Analysis of hypoxia responsive element enhancer sequences for hypoxia-targeted gene therapy applications.

A Thesis Submitted To the University of Manchester for the Degree of Doctor of Philosophy (Ph.D) in the Faculty of Medicine.

2001

Suzanne Karen Robinson

Department of Experimental Oncology, School of Medicine, Dentistry, Nursing and Pharmacy

ProQuest LLC.
789 East Eisenhower Parkway
P.O. Box 1346
Ann Arbor, MI 48106 – 1346

Contents

Contents 2

List of Figures 5
List of Tables 9
Abstract 11

Declaration 13

Copyright 14

Acknowledgements 15

Dedication 16

Chapter 1 17

Introduction 17

1.1 Treatment and Survival of Malignant Disease 17
1.2 Hypoxia and cancer therapy 20
1.2.1 Hypoxia 20
1.2.2 Radiotherapy 25
1.2.3 Chemotherapy 26
1.2.4 Chemo- and Radio-Resistance 27
1.2.5 Exploiting tumour hypoxia 28
1.3 Regulation of gene expression 30
1.4 Cellular responses to hypoxia 31
1.4.1 Hypoxia-Inducible Factor-1 (HIF-1) 32
1.4.2 Clinical evidence for HIF-1 expression 38
1.4.3 Oxygen sensing and signal transduction 39
1.4.4 Analysis of Hypoxia responsive elements (HREs) 41
1.5 Combination Therapy 53
1.5.1 Cyclic AMP 53
1.5.2 Radiation 56
1.5.2.1 Egr-1 and hypoxia 59
1.6 Aims of this Study 61

Chapter 2 63

Materials and Methods 63

2.1 General Techniques 63
2.1.1 Cell Culture 63
2.1.2 Cell Counts 65
2.1.3 Irradiation 66

2.2 DNA Handling 66
2.2.1 Digestion of DNA with Restriction Endonucleases 66
2.2.2 Agarose Gel Electrophoresis 67
2.2.3 Extraction and Elution of DNA Fragments from Agarose Gels 67
2.2.4 Ligation of DNA 68
2.3 Transformation of Competent Bacteria 70
2.4 Preparation of Plasmid DNA 72
2.4.1 Small Scale: Mini-Prep 72
2.4.2 Large Scale: Maxi-Prep. 73
2.4.3 Analysis of Plasmid DNA. 75
2.5 Transfection of Mammalian Cells 76
2.5.1 Electroporation 76
2.5.2 Calcium Phosphate 77
2.6 Assays 79
2.6.1 Dual-Luciferase Reporter Assay (DLR) System 79
2.6.2 DNA Sequencing 80
2.7 Solutions and Reagents 82

Chapter 3 84

Optimisation of Transfection Efficiency, Orientation, and Reoxygenation Phenomena of Hypoxia-Responsive Element Enhancer Sequences in a Panel of Human Carcinoma Cell Lines 84

3.1 Introduction 84
3.2 Methods 85
3.3 Results 87
3.3.1 Optimisation of DNA quantity and ratio 87
3.3.2 pRL.TK versus pRL.CMV 97
3.3.3 Determination of optimal reoxygenation time 100
3.3.4 Importance of the core HIF-1 binding site for HRE function 102
3.3.5 Calcium phosphate versus electroporation as a method for transfection 104
3.4 Discussion 105

Chapter 4 109

Optimisation of hypoxia responsive elements (HREs) for gene therapy 109

Part 1: Comparitive hypoxia-inducible expression of previously 'optimised' HREs 109
4.1.1 Introduction 109
4.1.2 Methods 113
4.1.3 Results 114
4.1.4 Discussion 117
Part 2: Dissection of the LDH-A and Glut-1 enhancer sequences 120
4.2.1 Introduction 120

4.2.2 Methods 121
4.2.3 Results 121
4.2.4 Discussion 131
Part 3: Preferential hypoxia response element transactivation by HIF-1α and EPAS-1 oxygen-responsive signalling pathways 133
4.3.1 Introduction 133
4.3.2 Methods 134
4.3.3 Results 134
4.3.4 Discussion 140

Chapter 5 143

Optimisation of the novel LDH-A hypoxia responsive enhancer. 143

5.1 Introduction 143
5.2 Methods 146
5.3 Results 146
5.4 Discussion 156

Chapter 6 158

Co-operative interaction between the hypoxia and PKA response pathways 158

6.1 Introduction 158
6.2 Methods 160
6.3 Results 160
6.4 Discussion 170

Chapter 7 172

Integrating the Transcriptional Response to Hypoxia and Ionising Radiation 172

7.1 Introduction 172
7.2 Methods 174
9.3 Results 177
7.3.1 pGL3.Epo.Egr-1: Transcriptional response to hypoxia and ionising radiation. 177
7.3.2 pGL3.Epo.CArG: Transcriptional response to hypoxia and ionising radiation. 186
7.3.3 Synergistic response of HREs to hypoxia and ionising radiation 188
7.4 Discussion 193

Chapter 8 196

Discussion 196

References 206

Appendices 231

List of Figures

Figure 1.1a: Illustration of the principle differences between the vasculature of normal and malignant tissues. 19
Figure 1.1b: Diagrammatic representation of tumour tissue surrounding a capillary showing regions of chronic hypoxia. 19
Figure 1.2: Frequency distributions of measured oxygen partial pressures (pO2 histograms) for malignant tissues of the breast and cervix, at either stage 1-2 or 3-4. Data adapted from various sources: Breast, Hoeckel et al. (1992); cervix, Schlenger et al. (1991). 22
Figure 1.3: Frequency distributions of measured oxygen partial pressures (pO2 histograms) for normal vs. malignant tissues of the breast, and cervix. 23
Figure 1.4: Schematic representation of the relative radiosensitivity as a function of O2 partial pressure (pO2) in the cellular environment. 26
Figure 1.5: Hypoxia and dioxin activated signal transduction pathways. 37
Figure 1.6: Comparative sequence homology of HIF-1 binding sites in HREs from various hypoxia-inducible genes 44
Figure 1.7; Transcriptional regulation of genes encoding glycolytic enzymes by HIF-1. (Firth et al., 1994, 1995; Semenza et al., 1996; Semenza et al., unpublished). 48
Figure 1.8: Regulation of the GLUT-1 enhancer, pG[1-610]α_1, by various stimuli, either in combination with or without hypoxia (1% O_2) in the human breast adenocarcinoma cell line MDA 468. 52
Figure 1.9: Mode of action of protein kinase A (PKA) 54
Figure 1.10: Consensus HIF-1 and CRE DNA binding sites. 55
Figure 1.11: Diagramatic representation of the the Egr-1 promoter (-935 to –65bp) showing co-operative *cis*-acting elements. 57
Figure 1.12: TNFα activity after transient transfection of the Epo-Egr-TNFα vector and treatment with hypoxia and radiation in combination and alone (TNFa : pg / million cells; error bars = sd) 60
Figure 2.1: Structure of pGL3.promoter plasmid supplied by Promega. 69
Figure 2.2: pGL3 vector showing upstream and downstream cloning sites and the locations of the sequencing primers, Rvprimer3 and Glprimer2. 80
Figure 3.1: Sequence comparison of PGK^{+++}, PGK^{--}, PGK^{mut}. 86
Figure 3.2: Normalised expression of pGL3.Control, pGL3.PGK^{+++} and pGL3.PGK^{--} amplitude in the human carcinoma cell line MDA 468, exposed to 16 hours air or anoxia, n=3 93
Figure 3.3: Normalised expression of pGL3.Control, pGL3.PGK^{+++} and pGL3.PGK^{--} amplitude in the human fibrosarcoma cell line HT1080, exposed to 16 hours air or anoxia (n=3). 94
Figure 3.4: Normalised expression of pGL3.Control, pGL3.PGK^{+++} amplitude in the human head and neck carcinoma cell line SQ20B, exposed to 16 hours air or anoxia (n=2) 96
Figure 3.5: Expression of pGL3.PGK^{+++} co-transfected with either pRL.TK or pRL.CMV in the HT1080 cell line. (n=2) 98
Figure 3.6: Amplitude of pRL.TK and pRL.CMV at different oxygen tensions, n=2. ...99

Figure 3.7: Normalised expression of pGL3.PGK^{+++} and pGL3.PGK^{-} amplitude in the human fibrosarcoma cell line HT1080, exposed to 16 hours air or anoxia and various periods of reoxygenation (n=3). (See appendix 3) 100
Figure 3.8: Normalised expression of pGL3.PGK^{+++} and pGL3.PGK^{-} amplitude in the human head and neck carcinoma cell line SQD9, exposed to 16 hours air or anoxia and various periods of reoxygenation (n=3). (See appendix 4) 101
Figure 3.9: Normalised expression of pGL3.PGK^{+++}, pGL3.PGK^{-} and pGL3.PGK^{mut} in two human carcinoma cell lines, SQD9 and HT1080, exposed to 16 hours air or anoxia and three hours reoxygenation (n=3) 103
Figure 3.10: Normalised expression of pGL3.PGK^{+++} transiently transfected into the human carcinoma cell lines MDA 468 and HT1080, at 40:1 and 10:1 ratios respectively, by electroporation. (n=2). 104
Figure 3.11: Induction of the CMV immediate early promoter under levels of hypoxia. 107
Figure 4.1: Hypoxia Response Elements and their co-operative cis-acting sequences .110
Figure 4.2: Mutations of the Epo HRE define the two functional regions required for hypoxic gene activation. 111
Figure 4.3: A schematic representation of the functional *cis*-acting elements within the Glut-1 enhancer sequence. 112
Figure 4.4: Amplitude of HRE-luciferase constructs exposed to 16 hours air, hypoxia or anoxia and three hours reoxygenation in the MDA 468 human breast carcinoma cell line. (n=3) 114
Figure 4.5: Amplitude of HRE-luciferase constructs exposed to 16 hours air, hypoxia or anoxia and three hours reoxygenation in the HT1080 human fibrosarcoma cell line. (n=3). 115
Figure 4.6: Amplitude of HRE-luciferase constructs exposed to 16 hours air, hypoxia or anoxia and three hours reoxygenation in the SQD9 human head and neck sarcoma cell line. (n=3). 115
Figure 4.7: Functional domains of LDH-A 120
Figure 4.8: Comparative expression of LDH-A (1+2+3) monomer, dimer and trimer, exposed to 16 hours air or anoxia in the HT1080 cell line, n=3. 122
Figure 4.9: Dissection of the functional elements of the LDH-A and Glut-1 enhancers in the MDA 468 human carcinoma cell line (n=3). 123
Figure 4.10: Dissection of the functional elements of the LDH-A and Glut-1 enhancers in the HT1080 human carcinoma cell line (n=3). 123
Figure 4.11: Dissection of the functional elements of the LDH-A and Glut-1 enhancers in the SQD9 human carcinoma cell line (n=3). 124
Figure 4.12: Expression of LDH $(1+2)^3$ in the forward and reverse orientation versus LDH $(1+2)^6$ in the negative orientation, in three human carcinoma cell lines, n=3. (See appendix 12) 126
Figure 4.13: Expression of PGK $(1+2)^3$ in the forward orientation versus PGK $(1+2)^6$ in the positive orientation in three human carcinoma cell lines, n=3 126
Figure 4.14: Expression of Epo $(1+2)^3$ in the forward orientation versus Epo $(1+2)^5$ in the positive orientation in three human carcinoma cell lines, n=3 127
Figure 4.15: Comparison of the amplitude of the 'optimal' HREs in the MDA 468 human carcinoma cell line, n=3. 129

Figure 4.16: Comparison of the amplitude of the 'optimal' HREs in the HT1080 human carcinoma cell line, n=3. 129
Figure 4.17: Comparison of the amplitude of the 'optimal' HREs in the SQD9 human carcinoma cell line, n=3. 130
Figure 4.18: Comparison of LDH (1+2) sequences. 132
Figure 4.19: Expression of LDH $(1+2)^{3-}$ in the C4.5 (wt) versus the Ka13 murine carcinoma cell line co-transfected with either none, or varying quantitites of HIF-1α, n=1 (except C4.5, n=3). 135
Figure 4.20: HRE expression in the parental, C4.5 cell line, n=3 (except at $1\%O_2$ n=2) (See appendix 15) 137
Figure 4.21: Ka13 cell line transiently co-transfected with pGL3.HREs plus pRL.CMV and 5μg pcDNA/^{Neo}/HIF-1α, n=3. 138
Figure 4.22: Ka13 cell line transiently co-transfected with pGL3.HREs plus pRL.CMV and 5μg pcDNA/^{Neo}/EPAS-1, n=3 139
Figure 5.1: HRE sequence exchanges. 144
Figure 5.2: Optimisation of the ChoRE from the LDH-A enhancer 145
Figure 5.2: Comparative expression of HREs containing either their natural site 2 or that from LDH-A in the MDA 468 cell line, n=3. 147
Figure 5.3: Comparative expression of HREs containing either their natural site 2 or that from LDH-A in the HT1080 cell line, n=3. 147
Figure 5.4: Comparative expression of HREs containing either their natural site 2 or that from LDH-A in the SQD9 cell line, n=3. 148
Figure 5.5: Comparative expression of the LDH HREs containing either its natural site 2 or that from Epo in the 3 human carcinoma cell lines, n=3. 149
Figure 5.6: Expression of LDH (1+2), with site 2 modifications in the MDA468 cell line, n=2. 151
Figure 5.7: Expression of LDH (1+2), with site 2 modifications in the SQD9 cell line, n=2. 151
Figure 5.8: Expression of HREs exposed to 16 hours air, hypoxia or anoxia and 3 hours reoxygenation in the A549 lung carcinoma cell line, n=3. 153
Figure 5.9: Expression of HREs exposed to 16 hours air, hypoxia or anoxia and 3 hours reoxygenation in the HCT116 colon carcinoma cell line, n=2. 154
Figure 5.10: Expression of HREs exposed to 16 hours air, hypoxia or anoxia and 3 hours reoxygenation in the T47D breast carcinoma cell line, n=3. 154
Figure 5.11: Expression of HREs exposed to 16 hours air, hypoxia or anoxia and 3 hours reoxygenation in the WiDr colon carcinoma cell line, n=3. 155
Figure 6.1: Comparative sequence homology of HIF-1 and CRE binding sites in various hypoxia-inducible genes. 159
Figure 6.2: Effect of 8-cl-cAMP on the expression of a variety on PGL3 HRE vectors in the MDA 468 breast carcinoma cell line, n=3. (See appendix 28) 161
Figure 6.3: Effect of 8-cl-cAMP on the expression of a variety on PGL3 HRE vectors in the HT1080 fibrosarcoma carcinoma cell line, n=3. (See Appendix 29) 162
Figure 6.4: HRE activity after 8 hours +/- a PKA analog followed by 16 hours air or anoxia and 3 hours reoxygenation in the MDA 468 cell line, n=3. 164
Figure 6.5: HRE activity after 8 hours +/- a PKA analog followed by 16 hours air or anoxia and 3 hours reoxygenation in the HT1080 cell line, n=3. 165

Figure 6.6: HRE activity after 8 hours +/- a PKA analog followed by 16 hours air or anoxia and 3 hours reoxygenation in the SQD9 cell line, n=3. 166
Figure 6.7: Expression of the dissected LDH-A elements 8 hours +/- a PKA analog followed by 16 hours air or anoxia and 3 hours reoxygenation in the HT1080 cell line, n=3. (See appendix 33) 168
Figure 6.8: Expression of the dissected LDH-A elements 8 hours +/- a PKA analog followed by 16 hours air or anoxia and 3 hours reoxygenation in the SQD9 cell line, n=3. (See appendix 34) 169
Figure 7.1: Schematic representation of pGL3.Epo.Egr-1 173
Figure 7.2: Schematic representation of pGL3.CArG and pGL3.Epo.CArG 174
Figure 7.3: Construction of pGL3.Egr-1 and pGL3.Epo.Egr-1 plasmids 175
Figure 7.3: Expression of Egr-1, Epo.Egr-1 and Epo exposed to 16 hours air or hypoxia, +/- 5Gy and 1 to 6 hours reoxygenation in the HT1080 cell line, n=3. 178
Figure 7.4: Expression of Egr-1, Epo.Egr-1 and Epo exposed to 16 hours air or hypoxia, +/- 5Gy and 1 to 6 hours reoxygenation in the MDA 468 cell line, n=3. 180
Figure 7.5: Expression of Egr-1, Epo.Egr-1 and Epo exposed to 16 hours air or hypoxia, +/- 5Gy and 1 to 6 hours reoxygenation in the DU145 cell line, n=3 182
Figure 7.6: Expression of Egr-1, Epo.Egr-1 and Epo exposed to 16 hours air or hypoxia, +/- 5Gy and 6 hours reoxygenation in the HepG2 cell line, n=1. 183
Figure 7.7: Expression of Egr-1, Epo.Egr-1 and Epo exposed to 16 hours air or hypoxia, +/- 5Gy and 3 hours reoxygenation in the HCT116 cell line, n=1 184
Figure 7.8: Expression of Egr-1, Epo.Egr-1 and Epo exposed to 16 hours air or hypoxia, +/- 5Gy and 3 hours reoxygenation in the WiDr cell line, n=1. 185
Figure 7.9: Expression of CArG.Epo versus CArG multimers exposed to 16 hours air or hypoxia and 3 hours reoxygenation in the HT1080 cell line, n=2. 186
Figure 7.10: Expression of CArG.Epo versus CArG multimers exposed to 16 hours air or hypoxia and 1 hour reoxygenation in the MDA 468 cell line, n=2. 187
Figure 7.11: Expression of CArG.Epo versus CArG multimers exposed to 16 hours air or hypoxia and 3 hours reoxygenation in the DU145 cell line, n=2. 187
Figure 7.12: HRE activity when exposed to hypoxia and radiation with 3 hours reoxygenation, in the HT1080 cell line, =3 (except Epo n=4) 189
Figure 7.13: HRE activity when exposed to hypoxia and radiation with 1 hour reoxygenation in the MDA 468 cell line, n=3 190
Figure 7.14: HRE activity when exposed to hypoxia and radiation with 1 hour reoxygenation in the DU145 cell line, n=2 (LDH (1+2); Epo^5), n=1 (PGK (1+2); LDH (1+2+3)). 191
Figure 7.15: HRE activity when exposed to hypoxia and radiation with 6 hours reoxygenation in the HepG2 cell line, n=1 192

List of Tables

Table 2.1: Description of human carcinoma cell lines used in this thesis. 65
Table 3.1: Representative raw data set for MDA468 transfected with either 15, 10 or 5 μg of total plasmid DNA (pGL3.Control, pGL3.PGK^{+++} and pGL3.PGK^{---}) at a reporter:control ratio (firefly:renilla) of 10:1 and 40:1. 89
Table 3.2: Normalised expression of pGL3.Control, pGL3.PGK^{+++} and pGL3.PGK^{---} in the human breast carcinoma cell line MDA 468, exposed to 16 hours air or anoxia. 91
Table 3.3: Induction of pGL3.Control, pGL3.PGK^{+++} and pGL3.PGK^{---} in the human carcinoma cell line MDA 468, exposed to 16 hours air or anoxia (n=3) 94
Table 3.4: Induction of pGL3.Control, pGL3.PGK^{+++} and pGL3.PGK^{---} in the human fibrosarcoma cell line HT1080, exposed to 16 hours air or anoxia (n=3). 95
Table 3.5: Induction of pGL3.Control, pGL3.PGK^{+++} and pGL3.PGK^{---} in the human head and neck carcinoma cell line SQ20B, exposed to 16 hours air or anoxia (n=2). 96
Table 3.6: pGL3.PGK^{+++} hypoxic and anoxic expression when co-transfected with either pRL.TK or pRL.CMV in the HT1080 cell line 97
Table 3.7: Expression of pRL.TK and pRL.CMV 99
Table 3.8: Induction of pGL3.Control, pGL3.PGK^{+++} and pGL3.PGK^{---} in the human fibrosarcoma cell line HT1080, exposed to 16 hours air or anoxia (n=3). 101
Table 3.9: Induction of pGL3.Control, pGL3.PGK^{+++} and pGL3.PGK^{---} in the human head and neck carcinoma cell line SQD9, exposed to 16 hours air or anoxia (n=3). 102
Table 3.9: Comparitive inducibility of the pGL3.PGK^{+++} vector transfected by either calcium phosphate (at chosen parameter, see earlier) or electroporation. 105
Table 4.1: Relative induction of 5 "optimal" HREs in 3 human carcinoma cell lines. (n=3) 116
Table 4.2: Comparative inducibility of LDH-A (1+2+3) monomer, dimer and trimer, exposed to 16 hours air or anoxia in the HT1080 cell line, n=3. 122
Table 4.3: Inducibility of the functional elements of the LDH-A and Glut-1 enhancers under hypoxia or anoxia in three human carcinoma cell lines. 124
Table 4.4: Induction of LDH, PGK and Epo multimers in the three human carcinoma cell lines. 127
Table 4.5: Amplitude and Induction of C4.5 and Ka13 cell lines transfected with pGL3.LDH (1+2)rev plus varying quantities of HIF-1α. 135
Table 5.1: Inducible expression of HREs containing site 2 sequence exchanges 150
Table 5.2: Induction of LDH (1+2), with site 2 modifications 152
Table 5.3: Induction of HREs exposed to 16 hours air, hypoxia or anoxia and 3 hours reoxygenation. 155
Table 6.1: HRE induction after 8 hours +/- a PKA analog followed by 16 hours air or anoxia and 3 hours reoxygenation 167
Table 6.2: Pairs of cAMP analogs that preferentially activate PKAI/PKAII 171
Table 7.1: Induction of Egr-1, Epo.Egr-1 and Epo exposed to 16 hours air or hypoxia, +/- 5Gy and 1 to 6 hours reoxygenation in the HT1080 cell line, n=3. 179

Table 7.2: Induction of Egr-1, Epo.Egr-1 and Epo exposed to 16 hours air or hypoxia, +/- 5Gy and 1 to 6 hours reoxygenation in the MDA 468cell line, n=3. 181
Table 7.3: Induction of Egr-1, Epo.Egr-1 and Epo exposed to 16 hours air or hypoxia, +/- 5Gy and 1 to 6 hours reoxygenation in the DU145 cell line, n=3 183
Table 7.14: Induction of HREs exposed to hypoxia and radiation in the HT1080 cell line 189
Table 7.15: Induction of HREs exposed to hypoxia and radiation in the MDA 468 cell line 190
Table 7.17: Induction of HREs exposed to hypoxia and radiation in the DU145 cell line. 191
Table 7.19: Induction of HREs exposed to hypoxia and radiation in the HepG2 cell line. 192

Abstract

Chemotherapeutic drugs and radiotherapy have a limited specificity for cancerous cells over normal, healthy tissues and thus produce significant toxic side effects. A reason for this is the requirement of oxygen for these therapies to be maximally cytotoxic. Therefore properties such as tumour blood flow, tissue oxygen and nutrient supply, pH distributuion and bioenergetic status can seriously alter the therapeutic response (Vaupel et al., 1989).

For a tumour to expand it must recruit its own vasculature from the existing host blood vessels. However, the growth of the tumour usually outstrips that of the recruited endothelial cells resulting in an inadequate and heterogenous vascular network and regions of hypoxia.

Tumour progression under conditions of hypoxic stress results in the over-expression of a number of specific genetic regulatory sequences, known as hypoxia response elements (HREs). HREs have been identified in a number of genes, such as those involved in angiogenesis, oxygen and glucose transport, and glucose metabolism, leading to increased protein synthesis, compared to aerobic cells. As these sequences are differentially expressed in tumour cells over healthy cells, they provide a mechanism by which treatment can be specifically targeted to cancerous cells.

The expression of these genes is regulated by the transcription factor, hypoxia-inducible factor-1 (HIF-1; Semenza et al., 1996). However, in a number of these genes there are multiple regulatory *cis*-acting elements. Evidence exists for the binding of *trans*-acting factors at adjacent sites and their cooperative interaction with HIF-1, to produce optimal transcriptional activation in response to hypoxia.

This study aims to optimise the functional amplitude of a number of HREs for use in gene therapy strategies. Constructs were made that contained synthetic hypoxia-

responsive enhancers, derived from Epo, VEGF, PGK, LDH-A and Glut-1. The HREs were driven by a heterologous SV40 promoter, linked to a luciferase transcription unit. Using Promega's Dual Luciferase Assay system, oxygen regulated transcription of each HRE was investigated in a panel of human carcinoma cell lines. From these results the LDH-A HRE was dissected and manipulated to allow further optimisation.

There is thought to be a level of integration between the PKA and oxygen sensing pathways. This was investigated by exposing carcinoma cells transiently transfected with HRE constructs to hypoxia and cAMP analogs. A marginal cooperative induction in response was observed.

Finally there have been attempts to make radiotherapy more specific by combining with gene therapy strategies to produce 'genetic radiotherapy'. This idea was expanded from previous studies to determine the combined effect of radiation and hypoxia on the Egr-1 gene, CArG elements and HREs in a wide range of human carcinoma cell lines.

Declaration

No portion of the work referred to in this thesis has been submitted in support of an application for another degree or qualification of this or any other university or other institute of learning.

Copyright

Acknowledgements

I would firstly like to thank my supervisors Dr Adam Patterson and Professor Ian Stratford for their help and advice throughout this Ph.D.

I must also thank all members of the Experimental Oncology group at the University of Manchester where this work was carried out.

Thank you, to the BBSRC for funding this work and my father for his financial support.

A final thank you to Jane Monaghan for sharing her computer expertise and all my friends and family for their support and encouragement throughout the last three years.

Dedication

To mum with all my love.

Chapter 1

Introduction

1.1 Treatment and Survival of Malignant Disease

Cancer is caused by a series of accumulated, acquired genetic mutations within somatic cells. These mutations are predominantly located in oncogenes and tumour suppressor genes, the consequences of which are disregulated cell division and uncoupled apoptotic signalling pathways. These genetic mutations are reproduced until a malignant clone arises, that ultimately proliferates outside normal tightly regulated controls, eventually killing its host. Cancer is rare as the body has evolved multiple mechanisms to check for and repair damaged DNA, e.g. immune-mediated or induced programmed cell death (apoptosis) of abnormal cells. Problems arise when these multiple checkpoints fail, and cells proliferate to form tumour foci. Eventually cells may infiltrate surrounding tissues and travel (metastasise), via the lymphatic or blood system, to other locations within the body to initiate secondary tumours.

Cancer is one of the biggest killers in the developed world, second only to heart disease. As imaging techniques improve, early detection of localised disease is becoming possible. At diagnosis, 70% of patients have no detectable distant metastasis and over half are cured by loco-regional treatment (Brady et al., 1990). However, of the patients treated for localised disease in Western Europe and the USA 22% are cured by surgery, 18% by radiotherapy and 5% by chemotherapy (DeVita, et al., 1983). These figures, in part, are a reflection of the fact that surgery and radiotherapy are largely employed to treat localised disease while chemotherapy is often utilised in the context of systemic disease, where prognosis is poor. Nevertheless, a critical limitation of conventional chemotherapy is the relative sensitivity of certain normal tissues with high proliferation rates.

It is becoming more widely accepted in the field of oncology that a contributory cause for these disappointing cure rates is the abnormal vasculature of tumours that can give rise to severe metabolite gradients e.g. oxygen, glucose, growth factors and other nutrients. Tumours, unlike normal tissues, often contain regions of low oxygen partial pressure (low pO_2; hypoxia) and extracellular acidity, particularly in areas with poor vascularisation. This is predominantly the result of the heterogenous and disorganised tumour blood flow, which can also result in poor chemotherapeutic drug penetration (figure 1.1a). In many cases, unless delivered by direct injection, reduced concentrations of chemotherapeutic drugs are possible in avascular regions of solid tumours. Furthermore, cells within this stressful microenvironment may be cycling very slowly or become quiescent (yet remain viable), and consequently are insensitive to conventional chemotherapeutics, which act predominantly on populations of proliferating cells. Thus the therapeutic index of chemotherapy is largely reliant upon differences in tumour versus normal tissue proliferation rates, a distinction that can be modest.

Moreover neoplastic cells often exist within a microenvironment that precludes optimal drug exposure and are sufficiently heterogeneous to allow adaptive survival of drug-resistant subpopulations. Despite a wealth of new agents there has been few examples of significant progress in the treatment of epithelial cancers. One approach has been to focus on developing "targeted" chemotherapy. It has been proposed that therapeutics could be made more specific by exploiting genetic or physiological differences between normal and cancerous tissues. Hypoxia is one such difference.

Figure 1.1a: Illustration of the principle differences between the vasculature of normal and malignant tissues.

(Taken from Brown 2000.)

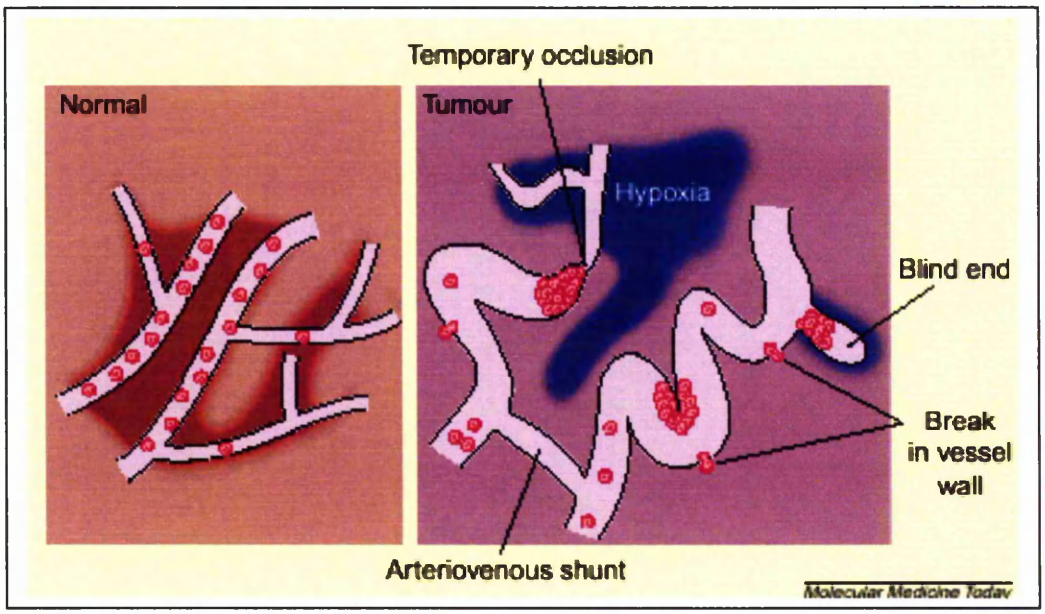

Figure 1.1b: Diagrammatic representation of tumour tissue surrounding a capillary showing regions of chronic hypoxia.

(Taken from Brown 2000.) Part of a tumour cord surrounding a capillary. (a) As the oxygen concentration decreases with increasing distance from the capillary, both cell proliferation rates and drug concentration decrease. (b) The level of cell kill in response to radiation, and to many other anticancer drugs, decreases with increasing distance from the capillary.

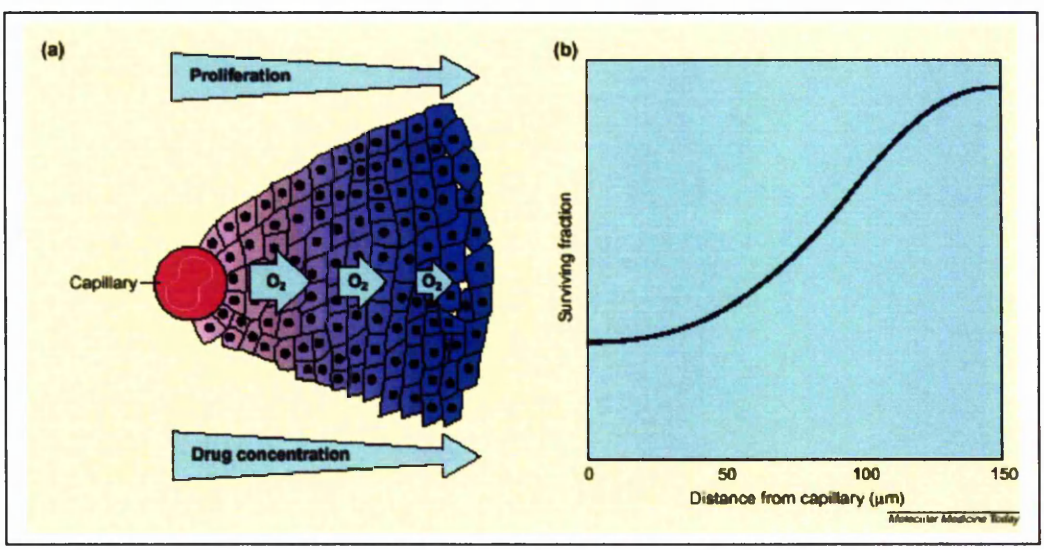

1.2 Hypoxia and cancer therapy

1.2.1 Hypoxia

Oxygen is rapidly metabolised in cells limiting its diffusion range. This results in cell populations within solid tumours that exist at intermediate and very low oxygen tensions (Gatenby et al., 1988) causing altered cellular metabolism. Thomlinson and Gray (1955), were the first to propose and model the existence of hypoxic cells, approximately 150-200μm (diffusion distance for oxygen) from a blood supply. Cells beyond 200μm from the circulatory network will have an oxygen concentration of zero leading to chronic, diffusion-limited hypoxia (figure 1.1b). For a tumour to grow and expand beyond a few mm^3 it must have an effective vasculature network to receive a supply of nutrients and oxygen and as well the removal of waste products. Initially a growing malignancy can exploit pre-existing host vasculature. However the host vessels per unit tumour mass do not increase in number leading to a reduction in the area available for the exchange of nutrients (Vaupel et al., 1989). As a tumour continues to proliferate it has to recruit its own blood supply. Angiogenic growth factors, e.g. vascular endothelial growth factor (VEGF), stimulate the growth of tumour vasculature via neovascularisation from venules within the tumour mass or from venules of the host tissue adjacent to the tumour front (Vaupel et al., 1989). This process is highly disorganised and the newly formed vessels lack any heirarcical structure. This results in tortuous, elongated and dilated venules, which can be obstructed or compressed (Vaupel et al., 1989). Tumour vessels are prone to occlusion or spontanaeous haemorrhage (Gatenby et al., 1988) resulting in hypoxic stress and regions of acute, transient perfusion-limited hypoxia.

Polarographic oxygen electrodes can be used to demonstrate the presence of hypoxic regions within tumours. The measuring device is a needle electrode with a membranised polarographic, microcathode tip in the form of gold wire. The electrode is calibrated in sterile phosphate-buffered saline (pH 7.4) prior to and immediately after pO_2 measurements (Vaupel et al., 1991).

Vaupel et al., (1993) measured oxygen concentrations in normal tissue to be in the range of 3.1% to 8.7% (pO_2; oxygen partial pressure of 24 to 66mmHg), whereas concentrations measured in human tumours showed a range of median oxygen from 1.3% to 3.9% (10 to 30mmHg). Readings of less than 0.3% (2.5mmHg) were frequent in over 80% of measurements taken. At 0.3% tissue O_2 cells are half-maximally resistant to radiotherapy (Hall, 1994). Regions of radioresistant hypoxic cells have been shown to exist within human solid tumours in a number of studies. 41 of 46 solid tumours studied were found to contain significant numbers of hypoxic cells (Moulder and Rockwell, 1987). In 6 out of 7 experimental model systems tested the hypoxic fraction was shown to increase with size; doubling the hypoxic fraction required an increase in the tumour diameter of about 1.5-fold. This increase in diameter corresponded to a volume increase of a factor of 3-fold. In broad agreement, tumour blood flow, tumour oxygenation, tissue pH distribution and high energy phosphates all decline as tumours enlarge. In each case the steepest decline occurs at a size range in which gross necrosis is rarely observed and in which a steep increase in the radiobiologically hypoxic fraction is also apparent (Vaupel et al., 1989). Vaupel et al. (1989), concluded that energy metabolism in the cell type tested (murine mammary adenocarcinomas) was limited by an inadequate O_2 supply which was manifest with tumour growth. However the strong correlation seen between tumour volume and hypoxic fraction is not observed in the clinical setting. The extent of hypoxia within a tumour cannot be predicted by tumour stage. For example there is no correlation between tumour stage and pO_2 frequency for carcinoma of the breast and cervix (figure 1.2). This makes it difficult to predict pO_2 within and between tumours and normal tissues. (Jiang et al., 1996),(figure 1.3), (figure 1.3; Hall, et al., 1998).

Figure 1.2: Frequency distributions of measured oxygen partial pressures (pO2 histograms) for malignant tissues of the breast and cervix, at either stage 1-2 or 3-4. Data adapted from various sources: Breast, Hoeckel et al. (1992); cervix, Schlenger et al. (1991).

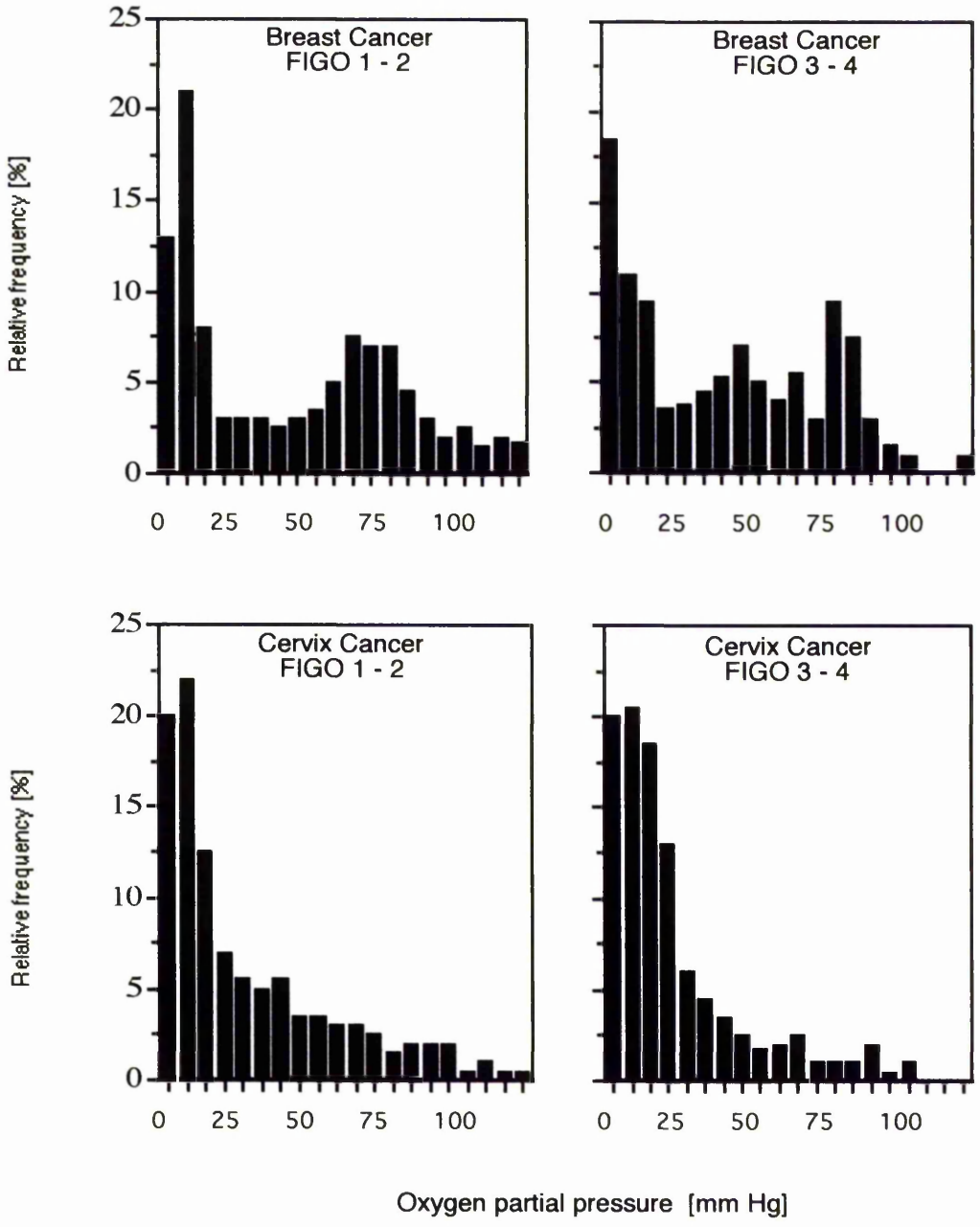

Figure 1.3: Frequency distributions of measured oxygen partial pressures (pO2 histograms) for normal vs. malignant tissues of the breast, and cervix.

Pooled data from various sources: Breast, Hoeckel et al. (1992); cervix, Schlenger et al. (1991); normal brain, Cooper et al. (1966), Roberts and Owens (1972) and Silver (1979).

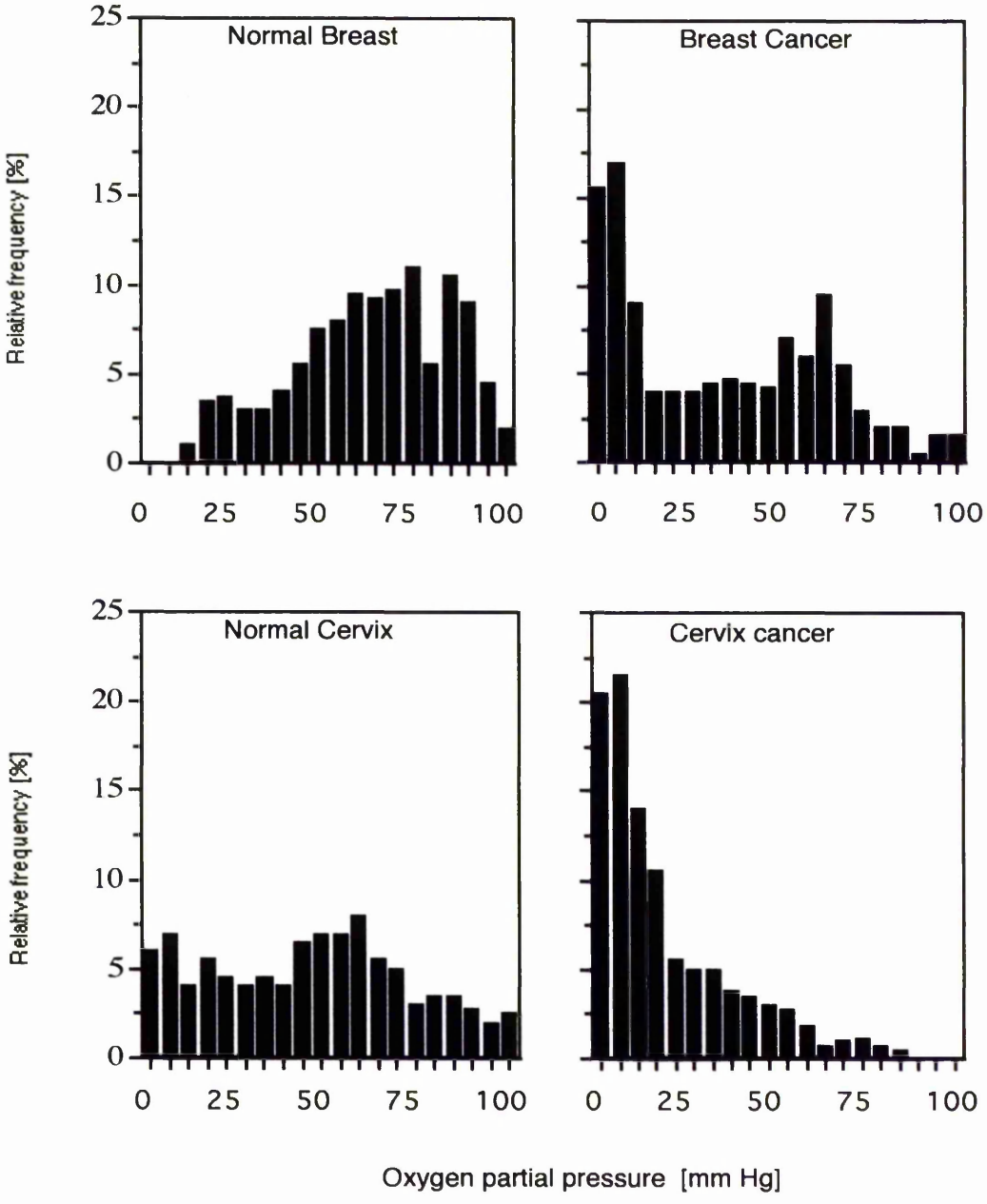

Hockel and colleagues (1996a), used the polarographic electrode assay to take up to 35 direct pO_2 measurements in at least two tumour tracks in cervical cancers of at least 3cm diameter in over 100 patients. They showed that a pre-therapeutic determination of tumour oxygenation status provides important information regarding malignant progression in terms of extra-cervical spread and radioresistance of locally advanced cancer of the uterine cervix. Patients with hypoxic tumours had significantly worse disease-free and overall survival probabilities compared to patients with non-hypoxic tumours, making tumour oxygen status a powerful pre-treatment prognostic indicator (Hockel, et al., 1996a).

There is significant hypoxic heterogeneity within solid tumours due to the chaotic vasculature and fluctuating blood flow, causing both chronic and acute hypoxia. Tissue pO_2 measurements don't necessarily reflect the temporal changes in oxygen flow that occur within the tumour microenvironment. Conflicting results obtained with differing hypoxic fraction measuring techniques may be explained by the presence of both chronic and acute hypoxia within the same tumour at the same time (Moulder and Rockwell, 1987). Thus it is difficult to predict oxygen levels within solid neoplasia, as there is no apparent relationship between oxygen concentrations in tumours of the same tissue type or with tumour grade.

1.2.2 Radiotherapy

Radiotherapy is almost exclusively a localised treatment. Tumour response to radiation is heterogenous, the response can be modified by intrinsic radiation sensitivity, rate of repopulation, and tumour size (Okunieff et al., 1994). Oxygen tension is possibly the most powerful predictor of radiation response in animal tumours as hypoxic cells are protected from the effects of radiation (figure 1.4; Suit et al., 1988). Many researchers have shown that ionising radiation, delivered as a single fraction, leads to the survival of hypoxic cells which can then repopulate the primary site (Review: Teicher, 1994). It is recognised that tumour hypoxia impacts less on treatment outcome if fractionated radiation is administered, allowing reoxygenation to occur between treatments (Suit et al., 1994, Kallman et al., 1972). Cells that were previously hypoxic may become aerobic and hence radiosensitised (Teicher, 1994). Fractionated radiation may partially overcome the effects of hypoxia, however, different tumours reoxygenate at different rates and reoxygenation between fractions is rarely complete. It has been suggested that both the initial ratios of acute and chronically hypoxic cells, and switching between these two states, may cause treatment failure (Okunieff et al., 1994; Stern and Guichard, 1996). This intrinsic heterogeneity of response within tumours and between patients remains a problem (Okunieff et al., 1994, Teicher, 1994). It has been proposed that tumour response is highly dependent on cells at intermediate levels of oxygen (0.5-20mmHg) and in most cases these cells are more important than the radiobiologically hypoxic fraction (Wouters and Brown, 1997). Wouters and Brown (1997) demonstrated that reoxygenation between radiation doses was much less than predicted, and hence had little impact on response.

Figure 1.4: Schematic representation of the relative radiosensitivity as a function of O2 partial pressure (pO2) in the cellular environment.

The range in values usually found in blood, normal tissues, and malignant tissues is illustrated. The pO2 at which the sensitizing effect is half-maximal is indicated. (Adapted from Vaupel, 1989a).

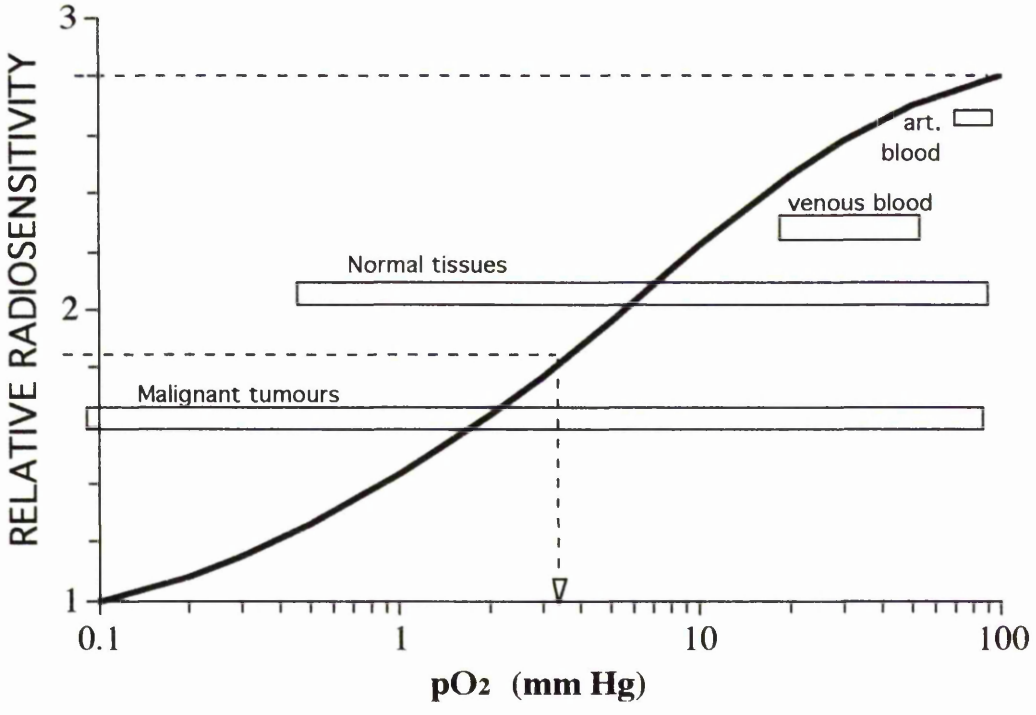

1.2.3 Chemotherapy

In contrast to surgery and radiation, chemotherapy can be used systemically to treat metastatic spread. Like radiation, chemotherapeutic drugs act by either inflicting genetic damage sufficient to kill cells directly, or by inducing apoptosis. (Hellman, 1996). However, the vast majority of these agents target DNA replication and are thus selective for proliferating cells. Consequently, chemotherapy is unable to distinguish between normal and cancerous cells as it has no inherent specifity for tumour cells. This

lack of selectivity means that these drugs are dose limited due to the array of toxic side effects.

1.2.4 Chemo- and Radio-Resistance

Hypoxic cells cycle at reduced rates (Durand, 1997) therefore, tend to be resistant to radiation and many chemotherapeutic drugs that act on rapidly dividing cells. Therapeutic responses are influenced by cellular heterogeneity due to genetic differences and physiological factors created by inadequate and heterogeneous vascular networks including tumour blood flow, tissue oxygenation, pH distribution and energy metabolism (Okunieff et al., 1994). Cells in the hypoxic state have been shown to remain viable for prolonged periods (Durand et al., 1997), and under conditions of reoxygenation may re-enter the cell cycle so repopulating a tumour, which had previously shown no responsiveness to therapy. Gatenby et al. (1988), demonstrated that response to radiation therapy was increased with increased oxygen concentration in squamous cell carcinomas of the head and neck. Tumours that recurred tended to have oxygen concentrations less than 10mmHg compared to those with over 10mmHg (Hoeckel et al., 1996). If tumours were hypoxic prior to treatment then the probability of developing distant metastasises was doubled (Brizel et al., 1996).

Alterations in gene expression, including oncogenes and tumour suppressor genes, can increase resistance to both radiation and chemotherapy. Under normal physiological conditions, apoptosis prevents the survival of mutated and transformed cells. A normal diploid copy of the tumour suppressor gene, p53, can facilitate apoptosis under low oxygen tensions such as those found within tumours (Graeber et al., 1996). Tumours that have no functional p53 have a significant reduction in hypoxia-mediated apoptosis, such that repeated hypoxia and repurfusion insult can favour the survival of p53-/- cells (Graeber et al., 1996; Giaccia et al., 1996). These data suggest hypoxia can provide a powerful selective pressure for cells that have mutated p53, an event that destabilises cells and encourages malignant progression. In addition, hypoxia results in

an increased mutation rate (Reynolds et. al., 1996) and a reduced DNA repair rate (Glazer et al., 2000). This genetic instability may contribute to the intrinsic and/or acquired drug resistance phenotype (Reynolds and Glazer, 1996). Since hypoxia can be an early event in the pathophysiological history of a solid neoplasia (Folkman, 1996), it is postulated that a clinically detectable tumour mass may have undergone durable clonal selection for many years. Thus tumour hypoxia may have an important role in the genotypic evolution of a growing tumour mass and suggests that hypoxia provides a physiological environment that is selective for malignant progression.

1.2.5 Exploiting tumour hypoxia

A number of strategies have been developed to overcome tumour hypoxia *in vivo*. The utility of fractionated radiation has already been discussed; others methods for overcoming radioresistance include breathing carbogen (95% O_2, 5% CO_2) concurrent to a regime of fractionated radiation (Review: Teicher, 1995), the combination of radiation with either nicotinamide and carbogen or carbogen and tirapazamine, (Stern and Guichard, 1996), or the use of hypoxic cell radiosensitisers. Radiosensitisers from the nitroimidazole class (eg. Nimorazole) are small freely diffusible compounds that are sufficiently lipophilic that they can distribute evenly within tumours, implying that they should be effective against both acutely and chronically hypoxic cells (Chaplin et al., 1987; Sutherland et al., 1996). This is in contrast to chemotherapeutic drugs that can have poor tissue diffusion properties i.e. if they are DNA-affinic or undergo metabolic consumption.

The presence of oxygen greatly increases the therapeutic response of solid neoplasms to radiotherapy and chemotherapy. A variety of techniques have been developed to increase oxygen delivery to tumours. For example the administration of an oxygen-carrying perfluorochemical emulsion prior to injection of bleomycin or etoposide produced significant tumour growth delays (Teicher, 1994). However, Chaplin and Hill (1995), suggest that if temporal changes in red blood cell flux and thus tumour

cell oxygenation, are a common feature of solid tumours, then procedures which improve the oxygen-carrying capacity of the blood will not be effective in reoxygenating all the hypoxic cell population.

A high percentage of tumour cells cycle through the hypoxic state (Wilson, 1996). The development of bioreductive prodrugs, or hypoxia selective cytotoxins (HSC), can be used to exploit hypoxia. HSC undergo metabolic reduction to generate cytotoxic metabolites. This bioactivation is suppressed in oxygenated cells providing a selective method of cytotoxicity to hypoxic tumour cell populations that are resistant to radiotherapy (Workman and Stratford, 1993; Denny et al., 1996). The bioreductive drugs that have been, or are currently, under investigation include; EO9, Porfiromycin, AQ4N and Tirapazamine. In general these agents tend to be DNA alkylating or DNA strand-breaking agents as their cytotoxic effects are not highly dependent on cell cycle status.

Vasoactive agents modify the blood flow so altering the perfusion of oxygenated blood to the tumour and thus the potential for bioreductive drug activation. An example is hydralazine, which preferentially causes arterial vascular smooth muscle to relax leading to vasodilation, a decrease in blood pressure and reduced blood flow to the tumour (Review: Teicher, 1995). Other antivascular agents include flavone acetic acid (FAA), a synthetic flavanoid, it causes a rapid and significant decrease in tumour blood flow *in vivo* and thus oxygen and nutrient delivery (Bibby et al., 1989; Edwards et al., 1989; Hill et al., 1989; Murray et al., 1989; Zwi et al., 1989). Combretastatin induces vascular shutdown in murine models, *in vivo*, (Chaplin et al., 1999) mediated by an induction in endothelial cell apoptois (Iyer et al., 1998).

1.3 Regulation of gene expression

Gene therapy is a novel method of therapeutic intervention against cancer targeted at the level of cellular gene expression. Gene therapy strategies offer the potential to achieve a much higher level of specificity than conventional therapeutics by virtue of the highly specific regulatory mechanism of gene expression that are targeted. This requires the identification of genetic regulatory sequences that are differentially expressed in cancerous cells over healthy cells providing a treatment that is more specifically targeted to neoplastic cells. By exploiting the tumour hypoxia that arises as a consequence of abnormal tumour physiology, regardless of tissue type, stage, or origin, a near universal transcriptionally selective strategy could be achieved. One promising application of gene therapy is gene directed enzyme-prodrug therapy (GDEPT). GDEPT involves the delivery and expression of a gene(s) to tumour cells that will confer conditional sensitivity to an inert prodrug (Connors 1995;). One possible level of specificity employs an integrated promoter (hypoxia responsive element; HRE) to drive the expression of the therapeutic enzyme in hypoxic cells (Connors, 1995; Springer et al., 2000).

The first hypoxia-targeted GDEPT strategy, *in vitro*, was described by Dachs et al. (1997); They transiently transfected a plasmid encoding a trimer of the hypoxia responsive element (HRE) from the phosphoglycerate kinase-1 (PGK-1) promoter, fused to a 9-27 promoter, linked to a gene encoding the enzyme cytosine deaminase, into the 9-3C (HT1080) human carcinoma cell line. On exposure to 16 hours anoxia, a 6.8-fold increase in cytosine deaminase activity was observed compared to normoxia and the parental (untransfected) cell line. On addition of the inactive prodrug, 5-fluorocytosine (5-FC), cytosine deaminase converts it to the active metabolite 5-fluorouracil (5-FU), which has demonstrated effectiveness in the treatment of colorectal carcinomas.

Prodrugs must distribute efficiently within hypoxic tumours and undergo selective metabolism, ideally producing a bystander effect by releasing a diffusible cytotoxin on activation (Denny et al., 1996). The metabolite produced should possess a

half-life sufficiently long to permit them to diffuse significant distances from the cell of origin. This would make a small proportion of hypoxic cells foci for the catalytic production of cytotoxic species, which can kill surrounding oxic tumour cells (Denny et al., 1996). The diffusion range of the cytotoxic species would not exceed that of oxygen (200μm) so limited localised cell killing occurs. It is unlikely that all cells in a tumour will be transfected thus a bystander effect is an essential property of any gene therapy strategy.

1.4 Cellular responses to hypoxia

Individual cells sense hypoxia and respond by altering the expression of specific genes, the products of which are involved in the maintenance of oxygen homeostasis under hypoxic conditions (Semenza, 1996). Responses to hypoxia can be systemic (including increased erythropoiesis, increased ventilation and cardiac output), or local (changes in vascular tone and neovascularisation; Semenza, 1996). Adaption is also achieved at the cellular level by cells switching from oxidative phosphorylation to the less efficient anaerobic glycolysis (Dang and Semenza, 1999). Molecular oxygen is the final electron acceptor in the respiratory electron transfer pathway through which mitochondrial redox potential is utilised to generate adenosine 5-triphosphate (ATP; Review: Wang and Semenza, 1996). Therefore, oxygen influences the pathway for glucose utilisation and thus the generation of ATP. Anaerobic glycolysis is 18-fold less efficient at producing ATP than the Krebs cycle, resulting in a higher rate of glucose utilisation (Pasteur effect) that is reliant on an increase in glucose transport. Consequently genes encoding enzymes involved in glucose transport (Glut-1, Glut-3) and glycolytic metabolism (PGK, ALDA, ENO-1, LDH-A) are upregulated.

The DNA regulatory elements controlling the expression of oxygen-responsive genes have been implicated or defined in most cases, and involve the specific binding and transactivation by various inducible, phosphorylation-dependent and/or redox sensitive transcription factors. Published evidence indicates that only hypoxia inducible

factor-1 α/β (HIF-1; Wang and Semenza, 1993a; 1993b), is specifically oxygen-responsive; HIF-1 operates at physiologically relevant oxygen tensions, in comparison, NF-κβ and the tumour suppressor p53, are induced by either near anoxic stress (0.02% O_2) or reoxygenation-dependent processes (Wenger and Gassman, 1997; An et al., 1998).

1.4.1 Hypoxia-Inducible Factor-1 (HIF-1)

HIF-1 is a heterodimeric transcription factor consisting of two polypeptides, a 120-kDa HIF-1α subunit complexed with a 91 to 94-kDa HIF-1β (ARNT) isoform (Wang and Semenza 1995). The amino terminal of each subunit contains basic helix-loop-helix (bHLH) and PER-ARNT-SIM (PAS) homology domains; the conserved PAS (Per-AHR-ARNT-Sim) domain has similarities to the *Drosophila* proteins period (Per) and single-minded (Sim) involved in circadian regulation and neurogenesis, respectively (Review: Littlewood and Evan, 1995; Wang et al., 1995). In mammals, the PAS domain is thought to be involved in heterodimerization, DNA binding and transactivation (Wenger and Gassman, 1997). In contrast, the HLH domain mediates dimerisation whilst the basic domain contacts the DNA of a large family of dimeric eukaryotic transcription factors (Review: Semenza, 2000).

HIF-1α is an 826 amino acid protein novel to HIF-1, its only known function is in hypoxia-specific gene regulation (Huang, 1996). HIF-1α mRNA is constitutively present in normoxic cells, but under hypoxic conditions, HIF-1a protein rapidly accumulates. HIF-1 levels are usually tightly regulated by cellular oxygen (Wang et al., 1995) as both hypoxia-induced HIF-1 binding, and HIF-1α protein levels rapidly and drastically decrease in response to reoxygenation (half life of less than 5 minutes in normoxia; Huang et al., 1996). However, HIF-1α is also expressed in normoxic human prostate (Zhong et al., 1999) and lung (Volm and Koomagi 2000) cancer cells *in vitro*, suggesting that mutations exist that bypass the normal HIF-1 degredative pathways in the presence of oxygen. HIF-1α protein levels are regulated, in part, through

posttranslational alterations in stability (Huang et al. 1996): Removal of PEST-like domains (proline, glutamic acid, serine, threonine; Rogers et al., 1986; Wang et al., 1995; Huang et al., 1996; Rechsteiner et al., 1997; Salceda et al., 1997), in the C-terminal portion of the protein (Wang et al., 1995) results in an oxygen insensitive, stable protein (Richard et al., 2000). A recent study by Salceda and Caro, 1997, suggested that the lack of HIF-1α protein under normoxic conditions was a result of rapid degradation by the ubiquitin-proteasome system, a mechanism involving PEST-like domains in other proteins. HIF-1α and thus the HIF-1 complex could be stabilised (even under normoxia) by blocking this pathway with proteosome inhibitors (Salceda and Caro 1997; Huang et al., 1998; Richard et al., 1999). This and previous data (Huang et al., 1996) suggest that the hypoxia induced changes in HIF-1α stability and subsequent gene activation are mediated by redox-induced changes.

In contrast, HIF-1β, has been shown to encode 774 and 789 amino acid isoforms. As well as dimerising with HIF-1α, HIF-1β, also known as aryl hydrocarbon nuclear translocator (ARNT) in the xenobotic response, can heterodimerise with the aryl hydrocarbon receptor (AHR) in cells exposed to xenobiotic ligands such as dioxin and other aryl hydrocarbons to form the AHR complex (Huang, 1996; Semenza et al., 1997; Wenger and Gassman, 1997). The AHR complex binds to the xenobiotic response element and regulates expression of genes involved in xenobiotic metabolism (figure 1.5; Wenger and Gassman, 1997). HIF-1β protein is constitutively expressed in normoxic cells and its level is not affected by changes in oxygen concentrations (Semenza et al., 1996; Wood et al., 1996). The N-terminal region of HIF-1β is vital for DNA binding and heterodimerisation, in contrast the C-terminal region mediates transactivation (Li et al., 1996). HIF-1β deficient Hepa-1 cells transiently transfected with a hypoxia responsive gene (HRE from PGK-1) showed no response to reduced oxygen (Li et al., 1996) demonstrating that HIF-1β is an essential component of hypoxia-inducible HIF-1 DNA binding and oxygen-regulated reporter activity (Li et al., 1996; Gassman et al., 1997; Maxwell et al., 1997).

There is evidence that HIF-1α and HIF-1β steady state mRNA levels remain constant at varying oxygen concentrations (between 20 and 0.5% in a variety of human carcinoma cell lines tested *in vitro*) suggesting that the induction of HIF-1 DNA binding is regulated at the post-transcriptional level (Wenger et al., 1997). The prevalent mode of HIF-1α induction seems to be translational up-regulation and/or protein stability (Wenger et al. 1997). HIF-1 is induced by hypoxia, cobalt chloride ($CoCl_2$) and desferrioxamine and inhibited by cyclohexamide, a protein synthesis inhibitor known to block induction of Epo mRNA (Goldberg et al., 1988) and actinomycin D, a protein kinase inhibitor (Wang and Semenza, 1993a) in hypoxic Epo (Hep3B) and non-Epo producing cells. This suggests a general role for HIF-1 in hypoxia signal transduction and transcriptional regulation (Semenza, et al., 1994). This suggests that both de novo transcription and translation is required for the induction of HIF-1 activity in hypoxic cells (Wang and Semenza, 1993a).

A study by Gradin et al. (1996), found HIF-1α stably associated with the molecular chaperone heat shock protein 90 (hsp90), suggesting that HIF-1a may be regulated by hsp90 in a manner similar to the dioxin receptor (figure 1.5). HIF-1α and AHR both contain ligand and hsp90 binding sites in the C-terminal half of the PAS domain (Wenger and Gassman, 1997). Prior to heterodimerisation with ARNT, the AHR transcription factor is located in the cell cytoplasm complexed with two molecules of hsp90. Ligand binding (by dioxins) causes activation of the AHR, it is then released from the hsp90, a mechanism possibly associated with ARNT, and translocates to the nucleus to heterodimerise with ARNT a HLH protein essential for both dioxin and HIF-1α mediated pathways (Gradin et al. 1996). Minet and colleagues (1999), demonstrated that hsp90 was essential for HIF-1 activation in hypoxia, as with AHR, hsp90 was not co-translocated with HIF-1α into the nucleus. Hsp90, as well as acting as a molecular chaperone, prevents the aggregation of unfolded proteins subjected to heat, oxidative or ischaemic stress, and also binds to zinc finger proteins so may have a role in oxygen sensing (Scandurro et al., 1997; Minet et al., 1999).

It has been demonstrated that HIF-1α and β subunits can independently co-*trans*activate the Epo enhancer, but binding of both subunits and a hypoxic environment was necessary for maximal transactivation (Madan et al., 1997). However this does suggest the presence of transcription factor(s) that may possess some homology to either HIF-1α or HIF-1β. Recently a HIF-1a-like bHLH factor was identified in independent studies (HIF-1a-like factor, HLF, Ema et al., 1997; HIF-related factor, HRF, Flamme et al., 1997; endothelial PAS domain protein 1, EPAS-1, Tian et al., 1997) with 48% similarity to HIF-1α (Wenger and Gassman, 1997). For the purpose of this thesis, we will refer to this factor as EPAS-1 and the EPAS-1/HIF-1β complex, as HIF-2. EPAS-1 is activated by hypoxia and can heterodimerise with HIF-1β to activate genes via the same HIF-1 binding sites as HIF-1, such as VEGF (Wenger and Gassman, 1997; Wiesener et al., 1998). The inducible responses of EPAS-1 to hypoxia are similar to that seen in HIF-1α, however EPAS-1 was slightly more abundant in normoxic and mildly hypoxic cells (Wiesener et al., 1998). EPAS-1 mRNA expression has been identified in highly vascularised tissues in adults and endothelial cells during embryogenesis, mouse embryonic stem cells lacking EPAS-1 developed severe vascular defects and die early in development (Peng et al., 2000). EPAS-1 has a high target specificity for VEGF, upregulating gene expression through its HIF-1 binding site (Maemura et al., 1999) compared to other HREs tested (Wiesener et al., 1998), demonstrating the important role of EPAS-1 in vascular development.

The C-terminal region of HIF-1α has been shown to associate to the transcriptional co-activator protein, p300 in a hypoxia-induced DNA-bound complex leading to the transcriptional activation of Epo and VEGF (Arany, et al., 1996). p300 is a general transcriptional activator with close homology to CREB binding protein (CBP), it interacts with transcription factors, such as HIF-1, cyclic AMP-responsive element binding-1 (CREB) and activating transcription factor-1 (ATF-1), as an adaptor protein rather than binding to DNA directly (Goldberg et al., 1988). p300/CBP may act by signalling between DNA-bound transcription factors and the basic transcriptional machinery (Arany et al., 1996) which may play a critical role in regulating HIF-1α activity, e.g. it may have activity with HIF-1 accessing its binding site (Arany et al.,

1996; Huang et al., 1997; Wenger and Gassman, 1997). If activity of p300/CBP was blocked by the adenovirus E1A oncoproteins, hypoxic Epo and VEGF gene activation was prevented in Hep3B cells, in contrast, enhanced expression of p300/CBP increased hypoxia-induced transcription (Arany et al., 1996; Wenger and Gassman 1997; Huang et al., 1997). This process may occur in other HREs, such as the LDH-A gene, which relies on the cooperative interaction of HIF-1 and CRE binding sites for function (Firth et al., 1995). If cells were exposed to cyclicAMP the transcription factor, CREB, is stimulated to bind to the cyclic AMP responsive element (CRE) DNA sequence and recruits the transcriptional adaptor CBP (Review: Arany et al., 1996).

Figure 1.5: Hypoxia and dioxin activated signal transduction pathways.

(Taken from Gassman et al., 1997) As a result of hypoxia, HIF-1α is released from hsp90 and translocates to the nucleus where it rapidly accumulates (Wang et al, 1995), and binds with HIF-1β to form the HIF-1 complex. Other co-activators may bind to HIF-1, prior to HIF-1 binding the core DNA sequence 5'-ACGTG-3', eg. CREB-1/ATF-1, or may compete for binding of the HIF-1 site. Binding of the HIF-1 complex to its DNA regulatory sequence leads to the transcriptional activation of a number of hypoxia responsive genes.

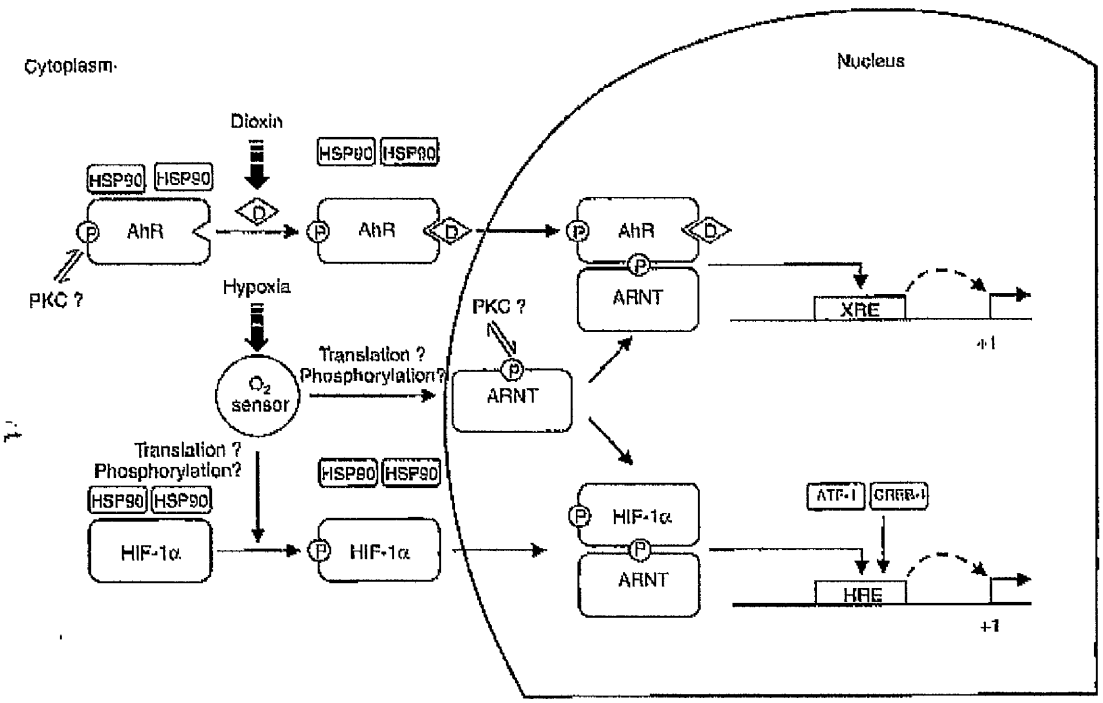

1.4.2 Clinical evidence for HIF-1 expression

Overexpression of HIF-1α protein can occur early in carcinogenesis, eg. in premalignant lesions of colon adenoma and breast carcinoma *in situ*, in comparison, benign tumours so far analysed do not overexpress HIF-1α (Zhong et al., 1999). Zhong and colleagues (1999), are continuing their studies to discover whether HIF-1a could become a novel biomarker of pre-cancerous lesions, thus allowing early therapeutic intervention.

Hypoxia causes the upregulation of a number of genes through HIF-1 activity, such as lactate dehydrogenase A (LDH-A) or thymidine phosphorylase (TP; Matsushita et al., 1999) both of which have long been used as markers of neoplasia (Wang et al., 1995) which lead to a poor prognosis.

The mutation of tumour suppressor genes and oncogenes, leading to their inactivation or activation respectively, results in increased expression of HIF-1α protein and HIF-1 DNA binding activity ultimately causing increased transcription of genes encoding, among others, VEGF and glycolytic enzymes (Review; Semenza et al., 2000). Accumulation of the tumour suppressor gene, p53, occurs in the hypoxic state where it can bind directly to HIF-1α through an interaction with p300 (An et al., 1998; Richard et al., 2000). Tumours lacking a second tumour suppressor gene, Von Hippel Lindau (VHL), over-express HIF-1 induced genes such as VEGF and Glut-1 in an oxygen-independent fashion resulting in highly vascularised tumours (Iliopoulos et al., 1996; Maxwell et al., 1999; Richard et al., 2000).

HIF-1α, at low oxygen tensions, is involved in maintaining oxygen homeostasis by increasing glycolysis, erythropoeisis and angiogenesis (Carmeliet et al., 1998), tumours lacking HIF-1 expression have a slower growth rate and are poorly vascularised (Maxwell et al., 1997; Jiang et al., 1997). Carmeliet and colleagues (1998) demonstrated that a lack of oxygen and glucose (hypoxia and hypoglycaemia respectively) reduced cellular proliferation and increased apoptosis, this was not seen in cells deficient in HIF-

1α, suggesting HIF-1α as a mediator of hypoxia and hypoglycaemia induced apoptosis. Thus a lack of HIF-1α would promote tumour regression by reducing hypoxia-induced expression of growth factors that allow the formation of new blood vessels, leading to a reduced vasculature (Carmeliet et al., 1998). Mice embryos lacking HIF-1α die at embryonic day 10.5; inadequate vascularisation, cardiac and neuronal abnormalities were observed in HIF-1α deficient mice, both these data indicate that HIF-1α plays a critical role in embryogenesis and neovascularisation (Carmeliet et al., 1998; Richard et al., 1999).

1.4.3 Oxygen sensing and signal transduction

Biological signalling involves a ligand binding to a cognate receptor in a stereospecific manner, this allows transduction of a signal that impacts on cellular function either directly or by altering gene expression (Bunn and Poynton, 1996). Nuclear receptors bind to their ligands in the cytosol, travel to the nucleus and bind to target genes, so functioning directly as transcription factors (Bunn and Poynton, 1996).

It was Goldberg et al. (1988), who originally demonstrated that a ligand-dependent conformational change in a heme-protein was likely to account for the mechanism by which hypoxia stimulates a signal transduction pathway leading to the induction of HIF-1a and the production of Epo. Oxygen is known to bind to and react with heme proteins, Goldberg and colleagues (1988), hypothsised that the oxygen sensor was a high turn-over heme-protein. Evidence to support this came from studies showing that Epo production was inhibited at low partial pressures of oxygen by carbon monoxide (the only known targets for carbon monoxide are reduced heme proteins). Secondly, Epo was induced by transition metals, namely iron; a heme protein acted as an oxygen sensor for Epo expression. Cobalt, nickel and manganese atoms can substitute for the iron atom in the heme moiety by changing their redox state (Bunn and Poynton, 1996; Ehleben et al., 1997; Huang et al., 1997; Salnikow et al., 2000). Blocking heme

synthesis in Hep3B cells, impaired the oxygen sensing mechanism and markedly reduced hypoxia-, cobalt-, and nickel-induced Epo production (Goldberg et al., 1988).

This response was also seen in non Epo-producing cells (Bunn and Poynton, 1996). It is hypothesised that the sensor is a cytochrome-b type oxidase, probably cytosolic and membrane-bound, that binds oxygen and reduces it to superoxide so producing reactive oxygen intermediates (ROI) (Bunn and Poynton et al., 1996; Wang and Semenza, 1996; Fandrey et al., 1997). The formation of ROI may be catalysed by iron (Iwai et al., 1998) and ROI may act as chemical signals which impact on transcription factors such as HIF-1 (possibly to stabilise and activate HIF-1 complex) to alter oxygen-responsive gene expression (Reviewed in Bunn and Poynton, 1996).

Cells may transduce signals through conformational changes, enzyme activities or by interacting with other molecules, all of which require free energy. This free energy, may be provided by the transfer of phosphate groups to a protein, or via redox regulation (Wang and Semenza 1996). The signals transduced by hypoxia are likely to involve both protein phosphorylation and redox chemistry (Bunn and Poynton, 1996). HIF-1 DNA binding activity and the steady-state level of Epo RNA induced by hypoxia was reduced significantly when Hep3B cells were incubated with cyclohexamide or 2-aminopurine (2-AP; protein kinase inhibitors), under hypoxia, indicating that protein synthesis and phosphorylation was essential prior to an increase in mRNA (Goldberg et al., 1988; Wang and Semenza, 1993). Therefore, phosphorylation of HIF-1 may be required for DNA binding. It is thought that HIF-1a may be phosphorylated before translocating to the nucleus (figure 1.5; Richard et al., 1999). Wang and Semenza (1996), suggested that both pathways may act co-operatively to transduce cell signals and regulate gene transcription. Evidence supporting this demonstrates that HIF-1 must be in the reduced state (Wang et al., 1995) and undergo phosphorylation (Wang and Semenza, 1993a) for DNA binding to occur (Bunn and Poynton).

1.4.4 Analysis of Hypoxia responsive elements (HREs)

Erythropoietin (Epo): The molecular mechanisms that mediate genetic responses to hypoxia were first studied in erythropoietin (Epo) gene regulation (Wang and Semenza 1995). Oxygen dependent Epo gene expression has been observed in the tissue culture hepatoma cell lines Hep3B and HepG2 (Goldberg et al., 1988). Epo is a glycoprotein growth factor that stimulates proliferation and differentiation of erythroid progenitor cells (Wang and Semenza 1995; Wenger and Gassman, 1997). The primary stimulus of Epo production is a decrease in blood oxygen levels, for example the hepatoma cell line, Hep3B, produces higher levels of Epo mRNA under hypoxia (1% oxygen) than at 20% oxygen (ie. decreased O_2 leads to increased Epo production). Epo mRNA levels are determined by both the rate of gene transcription and posttranscriptional events (Goldberg et al., 1991). A functionally tripartite 50 nucleotide (nt), *cis*-acting hypoxia-inducible enhancer was identified in the 3'-flanking region of the Epo enhancer (Pugh et al., 1991; Semenza and Wang 1992). The enhancer element contains a hypoxia responsive site (nt 1-24; Blanchard et al., 1992; Galson et al., 1992; Semenza and Wang 1992). By studying hypoxic extracts, this site alone was shown to bind a nuclear protein in both Epo-producing and non-Epo-producing cells (Beck et al., 1993) identified as the HIF-1 complex (Semenza and Wang 1992). Wang and Semenza (1993), demonstrated that HIF-1 recognises an 8 base pair (bp) DNA sequence, (nt 5-12) 5'-TACGTGCT-3', of the Epo enhancer. An essential second element, (nt 20-24) 5'-CACAG-3' was identified 5' to the HIF-1 binding site (Wang and Semenza, 1993). A highly conserved third element was found in the 3' portion of the enhancer (nt 26-48) which binds the tissue-specific transcription factor, hepatic nuclear factor-4 (HNF-4; Blanchard et al., 1992; Galson et al., 1992; Semenza and Wang 1992). HNF-4 consists of two direct repeats of a hexonucleotide putative thyroid-steroid hormone receptor superfamily binding site, (HNF-4), evidence suggests it may be involved in transducing a signal to the Epo promoter to amplify the hypoxic response (Galson et al., 1995; Zhang et al., 1999), allowing an increased rate of transcription as well as tissue specificity (its expression is limited to sites of renal cortex and liver Epo production; Goldberg et al., 1988). Mutation of any of the three sites ablated the hypoxic response

(Semenza and Wang 1992; Galson et al., 1995). Whilst the transcriptional response of the human Epo gene to hypoxia is mediated in part by the HNF-4 binding site, a minimal 24bp *cis*-acting enhancer element (nt 1-24) the hypoxia responsive element (HRE), located in the enhancer region, was shown to be essential and sufficient for transcriptional activation in response to hypoxia (Madan and Curtin, 1993; Pugh et al., 1994).

Maxwell et al. (1993) used transient transfection experiments, to show that the Epo 3' enhancer previously described, could produce similar oxygen related responses in a wide variety of cell types which do not express the erythropoietin gene and were not derived from tissues that make the hormone, e.g. lung, ovary and skin. Transcriptional activation, in response to hypoxia is mimicked by cobalt (Schuster et al., 1989) and desferrioxamine (Wang and Semenza 1993) and blocked by cyclohexamide and 2-aminopurine, implying new protein synthesis and phosphorylation was essential (Wang et al., 1995; Ratcliffe et al., 1997). However respiratory chain (mitochondrial) inhibitors, eg. cyanide, do not stimulate the hypoxic response suggesting that the sensing system is specific to hypoxia and not responsive to the metabolic consequences of interrupting mitochondrial electron transport (Maxwell et al., 1993). These and other results suggest that a similar oxygen sensing and signal transduction mechanism, identical to that controlling Epo expression, was widespread in mammalian cells (Maxwell et al., 1993; Pugh et al., 1994) and it could interact with sequences within the Epo 3' enhancer (Ratcliffe et al., 1997). It is likely that the system was operating on other genes in non-erythropoietin producing systems (Ratcliffe et al., 1997). The evidence strongly suggests that HIF-1 has an essential role in the modulation of other oxygen dependent genes. A number of other genes have been identified which show hypoxic inducibility similar to that seen by the Epo gene (Firth et al., 1994; Ratcliffe et al., 1997). These genes are found in pathways involved in angiogenesis, vascular endothelial growth factor, VEGF; increased glucose transport, glucose transporter-1, Glut-1; and anaerobic glycolysis, glycolytic enzymes. Detailed examination of their *cis*-acting control elements showed the presence of HREs containing HIF-1 binding site(s), suggesting that oxygen sensing, signal transduction and gene activation mechanisms very similar, if not identical, to

those present in Epo-producing cells must be widespread (figure 1.6; Firth et al., 1994). Studies by Wang et al., (1993) suggest that HIF-1 and its cognate recognition sequences are components of a universal mammalian cellular response to hypoxia.

Figure 1.6: Comparative sequence homology of HIF-1 binding sites in HREs from various hypoxia-inducible genes.

Gene	Species	HIF binding site
Erythropoetin	human	GCCCTACGTGCTGTCTCA
Erythropoietin	mouse	GCCCTACGTGCTGCCTCG
PFK-L	mouse	GGCGTACGTGCTGCAG
Aldolase A	human	CTCGGACGTGACTCGGAC
PGK-1	human	GTGAGACGTGCGGCTTCC
PGK-1	mouse	TTGTCACGTCCTGCACGA
Enolase 1	human	TGAGTGCGTGCGGGACTC
Enolase 1	human	GGAGTACGTGACGGAGCC
LDH-A	mouse	AGCGGACGTGCGGGAACC
Glut-1	mouse	CACAGGCGTGCCGTCTGA
VEGF	human	TGCATACGTGGGCTCCAA
VEGF	Rat	TGCATACGTGCTGCCTAG
iNOS	human	TGACTACGTGCTGCCTAG
Heme Oxygenase-1	mouse	AGCGGACGTGCTGGCGTG
Heme Oxygenase-1	mouse	AGAGGACGTGCCACGCCA

Vascular endothelial growth factor (VEGF): HIF-1 also targets angiogenic growth factors the most important being VEGF. VEGF is a secreted 34-43 kD dimeric glycoprotein, it is a potent inducer of angiogenesis *in vivo*. This is an adaptive process leading to increased blood capillary density and delivery of oxygen and nutrients to the tumour tissue and removal of waste products, thus promoting tumour progression (Shweiki et al., 1992; Berkman et al., 1993; Plate et al., 1993; Wenger and Gassman, 1997). Expression of VEGF mRNA was originally identified in cells surrounding expanding vasculature in a number of angiogenic processes, the highest expression was noted in tissues aquiring new capillary networks as well as adjacent to areas of necrosis (Shweiki et al., 1992; Brown et al., 1993a/b; Plate et al., 1993). VEGF mRNA and protein expression has been demonstrated in a variety of tumours *in situ*, by *in situ* hybridisation and immunohistochemistry, in accordance with the degree of hypoxia, eg. human gliomas (Plate et al., 1992; Samoto et al., 1995), neoplasms of the central nervous system (CNS; Berkman et al., 1993), kidney (Brown et al., 1993a; Takahashi et al., 1994), colon (Brown et al., 1993b), mammary fibroblasts (Hlatky et al., 1994) and ovary (Olson et al., 1994).

VEGF-binding activity has been seen on endothelial cells of both quiescent and proliferating blood vessels (Shweiki et al., 1992). When expressed, VEGF binds to and upregulates specific tyrosine kinase receptor proteins, *Flt-1* and *KDR*, whose mRNA has been shown to be upregulated in hypoxic endothelial cells *in situ* (Plate et al., 1992; Brown et al., 1993a/b; Brown et al., 1994). Increased expression of VEGF and its receptor, KDR, may correlate directly with the extent of neovascularisation and the degree of proliferation therefore may enhance tumour angiogenesis and may promote metastasis (Takahashi et al., 1995; Rofstad and Danielson, 1999). High levels of VEGF expression may be associated with bulky tumours and poor prognosis, if VEGF function was inhibited with a specific monoclonal antibody, then angiogenesis and vessel density was reduced and this in turn decreased tumour growth (Kim et al., 1993). The evidence suggests tumour angiogenesis may be regulated by paracrine mechanisms within hypoxic tumour regions (Hlatky et al., 1994).

In contrast to Epo, VEGF expression, was also induced by low glucose and inhibitors of oxidative phosphorylation (Shweiki et al., 1994; Levy et al., 1995). Evidence suggests that stimulation of VEGF may require the binding of *trans*-factors to co-operative *cis*-acting elements; AP-1 and SP-1, both redox sensitive transcription factors, which have binding sites within the VEGF promoter in close proximity to the HIF-1 binding site (Levy et al., 1995). A 35bp sequence has been identified as a hypoxia-inducible enhancer within VEGF (Levy et al., 1995; Liu et al., 1995). VEGF contains a critical HIF-1 binding site and a 5bp element (5'-CACAG-3'), also seen in the Epo enhancer in the same orientation and position to the HIF-1 site (Levy et al., 1995).

Hypoxia also stimulates the expression of other proteins involved in tissue perfusion, such as nitric oxide synthase (iNOS) (Reviewed in Semenza, 1996). iNOS contains a HIF-1 binding site in its 5'-flanking region, under low oxygen increased transcription of iNOS was responsible for the synthesis of the vasoactive mediator, nitric oxide (NO) (Reviewed in Semenza, 1996). NO itself can bind to the HIF-1 site of the VEGF promoter so regulating transcription (Kimura et al., 2000). Another example is heme oxygenase-1 (HO-1), HO-1 catalyses the synthesis of the vasoactive mediator carbon monoxide (CO) through increased transcription via a HIF-1 site in its 5'-flanking region (Review: Semenza, 1996). Carbon monoxide therefore inhibits the hypoxic induction of both Epo and VEGF (Goldberg et al., 1994).

Glucose transporter-1 (Glut-1) and the glycolytic enzymes: Oxygen is the final electron acceptor in respiratory redox reactions in mammalian cells, hence hypoxia provokes acute as well as long term physiological responses (Wang et al., 1995). Oxidative phosphorylation is the major metabolic pathway for ATP synthesis, an intracellular process that consumes oxygen in mammalian cell types. In situations of low oxygen tension there is an inhibition of mitochondrial respiration and cells switch from oxidative phosphorylation to obligate anaerobic glycolysis to generate ATP in an oxygen independent manner, thus genes encoding glucose transporter 1 (GLUT-1) and enzymes in the glycolytic pathway are upregulated (Pasteur Effect; figure 1.7; Stein et

al., 1995; Webster et al., 1990) thus allowing ATP synthesis to continue (Semenza, 1996). Glucose uptake *in vivo* has been demonstrated to be much higher in tumours than normal tissues, and correlates with tumour aggressiveness and prognosis (Dang and Semenza, 1999). The ATP yield is 18-fold lower in the glycolytic pathway compared to the oxidative Krebs pathway, the rate of glucose consumption must therefore increase, as must glucose transport for cellular adaption to hypoxia (Bunn and Poynton, 1996). Expression of glucose transporter-1 (Glut-1) mRNA was increased in response to hypoxia (Loike et al., 1992) in a HIF-1 dependent manner, similar to Epo (Ebert et al., 1996). Glut-1 was found in most cells, its expression was regulated by a variety of ligands thus its regulation depends on the cooperative interaction of a variety of *cis*-acting transcription factors (phorbol ester response elements, TRE; cAMP response element, CRE; serum response element, SRE; and HIF-1; see section 1.5) (Reviewed in Bunn and Poynton, 1996).

Figure 1.7; Transcriptional regulation of genes encoding glycolytic enzymes by HIF-1. (Firth et al., 1994, 1995; Semenza et al., 1996; Semenza et al., unpublished).

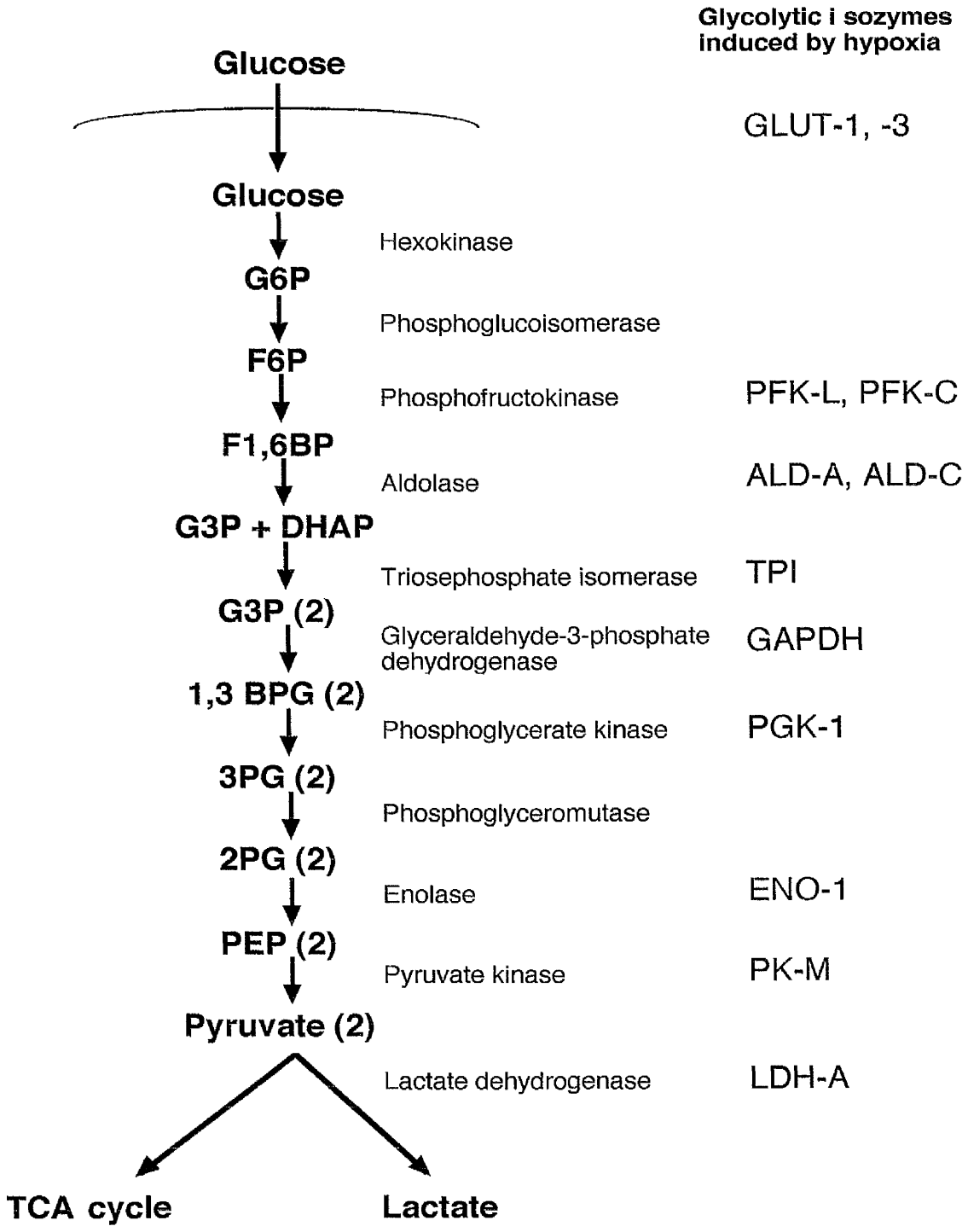

Similar cis-acting control sequences, containing HIF-1 binding sites, responsible for hypoxia-inducible expression, were identified in the 5' flanking sequences of PGK-1, LDH-A (Firth et el., 1994), aldolase A (ALDA), enolase 1 (ENO1) and phosphofructokinase L (PFKL; Semenza et al., 1994). All responded to cobalt, desferrioxamine, cyanide and cyclohexamide in a manner similar to Epo, VEGF and Glut-1 (Firth et al., 1994). An 18bp element was shown to be the crucial element in the PGK-1 enhancer and sufficient to confer hypoxic inducibility (Firth et al., 1994). Firth and colleagues (1994), demonstrated sequence homology between this 18bp PGK element and the 24bp Epo 3' enhancer (figure 1.6); the PGK-1 element has a 9bp region overlapped with 7 of the 8bp in the Epo enhancer except for a G-C substitution (Firth et al., 1994; Wang and Semenza, 1993). Three repeats of this single 18bp sequence was sufficient to confer hypoxic inducibility on a heterologous promotor (Firth et al., 1994). Semenza and colleagues (1994), showed that dimerisation of a 24bp sequence, containing a second domain similar to that of the Epo enhancer, also displayed hypoxic function.

Data suggests that HREs from these genes consist of at least one HIF-1 binding site, core sequence 5'-RCGTG-3', as well as possible additional cooperative transcription binding sites. The PGK, LDH-A and ENO1 promoters, contain functionally essential HIF-1 sites arranged as direct and inverted repeats separated by 4-10 bp (Semenza et al., 1996). Mutations within the core HIF-1 binding sites of these genes, not only eliminates HIF-1 binding but also transcriptional activation (Semenza et al., 1996). The VEGF, LDH-A and ADLA HREs contain a DNA sequence, similar to the Epo sequence 5'-CACAG-3', 4-6 nt 3' to the HIF-1 site, mutation of which results in a loss of HRE function (Semenza and Wang 1992; Firth et al., 1995). Co-operative *cis*-acting elements may be inducible by stimuli other than hypoxia and are likely to be required for maximal hypoxic induction, eg., CRE, AP-1, SRE, ChoRE (Semenza et al., 1996, 1997). Factors that recognise multiple sites within the HRE may function cooperatively either at the level of DNA binding or transactivation (Semenza et al., 1996). The evidence suggests that HIF-1 regulates the induction of glycolytic enzymes, in hypoxic cells, at the transcriptional level (Semenza et al., 1996).

Lactate dehydrogenase-A catalyses the interconversion of pyruvate and lactate. The LDH-A gene encodes the M-subunit of the enzyme, the isoform that is adapted for anaerobic function (Firth et al., 1995). Each LDH isoform (A,B,C) predominates in different regions (A in skeletal muscle and liver; B in the heart; and C in testes and spermatozoa) and is encoded by genes located on different chromosomes, all suggesting isoform-specific functions (Review: Jungmann et al., 1998). Increased expression of LDH under low oxygen tensions is specific to the LDH-A isoform (Ebert et al., 1996; Jungmann et al., 1998). Expression of LDH-A is also regulated at the transcriptional level by the protein kinase A (PKA) and C (PKC) pathways via the CRE and AP-1 *cis*-acting promoter elements respectively. Other elements identified in the LDH-A promoter region include two Sp-1 sites (involved in basal transcription level activity), a negative regulatory element (NRE) and two functional E-box sites implying LDH-A is transactivated by the oncoprotein, c-Myc (Review: Jungmann et al., 1998).

Mutational analysis of the LDH-A promoter in HeLa cells identified a 56bp region, as being necessary for hypoxic inducibility (Firth et al., 1995). Within this region, three domains were identified, each with distinct functionality, but all crucial for hypoxic regulation (Firth et al., 1995). One of these sites was a HIF-1 binding site, mutation of which completely abolished oxygen-regulated expression. The other two domains were located either side of the HIF-1 motif (Firth et al., 1995). Lying 5' to the HIF-1 site, Firth and colleagues (1995), defined a functionally critical 4bp domain at the same position (7 and 11bp 3' to the HIF-1 site, LDH-A in reverse orientation) of sequence homology, between the mouse LDH-A and mouse Epo enhancers (Firth et al., 1995). In LDH-A, but not Epo, this sequence is the conserved consensus E-Box, Myc/Max binding site (5'-CACGTG-3'; Anthony et al., 1992), also defined as a carbohydrate response element (ChoRE; Towle et al., 1995; Grandori et al., 1997). The E-box interacts with bHLH proteins, primarily c-Myc, which functions in cellular transformation, mitogenesis and is an inducer of apoptosis, suggesting a role in tumour progression (Amati et al., 1993; Jungmann et al., 1998). The oncogenic activity of c-Myc in rodent fibroblasts means they continually cycle, unable to exit the cell cycle, ultimately undergoing apoptosis (Evans et al., 1992; Amati et al., 1993). Myc is unable

to bind DNA directly, Myc either forms a heterodimer with its partner, Max, or alternatively Max-Max homodimers are formed via their leucine zipper regions, both of which bind to 5'-CACGTG-3' DNA sequences (Review: Amati et al., 1993). However, Max-Max homodimers are much weaker activators of transcription than Myc-Max heterodimers (Fisher et al., 1993).

The third domain was an 8bp region that lies 3' to the HIF-1 site and is characteristic of a cyclicAMP response element (CRE, 5'-TGACGTCA-3') (Roesler et al., 1988). The CRE is recognised by the CRE-binding protein (CREB). Forskolin, a cAMP analogue has been shown to modulate the cAMP system by interacting with the CREB via the protein kinase A (PKA) pathway (see 1.5.1) and has been shown to further upregulate LDH-A mRNA under hypoxic, but not normoxic conditions (Firth et al., 1995). Mutations of the CRE abolish cAMP-mediated induction and hypoxic function of LDH-A is reduced if either the CRE or E-box motifs are mutated (Firth et al., 1995). In contrast combination of the HIF-1 domain accompanied by either of the other two domains could convey inducible function (Firth et al., 1995). This and the fact that the HIF-1 site alone, even when multimerised, could not confer a hypoxic response, indicated that a cooperative interaction between factors binding at these sites was necessary for hypoxic function.

These hypoxically responsive genes are all functionally dissimilar but yet linked by what appears to be a common control system (Ratcliffe et al., 1997). There is cross-competition for binding of hypoxia-inducible factor(s) between these sequences, which is lost when the HIF-1 binding site is mutated (Firth et al., 1995). The cooperative HRE sites appear to convey little hypoxic inducibility alone but mutation abolishes or severly reduces function of the enhancers (Ratcliffe et al., 1997). However, synthetic enhancers containing multimers of the respective HIF-1 binding sites alone retain enhancer inducibility (Semenza and Wang, 1992; Pugh et al., 1994; Firth et al., 1995). LDH-A seems to have a broader range of inducing stimuli, this phenomena is apparent to a greater extent in the Glut-1 enhancer. As shown in figure 1.8, different *cis*-acting elements, within the HRE of Glut-1, responded to different stimuli; The HIF-1 site

mediated the hypoxic response, a serum response element (SRE) was sensitive to mitochondrial inhibitors, CRE to PKA agonists and may involve the co-activators p300/CBP, and the AP-1 site was involved in the protein kinase C (PKC) pathway (Ebert et al., 1995). This evidence suggests that other pathways may be stimulated in combination with hypoxia to obtain a super-induction of the HRE thus producing a synergistic response.

Figure 1.8: Regulation of the GLUT-1 enhancer, pG[1-610]α_1, by various stimuli, either in combination with or without hypoxia (1% O_2) in the human breast adenocarcinoma cell line MDA 468.

(Taken from Patterson 1998)

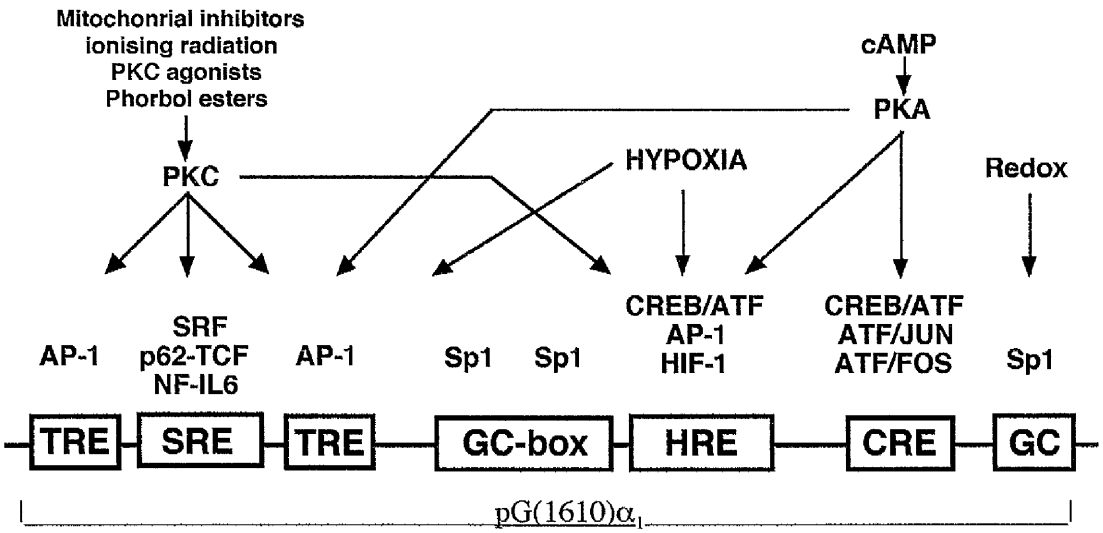

1.5 Combination Therapy

1.5.1 Cyclic AMP

cAMP is present in all cells and tissues, from bacteria to humans (Robinson, 1973). It is a mediator of hormonal signals, being involved in processes such as glycogen metabolism, regulation of glycolysis, amino acid breakdown, and regulation of gene expression to name just a few (Sporn et al., 1994). The primary mediator of cAMP action in eukaryotic cells is cAMP-dependent protein kinase (PKA; Kuo et al., 1969; Krebs et al., 1983). All the actions of cAMP that are implicated in a variety of cellular functions are related to protein phophorylation of CREB, prior to DNA binding, through the activation of PKA (Nichols et al., 1992; Rohlff et al., 1995).

PKA is composed of two genetically distinct catalytic (C) and regulatory (R) subunits; two C subunits bound to a R subunit dimer (C_2R_2; Rohlff et al., 1995). The PKA holoenzyme is enzymatically inactive in the absence of cAMP, activation occurs at cAMP concentrations of 10^{-8} to 10^{-6}M (Adams et al., 1991). As shown in figure 1.9, the activating ligand, cAMP, binds to the R subunit, inducing conformational changes and dissociates the holoenzyme R_2C_2 into an R_2 $(cAMP)_4$ dimer and two free C subunits that are catalytically active (Bramson et al., 1983; Beebe et al., 1986). The C subunit translocates to the nucleus and appears to be essential for the induction of cAMP-regulated genes (Roesler et al., 1988). An induction in CRE gene transcription is thought to result from changes in the ratio of type I to type II PKA holoenzymes, rather than a change in the level of the catalytic subunit. PKA stimulates the transcription of multiple genes containing CREs via phosphorylation of serine-133 residue of CREB.

Figure 1.9: Mode of action of protein kinase A (PKA)

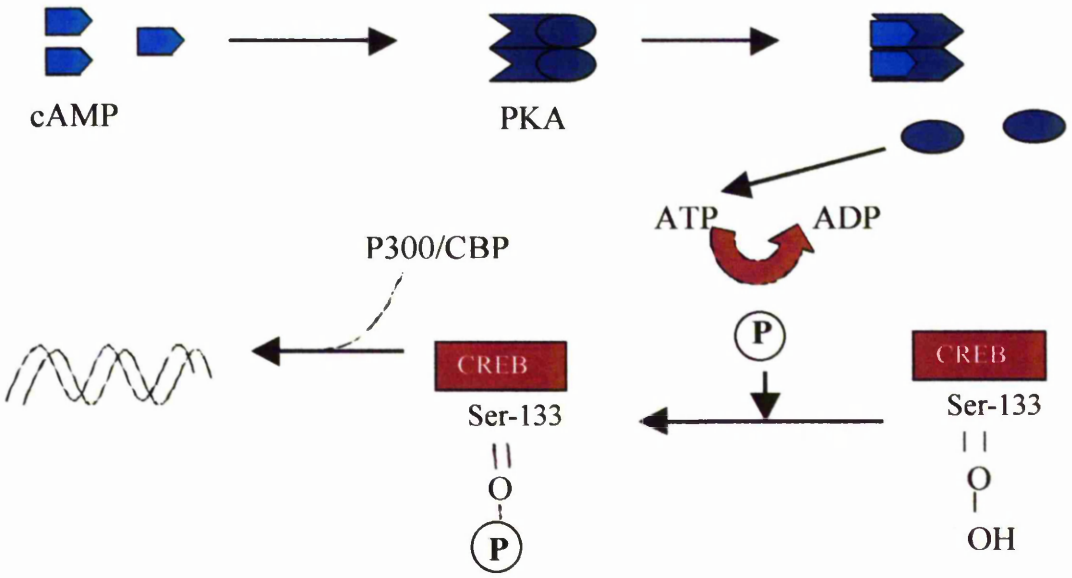

There are two isoforms of PKA, type I and II, which contain distinct R subunits, RI and RII respectively, that interact with common C subunits, Cα, Cβ, and Cγ (Beebe et al., 1986). The two PKA isoforms have different affinities for cAMP and different turnover rates indicating functional differences between type I and type II PKA isoforms (Cadd et al., 1990). This may relate to transient versus sustained responses, respectively, to hormones and other modulators of enzymatic activity (Weber, 1986). Expression of type II PKA predominates in normal cells, in malignant, non-dividing cells, type II is down-regulated and type I PKA is over-expressed. The functional balance can be restored by addition of cAMP analogues such as 8-cl-cAMP which down-regulates type I and upregulates type II (Cho-Chung, 1990).

The CRE recognition site shows sequence homology with the core 8bp HIF-1 binding site (figure 1.10). The HIF-1 site has been shown to be responsive to cAMP analogues (8-cl-cAMP, forslokin) under hypoxic but not normoxic conditions in a dose dependent manner (Kvietikova, et al., 1995). Results by Kvietikova et al. (1995) suggest

that oxygen-dependent gene expression is enhanced by the PKA pathway, mediated via the HRE. They demonstrated that a CREB and ATF-1 efficiently competed for binding of a HIF-1 probe either as homo- or heterodimers in hypoxic nuclear extracts. However, this competition for binding did not affect HIF-1 activity. A luciferase plasmid containing three copies of an PGK18bp HIF-1 oligonucleotide was transiently transfected into HeLa cells and incubated under normoxia and hypoxia in combination with the cAMP analogue, 8Br-cAMP. A 6.3-fold increase in luciferase expression was seen under hypoxia alone, however, the combination of hypoxia and 8Br-cAMP produced a further 64% increase in luciferase expression. This data suggests that HIF-1 is cAMP responsive through the activation of the protein kinase A (PKA) pathway (Kvietikova et al., 1995). This indicates cAMP is not a crucial element of the hypoxia signal transduction pathway and its effects may be mediated by the HRE itself, thus HREs other than those which contain the CRE site may be responsive to cAMP stimulation.

Figure 1.10: Consensus HIF-1 and CRE DNA binding sites.

HIF-1	(G/A)CGT(C/G)C
CRE	TGACGTCA
Human PGK	AGACGTGC
Mouse PGK	TCACGTCC
Mouse LDH-A	GGACGTGC
Mouse Glut-1	AGGCGTGC

1.5.2 Radiation

The Glut-1 enhancer was shown to be responsive to a number of stimuli including ionising radiation. Evidence suggests that it may be possible to combine the gene therapy techniques described with ionising radiation to provide "genetic radiotherapy".

In a variety of cell types, the early response genes c-Jun, c-Fos and Egr-1 are transcriptionally activated in response to ionising radiation, the products of these genes are important in the adaption of cells to radiation-induced stress (Weichselbaum et al., 1994). It is thought that c-fos and Egr-1 are involved in normal development, they have similar patterns of expression and are often co-regulated *in vivo*, therefore may share cis-acting 5' regulatory elements however, they are structurally unrelated (Sukhatme 1991). c-fos and Egr-1 are activated in a range of cell types (fibroblast, epithelial, lymphocyte) during cardiac and neural cell differentiation (Tsai-Morris et al., 1988) and by mutagens and changes in intracellular redox levels. Egr-1 is a nuclear intermediatary in signal transduction and initiates a cascade leading to increased DNA sythesis and cellular proliferation (Joannidid 1997) mediated by serum response elements (SRE); regulatory elements found in many growth factor regulated promoters that directs the rapid induction of gene expression (Treismann 1990).

The Egr-1 gene encodes a phosphoprotein with a zinc finger motif and binds to a single, high affinity Egr-1 binding site (EBS), 5'-CGCCCCCGC-3' (Christy et al., 1989; Weichselbaum et al., 1994) through which it is thought to have a suppressive effect on tumour cell growth in a variety of human tumour cell lines (fibroblast, epithelial, lymphocyte; Huang et al., 1995). Transcriptional activation of Egr-1 by ionising radiation is a direct consequence of the production of reactive oxygen intermediates (ROI; Datta et al., 1993) which activates early response genes (including Egr-1), possibly via the PKC pathway, initiating a cascade of cytoplasmic signalling events, providing an adaptive response to radiation-induced damage (Hallanhan et al., 1991). As shown in fiure 1.11, the Egr-1 upstream region contains 5 domains of 10 nucleotides,

which form the inner core of the serum response elements (SREs) $CC(A/T)_6GG$, referred to as CArG boxes, which bind the serum response factor (SRF). The ability of ionising radiation, and serum, to induce Egr-1 transcription is mediated through the five CArG domains (Datta et al., 1992), both the PKC and PKA pathways converge on this element (Sukhatme 1990). The presence of multiple CArG elements may account for the 5-10 fold greater serum induction of Egr-1 compared to c-fos, which has a SRE of 22 nucleotides which displays dyad symmetry (Tsai-Morris et al., 1988; Sukhatme 1990). Also identified within the Egr-1 promoter were 4 SP-1, 2 AP-1, and 2 CRE sequences, bound by the transcription factors SP-1, fos/jun heterodimers, and CREB respectively suggesting that Egr-1 gene expression is also modulated by a number of other ligand receptors interactions (Tsai-Morris et al., 1988; Sakamoto et al., 1991).

Figure 1.11: Diagramatic representation of the the Egr-1 promoter (-935 to –65bp) showing co-operative *cis*-acting elements.

(Adapted from Yan et al., 1999)

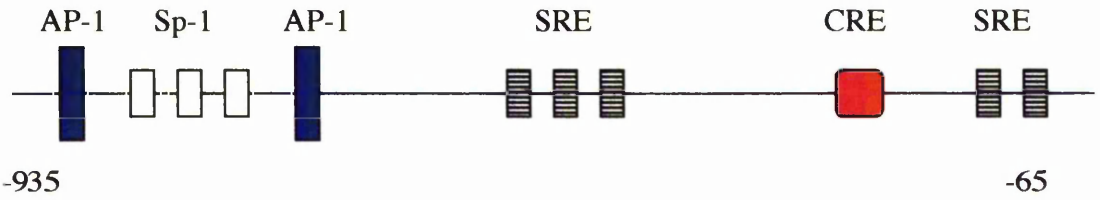

Manome et al. (1998), used an adenoviral vector to deliver the radiation inducible Egr-1 promoter driving the b-galactosidase reporter gene in glioma cells. As little as 2Gy was sufficient to demonstrate Egr-1 induction, evidenced by up to a 3-fold increase in b-galactosidase expression in 9L rat glioma cells *in vitro*. In a separate study, a vector containing a 425bp radiation inducible sequences from the Egr-1 gene (containing the five CArG elements), driving the cDNA for TNFα (Egr-TNF named pE425-TNF; Weichselbaum et al., 1994) was delivered, using an adenoviral vector or liposomes, to either a human prostate cancer PC3 xenograft or the murine fibrosarcoma

cell line, P4L, respectively, followed by exposure to radiation. The cytokine, TNF-α, is directly toxic to some tumour cells and can potentiate the cytotoxic effects of radiation *in vivo*. In both studies, the combination of the two strategies produced a marked reduction in tumour growth (Seung et al., 1995; Chung et al., 1997).

Egr-1 gene activation in the perfused rat kidney came during reperfusion after periods of ischeamia, it is unclear whether activation of immediate early genes (IEG) is a result of hypoxia or reperfusion (Bonventre et al., 1991). Hypoxia causes increased expression of the tissue factor gene mediated by activation of the transcription factor Egr-1 (Yan, 1998) and an increase in the DNA-binding activity of the Egr-1 protein (Bae et al., 1999). Signalling pathways activated by serum (PKC-independent) target the SRF-SRE binary complex. PKC-dependent pathways necessitate Elk-1 and SRF forming a ternary complex. The SRF binds to the SRE, whilst the C-terminal domain of Elk-1, a ternary complex factor, is phosphoryated at low oxygen tensions, by mitogen-activated protein kinases (MAPK) and Raf-1 kinase, prior to DNA binding. The N-terminal region mediates DNA contact and ternary formation leading to a conformational change and increased transcription (Hipskind et al., 1994; Muller et al., 1997). This suggests a dual function of the ternary complex that may allow the activation of two sets of genes (Janknecht et al., 1993). The Elk-1 ternary complex is hypoxically responsive. Yan et al. (1999), localised the region responsible for hypoxia-induced expression to the EBS-SRE-EBS (Elk-1 binding sites) and SRE-EBS-SRE elements, the former of which are critical for gene expression under hypoxia.

1.5.2.1 Egr-1 and hypoxia

In the Glut-1 enhancer a SRE cooperates with HIF-1 binding sequences (Ebert et al., 1995). Muller et al. (1997), suggested that the SRF and/or ternary complex factor, Elk-1 may be able to cooperate with HIF-1 to activate hypoxia inducible genes. In a more recent study by Saunders et al. (2000), a pentimer of the 24bp Epo HRE was inserted into the Egr-TNF vector (pE425-TNF) 5' to the Egr-1 gene (Epo-Egr-TNF). Therefore, transcription of TNF-α was modulated by both hypoxia and ionising radiation. When this construct was transiently transfected into the HCT116 human colon carcinoma cell line and exposed to both stimuli a 10-fold increase in TNF-α activity was seen compared to a 3-fold increase with either hypoxia or radiation alone (figure 1.12).

Figure 1.12: TNFα activity after transient transfection of the Epo-Egr-TNFα vector and treatment with hypoxia and radiation in combination and alone (TNFa : pg / million cells; error bars = sd).

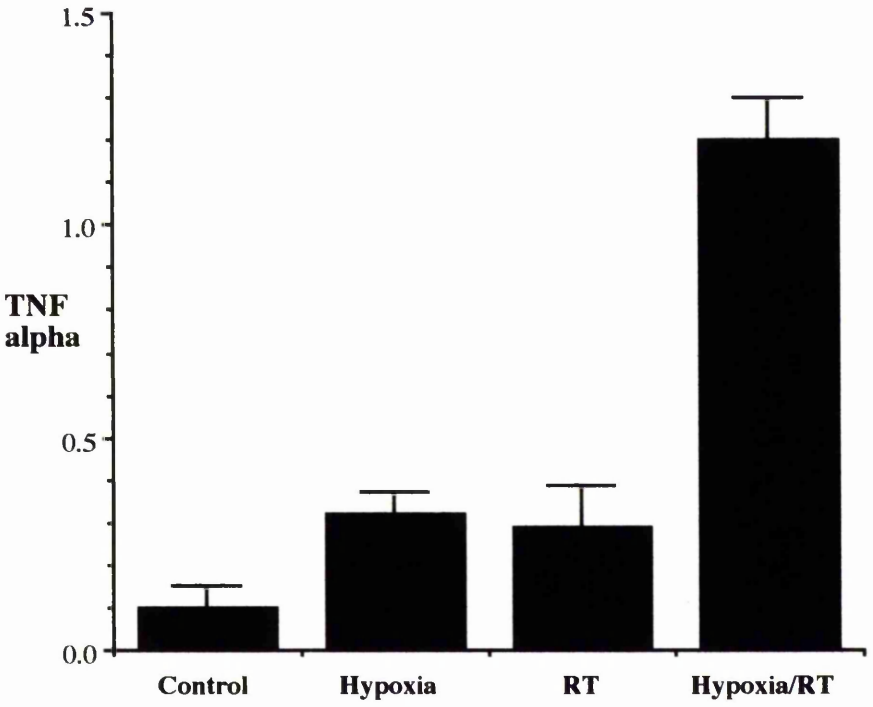

It is known that both the PKC and PKA pathways can converge on the CArG element (Sukhatme 1990) and that CREB competes with HIF-1 for binding of the HIF-1 site. The synergistic response produced by both hypoxia and radiation may be via the co-operative binding of HIF-1 and the SRF to their corresponding sites, not only by hypoxia responsive pathways but maybe also via PKC and PKA signalling. Similar co-operative interactions have previously been demonstrated between the *cis*-acting elements of the LDH-A and Glut-1 enhancer sequences.

1.6 Aims of this Study

During the course of this work several attempts have been made by other investigators to 'optimise' synthetic hypoxia responsive elements (HREs) for use in therapeutic vectors. However in each case copy, number, orientation and spacing have not always remained constant between the HREs tested and evaluation has been limited to only a single cell line. The effect of reduced oxygen tensions on hypoxia responsive genes varies among cell types, hence it is important that the HRE sequences tested are optimised in a panel of human carcinoma cell lines.

The overall aim of this work was to find the HRE with the most robust hypoxic (1% oxygen) and anoxic (less than 0.002% oxygen) response across a panel of human carcinoma cell lines, producing targeted gene expression that confers both low basal expression under normoxia and a high level of activated expression under hypoxia and anoxia. This will allow the unambigous optimisation of the context and functional amplitude of HREs, which can be exploited using gene therapy strategies in the treatment of oxygen deprived tumours.

Evidence indicates that the HIF-1 site may require the interaction of other cis-acting elements to function optimally. A number co-operative elements have been identified (CRE, SRE, AP-1, ChoRE) located in close proximity to the HIF-1 site in certain enhancers which can be activated by stimuli other than hypoxia, e.g. cAMP and ionising radiation. This suggested that the HIF-1 site, although absolutely necessary may not be sufficient for optimal inducible activity in response to low oxygen levels. Through the combination of specific transcriptional target sites it is possible to integrate the responses of a number of pathways, e.g. LDH-A contains a HIF-1 site and a CRE (activated by hypoxia and PKA agonists); Glut-1 has numerous cis-acting elements inducible by hypoxia (HIF-1) cAMP (CRE) and ionising radiation (SRE). A further purpose of this thesis was to investigate the integration of the hypoxia and cAMP signalling pathways on each of the HREs (PGK, Epo, LDH-A, VEGF, Glut-1) in an attempt to amplify their response to reduced oxygen. Finally it has been demonstrated

previously in our laboratory that it is possible to produce a dual radiation and hypoxia responsive promoter (Epo.Egr-1) allowing the development of 'targeted radiotherapy'. This work aimed at expanding initial observations to a wider panel of cell lines and combining the radiation responsive gene with the optimal HRE as identified in this work.

Specific Objectives

- Determination of optimal experimental parameters pertaining to all work in this thesis (chapter 3).
- Optimisation of previously identified HREs across a human carcinoma cell line panel (chapter 4).
- Dissection of the functional elements of the LDH-A HRE to determine their importance in the transcriptional response to reduced oxygen tensions (chapter 5).
- Integration of the hypoxia and cAMP response pathways in a attempt to obtain a super-induction of the HREs under hypoxic conditions (chapter 6).
- Further analysis of the functionality of the Epo.Egr-1, hypoxia and radiation responsive promoter in a broader cell line panel (chapter 7).

Chapter 2

Materials and Methods

2.1 General Techniques

All cell culture work was performed in category II laminar flow hoods. Standard laboratory clothing was worn at all times when handling cell lines, DNA, bacteria and all reagents. Solutions required were prepared using millipore grade water and sterilised by autoclaving (121°C /15 p.s.i. / 20 min) or filtering using Nalgene disposable filters (0.2μm). All centrifugation steps were carried out at 10000g unless otherwise stated. All waste was soaked in chloros for 24 hours prior to disposal. Glassware was soaked in lipsol (LIP) overnight, rinsed in distilled water and sterilised in a drying over (160°C) for 6-12 hours before use.

2.1.1 Cell Culture

The human head and neck carcinoma cells lines (SQ20B and SQD9) were kindly donated by Conchita Vens, The Netherlands Cancer Institute and the Ka13.5 chinese hampster ovary, HIF-1a deficient cell line by Professor Peter Ratcliffe. All cell lines were maintained in 1X Dulbeccos Modification of Eagles Media (DMEM), supplemented with 2mM glutamine and 10% foetal calf serum. All media was purchased, already reconstituted, in a 10X DMEM form (Gibco BRL). Cells were subcultured in antibiotic-free media and routinely screened for mycoplasma (Mycotect Kit (Gibco BRL)).

Established cell lines were grown as monolayers in γ-irradiated, vented, tissue culture grade flasks and plates supplied by Nunc and Falcon respectively. All cells were

routinely passaged every three to four days. To subculture, cell monolayers were washed twice with phosphate buffered saline (PBS), then 5ml trypsin / EDTA (TE) was added and the culture vessel was incubated at 37°C for approximately 5 minutes (depending on cell line). The TE caused disruption of cell surface adhesion proteins leading to cell detachment. The cells were decanted into a sterile, plastic *bijou* vessel containing 20ml of pre-warmed culture media to inactivate the trypsin. Cells were then reseeded by splitting either one in three or one in six, depending on the cell line, into 75 or 175cm^2 tissue culture flasks and placed in a 37°C humidified air / 5% CO_2 incubator.

Samples of cells were frozen down to produce stocks for later work thus allowing identical or similar passages to be used for related experiments. Cells were harvested and a cell pellet produced. The pellet was resuspended in 10% DMSO (dimethyl sulphoxide, Sigma chemical company Ltd) and culture media containing 15% FCS. 1ml aliquots were pipetted into sterile cryotubes (Nalgene), and placed into a freezing tub containing isopropanol (cryotub™). The isopropanol ensures that the temprature change was 1°C / min preventing the formation of ice crystals during freezing. Similarly cells were thawed rapidly to prevent damage by transiently formed ice crystals. Cryotubes (Nunc) were incubated in a 37°C waterbath for 1 to 2 minutes. Before decanting the contents into a 75cm^2 flask containing equilibriated media, the cryotubes were sterilised by wiping with 70% ethanol. The media in the flask was replaced after 24 hours to remove traces of DMSO.

All anoxic work was carried out in an anoxic cabinet, which contained an internal 37°C incubator for cell culture work. Within this unit there were two palladium catalysts, two silica gel, and two activated charcoal containers. One set of each were reactivated, every second day, by heating to 160°C overnight, and returned to the cabinet to cool. This catalyst-induced anoxia was expected to be below 0.002% O_2. For hypoxic work, cells were exposed to pre-humidified 1% O_2. 24 well tissue culture plates were placed in airtight containers and flushed with 1% O_2, 5% carbon dioxide and balance nitrogen (BOC) in a 37°C incubator.

Table 2.1: Description of human carcinoma cell lines used in this thesis.

Cell Line	Tissue Type	Growth Media	Morphology	Karyotype
A549	Lung	DMEM	Epithelial	2n=46
CNS-1	Glioblastoma	DMEM	Epithelial	2n=46
DU145	Prostate	DMEM	Epithelial	2n=46
HCT116	Colon	DMEM	Epithelial	2n=46
HT1080	Fibrosarcoma	DMEM	Epithelial	2n=46
MDA 468	Breast	DMEM	Epithelial	2n=46
*SQ20B	Head and neck sarcoma	DMEM	Epithelial	
SQD9	Head and neck sarcoma	DMEM	Epithelial	2n=46
T47D	Breast	DMEM	Epithelial	2n=46
WiDr	Colon	DMEM	Epithelial	2n=46

*This cell line consisted of two cell populations, diploid and tetraploid. The SQD9 cell line contains only the diploid population.

2.1.2 Cell Counts

Cell counts were performed using an Improved Neuberger Haemocytometer. Cells were harvested and centrifuged to produce a cell pellet. The supernatent was discarded and the cell pellet was resuspended in 1ml of culture media. A coverslip was pressed onto the haemocytometer slide until Newton's rings were visible. 10µl of the cell suspension were pipetted onto the haemocytometer and viewed under the microscope. The number of cells in the 16 square (4x4) grid were counted, each square

has a total volume of 0.1mm^3 (10^{-4}cm^3), hence the cell concentration per ml equalled the cell count x 10^4. After use the haemocytometer was cleaned and stored in 70% ethanol.

2.1.3 Irradiation

Cells were irradiated in 24 well tissue culture plates (Falcon) using a 250 kV orthovoltage tube at a dose of 5Gy, administered over a period of 6.8 minutes, at an ambient temperature of 37°C.

2.2 DNA Handling

2.2.1 Digestion of DNA with Restriction Endonucleases

Type II restriction endonucleases (RE, New England Biolabs) were used to cut DNA at specific recognition sequences, either to linearise plasmid DNA or to generate defined fragments for quantification or ligation reactions. The RE's were stored in glycerol; hence the total volume of RE never exceeded one tenth of the digestion reaction. Plasmid DNA was routinely digested for 16 hours in a 37°C waterbath with 1:10 of 10X manufacturers recommended buffer, 1:100 100X bovine serum albumin (BSA; if required for RE being used), and 1 - 2µl (as recommended by manufacturer) RE. This was made up to a final volume with sterile, distilled water. RE's were inactivated by heating to 65°C for 20 minutes or by ethanol precipitation of the DNA. An aliquot of the digested DNA was electrophoresed against undigested DNA and an appropriate DNA double-strand (ds) ladder on an agarose gel to ensure the digest was complete. If the DNA had been cleaved at the correct points discrete bands of DNA fragments equivalent to the number of restriction sites were seen on the gel at corresponding points according to their known ds-base-pair markers.

2.2.2 Agarose Gel Electrophoresis

Agarose gel electrophoresis was used for the sizing and separation of DNA fragments produced by the action of restriction endonucleases. Gels were made by heating standard electrophoresis grade agarose (Gibco BRL) in 1 X Tris-EDTA (TAE) buffer. After cooling to 50°C, 0.5µg/ml ethidium bromide (EtBr) was added, and the melted agarose was cast into a horizontal tray. Once set, the gel was submerged in 1 X TAE buffer in a flatbed apparatus (Pharmacia). 1:6 of 6x gel loading buffer (New England Biolabs) was added to the DNA samples prior to loading into individual wells. Samples were run alongside an appropriate ds-DNA marker to allow calibration of unknown fragments (100bp, 1kb, or Lambda Hind III from NEB) according to their known ds-base-pair markers, at an optimum voltage of 5V / cm / gel length. At higher voltage, larger molecules moved proportionately faster than smaller molecules, thus better resolution was seen at lower voltages. EtBr dye binds to the DNA fragments by intercalating between the bases, and fluoresces in the visible red-orange range when stimulated by UV light. The position of the DNA fragments on the gel were visualised using an UV transilluminator. A permanent record of all gels were obtained by photographing the gel using a polaroid camera and film.

2.2.3 Extraction and Elution of DNA Fragments from Agarose Gels

DNA of 70bp to 5kb was extracted from standard agarose gels in 1 x TAE buffer using the QIAquick II kit (Qiagen). The procedure was as described below.

The DNA band was excised from the gel and placed into a pre-weighed tube and re-weighed. The gel was dissolved in three volumes of solubilisation and binding buffer (QG) e.g. 300μl buffer QG to every 100mg gel, by incubating in a 50°C waterbath for 10 minutes. The buffer contained a pH indicator as DNA adsorption is only efficient at ≤pH7.5, if the indicator changed from yellow to an orange or violet colour, then 10μl of sodium acetate (NaAc), pH 5 was added and the solution gently mixed. One gel volume

of isopropanol was added to the solution to increase the yield of DNA and mixed. After pipetting into a QIAquick spin column, the sample was microcentrifuged for 1 minute. The DNA bound to the column and the flow-through was discarded. A further volume of buffer QG was added to remove residual agarose. After centrifugation, 0.5ml buffer PE, containing ethanol, was added to the column to remove any remaining salts. The QIAquick spin column was placed in a clean, 1.5ml microcentrifuge tube and the DNA was eluted by adding 50μl of low salt elution buffer (10mM Tris.Cl, pH 8.5) or water to the centre of the column. The column was left to stand for 1 minute to increase the DNA concentration eluted and then centrifuged for 1 minute. The average eluate was 48μl from 50μl elution buffer volume. A 2 to 5 µl aliquot was electrophoresed on an agarose gel to ensure the presence of DNA in the sample. The DNA was stored at -20°C to prevent degradation.

2.2.4 Ligation of DNA

The same procedure for ligation was carried out in all cases. All HRE constructs used in this thesis were inserted into the luciferase pGL3.promoter / basic vectors supplied by Promega (figure 2.1) for details of the restriction sites each HRE was inserted see individual chapters. Using REs the vector (V; pGL3.promoter or pGL3.basic) was linearised and the insert (I; a HRE derived from an oxygen-regulated gene) was either cleaved from its original plasmid or an oligonucleotide (oligo) was constructed (Sigma Genosys) with BamHI/BglII ends, to produce compatible cohesive ends. The DNA was run on an appropriate density agarose gel to ensure complete cleavage of restriction sites had occurred; Fragments smaller than 1kb were run on a 2.5% gel against a 100bp marker, those over 1kb were isolated on a 0.8% gel against a 1kb marker. The DNA fragments were then isolated from the gel and cleaned. To determine the concentration of each DNA sample a known aliquot (usually 1µl) of each was electrophoresed against 1µl of the λ Hind III molecular weight marker. By comparing their relative intensities under UV light, an approximation of the relative amounts of V and I were derived. Whilst keeping the vector concentration constant,

ligation reactions were set up at varying vector:insert (V:I) ratios. 1µl of T4 DNA ligase and 10% 10X ligase buffer were added to each ligation reaction and made up to a final concentration with sterile distilled water. The mixture was incubated in a 16°C waterbath for 12-16 hours.

Figure 2.1: Structure of pGL3.promoter plasmid supplied by Promega.

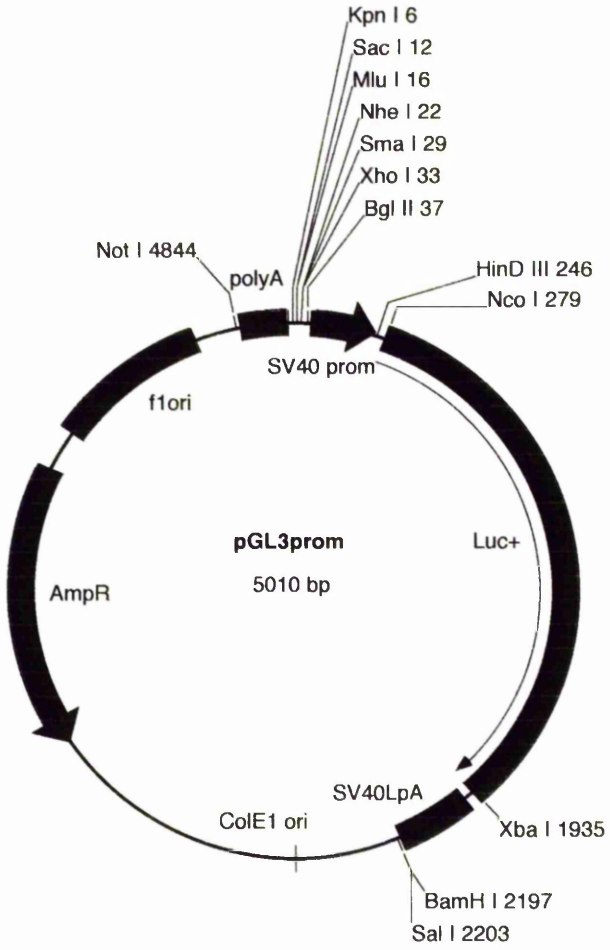

2.3 Transformation of Competent Bacteria

Transformation occurs when circular plasmid DNA was inserted into competent cells allowing large quantities of plasmid DNA to be obtained. The DNA plasmid must contain an origin of replication and an antibiotic resistance gene to yield a transformed colony capable of growing on a selective media. The bacterial cells used in these experiments were *E. coli* DH5a. DH5-a are a recombiation deficient strain used for plating and growth of plasmids and cosmids. They contain the *recA1* mutation, reducing the frequency of homologous recombination that might rearrange the structure of cloned DNA inserts and the *deoR* mutation facilitates the uptake of large DNA fragments.

Preparation of Competent Bacteria.

L broth (LB) plates were streaked with *E. coli* strain DH5-α to obtain a stock of single colonies and incubated at 37°C for 16 hours, usually overnight. 24 hours prior to competent cell preparation, 2ml of LB broth was inoculated with a single *E. coli* strain DH5-α colony from an agar plate using a sterile inoculating loop. The tube was capped and incubated in a shaker at 250rpm / 37°C overnight. 500ml LB medium was inoculated with the overnight culture and grown until it reached an OD_{600} of between 0.25 and 0.4. Bacterial cells were transferred to two sterile 500ml polypropylene bottles and incubated on ice for 5 minutes. Cells were gently resuspended in 40ml ice-cold calcium / glycerol (Ca/Gly) buffer by repeated pipetting. The last two steps were repeated, then the cell suspension was incubated in Ca/Gly buffer on ice for 30 minutes. Cells were pelleted by centrifugation in a Sorval GSA at 6000g for five minutes, at 4°C. The supernatant was discarded and the pellet resuspended in 6ml Ca/Gly buffer. 24 x 0.5ml aliquots of competent cells were dispensed into individual microcentrifuge or Nunc tubes prechilled on powdered dry ice. Aliquots were stored at -80°C until required for transformation. Cells were stable for several months.

Procedure for Transformation

An aliquot of competent cells was thawed slowly on ice. Approximately 20-250ng of the plasmid vector, or a ligation reaction, to be transformed, was placed into a sterile

tube (Falcon, 15ml). 100μl of thawed, competent DH5a cells were pipetted into each tube. When transforming a modified plasmid a minimum of four controls were set up in parallel:

- Original, uncut vector
- Linearised vector, plus ligase
- Linearised vector, minus ligase
- Insert only

Each of the tubes were incubated on ice for 10-20 minutes, mixing every 4-5 minutes. Cells were heat shocked at 42°C for exactly 45 seconds; this increased the transformation efficiency. Timing was important as prolonged exposure to heat in calcium/glycerol buffer kills competent cells. The reaction tubes were returned to ice for 2 minutes. 900µl of 37°C SOC buffer (Gibco BRL) was aliquoted into each tube; they were then shaken at 37°C, 250rpm, for 45-60 minutes. During this time competent cells recover and transformed cells express the antibiotic resistance gene needed to replicate on selective plates. Using a sterile glass spreader, 100μl of each sample was spread onto the surface of separate LB agar plates supplemented with the antibiotic, ampicllin (100µg/ml). The spreader was sterilised between samples by immersion in 95% ethanol, flaming and cooling for 30-60 seconds. Plates were incubated facing up for several minutes while inoculum of cells was completely absorbed into the agar, then inverted, so that the agar faced down, and incubated at 37°C in the plate incubator for 16 hours.

Materials

LB media: 500ml distilled water, plus 10g LB broth powder. Autoclaved at 121°C for 15 minutes or filter sterilised.

LB agar plates: 500ml distilled water, 10g LB broth powder, and 7.5g agar noble. Autoclaved at 121°C for 15 minutes. The agar was microwaved to liquefy and left to cool in a 55°C waterbath. Where required (for transformation of ligation reactions) ampicillin (100μg/ml) was added to 500ml agar when the temperature was below 55°C. 20ml of LB agar was poured into 10cm plates in laminar flow hoods to exclude other micro-organisms and left to set with lids half removed. Once set the lids were replaced

and the plates transferred to a 37°C incubator to remove excess moisture. Plates were stored at 4°C until required (max. 10-days).

Calcium/glycerol buffer: Combine 100ml 0.6M $CaCl_2$

20ml 0.5M Pipes pH 7.0

150ml glycerol

730ml water

Sterilise by autoclaving or filtering.

2.4 Preparation of Plasmid DNA

2.4.1 Small Scale: Mini-Prep

The QIAprep miniprep kit (QIAGEN) was used for high through-put purification of up to 20μg of plasmid DNA. It is based on alkaline lysis of the *E. coli*, followed by adsorption of the DNA onto a silica-gel resin in high salt concentrations. A single transformed *E. coli* colony was shaken in 5ml of LB, containing antibiotic selection, at 37°C for 14 to 16 hours. 4ml of this culture was used in the mini-prep protocol. The remaining 1ml was mixed with 1ml of 100% sterile glycerol (Gibco BRL), 1ml of this mixture was snap frozen in Nunc cryotubes. Those minis containing the pGL3.promoter plus Insert ligated in the correct (desired) manner, were stored at -80°C. The plasmid DNA was removed from the *E. coli* host by alkaline-SDS lysis followed by adsorption of DNA onto a silica-gel resin in the presence of a high salt concentration. The larger chromosomal DNA, with the lysed debris, was cleared by centrifugation. Incubation with RNase A, digested contaminating *E. coli* RNA. The plasmid DNA was purified from proteins by SS-phenol/chloroform extraction and concentrated by ethanol precipitation.

Procedure

The bacterial culture was centrifuged to pellet the bacterial cells. The supernatent was discarded. The pellet was resuspended in 250μl buffer P1 containing RNaseA and pipetted into a 1.5ml eppendorf tube. The bacteria were lysed by addition of 250µl of alkaline-SDS lysis buffer (P2). The tubes were incubated at room temperature for 5 minutes. 350μl of buffer N3 was added and mixed by inverting 4 to 6 times to stop the lysis reaction and prevent shearing of the DNA. The sample was centrifuged for 10 minutes to remove cell debris and unwanted chromosomal DNA. Buffer N3 has a high salt concentration to allow optimum adsorption to the silica-gel column. The supernatent was decanted into a QIAprep spin column and microcentrifuged at full speed for 30 to 60 seconds. The DNA bound to the resin and the flow through was discarded. The column was washed by adding 500µl of buffer PB and centrifuging for 30-60 seconds the flow through was discarded. The QIAprep spin column was washed again by addition of 750µl of buffer PE and centrifuging for 30-60 seconds. The flow through was discarded and the column was centrifuged for a further minute at full speed to remove residual wash buffer. The DNA was eluted into a clean, 1.5ml microcentrifuge tube by applying 50μl of buffer EB (10mM Tris.Cl, pH 8.5) or sterile distilled water to the centre of the QIAprep column. It was left to stand for 1 minute and then centrifuged for 1 minute at full speed. The eluate was collected in a sterile 1.5ml eppendorf tube and stored at -20°C.

The Qiaprep miniprep procedure was analysed via agarose gel electrophoresis.

2.4.2 Large Scale: Maxi-Prep.

The EndoFree Plasmid Maxi Kit supplied by QIAGEN can be used to isolate and purify plasmids of up to approximately 150kb. The protocol was used to purify up to 500µg of plasmid DNA. The principles are similar to that of the mini-prep protocol. 100ml of LB broth containing ampicillin (100µg/ml) was inoculated with 20-50µl of a

mini-prep culture and shaken for 12 to 16 hours at 37°C. The QIAGEN protocol described below was then followed.

Procedure

The bacterial culture was centrifuged in a Sorvall GSA at 6000g for 15 minutes at 4°C. The supernatent was discarded and the bacterial pellet was resuspended in 10ml of buffer (P1) containing RNase A. The culture was transferred to a 50ml screw cap tube and incubated with 10ml of lysis buffer (P2) at room temperature for a maximum of 5 minutes. The lysis reaction was stopped by addition of 10ml of chilled neutralisation buffer (N3), which increased the salt concentration of the sample to allow optimum binding to the silica-gel column. The lysate was centrifuged at 6000g for 20 minutes. The supernatant / lysate was decanted/ pipetted into the barrel of a QIAfilter cartridge and incubated at room temperature for 10 minutes so that a precipitate of proteins, genomic DNA and detergent formed a layer on top of the solution. The cell lysate was filtered into a 50ml tube, approximately 25ml of lysate was recovered. 2.5ml of endotoxin removal buffer (ER) was added to the filtered lysate and incubated on ice for 30 minutes. The cleared lysate was decanted into a QIAGEN-tip 500, previously equilibriated with 10ml equilibriation buffer (QBT). 2 x 30ml of wash buffer (QC) was applied to the column to remove any contaminants. The DNA was eluted by applying 15ml of elution buffer (QN) to the column. The flow-through was collected in a 30ml sterile tube. 10.5ml (0.7 volumes) room temperature isopropanol was added to precipitate the DNA and the solution was immediately centrifuged in a Sorvall SS-34 rotor at 15000g for 30 minutes at 4°C. The DNA pellet was washed with 2.5ml endotoxin-free, room temperature 70% ethanol (40ml of 96-100% ethanol was added to the endotoxin-free water supplied) and centrifuged for 10 minutes at 15000g. The supernatent was decanted. The pellet was air-dried for 5-10 minutes dissolved in 300µl of buffer TE and stored in a sterile 1.5ml eppendorf tube at -20°C.

Buffers

Buffer P1 (Resuspension Buffer): 50mM Tris.Cl, pH 8.0; 10mM EDTA; 100µg/ml RNase A. Store at 4°C after addition of RNase A.

Buffer P2 (Lysis Buffer): 200mM NaOH, 1% SDS.

Buffer P3/N3 (Neutralization Buffer): 3.0M potassium acetate, pH 5.5.

Buffer QBT (Equilibration Buffer): 750mM NaCl; 50mM MOPS, pH 7.0; 15% isopropranol; 0.15% Triton X-100.

Buffer QC (Wash Buffer): 1.0M NaCl; 50mM MOPS, pH 7.0; 15% isopropanol.

Buffer QF (Elution Buffer): 1.25M NaCl; 50mM Tris, Tris.Cl, pH 8.5; 15% isopropanol.

Buffer QN (Elution Buffer): 1.6M NaCl; 50mM MOPS, pH 7.0; 15% isopropanol.

TE: 10mM Tris.Cl, pH 8.0; 1mM EDTA.

All buffers were stored at room temperature unless stated otherwise.

2.4.3 Analysis of Plasmid DNA.

A 10µl aliquot of the TE/DNA mix was pipetted into an eppendorf containing 490µl of distilled water. Quartz cuvettes were used to read both the blank (distilled water) and test samples. The optical density (OD) was read at 260nm and 280nm. The OD's were applied to the equations below to determine the purity and quantity of plasmid DNA recovered.

$$\text{Purity of DNA:} \quad \frac{\text{OD 260nm}}{\text{OD 280nm}}$$

OD260/280 ≤ 1.7 indicated the plasmid preparation was free of protein contamination

$$\text{Quantity of DNA (µg/µl):} \quad OD_{260} \times \text{Dilution} \times 50$$

OD of 1 = 50µg/ul of DNA

2.5 Transfection of Mammalian Cells.

All the methods described below were used for co-transfection of two recombinant plasmids. Each novel HRE sequence was attached to a luciferase reporter gene and independently co-transfected, with a control CMV-driven reporter plasmid, into a panel of human carcinoma cell lines. The capacity of each vector construct to regulate gene expression in response to low oxygen was quantified relative to an SV40 early gene promoter/enhancer.

2.5.1 Electroporation

Human cell lines were electroporated using cytomix prepared as described in Van Den Hoff et al. (1992). Exponentially growing cells were harvested to produce a cell pellet, which was resuspended in 20ml of PBS at room temperature. The cells were counted using an improved Neuberger haemocytometer to obtain aliquots of 5 x 10^6 cells, centrifuged to produce a cell pellet and the supernatent was discarded. The electroporation medium was prepared and made up to a final volume with millipore water. An appropriate amount of ATP and glutathione were added to the cytomix just before use. The solution was pH adjusted to 7.6 using 1M KOH and then filter sterilised. Each aliquot of 5 x 10^6 cells were resuspended in 1ml cytomix and pipetted into an electroporation cuvette containing 20μg of purified plasmid DNA and incubated at room temperature for a maximim of 3 minutes. An electrical pulse (1500μF @ 280V, 320V for MDA 468, C4.5 and Ka13) was applied to each cuvette. Immediately after the electrical pulse, the cell / cytomix solution was transferred to a 75cm^2 flask containing 20ml complete, pre-warmed media. The flasks were placed in a 37°C, 5%CO_2 humidified incubator overnight.

Materials

120mM Potassium Chloride (KCl) MW 74.55

0.15mM Calcium Chloride ($CaCl_2$) MW 147.0

10mM Potassium Hydrogen Phosphate (K_2HPO_4), MW 174.18, pH 7.6

25mM Hepes, MW 238.3, pH 7.6

2mM Ethyleneglycol-bis-(b-aminoethyl ether)N,N,N',N',-tetraacetic acid (EGTA), MW 380.4, pH 7.6

5mM Magnesium Chloride ($MgCl_2$) MW 203.3

pH 7.6 with 1M Potassium Hydroxide (KOH) MW 56.11

All solutions were made at a 10X stock, filter sterilised (0.2μm) and stored at room temperature.

2mM Adenosine Triphosphate (ATP), MW 551.1, pH 7.6

5mM Glutathione, MW 307.3

Solutions were prepared fresh each time.

All reagents were purchased from Sigma.

2.5.2 Calcium Phosphate

24 hours before transfection, adherent cells were harvested, pelleted and counted using an improved Neuberger haemocytometer. 2 X 10^5 cells were seeded into an individual well of a 6 well plate with 2ml of complete DMEM. The plate was incubated overnight by which time the cells should be no more than 80% confluent. 10μg of DNA were pipetted into a sterile bijou tube containing 250μl of 0.25M $CaCl_2$. The $CaCl_2$ / DNA mix was slowly and gently, pipetted dropwise down the side of a pasteur pipette into a fresh 5ml bijou containing 250μl of BES, the solution turned milky, it was incubated at room temperature for 10-20 minutes. Fresh media was added to the cells and the calcium chloride / DNA solution pipetted dropwise onto the cells whilst swirling the plate in a circular manner to ensure an even distribution of the plasmid DNA. The plate was incubated in a humidified 95% air, 3% CO_2 atmosphere for 12-18 hours at 35°C. The plate was examined under the microscope for an even precipitate. A fine

precipitate indicated too much DNA was added, whilst a clumpy precipitate suggested too little. The plate washed twice with 5ml PBS and fresh complete media was added.

Materials

2.5M $CaCl_2$ (Sigma Chemicals Co. Ltd).

36.75g in 100ml distilled water.

Filter sterilised and stored at -20°C in 5ml aliquots.

Diluted to 0.25M for transfection.

2 X BES: Buffered solution (BBS): 50mM BES (MW 213.25), 10.663g/L.

280mM NaCl (MW 58.44), 16.363g/L.

1.5mM Na_2HPO_4 (MW 141.96), a 15mM stock was made (0.426g in 200ml), pH adjusted to 6.95 with HCl. 100ml was added to 1L to give a 1.5mM solution.

BES and NaCl were added to a 1L flask, to this was added 700µl distilled water, 100ml 1.5mM Na_2HPO_4, pH to 6.95-6.98 with 1M NaOH and made up to a total volume of 1L. The solution was filter sterilised and stored in 50ml aliquots at -20°C.

24 hours after transfection, each flask of transfected cells was harvested, pelletted and resuspended in 1ml of pre-warmed culture media. A cell count was performed on each sample and 3 x 10^4 cells were reseeded into duplicate wells of a 24 well plate (Monaghan, 2000). The cells were allowed 4-6 hours to attach and then triplicate plates were exposed to 16 hours air (37°C, 5% CO_2 humidified incubator), hypoxia (1% O_2, 5% CO_2, 94% N_2 humidified), or anoxia (≥ 0.002% O_2). Following exposure, cells were returned to normoxia for 3 hours and subsequently were lysed and assayed for firefly and renilla luciferase activities.

2.6 Assays

2.6.1 Dual-Luciferase Reporter Assay (DLR) System

The DLR system was used to study the transcriptional response of a variety of genes to both aeorobic and hypoxic conditions. A modified version of the recommended procedure was used. Cells were seeded into 24 well plates for all experiments, for more details see section 2.5. The culture media was apirated from the cells and they were washed with 200µl of PBS. 100µl of 1 X passive lysis buffer PLB (supplied by Promega) was then applied to each well of a 24-well plate. The plate was placed on a plate shaker (Heidolph, Titramax 1000) for 15 minutes at room temperature to ensure complete coverage and lysis of the cells. The Luciferase Assay Reagent II (LAR II) was prepared by resuspending the lyophilized Luciferase Assay Substrate in 10ml of Luciferase Assay Buffer. A 50X stock of the Stop and Glo Solvent was prepared by adding 200µl of Stop and Glo Substrate Solvent to the dried Stop and Glo Substrate. Both of these reagents were stable at –20°C (for one month), or –70°C for long term storage (up to one year). The Stop and Glo Reagent was prepared fresh by adding 50 volumes of Stop and Glo Buffer to one volume of Stop and Glo Substrate in an amber vial. To ensure minimal background activity a lysate of untransfected control cells and cells expressing high levels of firefly luciferase were prepared. 10µl of each lysate (test and control) were dispensed into duplicate wells of a 96 well luminometer plate (Dynex). **Luminescence was determined by measuring the luminescence activity produced by addition of 50µl LARII followed by 50µl Stop & Glo; A reagent injector dispensed 50µl of LARII into a single well, the luminometer performed a two-second pre-measurement delay followed by a ten-second measurement period for each reporter assay. A second injector then dispensed 50µl of Stop and Glo into the same well and performed a ten-second measurement. A mean of each value was calculated per sample and normalised against the aerobic control to give luciferase expression (see 3.3.1).

2.6.2 DNA Sequencing

All plasmids generated for this study were sequenced using the the ABI PRISM BigDye™ Terminator Cycle Sequencing Ready Reaction Kit supplied by PE Applied Biosystems. The kit consists a single reagent containing four dye-labelled dideoxy nucleotides. This was added to the primer and vector template and prepared for the automatic DNA sequencer using a modified method to the suppliers recommended procedure. Modified pGL3 vectors were sequenced clockwise form the upstream cloning site using the Rvprimer3 and counterclockwise upstream of *luc*+ with the Glprimer2.

Figure 2.2: pGL3 vector showing upstream and downstream cloning sites and the locations of the sequencing primers, Rvprimer3 and Glprimer2.

(Taken from pGL3 Luciferase Repoter Vectors, technical manual, Promega.)

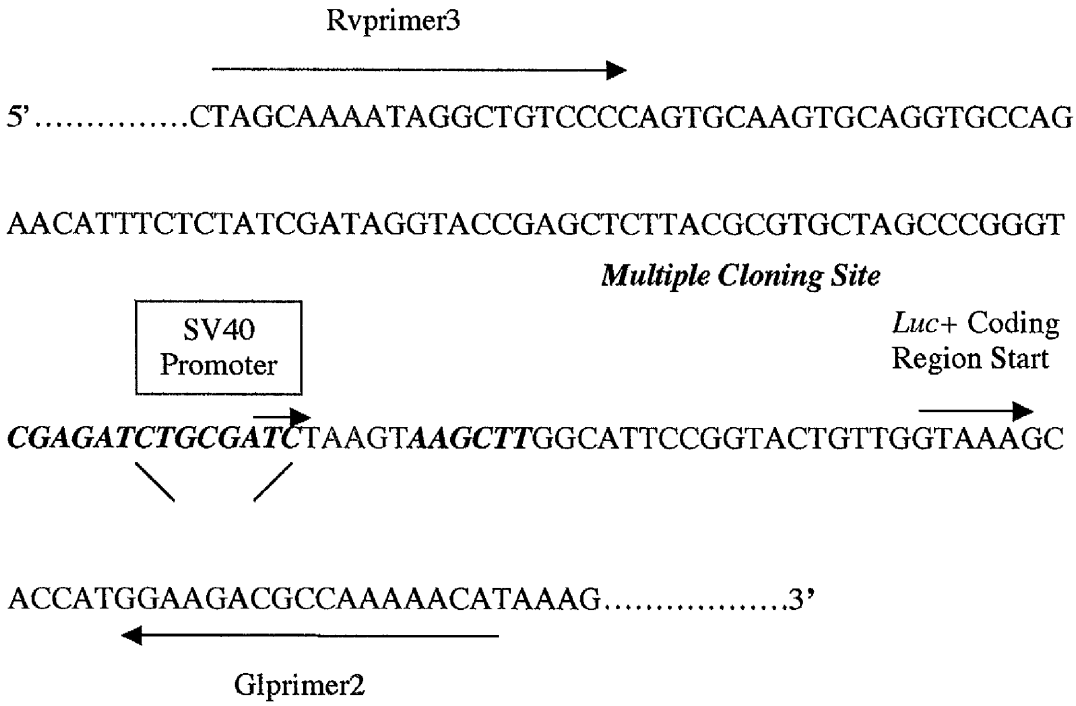

Procedure

1µl of each vector to be sequenced was run on an agarose gel against 1µl of the Lambda (l) HindIII (NEB) molecular weight DNA marker to accurately determine its concentration. For each sequencing reaction 200 to 500ng of double stranded DNA were dispensed into a 0.5ml thin-walled PCR reaction tube (Eppendorf). Added to this were 5pmol primer (Promega), 1µl DMSO, 8µl Terminator Ready Reaction mix (Applied Biosystems) and made up to a final volume of 20µl with millipore grade water and mixed well. The tube(s) was placed in a Techne thermal cyler. The solution was exposed to 96°C for four minutes followed by 30 cylces of:

- Rapid thermal ramp to 96°C
- 96°C for 30 seconds
- Rapid thermal ramp to 50°C
- 50°C for 10 seconds
- Rapid thermal ramp to 60°C
- 60°C for 4 minutes

After the 30 cycles there was a rapid thermal ramp to 4°C, this temperature was held until the sample was ready to be purified.

The tubes were briefly spun and the contents were pipetted into individual, clean 1.5ml eppendorf tubes containing 2µl of 3M sodium acetate (NaOAc) pH 4.6 and 50µl of 95% ethanol (EtOH). The tubes were vortexed then left at room temperature for 15 minutes to precipitate the DNA. The tubes were spun in a microcentrifuge for 20 minutes at maximum speed. The supernatent containing unbound dye terminators was removed and the pellet rinsed by addition of 250µl of 70% ethanol. After vortexing the tube was centrifuged again and supernatent discarded. The tube was then placed in a heated block (90°C) with its lid open for one minute to dry the pellet. Each sample was kindly electrophoresed by Dr. Lawrence Hall, at the Medical School, University of Manchester.

2.7 Solutions and Reagents

Dulbeccos modification of eagles media (DMEM)

Reagents

10X DMEM (Gibco BRL)

Foetal calf serum (FCS; Labtech)

7.5% sodium bicarbonate ($NaHCO_3$; Sigma)

L-glutamine (200mM; Imperial Labs)

1M sodium bicarbonate (NaOH; Sigma)

1M hydrochloric acid (HCL; Sigma)

Sterile distilled water

390ml of distilled water were aliquoted into 500ml bottles and autoclaved. Using aseptic techniques, 50ml 10X DMEM, 50ml FCS, 27.5ml 7.5% $NaHCO_3$, 5ml of 200mM L-glutamine and 7ml 1M NaOH were added to each bottle and gently mixed. The bottles of 1X DMEM were dated and stored at 4°C until required.

Phosphate Buffered saline (PBS)

Individual tablets (Oxoid) were dissolved in 500ml distilled water and autoclaved. The sterile PBS was a pH of 7.4.

Trypsin–EDTA

Trypsin was supplied in 100ml bottles by Gibco BRL as a 10X stock which was stored at -20°C. 1ml of 500mM EDTA was added to each thawed bottle of trypsin, which was aliqoted and stored at -20°C. Prior to use the trypsin-EDTA mix was diluted 10-fold in sterile PBS.

*0.5M EDTA (pH 8.0)**

186.1g of disodium ethylenediaminetetra-acetate.$2H_2O$ were added to 800ml of distilled water and pH adjusted to pH 8.0 with 1M NaOH. The solution was sterilised by autoclaving.

*50 x Tris-EDTA**

121g tris base (Sigma), 28.55ml glacial acetic acid (Gibco BRL), 50ml EDTA (0.5M, pH 8.0) were dissolved in 400ml of distilled water. The solution was made up to a total volume of 500ml with distilled water and vigorously stirred on a magnetic stirrer.

*Ethidium bromide (EtBr)**

1g of EtBr was added to 100ml of distilled water and placed on a magnetic stirrer to ensure the dye fully dissolves. The solution was transferred to a dark bottle and stored at room temperature.

* Recipes from Maniatas

Chapter 3

Optimisation of Transfection Efficiency, Orientation, and Reoxygenation Phenomena of Hypoxia-Responsive Element Enhancer Sequences in a Panel of Human Carcinoma Cell Lines.

3.1 Introduction

Prior to beginning the main set of experiments for this thesis, it was important to validate that the expression of the chosen HRE sequences under hypoxic and aerobic conditions was as a direct result of the binding and *trans*activation of the HRE and not artifacts inherent in the experimental procedures.

Since the PGK 18bp HRE is relatively well characterised in the published literature (Firth et al., 1994; Dachs et al., 1997; Boost et al., 1999), it was used to determine multiple experimental parameters such as quantity and ratio of DNA transfected and length of reoxygenation time after hypoxic and anoxic exposure. 16 hr (overnight) was nominally selected as the exposure time for all experiments as this appears to be the most common schedule used in the majority of HRE studies published to date and was logistically straightforward

It was considered important that the respective HREs were optimised under both intermediate hypoxia and anoxic conditions. 1% O_2 (1% O_2, 5% CO_2, 94% N_2, humidified), referred to hereafter as "hypoxia", and palladium catalyst-induced anoxia (≥0.002% O_2) referred to as "anoxia" were employed to represent these conditions. Ambient pO_2 (20.9% O_2) was used to represent normoxia. 1% O_2 represents the concentration of molecular oxygen that discriminates most clearly between tumour and

normal tissues (see chapter 1) and is known to evoke a HIF-1-dependent response. Anoxia was considered representative of the severe oxygen deprivation that occurs in tumour tissues following complete vascular occlusion. Initial experiments to determine optimisation of reporter: control plasmid ratios were performed under normoxia and anoxia only. Following this initial optimisation, experiments comparing the effectiveness of the phosphoglycerate kinase HRE in the homologous (positive) orientation (PGK^{+++}), reverse of homologous (negative) orientation (PGK^{---}), and in the homologous orientation but with a mutated HIF-1 binding site (PGK^{mut}) were performed. Further experiments to optimise reoxygenation times were carried out under normoxia, hypoxia and complete anoxia.

3.2 Methods.

The pGL3.PGK^{+++} and pGL3.PGK^{---} orientation were kindly donated by Oxford Biomedica, both contained an 18-bp trimer HRE. A pGL3.PGK^{mut} vector was constructed; an oligo of three copies of the PGK^{+++} sequence (SigmaGenosys), mutated at the core HIF-1 binding site, ACGT, and ligated into the pGL3.promoter expression vector (Promega) at the Bgl II site in the multiple cloning region, 5' to the SV40 enhancer (figure 3.1).

Figure 3.1: Sequence comparison of PGK^{+++}, PGK^{--}, PGK^{mut}.

PGK^{+++}

5'-TGTC**ACGT**CCTGCACGAC-*3'*

$PGL3.PGK^{--}$ was identical to $pGL3.PGK^{+++}$ except the PGK was inserted in the reverse orientation with respect to its homologous promoter context (Dachs et al., 1997).

$pGL3.PGK^{mut}$.

5'-TGTC**CATT**CCTGCACGAC-*3'*

The pGL3.PGK HRE construct encoding the SV40 minimal promoter and the firefly luciferase reporter gene was used to optimise transfection conditions. The pGL3.control plasmid containing the SV40 enhancer and promoter, both unresponsive to changes in O_2, was used to normalise HRE activity. pGL3.Control, $pGL3.PGK^{+++}$, $pGL3.PGK^{--}$, were transiently co-transfected with the control CMV-driven renilla reporter plasmid, pRL.CMV as described in section 2.5, into the MDA 468, HT1080 and SQ20B human carcinoma cell lines with different total quantities of plasmid DNA (5, 10, or 15μg), at varying ratios (10:1 or 40:1). In each case the quantity of the pRL.CMV remained at a constant ratio, whilst the absolute amount of pGL3.PGK was titrated. Cells were allowed 24hr to recover from transfection, whereupon they were reseeded into duplicate 24 well plates and exposed to 16 hours oxia (37°C, 5% CO_2 humidified incubator), or complete anoxia (≥0.002% O_2). Following exposure, cells were lysed and assayed for firefly and renilla luciferase activities using a Berthold model luminometer.

Using the optimal quantity and ratio of DNA the HT1080 cell line was transiently co-transfected with $pGL3.PGK^{+++}$ and either pRL.CMV or pRL.TK

(thymidine kinase promoter) under identical experimental conditions to determine the most appropriate internal control promoter to drive the transcription of the renilla cDNA for use in this study.

Follow up experiments were performed using the preferred renilla (pRL.CMV as determined by experiments in section 3.3.2) to determine the optimal reoxygenation period. Cells were exposed to 16 hours oxia, hypoxia or anoxia after which they were given varying periods of reoxygenation (0, 1, 2, 3, 4, and 6 hours), lysed and assayed for firefly and renilla activities.

Finally, to demonstrate the importance of the core HIF-1 binding site pGL3.PGK$^{+++/---}$ expression was compared with pGL3.PGK^{mut}.

3.3 Results

3.3.1 Optimisation of DNA quantity and ratio

The dual-luciferase assay involves the co-transfection of two plasmids. The first contains the HRE under evaluation, placed in the heterologous context of a minimal SV40 promoter with a firefly luciferase reporter gene readout (firefly: pGL3.HRE). The second was a renilla plasmid (pRL), a chimeric vector composed of a promoter that was found to be constant under all experimental conditions under investigation in this study, linked to a renilla luciferase reporter gene. The renilla vector allowed the transfection efficiency of each independent experiment to be accounted for, allowing normalisation of intra and inter experimental variations. There are currently two possible promoters used in the renilla plasmid, cytomegalovirus (CMV) or thymidine kinase (TK), denoted either pRL.CMV or pRL.TK respectively. Preliminary experiments were performed using the more robust pRL.CMV vector.

The table overleaf (3.1) shows the expression of pGL3.PGK^{+++} versus pGL3.PGK^{---} in the human carcinoma cell line MDA 468. Normalised values for the expression of each vector under air and complete anoxia were obtained as described below.

a) Firefly and renilla luciferase readings were taken from untransfected, wild-type, cells to account for any background noise registered by the luminometer.

b) This was subtracted from the sample values.

c) Duplicate readings of firefly and renilla activity were made for each sample, as described in 2.6 and the mean was calculated.

d) Mean firefly activity was divided by mean renilla activity (control of transfection efficiency) to internally normalise every independent cell lysate sample, thus accounting for transfection differences between both reporter plasmids and repeat experiments. This normalised value is nominally referred to as Relative Light Units (RLU).

e) In order to compare RLUs across multiple cancer cell lines this value was then normalised for each cell line by nominally assigning the aerobic pGL3.Control (full SV40 promoter/enhancer) RLU a value of 1.00. This value was unresponsive to changes in oxygen tension. All experiments were performed in triplicate and normalised intra-cell line values were averaged. Thus all variable parameters, both intra- and inter-experimental, were accounted for. Standard deviation and standard error values were determined from the mean. To calculate the amplitude of each HRE RLUs were normalised to that of normoxic expression in the pGL3.Control cells (RLU = 1.00).

f) Fold-induction ratios were calculated by dividing the normalised anoxic (or hypoxic) value by the corresponding aerobic value for each HRE.

Table 3.1: Representative raw data set for MDA468 transfected with either 15, 10 or 5 μg of total plasmid DNA (pGL3.Control, pGL3.PGK^{+++} and pGL3.PGK^{---}) at a reporter:control ratio (firefly:renilla) of 10:1 and 40:1.

10:1

15ug

			c	*a*				*b*	*b*	*c*	*d*	*e*	*f*
			MEAN							MEAN			
SAMPLE	FIREFLY	FIREFLY	FIREFLY	BCKGRD	MEAN	RENILLA	RENILLA	RENILLA	RENILLA	RENILLA	FIR/REN	NORMALISED	INDUCTION
CONTROL/AIR	93737	119251	106494	80	85	196177	279764	196092	279679	237886	0.4477	1.0000	0.9686
AnO_2	66080	63562	64821	83		164493	134654	164408	134569	149489	0.4336	0.9686	
PGK+++/AIR	7872	3793	5832.5	92		638934	408051	638849	407966	523408	0.0111	0.0249	24.4784
AnO_2	127118	130778	128948	81		511131	434506	511046	434421	472734	0.2728	0.6093	
PGK---/AIR	2034	7535	4784.5	92		448268	378628	448183	378543	413363	0.0116	0.0259	16.3341
AnO_2	77382	56872	67127	82		349223	361060	349138	360975	355057	0.1891	0.4223	

10ug

			MEAN							MEAN			
SAMPLE	FIREFLY	FIREFLY	FIREFLY	BCKGRD	MEAN	RENILLA	RENILLA	RENILLA	RENILLA	RENILLA	FIR/REN	NORMALISED	INDUCTION
CONTROL/AIR	66450	58397	62423.5			135351	139776	135266	139691	137479	0.4541	1.0000	0.8888
AnO_2	66194	54741	60467.5			168065	131780	167980	131695	149838	0.4036	0.8888	
PGK+++/AIR	3272	2535	2903.5			327818	276342	327733	276257	301995	0.0096	0.0212	22.0338
AnO_2	65123	57252	61187.5			326825	251018	326740	250933	288837	0.2118	0.4665	
PGK---/AIR	1499	1491	1495			169669	209659	169584	209574	189579	0.0079	0.0174	35.7295
AnO_2	46480	26211	36345.5			131030	127130	130945	127045	128995	0.2818	0.6205	

5ug

			MEAN							MEAN			
SAMPLE	FIREFLY	FIREFLY	FIREFLY	BCKGRD	MEAN	RENILLA	RENILLA	RENILLA	RENILLA	RENILLA	FIR/REN	NORMALISED	INDUCTION
CONTROL/AIR	85308	83066	84187			87513	92438	87428	92353	89890.5	0.9366	1.0000	0.7471
AnO_2	78736	87845	83290.5			98563	139691	98478	139606	119042	0.6997	0.7471	
PGK+++/AIR	7142	8011	7576.5			263581	283261	263496	283176	273336	0.0277	0.0296	16.5017
AnO_2	77009	82738	79873.5			177685	171731	177600	171646	174623	0.4574	0.4884	
PGK---/AIR	4630	2087	3358.5			99211	120352	99126	120267	109697	0.0306	0.0327	18.1397
AnO_2	29634	42516	36075			72747	57336	72662	57251	64956.5	0.5554	0.5930	

40:1

15ug

			MEAN							MEAN			
SAMPLE	FIREFLY	FIREFLY	FIREFLY	BCKGRD	MEAN	RENILLA	RENILLA	RENILLA	RENILLA	RENILLA	FIR/REN	NORMALISED	INDUCTION
CONTROL/AIR	188670	141034	164852	80	85	2790	1682	2705	1597	2151	76.6397	1.0000	0.8784
AnO_2	140072	177933	159003	83		1910	2984	1825	2899	2362	67.3169	0.8784	
PGK+++/AIR	14001	12667	13334	92		8661	13216	8576	13131	10853.5	1.2285	0.0160	22.9455
AnO_2	150319	120583	135451	81		5353	4427	5268	4342	4805	28.1896	0.3678	
PGK---/AIR	9983	17609	13796	92		8450	16764	8365	16679	12522	1.1017	0.0144	16.2041
AnO_2	120288	74307	97297.5	82		5112	5958	5027	5873	5450	17.8528	0.2329	

10ug

			MEAN							MEAN			
SAMPLE	FIREFLY	FIREFLY	FIREFLY	BCKGRD	MEAN	RENILLA	RENILLA	RENILLA	RENILLA	RENILLA	FIR/REN	NORMALISED	INDUCTION
CONTROL/AIR	45806	54856	50331			1140	876	1055	791	923	54.5298	1.0000	0.5451
AnO_2	29499	25642	27570.5			1176	849	1091	764	927.5	29.7256	0.5451	
PGK+++/AIR	11350	10375	10862.5			9410	4587	9325	4502	6913.5	1.5712	0.0288	21.5910
AnO_2	119741	75965	97853			3995	1944	3910	1859	2884.5	33.9237	0.6221	
PGK---/AIR	7902	8470	8186			4923	6310	4838	6225	5531.5	1.4799	0.0271	26.2123
AnO_2	84498	117760	101129			2921	2463	2836	2378	2607	38.7913	0.7114	

5ug

			MEAN							MEAN			
SAMPLE	FIREFLY	FIREFLY	FIREFLY	BCKGRD	MEAN	RENILLA	RENILLA	RENILLA	RENILLA	RENILLA	FIR/REN	NORMALISED	INDUCTION
CONTROL/AIR	11923	17730	14826.5			1027	1508	942	1423	1182.5	12.5383	1.0000	0.6413
AnO_2	8538	8837	8687.5			1507	824	1422	739	1080.5	8.0403	0.6413	
PGK+++/AIR	4616	1635	3125.5			5408	10806	5323	10721	8022	0.3896	0.0311	11.0910
AnO_2	14715	34763	24739			3096	8524	3011	8439	5725	4.3212	0.3446	
PGK---/AIR	455	529	492			4391	5471	4306	5386	4846	0.1015	0.0081	32.6848
AnO_2	6909	3972	5440.5			2356	1093	2271	1008	1639.5	3.3184	0.2647	

Within the tables and figures in this study, aerobic values (37°C, 5% CO_2) are denoted by AIR, hypoxic values (1% O_2, 5% CO_2, 94% N_2) by 1%O_2 and anoxic values (≥0.002% O_2) by AnO_2.

The experiment was performed in triplicate. The mean of the normalised values was calculated and plotted as normalised expression of RLU of luciferase at normoxia and anoxia. The final normalised values can be seen in table 3.2.

Table 3.2: Normalised expression of pGL3.Control, pGL3.PGK^{+++} and pGL3.PGK^{---} in the human breast carcinoma cell line MDA 468, exposed to 16 hours air or anoxia.

(Mean values are shown in italics.)

10;1

15ug

	AIR	AIR	AIR	*AIR*	Sdev	SE
Control	1.0000	1.0000	1.0000	*1.0000*	0.0000	0.0000
PGK+++	0.0249	0.0399	0.0230	*0.0292*	0.0092	0.0054
PGK---	0.0259	0.0232	0.0227	*0.0239*	0.0017	0.0010

	AnO_2	AnO_2	AnO_2	*AnO 2*	Sdev	SE
Control	0.9686	1.1668	1.0377	*1.0577*	0.1006	0.0588
PGK+++	0.6093	1.2160	2.0970	*1.3074*	0.7480	0.4374
PGK---	0.4223	0.7159	1.1388	*0.7590*	0.3602	0.2106

10ug

	AIR	AIR	AIR	*AIR*	Sdev	SE
Control	1.0000	1.0000	1.0000	*1.0000*	0.0000	0.0000
PGK+++	0.0212	0.0433	0.0183	*0.0276*	0.0136	0.0080
PGK---	0.0174	0.0125	0.0286	*0.0195*	0.0082	0.0048

	AnO_2	AnO_2	AnO_2	*AnO 2*	Sdev	SE
Control	0.8888	1.1018	0.9440	*0.9782*	0.1106	0.0647
PGK+++	0.4665	1.3895	1.5472	*1.1344*	0.5837	0.3414
PGK---	0.6205	0.8925	1.2074	*0.9068*	0.2937	0.1718

5ug

	AIR	AIR	AIR	*AIR*	Sdev	SE
Control	1.0000	1.0000	1.0000	*1.0000*	0.0000	0.0000
PGK+++	0.0296	0.0679	0.0213	*0.0396*	0.0249	0.0145
PGK---	0.0327	0.0088	0.0168	*0.0194*	0.0122	0.0071

	AnO_2	AnO_2	AnO_2	*AnO 2*	Sdev	SE
Control	0.7471	0.9951	0.9425	*0.8949*	0.1307	0.0764
PGK+++	0.4884	1.3597	2.1671	*1.3384*	0.8395	0.4910
PGK---	0.5930	0.3571	1.4082	*0.7861*	0.5515	0.3225

40;1

15ug

	AIR	AIR	AIR	*AIR*	Sdev	SE
Control	1.0000	1.0000	1.0000	*1.0000*	0.0000	0.0000
PGK+++	0.0160	0.0297	0.0140	*0.0199*	0.0086	0.0050
PGK---	0.0144	0.0240	0.0094	*0.0159*	0.0074	0.0044

	AnO_2	AnO_2	AnO_2	*AnO 2*	Sdev	SE
Control	0.8784	1.2497	1.0091	*1.0457*	0.1884	0.1102
PGK+++	0.3678	1.0521	1.2494	*0.8898*	0.4627	0.2706
PGK---	0.2329	0.9954	0.6189	*0.6157*	0.3812	0.2229

10ug

	AIR	AIR	AIR	*AIR*	Sdev	SE
Control	1.0000	1.0000	1.0000	*1.0000*	0.0000	0.0000
PGK+++	0.0288	0.0263	0.0181	*0.0244*	0.0056	0.0033
PGK---	0.0271	0.0129	0.0104	*0.0168*	0.0090	0.0053

	AnO_2	AnO_2	AnO_2	*AnO 2*	Sdev	SE
Control	0.5451	1.2149	1.2112	*0.9904*	0.3856	0.2255
PGK+++	0.6221	0.6264	1.2194	*0.8226*	0.3436	0.2009
PGK---	0.7114	0.3380	0.7127	*0.5874*	0.2160	0.1263

5ug

	AIR	AIR	AIR	*AIR*	Sdev	SE
Control	1.0000	1.0000	1.0000	*1.0000*	0.0000	0.0000
PGK+++	0.0311	0.0256	0.0346	*0.0304*	0.0046	0.0027
PGK---	0.0081	0.0100	0.0558	*0.0246*	0.0270	0.0158

	AnO_2	AnO_2	AnO_2	*AnO 2*	Sdev	SE
Control	0.6413	0.8991	0.8349	*0.7918*	0.1342	0.0785
PGK+++	0.3446	0.9587	2.1226	*1.1420*	0.9030	0.5281
PGK---	0.2647	0.5952	1.3335	*0.7311*	0.5472	0.3200

The mean normalised values from triplicate experiments, shown in *italics*, are plotted graphically overleaf (figure 3.2). Normalised HRE ampliude (relative light units (RLU)) is shown on the y-axis. In future data will only be shown graphically, all corresponding tables can be found in the appendices. For convenience data will be presented as the mean of the normalised expression for each set of experiments throughout this thesis. All plots are the average of at least three independent experiments performed on different days.

Figure 3.2: Normalised expression of pGL3.Control, pGL3.PGK^{+++} and pGL3.PGK^{---} amplitude in the human carcinoma cell line MDA 468, exposed to 16 hours air or anoxia, n=3.

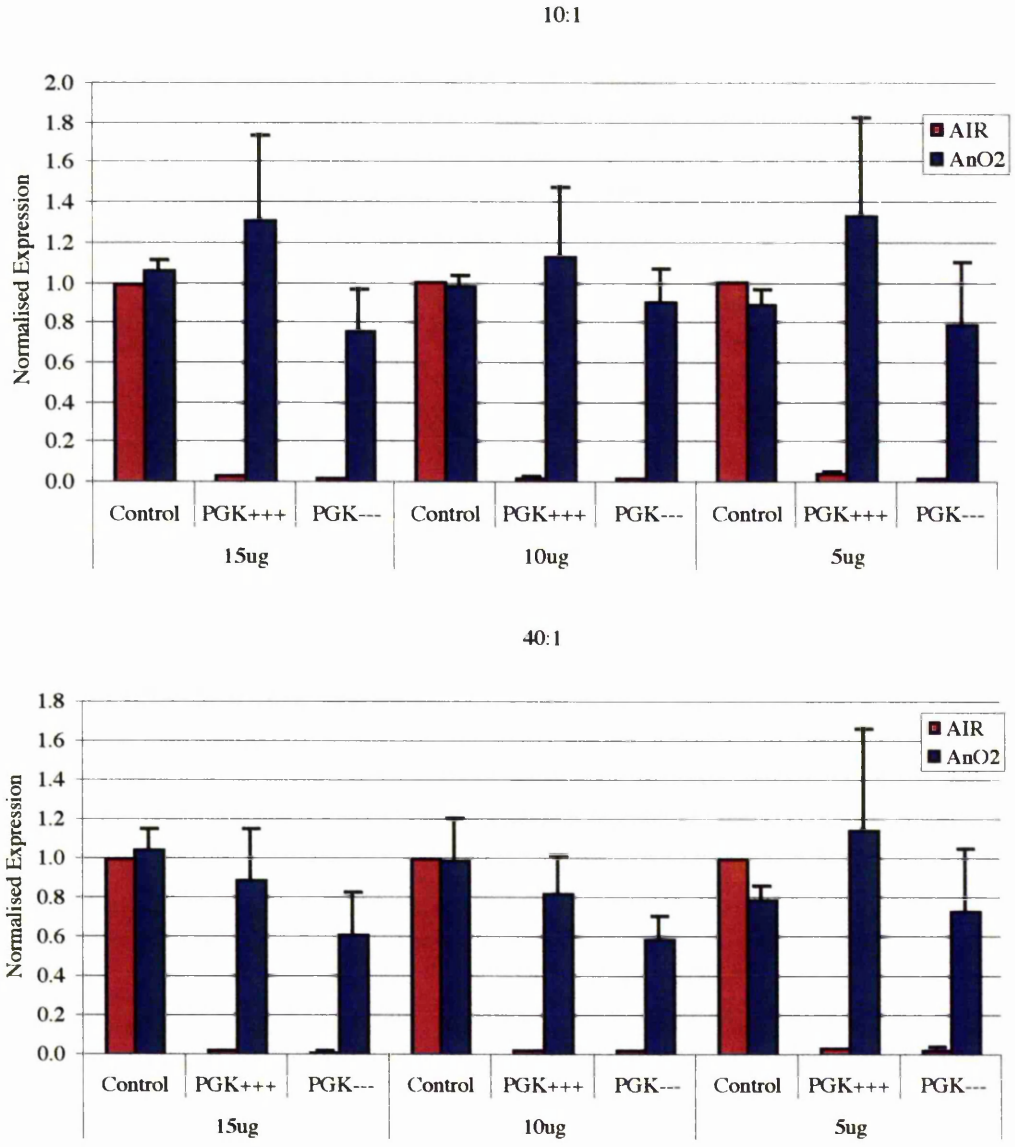

Table 3.3: Induction of pGL3.Control, pGL3.PGK^{+++} and pGL3.PGK^{---} in the human carcinoma cell line MDA 468, exposed to 16 hours air or anoxia (n=3).

DNA Ratio	Total DNA (ug)	Induction		
		Control	PGK+++	PGK---
10;1	15	1.1	44.7	31.7
	10	1.0	41.1	46.5
	5	0.9	33.8	40.4
40;1	15	1.0	44.7	38.7
	10	1.0	33.7	35.0
	5	0.8	37.5	29.7

The above experiment was repeated in the HT1080 (figure 3.3) and SQD9 (figure 3.4), human fibrosarcoma and head and neck cell lines respectively.

Figure 3.3: Normalised expression of pGL3.Control, pGL3.PGK^{+++} and pGL3.PGK^{---} amplitude in the human fibrosarcoma cell line HT1080, exposed to 16 hours air or anoxia (n=3).

(See appendix 1 for data)

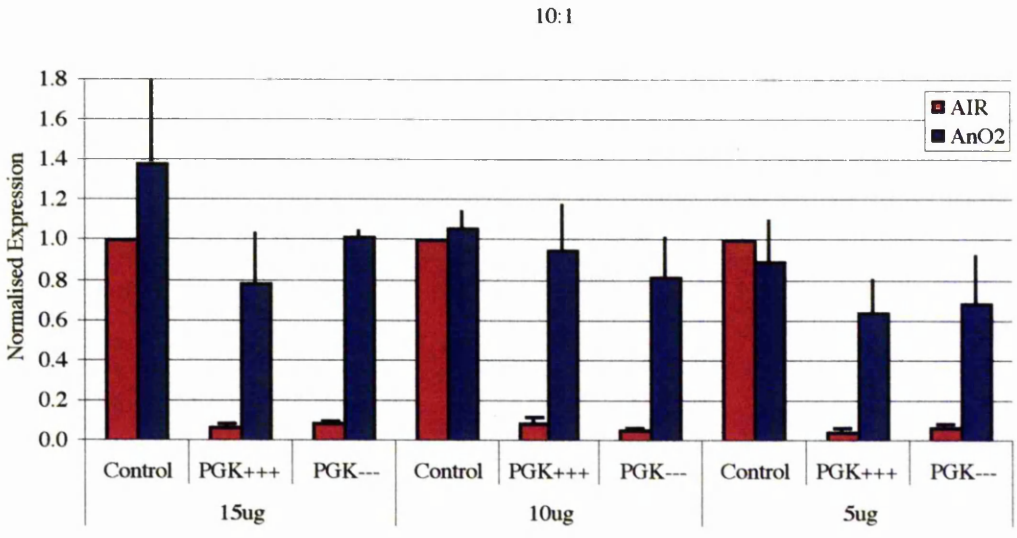

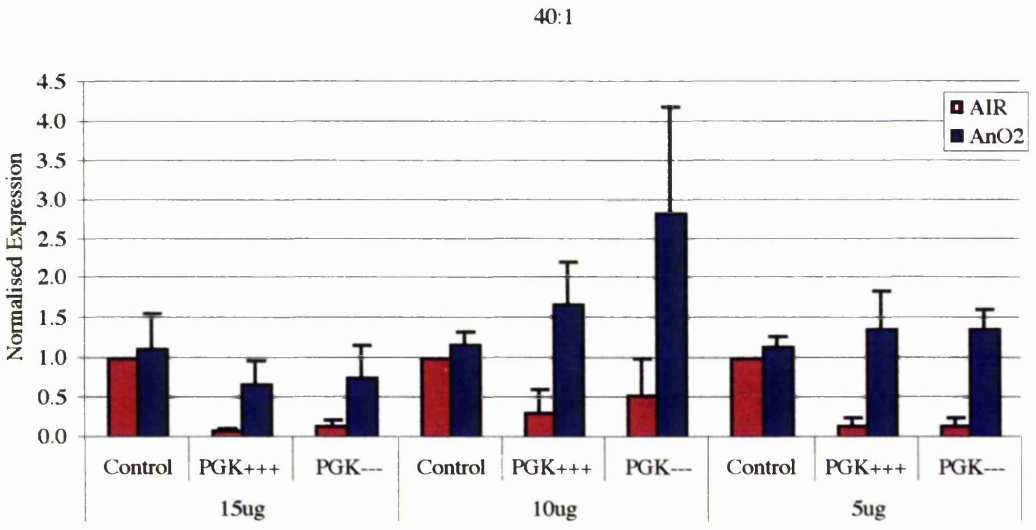

Table 3.4: Induction of pGL3.Control, pGL3.PGK^{+++} and pGL3.PGK^{---} in the human fibrosarcoma cell line HT1080, exposed to 16 hours air or anoxia (n=3).

DNA Ratio	Total DNA (ug)	Induction		
		Control	PGK+++	PGK---
10;1	15	1.4	11.6	12.2
	10	1.1	10.8	15.7
	5	0.9	13.2	11.2
40;1	15	1.1	8.2	5.8
	10	1.2	5.2	5.4
	5	1.1	9.8	9.7

Figure 3.4: Normalised expression of pGL3.Control, pGL3.PGK^{+++} amplitude in the human head and neck carcinoma cell line SQ20B, exposed to 16 hours air or anoxia (n=2).

(See appendix 2)

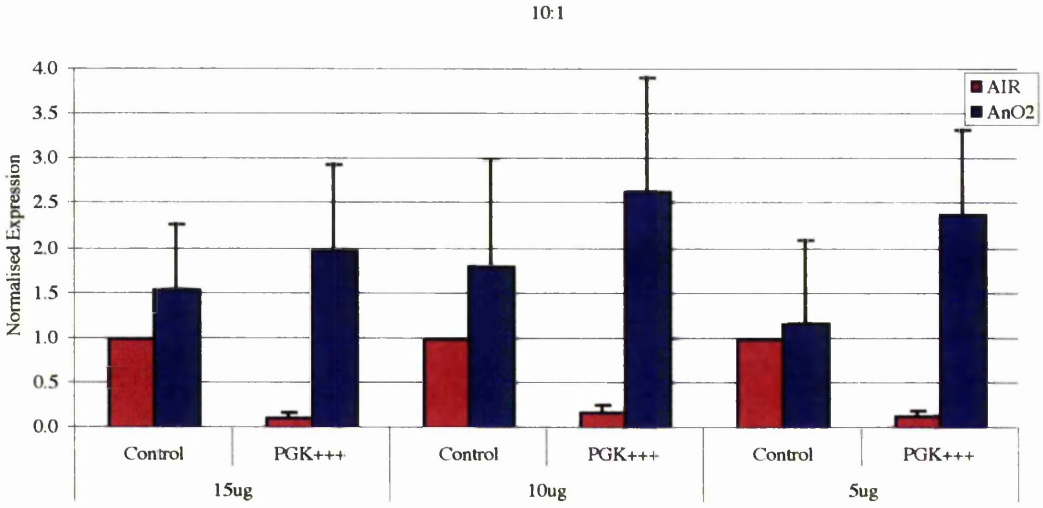

Table 3.5: Induction of pGL3.Control, pGL3.PGK^{+++} and pGL3.PGK^{---} in the human head and neck carcinoma cell line SQ20B, exposed to 16 hours air or anoxia (n=2).

DNA Ratio	Total DNA (ug)	Induction	
		Control	PGK+++
10;1	15	1.5	17.4
	10	1.8	15.6
	5	1.2	18.2

Experiments were begun with the human head and neck carcinoma cell line SQ20B. It was noted subsequently that this was a mixed diploid and tetraploid cell line, so the diploid SQD9 cell line was used in all further studies.

The figures (3.2-4) show the amplification of the PGK HRE (positive and negative orientations) gene expression under two experimental conditions (air and anoxia), normalised against the aerobic pGL3.Control vector which was non-responsive. The mean induction ratio, ie. (O_2 / AnO_2) for PGK^{+++} and PGK^{--} in each cell line is displayed in the tables. Data suggests that the anoxic inducibility of pGL3.PGK^{+++} was consistently higher in cells transfected with DNA at a 10:1 ratio compared to 40:1. However, there were no significant differences in the results. Collectively these observations imply that within the experimental parameters tested; 5 – 15 μg of vector at reporter/control ratios from 10:1 to 40:1, no artefacts are present. Early additional experiments (data not shown) suggested that extreme reporter/control ratios (e.g. ≤ 60:1) or very low total vector (≥ 2μg) resulted in abnormally high induction ratios and RLUs, respectively. Conversely, excess vector (<60 μg) resulted in a saturation of the transcriptional response to hypoxia.

3.3.2 pRL.TK versus pRL.CMV

Prior to optimising experimental conditions further, pRL.CMV was studied to ensure it was equal to, or superior in function to the pRL.TK. Experiments were performed as described.

Table 3.6: pGL3.PGK^{+++} hypoxic and anoxic expression when co-transfected with either pRL.TK or pRL.CMV in the HT1080 cell line.

			MEAN		
	AIR	AIR	AIR	Sdev	
PGK + TK	0.39	0.37	0.38	0.01	
PGK + CMV	0.10	0.09	0.10	0.01	
			MEAN		
	$1\%O_2$	$1\%O_2$	$1\%O_2$	Sdev	Induction
PGK + TK	0.53	0.90	0.71	0.26	1.88
PGK + CMV	1.06	0.42	0.74	0.46	7.47
			MEAN		
	AnO_2	AnO_2	AnO_2	Sdev	Induction
PGK + TK	0.83	0.67	0.75	0.11	1.97
PGK + CMV	1.18	0.56	0.87	0.44	8.82

Cells were exposed to 16 hours normoxia, hypoxia or complete anoxia, then assayed for firefly and renilla activities. Results were normalised against the aerobic control as described.

Figure 3.5: Expression of pGL3.PGK^{+++} co-transfected with either pRL.TK or pRL.CMV in the HT1080 cell line. (n=2)

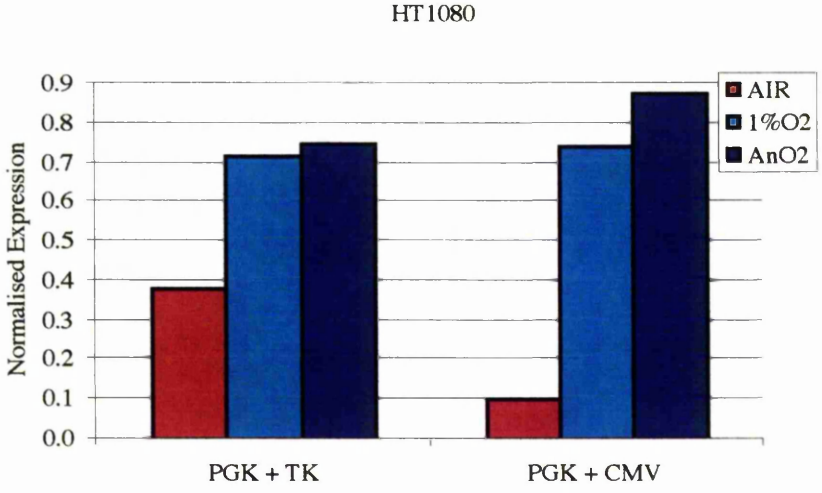

From table 3.6 and the graph above (figure 3.5), it can be seen that the choice of promoter to drive renilla expression has little effect on the hypoxic and anoxic PGK HRE expression. However, the 100-fold lower absolute level of renilla expression with pRL.TK compared to pRL.CMV, artificially elevated the aerobic baseline readings of pGL3.PGK^{+++} as shown in table 3.7 and figure 3.6 overleaf. Thus cells co-transfected with pRL.CMV have a much greater level of induction compared to those co-transfected with pRL.TK. While no internal transfection control existed in these experimental comparisons, cells were derived from single transfection events.

Table 3.7: Expression of pRL.TK and pRL.CMV.

Raw data at varying oxygen concentrations n=2.

	MEAN	
	AIR	Sdev
TK	250.5	111.0
CMV	26843.2	11324.5
	MEAN	
	$1\%O_2$	Sdev
TK	223.7	92.6
CMV	35485.8	21252.9
	MEAN	
	AnO_2	Sdev
TK	380.0	151.3
CMV	22922.5	14570.6

Figure 3.6: Amplitude of pRL.TK and pRL.CMV at different oxygen tensions, n=2.

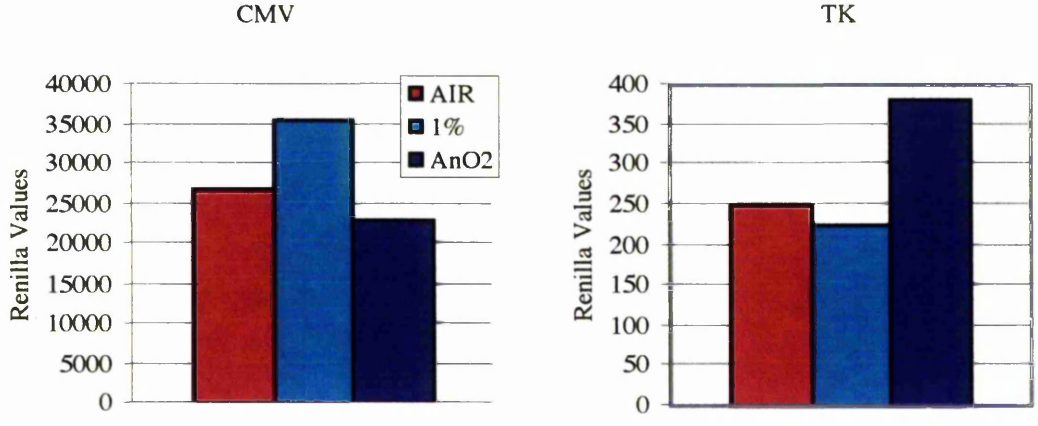

3.3.3 Determination of optimal reoxygenation time

Following the determination of optimal vector ratio, quantity and choice of internal control it was necessary to determine the most appropriate reoxygenation time for all subsequent studies, in order to obtain the optimal hypoxic and anoxic responses. This was intended to minimise any influence oxygen-deprivation may have upon the post-transcriptional processing of the luciferase mRNAs and polypeptide chains. Thus the experiment was repeated using the ratio of 10:1 and 10μg of plasmid DNA with pRL.CMV in two of the cell lines.

Figure 3.7: Normalised expression of pGL3.PGK^{+++} and pGL3.PGK^{---} amplitude in the human fibrosarcoma cell line HT1080, exposed to 16 hours air or anoxia and various periods of reoxygenation (n=3). (See appendix 3)

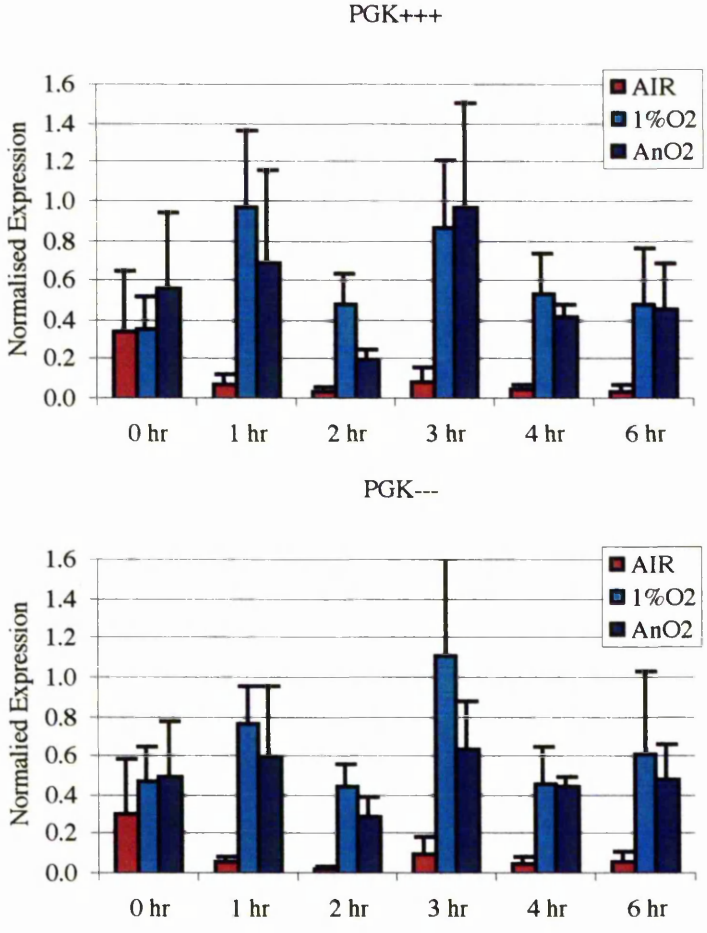

Table 3.8: Induction of pGL3.Control, pGL3.PGK^{+++} and pGL3.PGK^{---} in the human fibrosarcoma cell line HT1080, exposed to 16 hours air or anoxia (n=3).

	PGK+++		PGK---	
	$1\%O_2$	AnO_2	$1\%O_2$	AnO_2
No reox	1.1	1.6	1.5	1.6
1 hr reox	12.1	8.7	12.4	9.7
2 hr reox	11.9	4.9	17.8	11.9
3 hr reox	9.3	10.3	10.4	6.0
4 hr reox	11.4	9.0	8.6	8.3
6 hr reox	11.2	10.5	8.9	7.0

Figure 3.8: Normalised expression of pGL3.PGK^{+++} and pGL3.PGK^{---} amplitude in the human head and neck carcinoma cell line SQD9, exposed to 16 hours air or anoxia and various periods of reoxygenation (n=3). (See appendix 4)

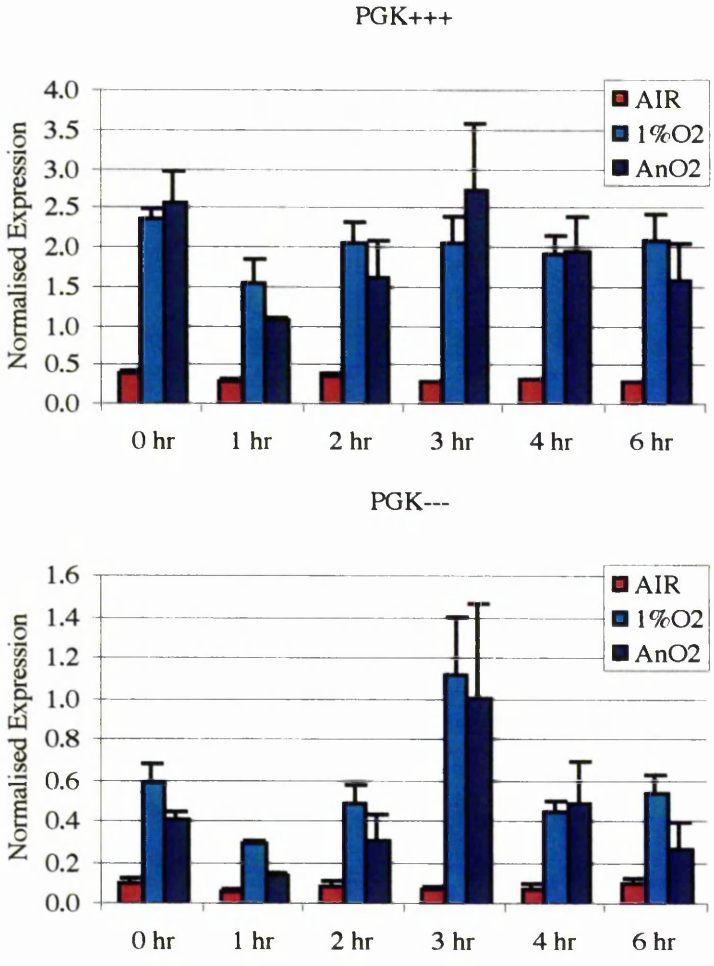

Table 3.9: Induction of pGL3.Control, pGL3.PGK^{+++} and pGL3.PGK^{---} in the human head and neck carcinoma cell line SQD9, exposed to 16 hours air or anoxia (n=3).

	PGK+++		PGK---	
	1%	ANO2	1%	ANO2
No reox	6.1	3.0	5.7	4.1
1 hr reox	5.3	1.4	4.4	2.1
2 hr reox	5.5	2.0	5.3	3.3
3 hr reox	7.0	3.1	13.7	12.3
4 hr reox	5.9	2.3	5.8	6.3
6 hr reox	7.3	1.9	5.2	2.7

There were no significant differences in PGK expression at varying reoxygenation times. However, there appeared to be a peak at one and three hours post-hypoxia in the HT1080 cells and three hours in the SQD9 cells.

3.3.4 Importance of the core HIF-1 binding site for HRE function

For further proof that it was the PGK HRE producing the oxygen related induction in luciferase expression, the PGK^{+++} was mutated at the core HIF-1 binding site (figure 3.1) to produce PGK^{mut}. The PGK constructs were transiently co-transfected, as previously described into the HT1080 and SQD9 cells and exposed to 16 hours air, hypoxia, or anoxia and three hours reoxygenation prior to assaying for firefly and renilla activities.

Figure 3.9: Normalised expression of pGL3.PGK^{+++}, pGL3.PGK^{---} and pGL3.PGK^{mut} in two human carcinoma cell lines, SQD9 and HT1080, exposed to 16 hours air or anoxia and three hours reoxygenation (n=3).

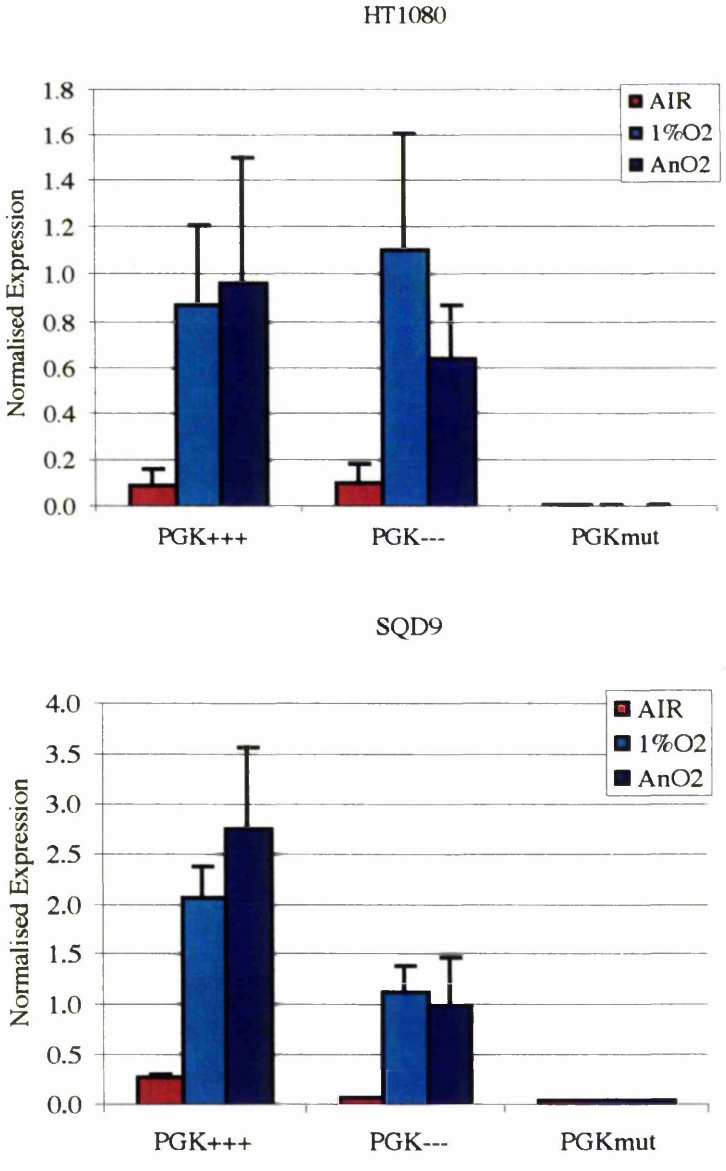

3.3.5 Calcium phosphate versus electroporation as a method for transfection

It was noted that some of the absolute luciferase values produced by the luminometer for certain cell lines were considerably lower than others. This suggested a reduced transfection efficiency, which hampered experimental reproducibility. Using the already optimised protocol, ie 10:1 ratio and three hours reoxygenation, two of the cell lines were transfected by electroporation to determine if this increased efficiency. They were electroporated at 280 or 320V (1500μF), depending on the cell line (See table 2.1) with various total quantities (μg) of DNA and the protocol was followed as previously described.

Figure 3.10: Normalised expression of pGL3.PGK^{+++} transiently transfected into the human carcinoma cell lines MDA 468 and HT1080, at 40:1 and 10:1 ratios respectively, by electroporation. (n=2).

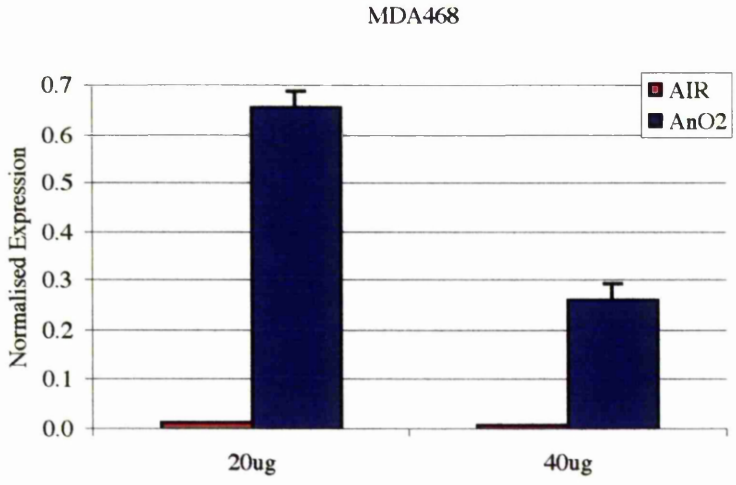

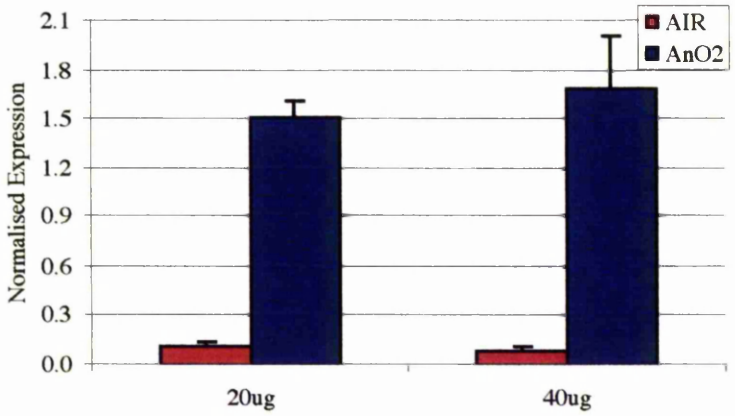

Table 3.9: Comparitive inducibility of the pGL3.PGK^{+++} vector transfected by either calcium phosphate (at chosen parameter, see earlier) or electroporation.

	PGK^{+++}		
	Calcium Phosphate	Electroporation 20ug	40ug
HT1080	5.2	13.5	17.9
MDA 468	41.1	48.8	31.9

3.4 Discussion

There was little difference in the amplitude of pGL3.PGK luciferase gene expression with the different quantities and ratios of total DNA used, irrespective of HRE orientation. It was considered that 5μg might encourage inaccuracies when aliquoting DNA and 15μg might possibly begin to saturate the transcriptional response in other cell lines that will be added to the panel later. Inducibility of the HRE appeared marginally higher at the 10:1 versus the 40:1 ratio. Using the 10:1 ratio could account for lower transfection efficiencies in the expanded cell line panel where it was possible that the pRL.CMV may become low enough to limit experimental accuracy at a ratio of 40:1. Therefore experiments were performed with 10μg of total DNA at a 10:1 ratio (firefly:renilla).

The pGL3.Control plasmid was minimally affected by changes in oxygen concentration in each of the cell lines tested. The level of expression produced by this construct was consistent between experiments within individual cell lines, thus providing a reproducible internal constant. All values were normalised against the aerobic pGL3.Control value (see 3.3.1), therefore inter-experimental and inter-cell line comparisons could be made.

A comparative evaluation of the pRL.CMV and pRL.TK plasmids, as internal transfection controls, clearly suggested the pRL.CMV vector was superior and would provide more reproducible values. CMV is one of the most efficient eukaryotic promoters in most cell types (Boshart et al., 1985). The amplitude of pRL.TK was exceptionally low, (ca. 250-400 light units; figure 3.6), and once background readings of wild-type cells were subtracted (in the range of 80-200 light units) this reading became highly inconsistent. One option would be to increase the pRL.TK values by altering the ratio from 10:1 to 3:1, for example. However, the protocol supplied by Promega recommends a ratio in the range of 10:1 to 60:1 and excessive renilla vector may compete for essential factors required for assembly of the transcription initiation complex. As more pRL.TK is introduced into the system there will be less HRE reporter for total DNA to remain constant. The data presented here demonstrates that the normalised ratios of pGL3.PGK when using either pRL.CMV or pRL.TK as the internal control are very similar irrespective of promoter usage (figure 3.5). This suggests that no promoter cross-talk (squelching) was occuring at these ratios. The greater amplitude of pRL.CMV (figure 3.6) introduces fewer issues of variability, ie 10 000-fold rather than 3-fold above background. To further support the use of renilla-CMV (pRL-CMV), published data by Boast et al., 1999, demonstrates no variation in CMV luciferase expression (CMV was inserted into the pGL3.basic vector, Promega) at a range of oxygen tensions and at 0.1% oxygen their PGK ($18bp^{-}$) HRE expression was greater than that of CMV in the human breast carcinoma cell line, T47D (figure 3.11). Thus collective experimental and published evidence supported the use of pRL.CMV in preference to pRL.TK.

Figure 3.11: Induction of the CMV immediate early promoter under levels of hypoxia.

Results are of triplicate experiments in the T47D human breast carcinoma cell line. Firefly luciferase activity was normalised to the renilla luciferase activity and these values were plotted below. (Taken from Boast et al., 1999)

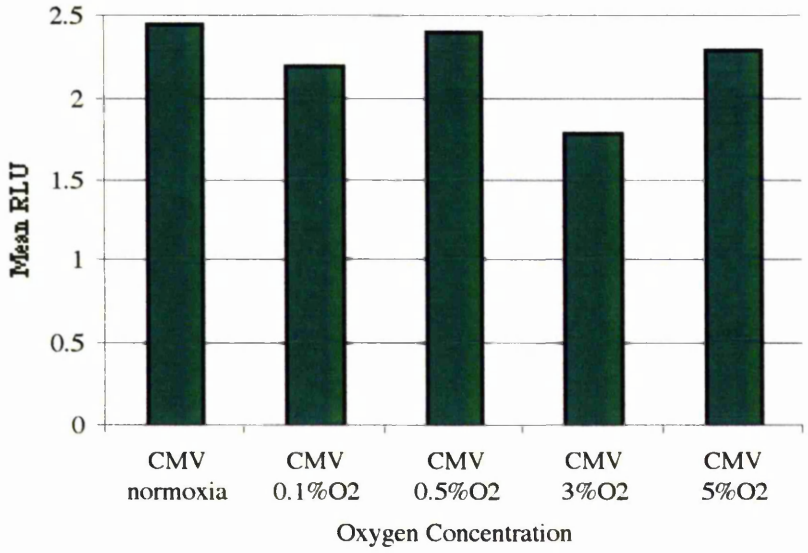

Due to the inter-experimental variability there were no significant differences in luciferase gene expression with varying length of reoxygenation ($P<0.05$). However, there may be a slight exception with a peak in both pGL3.PGK^{--} amplitude and induction at three hours reoxygenation, in the SQD9 cell line.

By changing the method of transfection from calcium phosphate to electroporation it was possible to increase the transfection efficiency of all three cell lines. This meant that in some cases (MDA 468) the raw data produced by the luminometer was significantly higher than background readings and in the case of the HT1080 cell line there was a greater HRE amplitude and induction with electroporation, compared to calcium phosphate transfection.

The induction ratio of pGL3.PGK^{+++} versus pGL3.PGK^{---} appeared to be cell line specific. Boast et al., 1999, indicated that the negative orientation of PGK had a far superior response. However, this result was only reported in a single cell line, the human breast carcinoma T47D. The data presented here suggests that the orientation phenomena of PGK is cell line specific. The mutation in the HIF-1 binding site in the PGK sequence severely reduced transcriptional activation of the luciferase reporter and probably eliminated this mutation has been shown to prevent HIF-1 binding in the hypoxic cells (Ebert et al., 1995).

In summary, the preliminary evaluation of the 18-bp trimer of PGK HRE allowed the determination and optimisation of:

1. enhancer orientation in the heterologus SV40 basal promoter context
2. total plasmid quantity per transfection ($CaPO_4$ and electroporation)
3. reporter : control vector ratios
4. control vector promoter usage
5. lack of reporter and control promoter "squelching"
6. reoxygenation phenomenon

Chapter 4

Optimisation of hypoxia responsive elements (HREs) for gene therapy

This chapter has been divided into three sections. Initial work compared the hypoxic and anoxic inducibility of a number of HREs (previously optimised by other investigators) in a panel of human carcinoma cell lines. Following on from this two of the HREs were selected for dissection of their functional elements and further optimisation in the same cell line panel. Finally, the *trans*activation of each HRE by either HIF-1a or EPAS-1 was studied in a modified cell line, Ka13, which does not express either of these transcription factors.

Part 1: Comparitive hypoxia-inducible expression of previously 'optimised' HREs

4.1.1 Introduction

A number of genes are upregulated in response to tissue hypoxia, including erythropoeitin (Epo), vascular endothelial growth factor (VEGF), phoshogycerate kinase 1 (PGK), lactate dehydrogenase A (LDH-A) and glucose transporter 1 (Glut-1). The transcriptional response of these genes to hypoxia is predominantly regulated by the transcription factor HIF-1, previously described in chapter 1. The HIF-1 binding site contained within each promoter is absolutely necessary but not always sufficient for hypoxia inducible activity. It is likely that there is a cooperative interaction between factors binding at adjacent *cis*-acting sites that are required for optimal hypoxic function. So far this study has only examined the PGK 18bp HRE, composed of a minimal HIF-1 binding region (site 1; figure 4.1), which has been shown to be 'optimal' for hypoxic

function in a heterologous SV40 or CMV promoter context (Boast et al., 1999). A number of independent studies have identified hypoxia responsive enhancer sequences within the gene regulatory sequences for; Epo (Pugh et al., 1993; Firth et al., 1994), VEGF (Liu et al., 1995), PGK (Firth et al., 1994; Boast et al., 1999 [18bp]; Semenza et al., 1994 [24bp and 26bp]), Glut-1 (Ebert et al., 1995), and LDH-A (Firth et al., 1995). However, these investigations were usually restricted to a single cell line. In this chapter the optimised sequences, described in earlier studies, were compared side-by-side for their response to low oxygen tensions in a panel of human carcinoma cell lines (MDA 468, HT1080, and SQD9). For ease, each site has been given a simple nomenclature to which it will be referred to for the remainder of this thesis (figure 4.1).

Figure 4.1: Hypoxia Response Elements and their co-operative cis-acting sequences

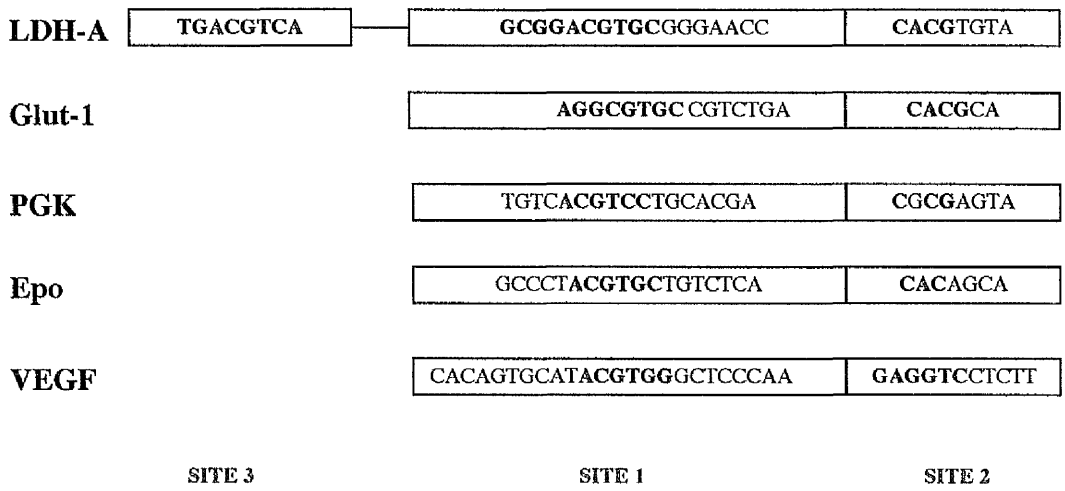

The HREs from each hypoxically regulated gene all contain core HIF-1 binding sites. However, they differ in their natural sequence context and their *cis*-acting co-activated enhancer sequences. Site 1 contains the core HIF-1 binding site, essential for oxygen-regulated gene transcription. The conserved sequence is shown in bold. Nucleotides ACGT have been shown to be essential for oxygen-regulated transcription

of the Epo gene by DNAse I protection assays (Wang and Semenza, 1993; Pugh et al., 1994).

Site 2 has been shown to be an essential second binding site within the 26bp Epo HRE and has been termed a carbohydrate response element (ChoRE) in the LDH-A HRE. As shown in figure 4.2, mutations at either site 1 (nucleotides 5-12) or 2 (nt 21-24) of the Epo HRE ablated the hypoxic response in HepG2 and CHO cells, as did increasing the natural spacing between these two sites from 4 to 8bp (Wang and Semenza, 1993; Pugh et al., 1994). This evidence suggests a cooperation between site 1 and 2 is essential, at least in the Epo HRE.

Figure 4.2: Mutations of the Epo HRE define the two functional regions required for hypoxic gene activation.

Mutations were made in the 26bp Epo HRE, sites of nucleotide substitutions are indicated. Plasmids containing the enhancer mutations were transiently transfected into HepG2 cells and exposed to either hypoxia or normoxia. Hypoxia inducible activity of the mutant enhancers is expressed as a percentage of that of the unmutated enhancer. Data shown is the mean of three independent experiments (Pugh et al., 1994).

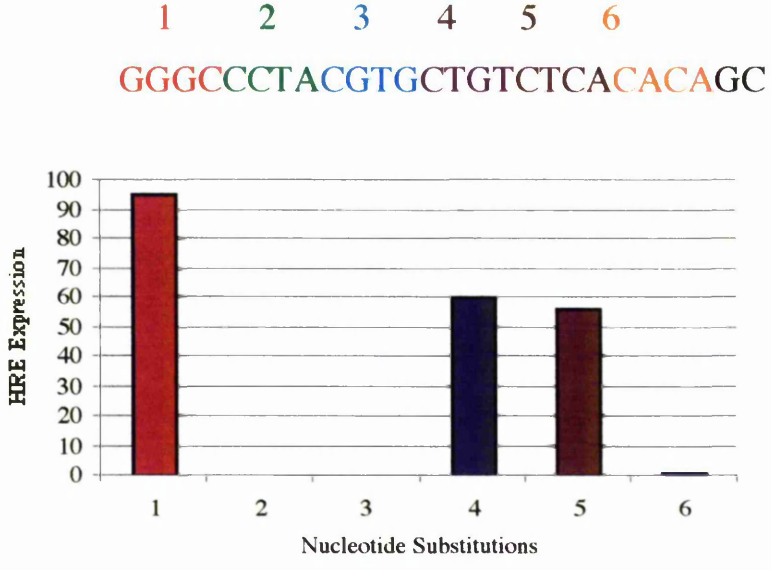

A similar interaction has been demonstrated for the LDH-A HRE. Mutation of site 1, 2 or 3 severly reduces or ablates the hypoxic response, however, constructs containing site 1 with either of the other two sites could confer a hypoxic response, although significantly reduced compared to the full HRE containing all three sites (Firth et al., 1995). Site 1 of the PGK HRE has been shown to function independently of site 2 if the sequence is multimerised, with a trimer of site 1 providing the optimal response in either orientation. The 24bp PGK HRE did not improve on the hypoxic response of PGK 18bp (Firth et al., 1994).

Site 3 is a cAMP response element (CRE). It should be noted that Glut-1 also contains CRE (site 3), but it is approximately 300bp downstream (3') of the HIF-1 binding site, as well as a number of other cooperative transcription sites (Figure 4.3).

Optimisation of each hypoxically regulated HRE, shown in figure 4.1, was determined to dissect out the importance of the different HIF-1 and co-activated enhancer sequences. Both the amplitude of response and the level of induction was determined under hypoxia and anoxia in relation to normoxia, in a panel of human carcinoma cell lines.

Figure 4.3: A schematic representation of the functional *cis*-acting elements within the Glut-1 enhancer sequence.

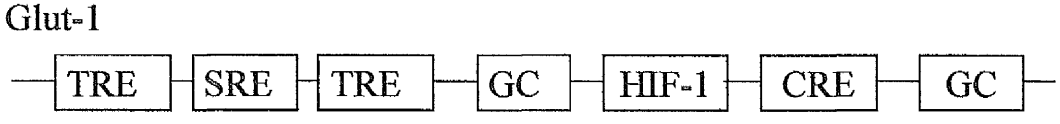

4.1.2 Methods

The pGL3 luciferase vector containing the HRE from LDH-A, was kindly donated by Oxford Biomedica. Oligonucleotides containing HREs from the genes encoding Epo, PGK and VEGF were synthesized by SigmaGenosys. They were designed with Bgl II and Bam HI sites at their ends so that they could be cloned into the Bgl II site, 5' of the minimal SV40 promoter in the pGL3.promoter vector (Promega). The 610bp HRE from the Glut-1 gene was isolated from Sp72 at Xba I (5') and Xba I (3') and cloned into the Nhe I site upstream of the minimal SV40 promoter in the pGL3.promoter vector. Each HRE sequence was inserted as a trimer, into the pGL3 vector in its homologous orientation (positive), the only exception to this was Glut-1, already 610bp long, as it proved impossible to construct multimers due to *in situ* bacterial rearrangement and was therefore tested as a monomer. The structure of each construct was confirmed by digestion with restriction endonucleases and dideoxy sequencing. The pGL3.control plasmid (Promega) that contains the SV40 enhancer and promoter was employed as an expression control (RLU = 1.00) to allow normalisation of all RLU values.

A trimer of each HRE sequence in the positive orientation, attached to a firefly luciferase reporter gene (reporter vector) was independently co-transfected, by electroporation, with a CMV-driven Renilla luciferase expression plasmid, into a panel of human carcinoma cell lines (20μg plasmid DNA at a 10:1 ratio (firefly:renilla), as optimised in chapter 3). The capacity of each vector construct to regulate gene expression in response to low oxygen was quantified relative to the pGL3.control vector (SV40 early gene promoter). After 24 hours recovery, cells were reseeded into a 24 well plate and exposed to 16 hours air (37°C, 5% CO_2 humidified incubator), hypoxia (1% O_2, 5% CO_2, 94% N_2, humidified) or anoxia (> 0.002%O_2). Following exposure, cells were returned to normoxia for three hours and subsequently were lysed and assayed for firefly and renilla luciferase activities (Promega Dual Luciferase assay system).

4.1.3 Results

Here we refer to the HREs contained within the pGL3 vectors as enhancers and to the region containing the transcriptional start site and the minimal SV40 promoter as a minimal promoter. To optimise oxygen regulated gene expression, each pGL3 vector contains three copies of the HRE each of which was in its homologous orientation denoted by '+', (reverse of homologous / negative orientation denoted by '-')with identical synthetic linkers between each HRE repeat to maintain a constant spacing phenomenon. The numbers in brackets, eg. PGK (1+2), denote the sites which compose each HRE from the respective gene (figure 4.1). The number displayed outside the brackets indicates HRE copy number. All experiments were performed in triplicate and results were calculated as previously described in section 3.3. The mean of the normalised values and the stanadard deviation (Sdev) and standard error (SE) of the mean were determined for each experiment. The amplitudes were plotted for each HRE under air, hypoxia and anoxia, for each cell line tested.

Figure 4.4: Amplitude of HRE-luciferase constructs exposed to 16 hours air, hypoxia or anoxia and three hours reoxygenation in the MDA 468 human breast carcinoma cell line. (n=3).

(See appendix 5)

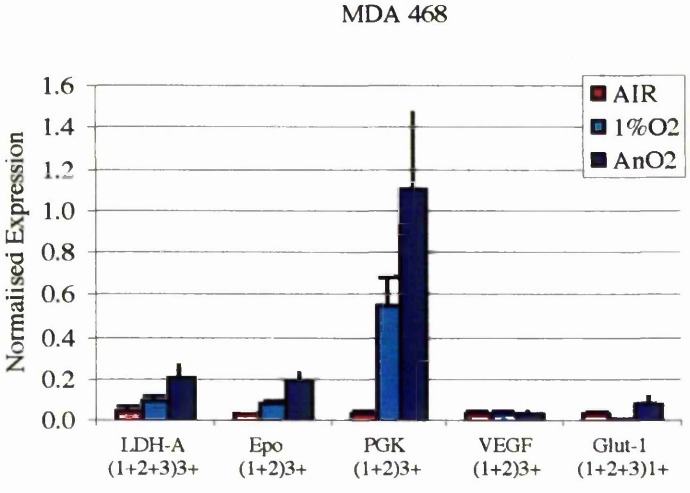

Figure 4.5: Amplitude of HRE-luciferase constructs exposed to 16 hours air, hypoxia or anoxia and three hours reoxygenation in the HT1080 human fibrosarcoma cell line. (n=3).

(See appendix 6)

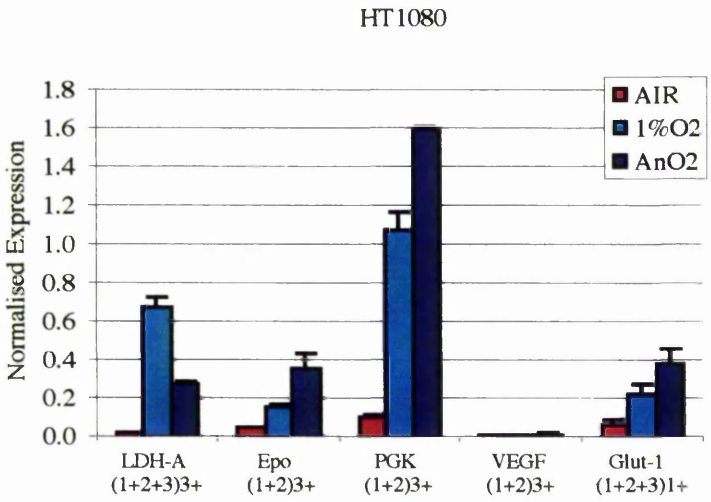

Figure 4.6: Amplitude of HRE-luciferase constructs exposed to 16 hours air, hypoxia or anoxia and three hours reoxygenation in the SQD9 human head and neck sarcoma cell line. (n=3).

(See appendix 7)

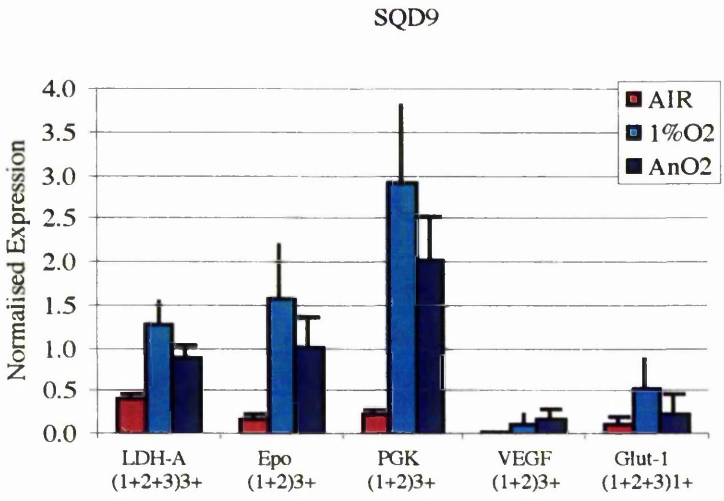

Table 4.1: Relative induction of 5 "optimal" HREs in 3 human carcinoma cell lines. (n=3).

	HRE Induction					
	MDA 468		HT1080		SQD9	
Gas-phase O_2	$1\%O_2$	AnO_2	$1\%O_2$	AnO_2	$1\%O_2$	AnO_2
LDH-A $(1+2+3)^{3+}$	2.0	4.0	22.7	9.1	3.2	2.2
Epo $(1+2)^{3+}$	2.8	5.9	3.3	7.3	9.2	5.9
PGK $(1+2)^{3+}$	17.0	33.8	9.7	14.6	12.1	8.4
VEGF $(1+2)^{3+}$	1.1	1.1	2.0	2.9	4.4	5.6
Glut-1 $(1+2+3)^{1+}$	2.0	2.8	3.2	5.5	4.1	1.9

The data above shows the amplification of HRE expression under the three experimental conditions (air, hypoxia and anoxia), normalised against the aerobic pGL3.Control vector which was non-responsive (data not show). In each cell line tested, PGK (1+2) gave the most robust response to both hypoxia and anoxia compared to the other HREs tested. The amplitude of the remaining four HREs, in relation to one another, appeared to be cell line specific.

The inducibility of each HRE, i.e. the expression under either hypoxia or anoxia relative to the basal (oxic) expression, between cell lines is shown in the table above (4.1). The most inducible being PGK (1+2) both within and between the cell lines tested.

4.1.4 Discussion

All HREs tested induced firefly luciferase expression, to varying degrees, by exposure to either hypoxia ($1\%O_2$) or complete anoxia ($\geq 0.002\%$ O_2). The basal (oxic) expression of each HRE was significantly lower than the hypoxic and anoxic. The normoxic expression of Epo was lower than PGK in all cases and in two out of three cases the LDH-A baseline was higher than Epo. PGK demonstrated a far superior hypoxic and anoxic (amplitude and induction) activity compared to the other HREs tested. This is supported by data from Boast et al. (1999), they showed a trimer of PGK, inserted into the pGL3.promoter expression vector (containing the minimal SV40 promoter), to be the most inducible to 0.1% O_2 when compared to the Epo, ENO1 and LDH-A HREs. The PGK $(1+2)^{3+}$ HRE had the lowest basal expression and greatest amplitude under hypoxia and anoxia in the MDA 468 cell line. This was not seen in the HT1080 and SQD9 cell lines; PGK had a lower inducibility, but it was still superior to the induction of the other HREs. Boast and colleagues (1999), concluded that the $PGK(1)^{-}$ construct has a superior response to both the fuller $PGK(1+2)^{3+}$ and the positive orientation i.e. $PGK(1)^{3+}$ and $PGK(1+2)^{3+}$ and was thus their 'optimised' HRE of choice. However, their data was derived from a single cell line, T47D. The results presented here and in Chapter 3, corroberate the general conclusion that the PGK HRE is the most robust HRE tested, however, the most active PGK variation appears to be cell line dependent.

The reduced oxygen tension had little effect on VEGF in all three cell lines tested, with inductions of 1.12 and 1.05 fold in the MDA 468's; 1.96 and 2.87 fold in the HT1080's; 4.43 and 5.62 fold in the SQD9's, at $1\%O_2$ and anoxia respectively. This is in contrast to recently published data by Shibata et al., 2000. Using a pentimer of the same VEGF sequence linked to a CMV minimal promoter, Shibata and colleagues (2000), demonstrated over a 500-fold induction in VEGF under hypoxia in the HT1080 cell line. From the data presented later in this chapter it is unlikely that increasing the copy number would alter the inducibility of VEGF from 1.96 to 500-fold. The work presented above uses the minimal SV40 promoter, which has a similar basal activity to the

minimal CMV promoter and yet in the same cell line only a 1.96-fold induction was seen under hypoxia. Results appear to have been normalised in the same way and experimental conditions were similar with the exception of the choice of the renilla control plasmid. Shibata and colleagues (2000), used the HRE and CMV promoter together in the pGL3 vector as well as pRL.CMV as the transfection control. It may be that there was cross-talk between the two promoters. The study by Lui et al. (1995), has shown the 35bp VEGF sequence described here to be optimal for oxygen-related gene expression. The work presented here and by Shibata et al. (2000) used the optimised 35bp sequence but there is significant discrepancy in the data. The results produced by Shibata and colleagues (2000), would suggest that VEGF has a greater activity than all other HREs tested in the HT1080 cell line. This could be investigated by independently transiently transfecting the HT1080 cells with each HRE, exposing to air or hypoxia and measuring changes in mRNA and protein levels of each HRE, as well as HIF-1a and EPAS-1 (see section 4.3).

VEGF gene induction in response to tissue hypoxia may be tissue specific *in vivo* (Sandner et al.,1996). Blancher et al. (2000), showed significant variation in VEGF and LDH-A mRNA levels across a panel of human breast carcinoma cell lines exposed to 16 hours hypoxia. The least aggressive cell lines (defined by clonogenic survival assays) had the lowest basal expression and the greatest inducibility (T47D; see chapter 5), whereas the more aggressive cell lines (MDA 468) had a higher normoxic expression and thus a lower level of induction. When the protein levels of HIF-1a and EPAS-1 were measured in these normoxic and hypoxic cell extracts it was observed that there was an inverse correlation between clonogenic survival and the induction of HIF-1a and EPAS-1 after hypoxic exposure. This implies cells with the greatest survival under hypoxia have the smallest induction in HIF-1a and EPAS-1 proteins (Blancher et al., 2000).

The results for LDH-A and Glut-1 activity correlate with those produced by Firth et al. (1995) and Ebert et al. (1995); they demonstrated a 1.67-fold ±0.26 (n=4) induction in LDH-A and a 3 to 5-fold induction in Glut-1 activity by exposure to 1%O_2 in the human cervical (HeLa) and fibrosarcoma (HT1080) cell lines, respectively. A

similar level of induction is shown in the data above (Table 4.1), the exception being the HT1080 cell line where LDH-A expression was much higher. The LDH-A and Glut-1 HREs also had very low levels of induction and a much higher baseline in the MDA 468 and SQD9 cell lines. The firefly values were not significantly low suggesting that this was not an artifact of transfection efficiency. It is more likely that they have a more modest inducibility compared to PGK and Epo because there is considerable constitutive activity. Oligonucleotides of the LDH-A and Glut-1 HREs have been shown to compete with PGK and EPO for binding at the HIF-1 site, with Glut-1 displaying the lowest affinity (Ebert et al., 1995). This competition was reduced if any of the HIF-1 sites were mutated, rendering them non-functional (Ebert et al., 1995; Firth et al., 1995). Another reason for their low amplitude could be attributed to the presence of a CRE binding site (site 3) in both LDH-A and Glut-1. This element is not contained within the PGK and Epo HREs. It may be possible that the CRE has a regulatory control over adjacent *cis*-acting elements, eg HIF-1 binding site, this will be explored in part 2 of this chapter.

HRE expression was slightly higher at 1%O_2 compared to anoxia in the SQD9 cell line, the opposite was seen in the HT1080 and MDA 468 cell lines. This demonstrates the importance of testing HRE expression at a range of low oxygen tensions and in a variety of human carcinomas originating from different tissues. In this section, the full sequences shown above, were tested for their ability to evoke both a hypoxic and anoxic response. The data presented not only demonstrates PGK (1+2) to be the superior HRE within the series tested, but also the importance for HRE optimisation across a panel of human carcinoma cell lines.

Part 2: Dissection of the LDH-A and Glut-1 enhancer sequences

4.2.1 Introduction

The molecular response to hypoxia involves a complex integration of signalling cascades that are triggered by diverse but related changes in tissue pO_2, cellular redox and metabolic status. Sequence conservation exists not only at HIF-1 binding sites, but also at adjacent sites shown to be of functional relevance. This interrelationship of *cis*-acting sequences suggests that the other factors which bind at these adjacent motifs are important for both the operation of HIF-1, and the co-operative induction of gene expression in response to low oxygen tension. For example the lactate dehydrogenase A gene (LDH A) is regulated by a tripartite enhancer element containing a central HIF-1 binding sequence, a cAMP-response element (CRE) and a carbohydrate-response element (ChoRE; figure 4.7). It has been reported that each element must be present for an intact hypoxic-response (Firth et al., 1994).

Figure 4.7: Functional domains of LDH-A

5'- GCTGACGTCAGAGTGGGAGCCCAGCGGACGTGCGGGAACCCACGTGTA – 3'
CRE HRE ChoRE

In part 1, it was observed that the complete hypoxia-responsive sequence from the LDH-A (1+2+3), and Glut-1 (1+2+3) enhancers, were less effective than the 'optimised' HREs derived from either that of Epo, or PGK-1. It was hypothesised that the CRE contained within the LDH-A and Glut-1 sequences might modulate the amplitude of the adjacent elements. Reporter constructs were made containing the distinct elements of the LDH-A enhancer, and the Glut-1 enhancer lacking the CRE (site 3), in multimerised form. These were compared to the original HRE sequences to determine if any improvement in hypoxic and anoxic activity could be achieved.

4.2.2 Methods

Oligonucleotides consisting of trimers of the individual domains of the LDH-A HRE were made (SigmaGenosys) with Bgl II and Bam HI ends and cloned into the Bgl II site of pGL3.promoter vector (Promega). The short, 326bp, Glut-1 sequence (Sites 1+2 only) was excised from Sp72 at Xba I (5') and Xba I (3'; Ebert et al., 1995) and cloned into the pGL3.promoter, as a dimer, at the Nhe 1 site. Both cloning sites were located upstream of the minimal SV40 promoter.

The DNA constructs encoding the firefly luciferase reporter gene, under the transcriptional control of the individual LDH-A functional domains or Glut (1+2) were transiently co-transfected with pRL.CMV, by electroporation, into a panel of human carcinoma cell lines (HT1080, MDA468, SQD9) as previously described. 24 hours after transfection, cells were reseeded into a 24 well plate and exposed to 16 hours air, hypoxia, or complete anoxia. Following exposure, cells were returned to normoxia for 3 hours and subsequently were lysed and assayed for firefly and renilla luciferase activities.

4.2.3 Results

The copy number of HREs is known to affect hypoxic inducibility (see later). An initial experiment was performed to ensure that the LDH-A (1+2+3) trimer was not saturating the hypoxic response. The results shown overleaf indicated that the LDH-A trimer had a far greater amplitude and inducibility, despite a slight increase in basal activity, than the corresponding monomer or dimer. It may be possible to make further improvements by increasing the copy number. However, the aim of this study was to compare HREs taking into account their natural co-activated enhancer elements rather than copy number. The experiment was repeated under both hypoxia and anoxia to test the activity of each of the functional elements of the LDH-A and Glut-1 enhancers.

Figure 4.8: Comparative expression of LDH-A (1+2+3) monomer, dimer and trimer, exposed to 16 hours air or anoxia in the HT1080 cell line, n=3.

(See appendix 8)

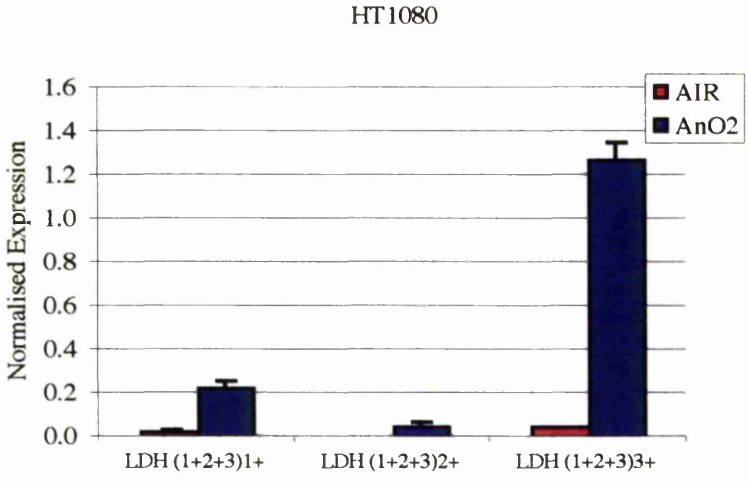

Table 4.2: Comparative inducibility of LDH-A (1+2+3) monomer, dimer and trimer, exposed to 16 hours air or anoxia in the HT1080 cell line, n=3.

	Induction ratio
LDH $(1+2+3)^{1+}$	9.6
LDH $(1+2+3)^{2+}$	16.6
LDH $(1+2+3)^{3+}$	28.7

Figure 4.9: Dissection of the functional elements of the LDH-A and Glut-1 enhancers in the MDA 468 human carcinoma cell line (n=3).

Cells were exposed to 16 hours air, hypoxia or anoxia followed by 3 hours reoxygenation. (See appendix 9)

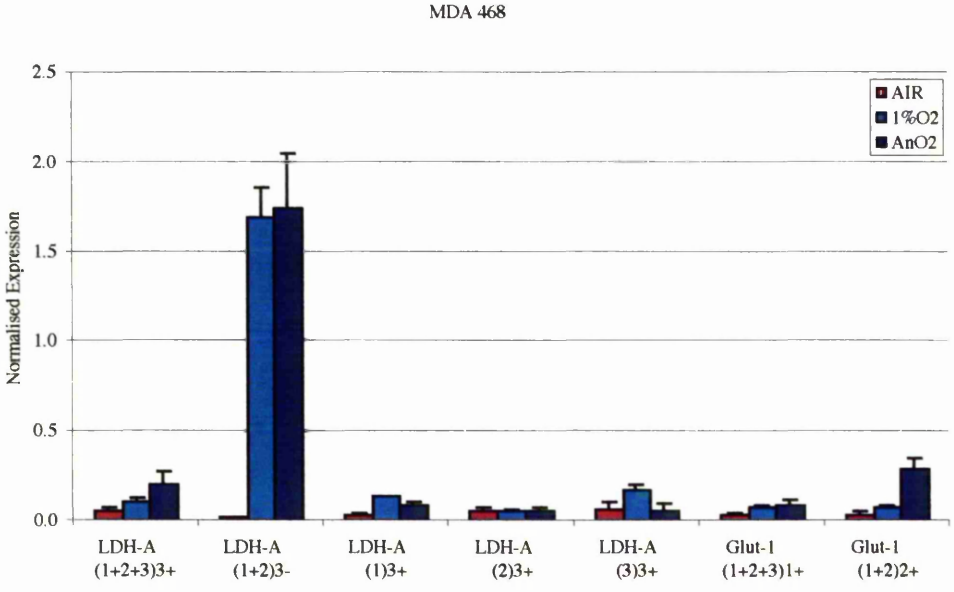

Figure 4.10: Dissection of the functional elements of the LDH-A and Glut-1 enhancers in the HT1080 human carcinoma cell line (n=3).

(See appendix 10)

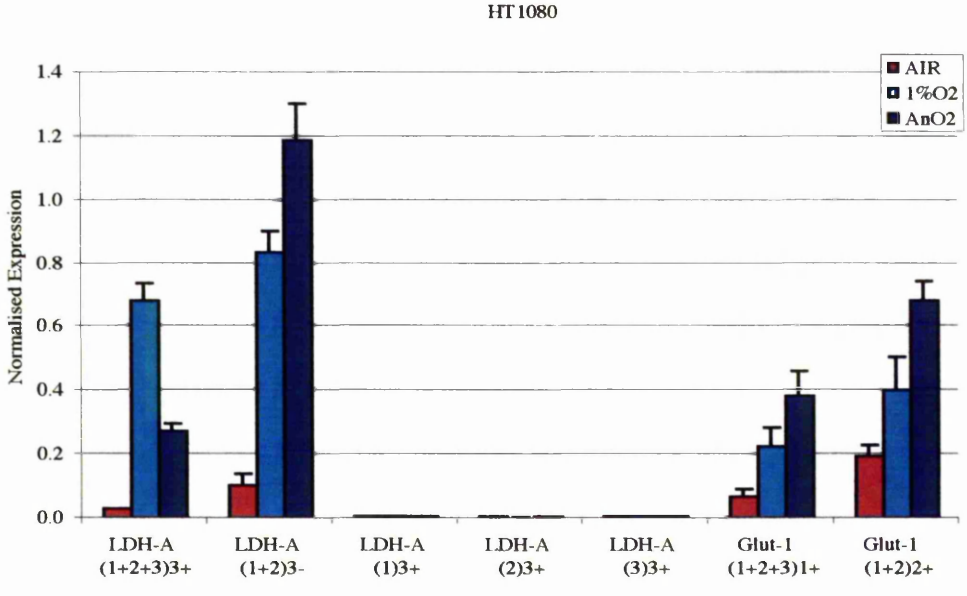

Figure 4.11: Dissection of the functional elements of the LDH-A and Glut-1 enhancers in the SQD9 human carcinoma cell line (n=3).

(See appendix 11)

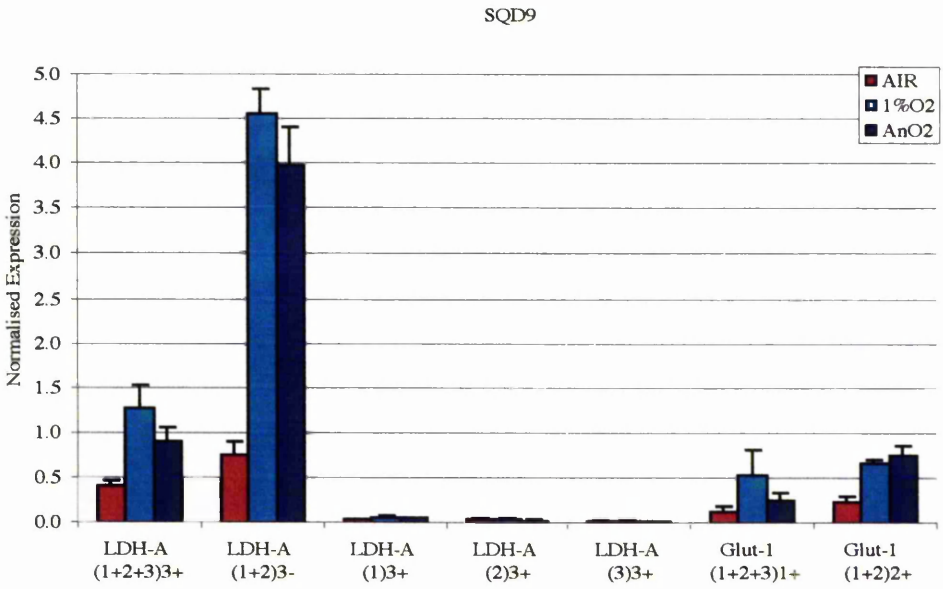

Table 4.3: Inducibility of the functional elements of the LDH-A and Glut-1 enhancers under hypoxia or anoxia in three human carcinoma cell lines.

	HRE Induction					
	MDA 468		HT1080		SQD9	
Gas-phase O_2	1%O_2	AnO_2	1%O_2	AnO_2	1%O_2	AnO_2
LDH $(1+2+3)^{3+}$	2.0	4.0	22.7	9.1	3.2	2.2
LDH $(1+2)^{3-}$	75.2	77.7	8.1	11.6	6.1	5.3
LDH $(1)^{3+}$	3.9	2.3	0.7	1.3	2.0	1.7
LDH $(2)^{3+}$	1.0	1.2	0.6	1.0	1.0	0.7
LDH$(3)^{3+}$	2.6	0.8	0.8	0.9	1.1	1.0
Glut-1 $(1+2+3)^{1+}$	2.4	2.8	3.2	5.5	4.1	1.9
Glut-1 $(1+2)^{3+}$	2.2	8.1	2.0	3.5	2.8	2.9

In each of the three cell lines tested, both LDH (1+2) and Glut (1+2) had a more robust hypoxic and anoxic activity compared to their corresponding HREs containing the CRE (site 3). Despite the improvement in Glut-1 activity it remains inferior to the PGK, Epo and LDH (1+2) HREs examined. Each of the three distinct elements from the LDH-A enhancer were essentially non-functionally when stimulated independently. The combination of LDH-A sites 1 and 2 produced an activity which was far greater than the full LDH-A (1+2+3) sequence and a maximal response under both hypoxia and anoxia in all three cell lines. In the HT1080 and SQD9 cell lines there were also an increase in LDH (1+2) basal expression, which is reflected in the poor induction ratios.

The data above employed the LDH (1+2) in the reverse (negative) orientation. As previously shown in chapter 3, it is important to investigate if any orientation phenomenon is apparent in this oxygen-regulated expression. Thus, both copy number and orientation were investigated for the three most robust HREs in this investigation, LDH $(1+2)^{3-}$, PGK $(1+2)^{3+}$, Epo $(1+2)^{3+}$. Cells were exposed to 16 hours air, hypoxia or anoxia, followed by 3 hours reoxygenation then lysed and assayed for firefly and renilla luciferase activities.

Figure 4.12: Expression of LDH $(1+2)^3$ in the forward and reverse orientation versus LDH $(1+2)^6$ in the negative orientation, in three human carcinoma cell lines, n=3. (See appendix 12)

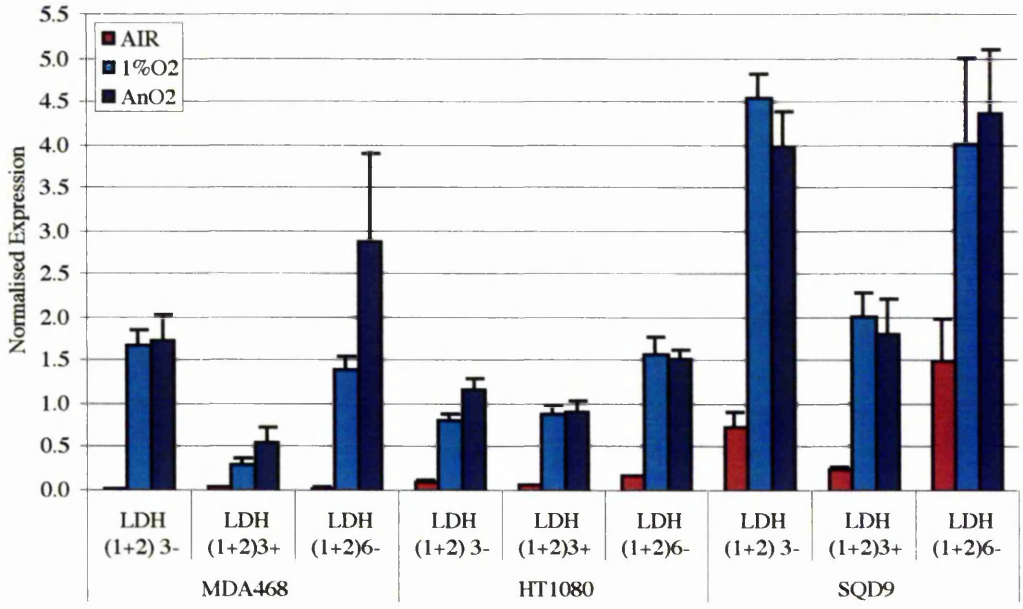

Figure 4.13: Expression of PGK $(1+2)^3$ in the forward orientation versus PGK $(1+2)^6$ in the positive orientation in three human carcinoma cell lines, n=3.

(See appendix 13)

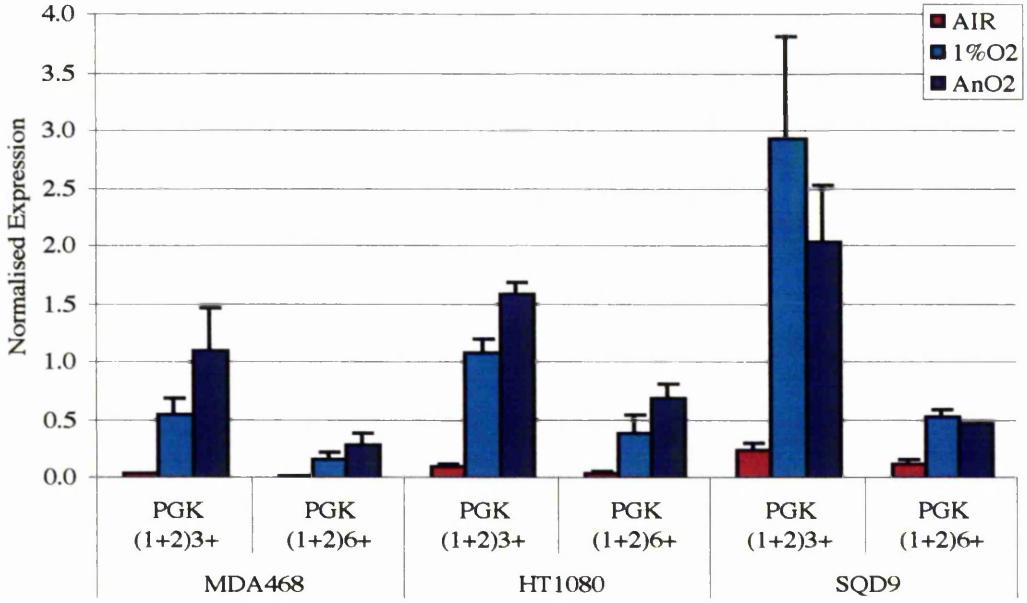

Figure 4.14: Expression of Epo $(1+2)^3$ in the forward orientation versus Epo $(1+2)^5$ in the positive orientation in three human carcinoma cell lines, n=3.

(See appendix 14)

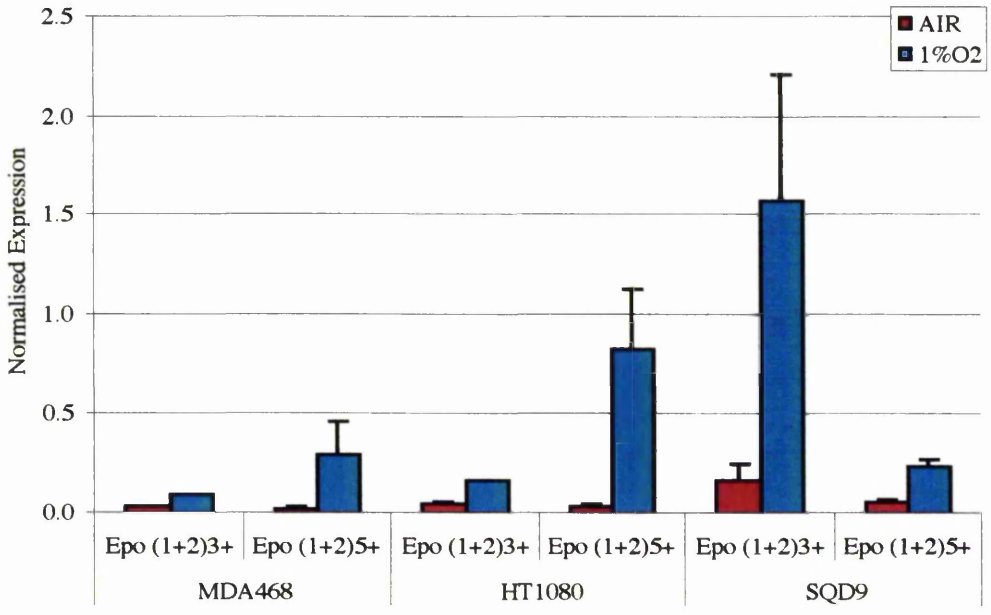

Table 4.4: Induction of LDH, PGK and Epo multimers in the three human carcinoma cell lines.

	HRE Induction					
	MDA 468		HT1080		SQD9	
Gas-phase O_2	$1\%O_2$	AnO_2	$1\%O_2$	AnO_2	$1\%O_2$	AnO_2
LDH-A $(1+2)^{3-}$	75.2	77.7	8.1	11.6	6.1	5.3
LDH-A $(1+2)^{3+}$	7.9	14.7	12.2	12.5	7.6	6.8
LDH-A $(1+2)^{6+}$	38.7	79.5	8.6	8.4	2.6	2.9
PGK $(1+2)^{3+}$	17.0	33.8	9.8	14.6	12.1	8.4
PGK $(1+2)^{6+}$	11.6	20.2	7.9	14.1	4.5	3.9
Epo $(1+2)^{3+}$	2.8		3.3		9.2	
Epo $(1+2)^{5+}$	14.1		20.4		3.9	

There was significant variation in the basal (oxic) activity between the three cell lines. Each variation of the LDH-A HRE had the greatest absolute activity in the SQD9 cell line, regardless of experimental conditions. This is reflected in low levels of induction (Table 4.4). The lowest basal expression (oxic) was observed in the MDA 468 cell line, which consequently produced the greatest induction ratios (Table 4.4). However, LDH $(1+2)^{3-}$ has a superior amplitude to LDH $(1+2)^{3+}$ in each of the three cell lines, demonstrating that orientation is important in the context of the LDH-A HRE. The LDH $(1+2)^{6-}$ has a higher basal activity in each cell line and an overall amplitude similar to that of LDH $(1+2)^{3-}$, therefore increasing the copy number had no significant advantage. The pattern of expression displayed by the three LDH HRE variants was consistent across the cell line panel, implying that the expression pattern was a property specific to the LDH HRE, not the activity of the cell line.

In contrast this correlation of increasing expression with increased HRE copy number was not observed with the PGK HRE. Increasing the copy number of the PGK HRE suppressed oxic (basal) expression but produced no further improvement in activity. A significantly poorer response was observed in each cell line tested.

In two out of three cell lines, an increase in the Epo HRE copy number produced an improved response under $1\%O_2$, with a minimal change in the basal activity. This was not seen in the SQD9 cell line. However, the S.D. for the $1\%O_2$ determination was large.

The results presented in figure 4.13 and 4.14 are supported by data published by Boast et al. (1999). They demonstrated that increasing PGK copy number from three to six resulted in a decrease in activity, whereas an increase in Epo copy number elevated expression.

The graphs overleaf compare the activities of the optimal LDH-A, Epo and PGK HREs in the three cell lines.

Figure 4.15: Comparison of the amplitude of the 'optimal' HREs in the MDA 468 human carcinoma cell line, n=3.

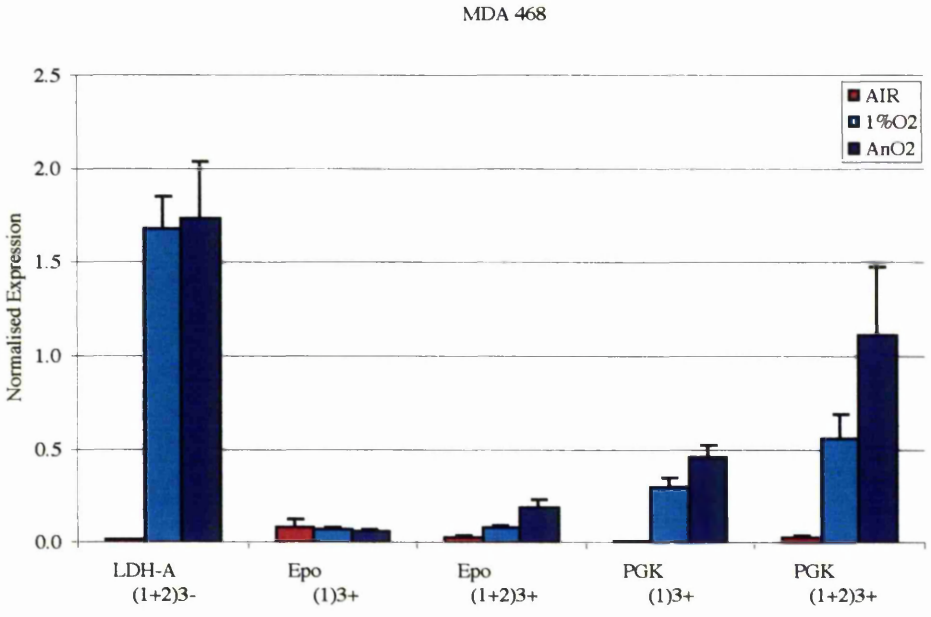

Figure 4.16: Comparison of the amplitude of the 'optimal' HREs in the HT1080 human carcinoma cell line, n=3.

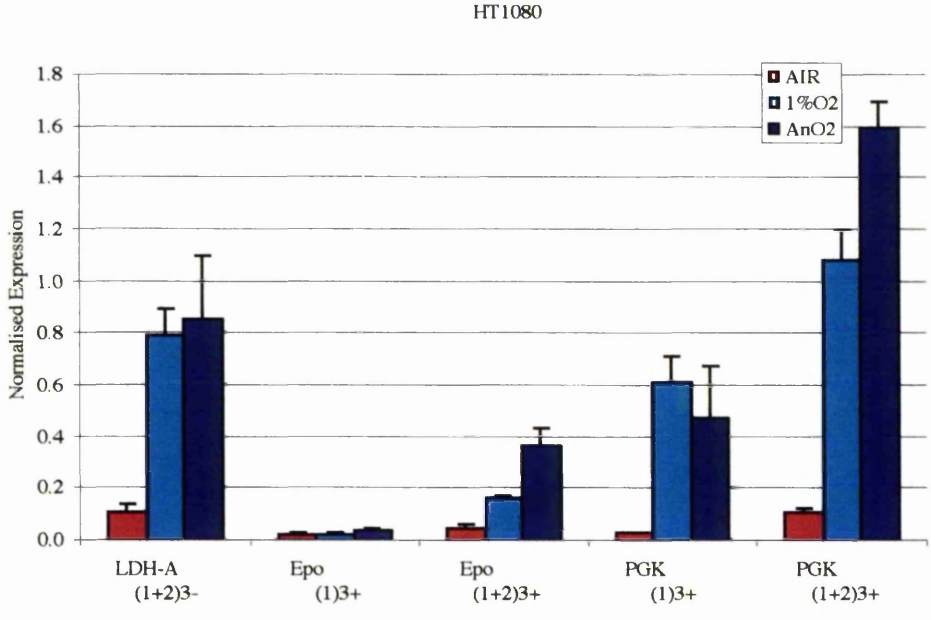

Figure 4.17: Comparison of the amplitude of the 'optimal' HREs in the SQD9 human carcinoma cell line, n=3.

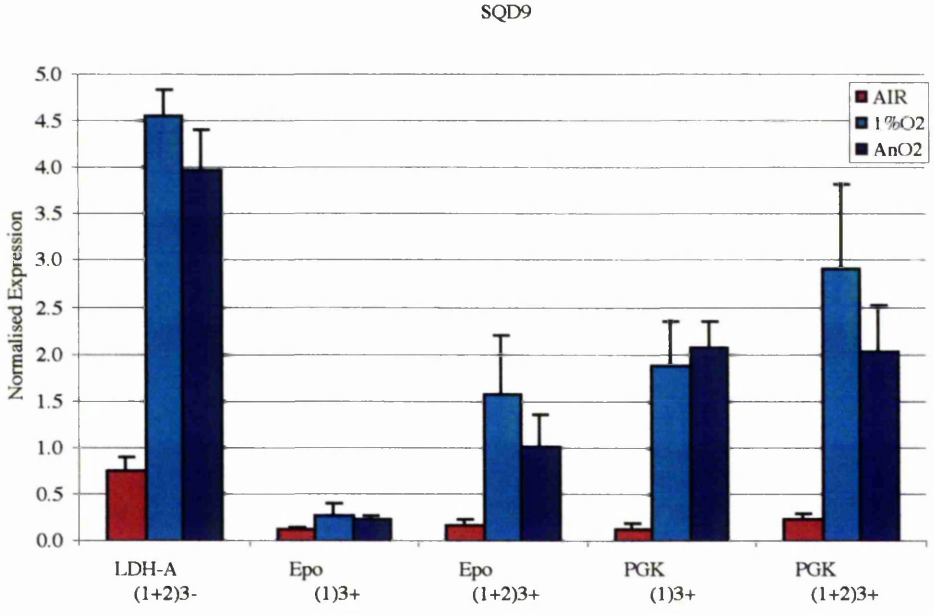

Epo and PGK site 1 only are also included to illustrate the importance of site 2 in these HREs. The data presented in figure 4.15-17 illustrates that site 2 is essential to the hypoxic response of the Epo HRE in each cell line tested, as previously demonstrated by Pugh et al. (1994) in HepG2 cells and Firth et al. (1994) in HeLa cells. In contrast, PGK site 1 can function independently of its site 2 when multimerised. Extension of the 18bp element to 24bp did not lead to a significant increase in activity in the data presented here or that by Firth and colleagues (1994). Site 2 appears to play a more significant role in inducibility in the Epo and LDH-A HREs compared to the PGK HRE in all three cell lines. In two of three cell lines LDH $(1+2)^{3-}$ has a greater amplitude under both hypoxia and anoxia compared to Epo and PGK.

4.2.4 Discussion

The Glut (1+2) 326bp and the LDH (1+2) 26bp sequences, both lacking the CRE site (site 3), had a significantly magnified hypoxic and anoxic activity resulting from an increase in the amplitude of expression rather than a decrease in basal (oxic) activity. This suggests that the CRE had a negative regulatory effect on the hypoxic expression of these enhancers. Ebert et al. (1995) also demonstrated the superior hypoxic response of the shorter Glut sequence, lacking site 3. However, in the HT1080 and SQD9 cells there appeared to be a poor level of induction due to a corresponding increase in normoxic expression (Table 4.2). Despite the increase in Glut (1+2) activity it remained inferior to that displayed by PGK (1+2) and LDH (1+2). Both the Glut-1 enhancer variations are significantly larger than any of the other HREs being examined and contain an increased number of *cis*-acting elements adjacent to the hypoxia responsive enhancer. It is probable that considerably more transcription factors are bound at adjacent sites, resulting in a more complex interaction between HIF-1 and its cognate HRE.

A significant improvement was made to the hypoxia regulated activity of LDH-A trimer by removal of site 3. The negative orientation of this construct, LDH (1+2) had the most robust hypoxic and anoxic response compared to LDH (1+2+3), PGK (1+2) and Epo (1+2) in two out of the three cell lines tested. No improvement in oxic/anoxic induction was made to the LDH (1+2) or PGK (1+2) HREs by increasing the copy number. In contrast, an Epo pentimer produced a response similar to that observed by the PGK trimer in the three cell lines and has been reported to be orientation independent (Beck et al., 1991).

Firth et al. (1995), produced evidence to show that none of the three domains found within the LDH-A HRE, either as monomers or as dimers, could independently drive hypoxic expression through a heterologous minimal promoter when compared to the full LDH-A HRE sequence containing all three sites. However, the combination of the HIF-1 binding site (site 1) with either of the other two sites conferred a marginal hypoxic response. The data presented in figures 4.9-11 supports these findings.

However, Firth et al. (1995), demonstrated the best response from the full LDH-A sequence containing all three domains. In contrast, results here indicate that the combination of site 1 and site 2 only produces an oxygen-regulated response far superior to that of LDH (1+2+3). To determine why this is, the different sequences used must be analysed (figure 4.18). There is only a single base difference between the sequences, highlighted in red. The single base, 'A' forms part of the ChoRE which resembles a Myc/Max responsive element (E-box) so it may be possible that the loss of this single base led to the reduced response seen by Firth et al. (1995) compared to data presented here. This discrepancy in the data resulting from a single base suggests that it may be possible to increase the oxygen regulated response of LDH (1+2) HRE by altering a single base within the ChoRE or even altering it to produce an optimized E-box.

Figure 4.18: Comparison of LDH (1+2) sequences.

LDH (1+2)

SR (2001)

GCGGACGTGCGGGAACCCACGTGTA

Firth (1995)

GCGGACGTGCGGGAACCC**ACGTGT**

Core HIF-1 and ChoRE binding sites shown in bold.

Part 3: Preferential hypoxia response element transactivation by HIF-1α and EPAS-1 oxygen-responsive signalling pathways.

4.3.1 Introduction

Hypoxia responsive genes have been shown to function in a HIF-1α dependent, eg. Glut-1 (Wood et al., 1995) or independent manner, eg. VEGF (Weisener et al., 1998). EPAS-1 is expressed across a variety of cell types (Talks et al., 2000) and induced by hypoxia at the protein but not mRNA level (Wiesener et al., 1998). A bHLH factor, EPAS-1 shows 48% homology to HIF-1α and can dimerise with HIF-1β. Studies in a mutant CHO cell line, Ka13, which does not express either HIF-1α or EPAS-1 demonstrated the ability of both HIF-1α and EPAS-1 to interact with HREs (Wood et al., 1995; Weisener et al., 1998) and led to the observation that each transcription factor may have different target specificities; VEGF is significantly more responsive to *trans*activation via EPAS-1 in comparison to HIF-1α (Wiesener et al., 1998).

To determine whether each of the HREs (Epo, PGK, LDH-A, VEGF and Glut-1) are preferentially *trans*activated by HIF-1α or EPAS-1 the pGL3.HRE plasmids were transiently transfected into the Chinese hampster ovary (CHO-K1) cell lines, C4.5 and Ka13. The former (parental, wild-type) expresses both HIF-1α and EPAS-1, and displays a functional hypoxic response. In contrast, the Ka13 cell line has a defect in HIF-1α expression, possibly due to a frame-shift mutation in the HIF-1α open reading frame. It is not defective in the oxygen sensing mechanism that stabilises and *trans*activates HIF-1α since transient transfections with HIF-1α restored hypoxia-inducible expression in a dose-dependent manner; the more HIF-1α that was transfected, the greater the HRE response leading to a progressive increase in HRE activity under normoxia. Transfection of EPAS-1 into Ka13 cells produced a similar pattern of results to transfection of HIF-1α, indicating that HIF-1α and EPAS-1 can independently produce hypoxia-inducible HRE expression, even under normoxia (Blancher et al., 2000). Using the Ka13 cell line it will be possible to determine the

comparative roles of HIF-1α and EPAS-1 dependent and independent pathways of hypoxia inducible expression.

4.3.2 Methods

HIF-1α and EPAS-1 cDNAs were ligated into the multiple cloning region of pcDNA3^{neo} vector, prepared by Dr Karen King in our laboratory (a gift from Prof. Peter Ratciffe). The Chinese hamster ovary, C4.5 and Ka13 carcinoma cell lines (CHO-K1) were co-transfected with a total of 20μg of plasmid DNA consisting of a pGL3.HRE construct and pRL.CMV at a 20:1 respectively, by electroporation at 320V as described in section 2.5. In addition, either 5μg (determined by prior titration experiments, figure 4.19) of HIF-1α or EPAS-1 were co-tranfected in combination with the pGL3 and pRL vectors into the Ka13 cells.

4.3.3 Results

Previous results in section 1 of this chapter suggest that LDH $(1+2)^{3-}$ would likely have the greatest activity in the CHO-K1 cell line, therefore optimisation experiments were carried out using this HRE. Both the C4.5 and Ka13 cell lines were transiently co-transfected with pGL3.LDH $(1+2)^{3-}$ and pRL.CMV. In addition the Ka13 cell line was also transfected with either 2, 3.5 or 5μg of pcDNA3/^{Neo}/HIF-1α, in an attempt to recapitulate the hypoxic response of LDH $(1+2)^{3-}$ seen in the C4.5 cell line, in the Ka13, HIF-1α deficient cell line.

Table 4.5: Amplitude and Induction of C4.5 and Ka13 cell lines transfected with pGL3.LDH (1+2)rev plus varying quantities of HIF-1α.

	AIR	AnO_2	Induction
C4.5	0.2164	1.8643	8.6152
Ka13	0.1218	0.1424	1.1695
Ka13 + 2ug	0.5525	1.3616	2.4643
Ka13 + 3.5ug	0.2795	0.8788	3.1439
Ka13 + 5ug	0.6914	1.8329	2.6511

Figure 4.19: Expression of LDH $(1+2)^{3'}$ in the C4.5 (wt) versus the Ka13 murine carcinoma cell line co-transfected with either none, or varying quantitites of HIF-1α, n=1 (except C4.5, n=3).

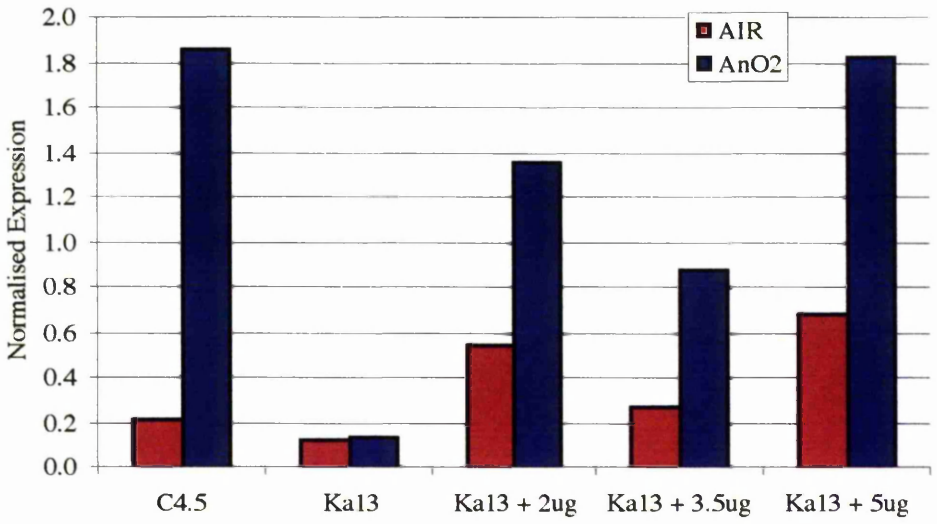

An 8-fold induction in the LDH (1+2) HRE was observed in the C4.5 cell line. There was an increase in the basal (oxic) activity of the Ka13 cells, when compared to the C4.5 cells, regardless of the quantity of pcDNA3/^{Neo}/HIF-1α co-transfected into the Ka13 cell line. The transfection of 5μg of pcDNA3/^{Neo}/HIF-1α DNA into the Ka13 cell line produced an anoxic LDH activity similar to that seen in the wild-type, C4.5 line.

However, the level of induction was significantly lower due to the increase in normoxic expression, suggesting that some level of oxic HIF-1α regulation has been lost.

The experiment was repeated for the range of HREs (PGK, Epo, VEGF, Glut-1, LDH-A) co-transfecting the pGL3 and pRL vectors with 5μg of either pcDNA3/^{Neo}/HIF-1α or pcDNA3/^{Neo}/EPAS-1. Identical amounts of EPAS-1 and HIF-1α expression vector were used so as to compare their *trans*activation potentials for each HRE construct.

Figure 4.20: HRE expression in the parental, C4.5 cell line, n=3 (except at 1%O_2 n=2) (See appendix 15)

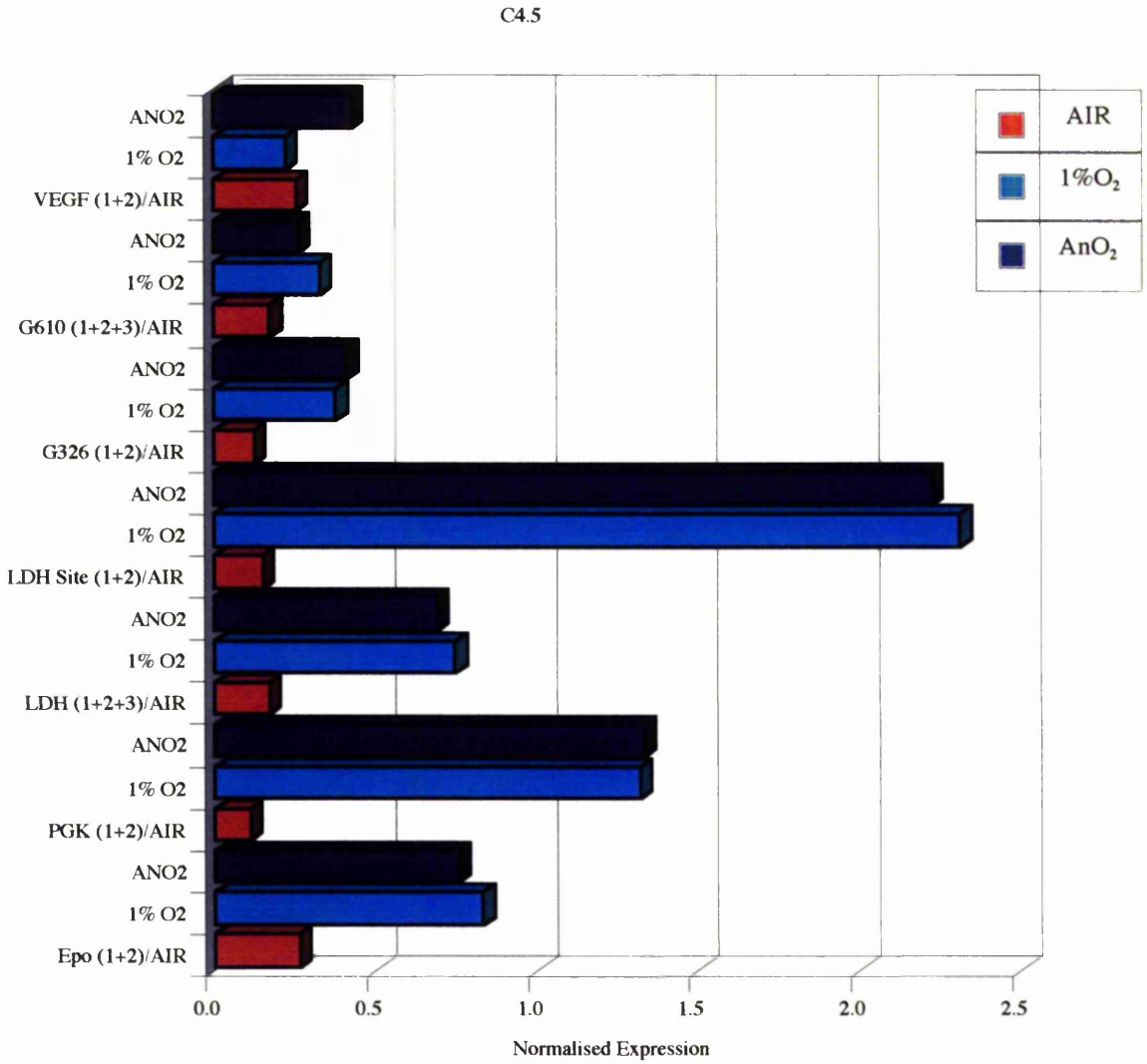

A similar pattern of HRE expression was seen in the C4.5 wild type cell line, as that previously described in parts 1 and 2. As expected LDH $(1+2)^{3-}$ is the most responsive and the short Glut-1 sequence has a marginally higher activity than the full Glut-1 HRE containing site 3. An induction in VEGF was measured under anoxia but not hypoxia, Wood et al. (1995), saw little or no induction of VEGF in the C4.5 cells at 1%O_2.

Figure 4.21: Ka13 cell line transiently co-transfected with pGL3.HREs plus pRL.CMV and 5μg pcDNA/^{Neo}/HIF-1α, n=3.

(See appendix 16)

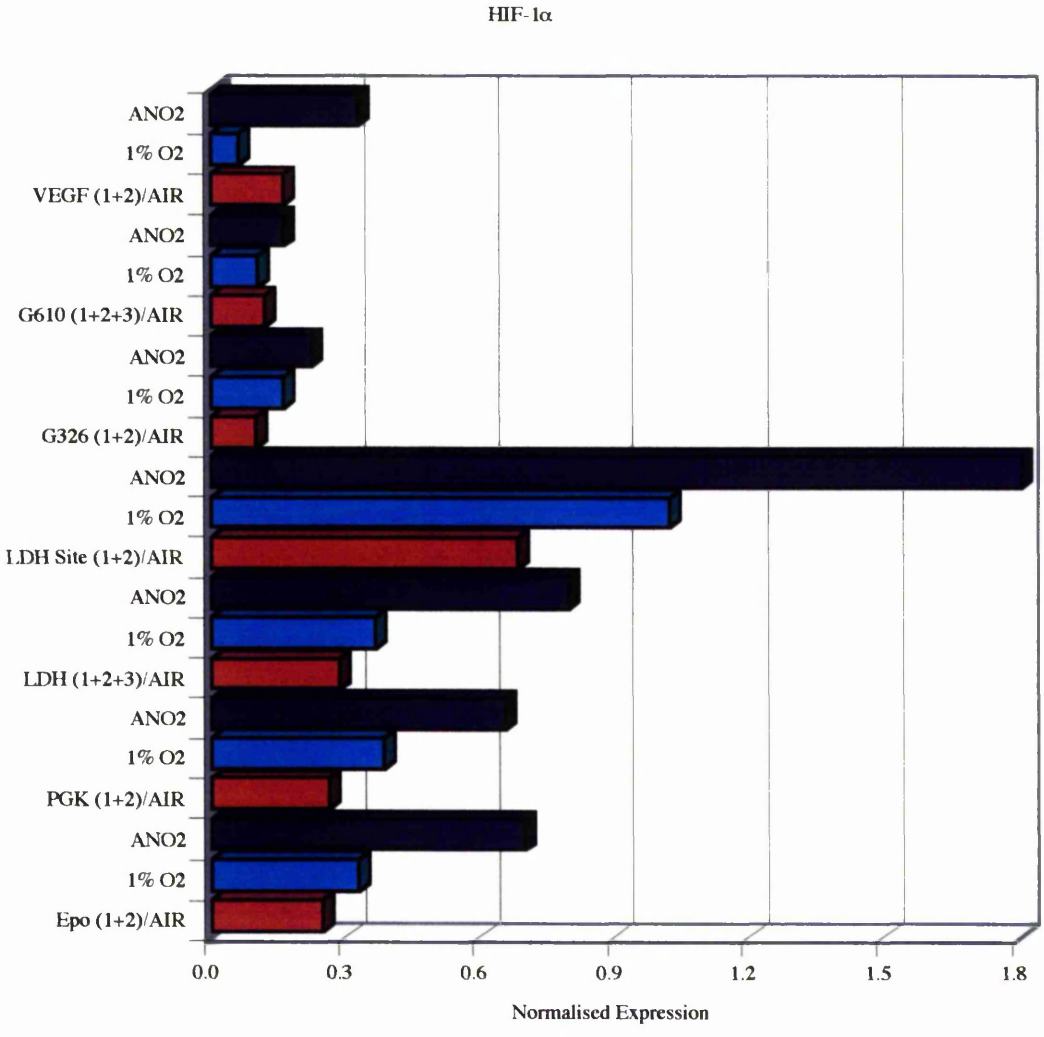

The data suggests that LDH $(1+2)^{3-}$ has the greatest transcriptional response to HIF-1α compared to all other HREs tested in the Ka13 CHO-K1 cell line. The amplitude of HRE expression is greater under anoxia compared to hypoxia in each system. There was a reduction in the VEGF and Glut (1+2+3) HRE activities under hypoxia when compared to normoxia.

Figure 4.22: Ka13 cell line transiently co-transfected with pGL3.HREs plus pRL.CMV and 5μg pcDNA/^{Neo}/EPAS-1, n=3.

(See appendix 17)

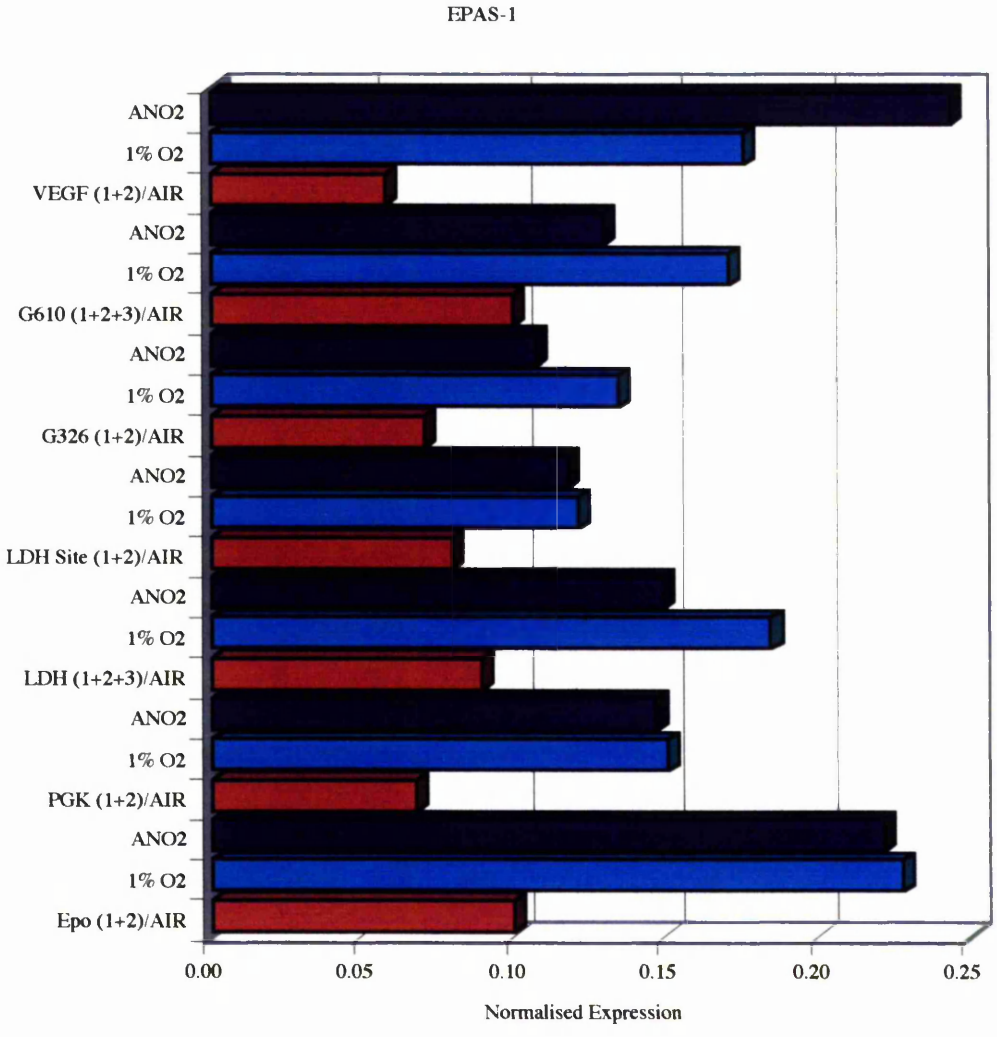

Expression of EPAS-1 in the Ka13 cells resulted in a significantly lower amplitude of HRE gene expression and less tightly controlled oxic expression than seen for HIF-1α. Results indicate that the Epo and VEGF HREs have the greatest response to EPAS-1 expression in the Ka13 CHO-K1 cell line. However, the reduction in HIF-1α mediated HRE performance at 1%O2 is not seen when co-transfected with EPAS-1.

Both the short and full-length Glut-1 sequences show similar responses to HIF-1α and EPAS-1, whilst there is approximately a 2-fold loss in Epo, PGK and LDH (1+2+3) activities and almost a 12-fold reduction in LDH (1+2) expression under anoxia with the notable exception of VEGF HRE. The hypoxic expression of most HREs at 1%O_2 is equal to or greater than the anoxic expression.

4.3.4 Discussion

The results presented here support previous experiments (Wood et al., 1995) suggesting that both HIF-1α and EPAS-1 can independently participate in hypoxia induced gene transcription.

The data in figure 4.19 demonstrates a progressive increase in normoxic LDH HRE activity as more HIF-1α was transfected into the Ka13 cells. This was also observed by Wood et al. (1995), with a similar pattern of EPAS-1 induced HRE expression. At high HIF-1α or EPAS-1 plasmid doses, HRE expression in the Ka13 cell line exceeded that of the wild type C4.5 cells (Wood et al., 1995).

Wiesener et al. (1998), showed EPAS-1 protein to be marginally more abundant in normoxic and mildly hypoxic cells than HIF-1α. When Ka13 cells were co-transfected with EPAS-1 (figure 4.22) there was a sharp increase in HRE expression at 1%O_2, in many cases in excess of that seen under anoxia. Co-tranfection with HIF-1α produced a marginally more pronounced response to anoxia compared to hypoxia for each HRE.

Wood et al. (1995), showed that Glut-1 expression was critically dependent on HIF-1α, in contrast the hypoxia-inducible expression of some other genes was HIF-1α independent. The activities of HIF-1α and EPAS-1 were distinct with respect to the transactivation of the VEGF HRE. EPAS-1 appeared to cause an increase in the transactivation of VEGF at 1%O_2 compared to anoxia. This was not seen when VEGF

was co-transfected with HIF-1α. From the results it seems that each of the HREs are minimally activated by EPAS-1, but are preferentially transactivated by HIF-1α, with the exception of VEGF. The presence of EPAS-1 has the potential to produce a hypoxic response at higher O_2 tensions. It would be interesting to examine HRE activity when co-transfected with both HIF-1α and EPAS-1 in the Ka13 cell line.

The abundance of EPAS-1 mRNA varies widely across a range of cell lines from identical and different tissues, in contrast, the level of HIF-1α mRNA is less variable (Blancher et al., 2000). HIF-1α, like EPAS-1 is a bHLH protein, hypoxic activation of HIF-1α results in altered protein levels independent of mRNA. Weisener et al. (1998), and Blancher et al. (2000) examined the pattern of normoxic and hypoxic expression of HIF-1α and EPAS-1 in a range of cell lines. Increases in both EPAS-1 and HIF-1α protein were detectable after 4 hours hypoxia compared to normoxic extracts. However, EPAS-1 is more responsive to mild hypoxia, being detected in some extracts at 5% and 3% O_2. EPAS-1 is detectable in endothelial and epithelial cells and fibroblast (Weisener et al., 1998). However, expression of HIF-1α is more prominent in human carcinoma cell lines than EPAS-1. This implies that the ratio of HIF-1α to EPAS-1 expression is cell line specific; e.g. the MDA 468 cell line expresses significantly higher levels of HIF-1α compared to EPAS-1, whereas, SKBr3 expresses similar levels of both (Blancher et al., 2000). Data presented in figure 4.20 shows the LDH (1+2) HRE to be selectively responsive to transactivation by HIF-1α compared to the other HREs tested. The MDA 468 breast carcinoma cell line expresses high levels of HIF-1α (compared to EPAS-1) protein thus may imply why the LDH (1+2) HRE is so responsive in this cell line compared to PGK, Epo, VEGF and Glut-1. In contrast the HT1080 cell line expresses moderately more HIF-1α protein than EPAS-1 in response to hypoxia, although the difference is not large (Wiesener et al., 1998). This may partly explain the poorer induction ratios in the HT1080 cell line, since EPAS-1 expression will tend to increase oxic HRE activity more readily.

The apparent selectivity of the LDH HRE for HIF-1α in preference to EPAS-1 is of therapeutic significance. Immunohistochemical analysis of human tumours of diverse

origin indicate that HIF-1α is expressed in 70% of all solid tumours, whereas EPAS-1 expression is much more sparodic. Furthermore evidence suggests that HIF-1α is expressed predominantly in epithelial tumour tissues, where as EPAS-1 is often confined to endothelial and stromal tissues (Semenza, 2000a,b,c). These observations have implications for the use of HREs to target gene expression in human solid tumours. It would suggest that, unless the intention is to deliberately target the tumour vasculature, HREs such as VEGF would be inappropriate and may lead to sparodic, heterogenous and inconsistent HRE activity. The induction of EPAS-1 by slightly less severe hypoxia compared to HIF-1α, suggests that EPAS-1 functions as a modulator of gene expression under normoxia and less severe hypoxia in contrast to HIF-1α (Weisener et al., 1998). Results show that all components of either HIF-1 or HIF-2 are required for the hypoxic response, but the ratios to which they occur may be HRE or cell line dependent.

Chapter 5

Optimisation of the novel LDH-A hypoxia responsive enhancer.

5.1 Introduction

The ChoRE binding site (site 2) of LDH-A HRE appears to play a critical role in the hypoxic inducibility of the LDH-A HRE as demonstrated in chapter 4. Similar binding sites have been found in each of the other HREs tested at almost identical positions, with respect to the HIF-1 binding site. However, the site 2 of PGK, Epo, and VEGF HREs seems to have a weaker activity than that found in LDH-A. The ChoRE (site 2) within the LDH-A HRE is identical to the core Myc/Max binding sequence (CACGTG). The Myc family of proteins are basic helix-loop-helix leucine zipper transcriptional factors, including C-Myc, N-Myc and L-Myc that form heterodimeric complexes with the Max protein (Max; Blackwell et al., 1990; Blackwood et al., 1991; Kretzner et al., 1992; Amati et al., 1992). Myc specifically binds the core nucleotide sequence CACGTG as Myc-Max heterodimers, rather than either Myc or Max homodimers, resulting in sequence-specific transcriptional activation.

To explore the underlying reasons for the superiority of the LDH (1+2) enhancer over that of PGK-1 and Epo, the ChoRE (site 2) was taken from the LDH HRE and interchanged with the minimal functional elements of Epo, VEGF and PGK-1 (figure 5.1a and b). Further, site 2 of Epo HRE was placed in the context of LDH site 1, since like LDH HRE, Epo HRE function is dependent upon the presence of site 2.

Figure 5.1: HRE sequence exchanges.

a)

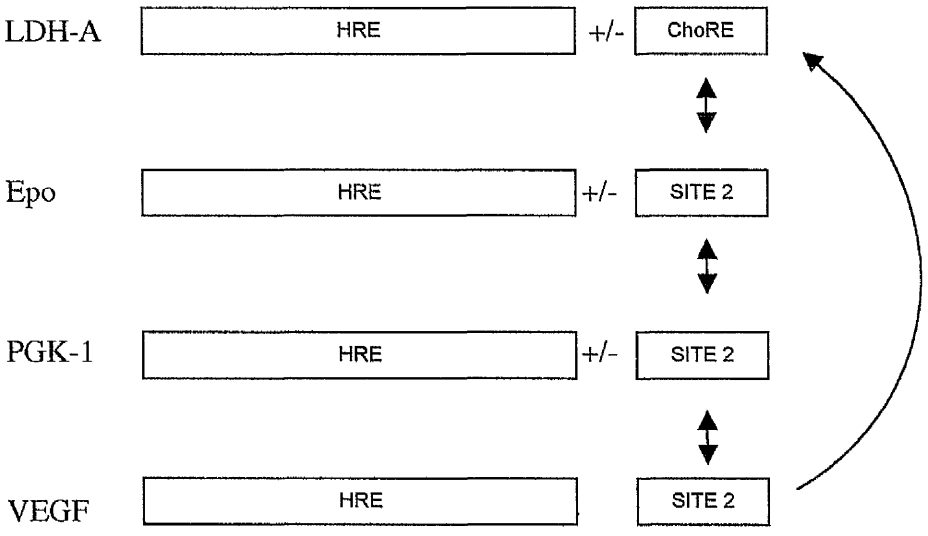

b)

LDH site 1 + LDH site 2

CGGACGTGCGGGAACC | **CACG**TGTA

PGK site 1 + LDH site 2

TGT**CACGTCC**TGCACGA | **CACG**TGTA

Epo site 1 + LDH site 2

GCCCT**ACGTGC**TGTCTCA | **CACG**TGTA

VEGF site 1 + LDH site 2

CACAGTGCAT**ACGTGG**GCTCCCAA | **CACG**TGTA

LDH site 1 + Epo site 2

CGGACGTGCGGGAACC | **CAC**AGCA

SITE 1 **SITE 2**

In an attempt to improve the existing LDH (1+2) HRE the ChoRE or E-box (an apparent consensus Myc/Max binding site, site 2) was altered. Transcriptional activation by Myc-Max is significantly reduced by specific base changes flanking the core sequence, CACGTG, possibly by altering the DNA binding activity (figure 5.2; Fisher et al., 1993). Fisher et al. (1993) showed that a T residue 5' of the CACGTG motif severely reduced gene activation by Myc-Max, whereas a G residue proved optimal. By substituting the C residue 5' of the CACGTG motif in the LDH ChoRE, or by altering the sequence to produce an optimised E-box motif, it may be possible to amplify or inhibit LDH-A gene transcription.

Figure 5.2: Optimisation of the ChoRE from the LDH-A enhancer

LDH (1+2)

CGGACGTGCGGGAACC**CACGTG**TA

LDH (1+2; Dest)

CGGACGTGCGGGAACT**CACGTG**TA

LDH (1+2; Opt)

CGGACGTGCGGGAACG**CACGTG**TA

LDH (1+2; A)

CGGACGTGCGGGAACA**CACGTG**TA

LDH (1+ E-box)

CGGACGTGCGGGCCA**CCACGTGG**TGCCTA

Finally, the activity of the optimal HREs as determined in this study were tested for their hypoxia induced expression in an extended cell line panel. It was important to include cell lines from different tissue origins, therefore the A549 (lung), HCT 116 (colon), T47D (breast) and WiDr (colon) were selected.

5.2 Methods

Oligonucleotides were constructed containing trimers of the modified HRE sequences (Sigmagenosys) with Bgl II and Bam HI ends and were cloned into the pGL3.promoter vector (Promega) at the Bgl II site, upstream of the minimal SV40 promoter. All vectors were sequenced to ensure integrity and orientation of the trimers.

Experiments were performed as previously described in Chapter 2 using the optimised conditions. All cell lines were transfected by electroporation.

5.3 Results

Statistics

Means of data sets were compared for the significance of the difference between them using a two-tailed two-sample T-test. p values ≤ 0.05 are shown with single asterisks over the relevant data sets.

Sequence Exchanges

The three human carcinoma cell lines MDA 468, HT1080 and SQD9 were independently co-transfected with PGK, Epo, and VEGF each of which had their natural site 2 replaced with the putative E-box from LDH-A. Cells were transfected in the usual way and exposed to 16 hours air, hypoxia and anoxia, followed by three hours reoxygenation and then lysed and assayed for firefly and renilla activities. The amplitude of HRE expression is plotted below for each cell line.

Figure 5.2: Comparative expression of HREs containing either their natural site 2 or that from LDH-A in the MDA 468 cell line, n=3.

* P≤0.05 vs air (See appendix 18)

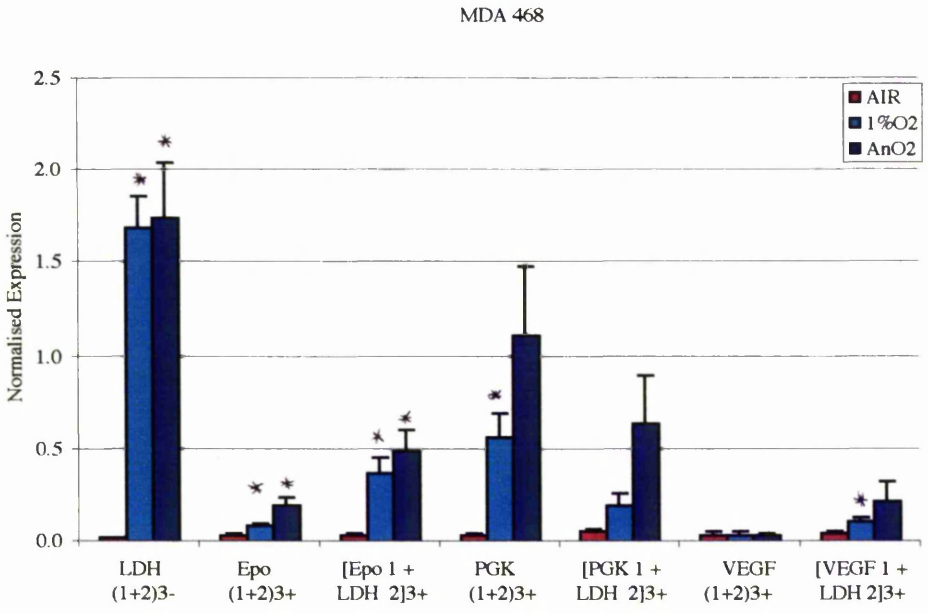

Figure 5.3: Comparative expression of HREs containing either their natural site 2 or that from LDH-A in the HT1080 cell line, n=3.

* P≤0.05 vs air (See appendix 19)

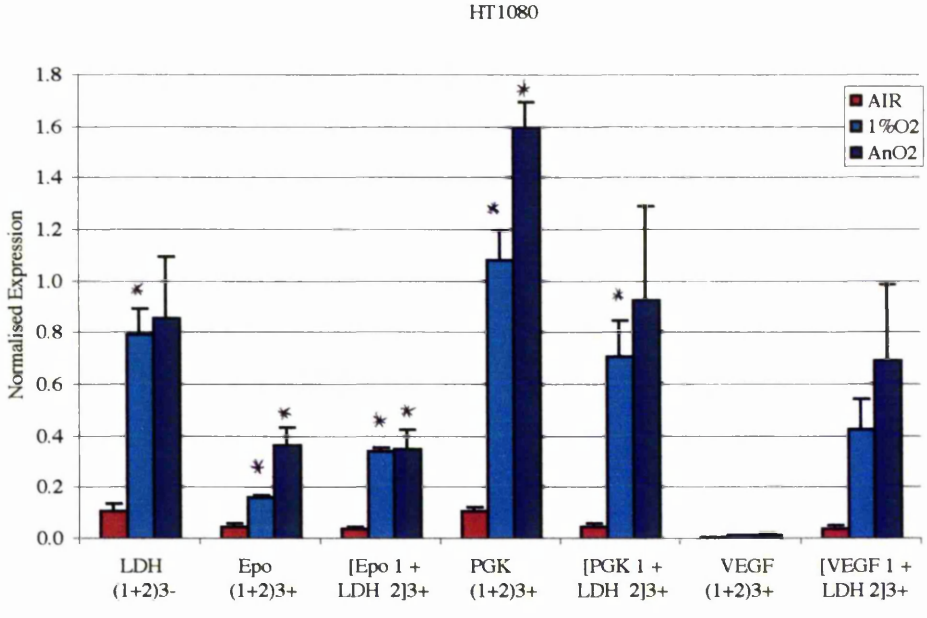

Figure 5.4: Comparative expression of HREs containing either their natural site 2 or that from LDH-A in the SQD9 cell line, n=3.

* P≤0.05 vs air (See appendix 20)

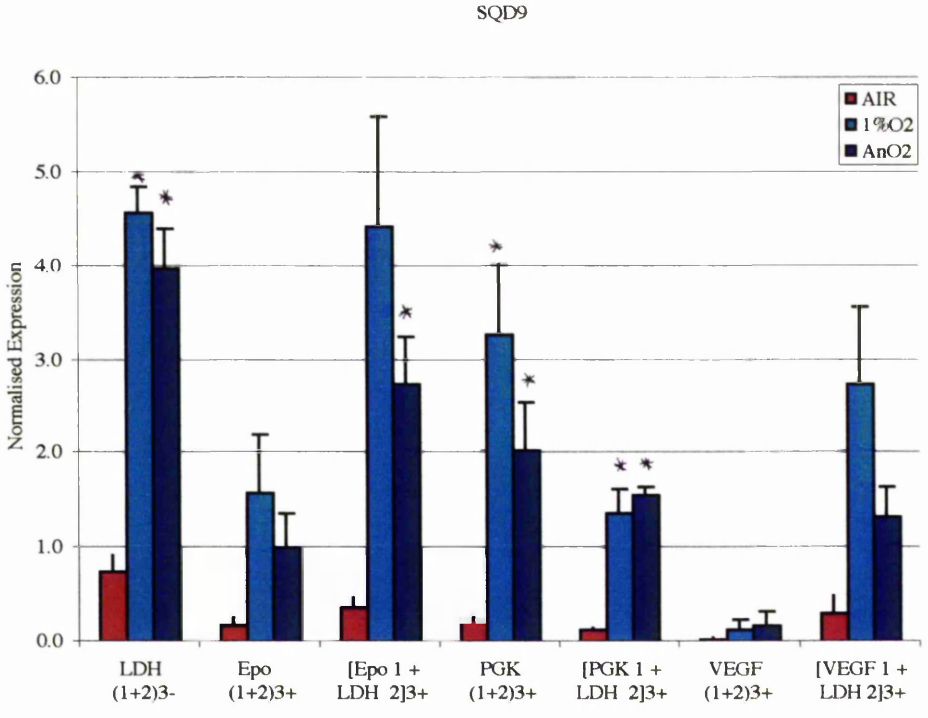

A similar pattern of HRE activity was observed across the three cell lines. Replacing site 2 of Epo and VEGF with that from the LDH-A HRE caused a significant increase in both hypoxic and anoxic regulated expression. Despite an increase in the basal activity, there was a marked increase in the inducibility of the modified Epo and VEGF HREs. This perhaps suggests that a constitutive *trans*acting factor binds site 2 of LDH HRE modestly stimulating oxic transcription. However under hypoxia it functions to efficiently recruit the now stabilised HIF-1 complex to the adjacent HRE, irrespective of the exact core sequence of site 1. In contrast, the PGK HRE appears to function optimally when the HIF-1 binding site (site 1) is combined with its homologous site 2 rather than the E-box from LDH-A. Interestingly, PGK HRE is the only known HRE that is functional in the absence of site 2 (Firth et al., 1994).

Site 2 from the Epo HRE functions to magnify the response to hypoxia and anoxia when found in its natural context (figures 4.15-17). The LDH (1+2) HRE was modified to exchange its natural site 2 for that of Epo. The experiment was performed as described previously. The data presented in figure 5.5 indicates that in striking contrast to LDH-A site 2, the Epo site 2 does not function outside its natural context in the LDH-A enhancer.

Figure 5.5: Comparative expression of the LDH HREs containing either its natural site 2 or that from Epo in the 3 human carcinoma cell lines, n=3.

* P≤0.05 vs air (See appendix 21)

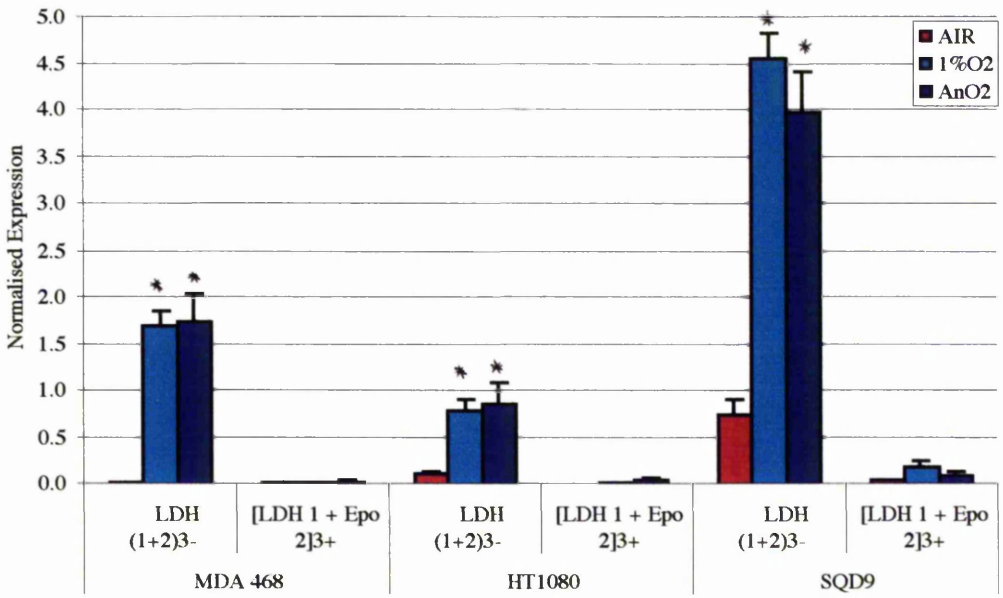

Table 5.1: Inducible expression of HREs containing site 2 sequence exchanges

	HRE Induction					
	MDA 468		HT1080		SQD9	
Gas-phase O_2	$1\%O_2$	AnO_2	$1\%O_2$	AnO_2	$1\%O_2$	AnO_2
LDH-A $(1+2)^{3-}$	75.2	77.7	7.2	7.8	6.1	5.3
Epo $(1+2)^{3+}$	2.8	5.9	3.4	7.3	9.2	5.9
[Epo 1 + LDH 2]$^{3+}$	10.2	13.2	9.3	9.6	12.3	7.6
PGK $(1+2)^{3+}$	17.0	33.8	9.8	14.6	13.5	8.4
[PGK 1 + LDH 2]$^{3+}$	3.8	12.5	15.2	19.9	11.2	12.9
VEGF $(1+2)^{3+}$	1.1	1.1	2.2	2.7	4.4	5.6
[VEGF 1 + LDH 2]$^{3+}$	2.7	5.5	11.4	18.4	8.9	4.3
[LDH 1 + Epo 2]$^{3+}$	1.3	2.1	1.4	6.2	4.6	2.7

Figure 5.6: Expression of LDH (1+2), with site 2 modifications in the MDA468 cell line, n=2.

(See appendix 22)

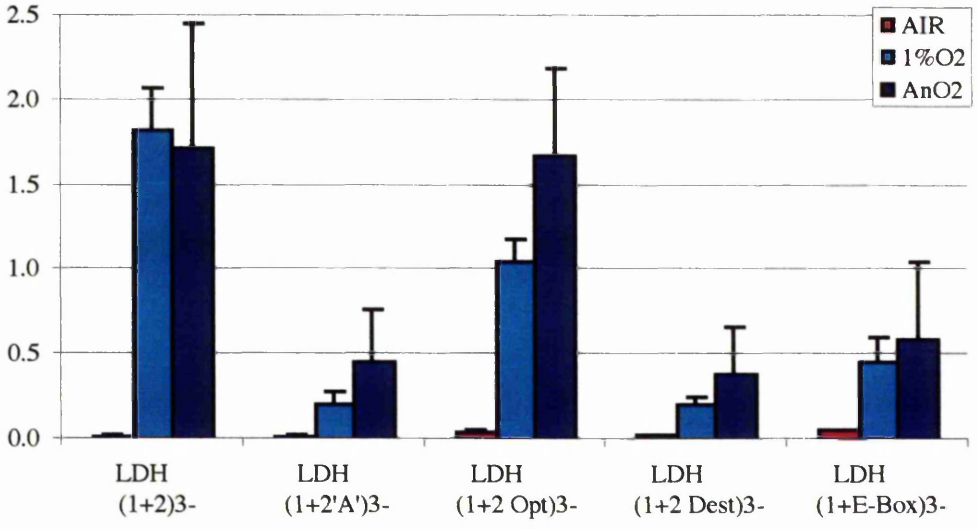

Figure 5.7: Expression of LDH (1+2), with site 2 modifications in the SQD9 cell line, n=2.

(See appendix 23)

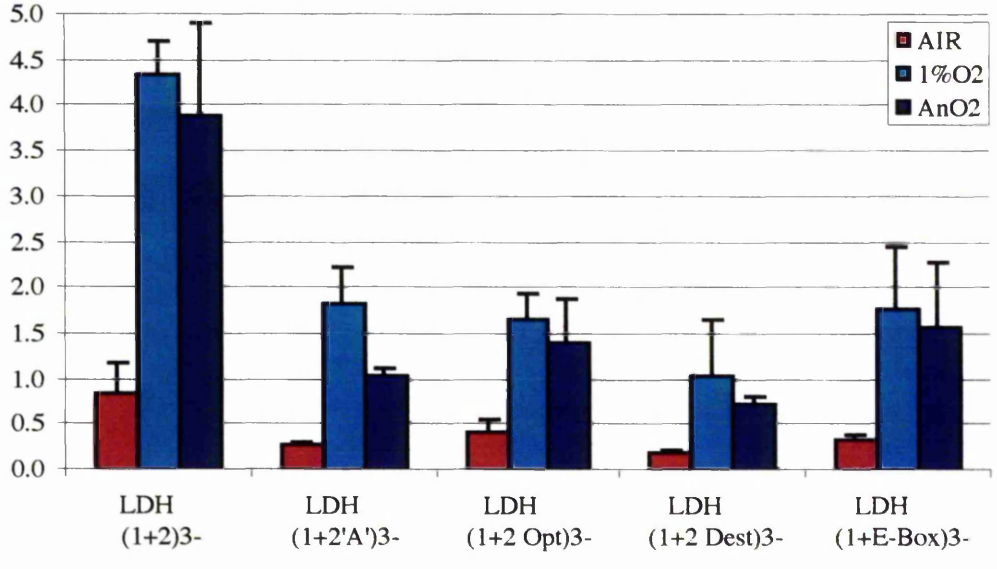

Table 5.2: Induction of LDH (1+2), with site 2 modifications

	HRE Induction			
	MDA 468		SQD9	
Gas-phase O_2	$1\%O_2$	AnO_2	$1\%O_2$	AnO_2
LDH $(1+2)^{3-}$	83.7	79.0	5.1	4.6
LDH $(1+2'A')^{3+}$	11.5	25.1	6.8	3.9
LDH $(1+2\ Opt)^{3+}$	24.2	38.3	4.1	3.5
LDH $(1+2\ Dest)^{3+}$	8.2	15.4	5.0	3.5
LDH $(1+E\text{-}Box)^{3+}$	8.7	10.9	5.1	4.5

Modification of the critical single nucleotide, identified as essential for Myc/Max binding, dramatically altered the functionality of LDH$(1+2)^{3-}$. Most strikingly, disruption of the E-box by a C→T mutation which is known to markedly reduce affinity for Myc/Max heterodimers (Fisher et al., 1995), also suppressed the hypoxic response 8-fold and 5-fold in the MDA468 and SQD9 cell lines respectively. However, neither replacing the C residue with an A or G nor optimising the E-box, improved the activity beyond that of LDH (1+2) containing the unaltered motif. In most cases there was an increase in the basal activity in the SQD9 cells. In contrast to the MDA 468 cell line there was a slight decrease in basal activity. For each of the novel LDH HREs, nucleotide spacing between site 1 and site 2 was preserved (see figure 5.2). The nucleotide spacing between site 1 and 2 has been shown to be important for the function of Epo HRE, where substitution of the 'natural' 4-bp spacer with an 8-bp oligonucleotide disrupted oxygen-regulated transcription (Pugh et al., 1994). Since spacing is preserved this might suggest that the intervening sequence contributes to functionality, perhaps by appropriating the correct secondary tortial DNA structure of the HRE to facilitate transcription factor interaction and cooperativity.

Expression of preferred HREs in an extended cell line panel

Expression of the three PGK and LDH-A HREs was investigated in an extended cell line panel composed of a human lung (A549), two colon (HCT116 and WiDr) and a second breast (T47D) human carcinoma cell line.

Figure 5.8: Expression of HREs exposed to 16 hours air, hypoxia or anoxia and 3 hours reoxygenation in the A549 lung carcinoma cell line, n=3.

* P≤0.05 vs air (See appendix 24)

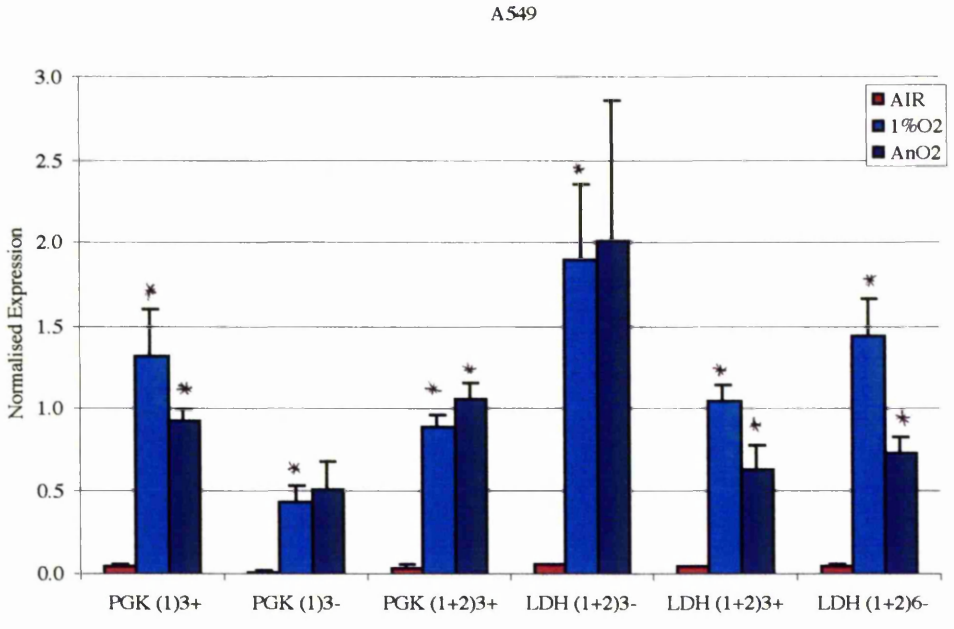

Figure 5.9: Expression of HREs exposed to 16 hours air, hypoxia or anoxia and 3 hours reoxygenation in the HCT116 colon carcinoma cell line, n=2.

(See appendix 25)

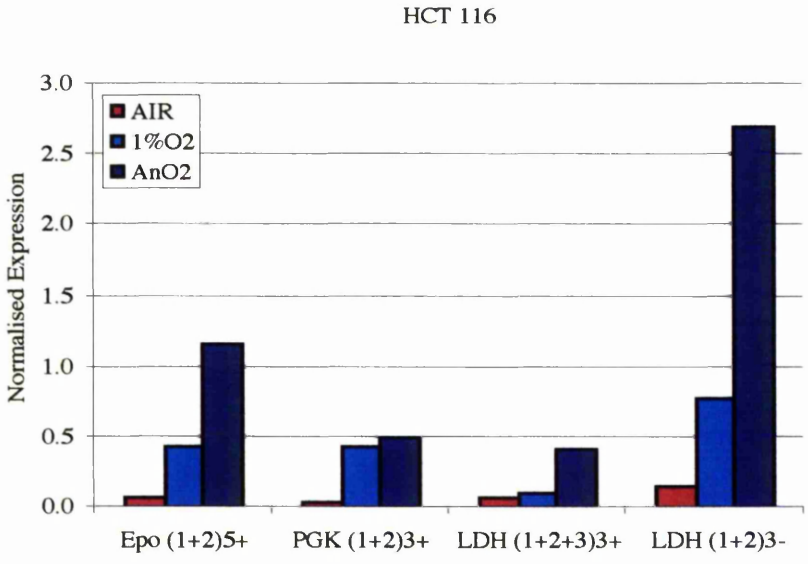

Figure 5.10: Expression of HREs exposed to 16 hours air, hypoxia or anoxia and 3 hours reoxygenation in the T47D breast carcinoma cell line, n=3.

* P≤0.05 vs air (See appendix 26)

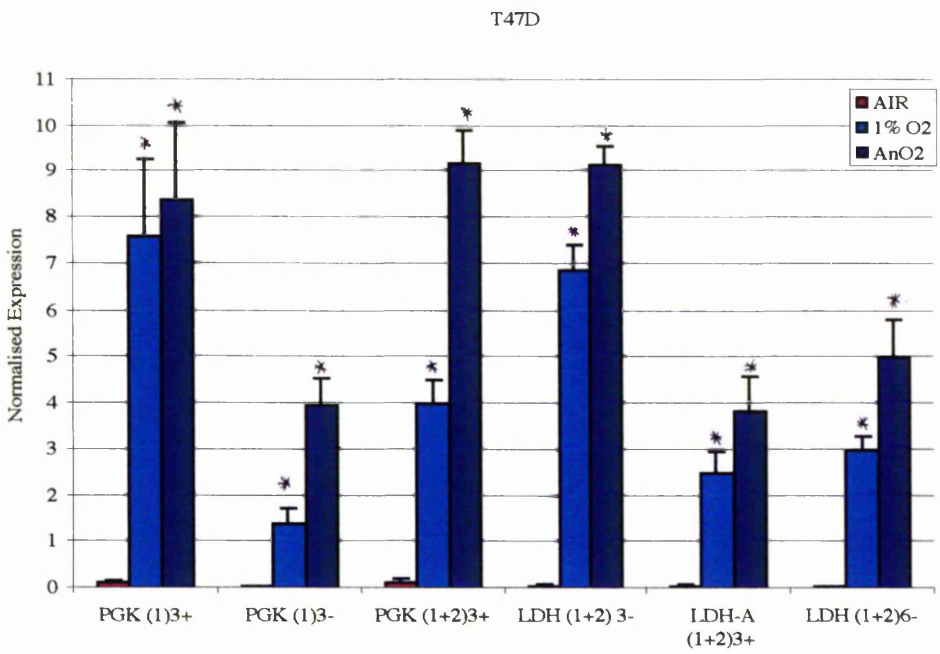

Figure 5.11: Expression of HREs exposed to 16 hours air, hypoxia or anoxia and 3 hours reoxygenation in the WiDr colon carcinoma cell line, n=3.

* P≤0.05 vs air (See appendix 27)

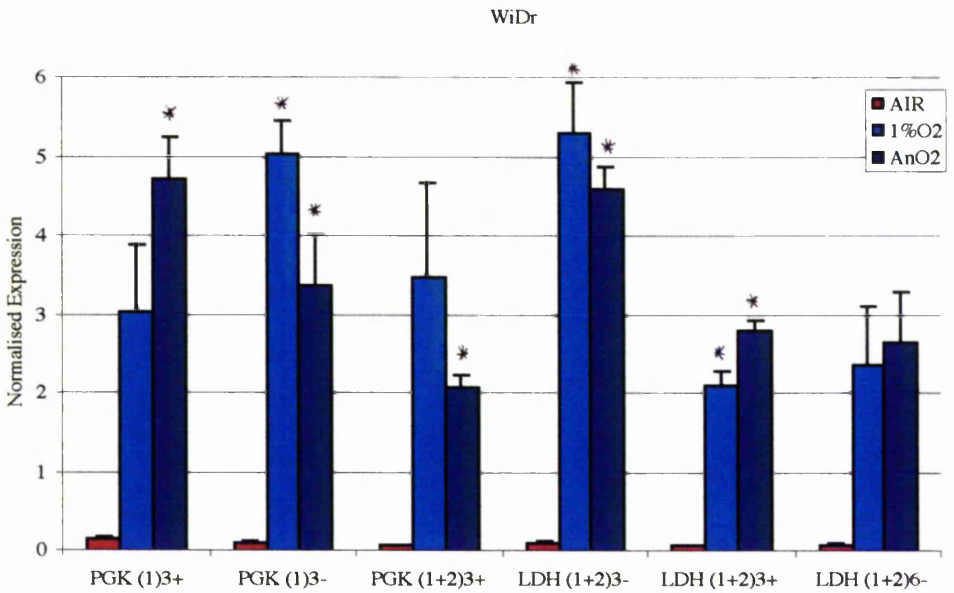

Table 5.3: Induction of HREs exposed to 16 hours air, hypoxia or anoxia and 3 hours reoxygenation.

	HRE Induction							
	A549		**HCT116**		**T47D**		**WiDr**	
Gas-phase O_2	$1\%O_2$	AnO_2	$1\%O_2$	AnO_2	$1\%O_2$	AnO_2	$1\%O_2$	AnO_2
PGK $(1)^{3+}$	24.5	17.3			63.7	70.5	20.7	32.2
PGK $(1)^{3-}$	24.3	28.8			28.6	81.3	47.0	31.5
PGK$(1+2)^{3+}$	22.2	26.4	11.1	13.1	27.6	63.1	42.9	25.7
LDH $(1+2)^{3-}$	32.9	34.9	4.9	17.2	129.4	172.0	48.2	41.8
LDH$(1+2)^{3+}$	22.7	13.7	1.5	6.6	50.3	77.5	30.0	40.0
LDH$(1+2)^{6+}$	27.7	14.0			94.3	158.6	26.3	29.5

In agreement with all the data generated for MDA468, SQD9 and HT1080 during the earlier HRE studies (chapter 4), LDH $(1+2)^{3-}$ is consistently the most active and inducible HRE trimer so far identified. Moreover, the absolute amplitude of gene expression under 1% O_2 and anoxia is consistently superior when viewed across the extented cell line panel (n=7). Thus it is predicably active in all cell lines, whereas both PGK and Epo demonstrated considerable cell line selectivity.

5.4 Discussion

As shown in chapter 4.2, site 2 of the Epo, VEGF, and LDH-A HREs are essential to the hypoxic and anoxic response. The short LDH-A (26bp) sequence comprising the HIF-1 (site 1) and ChoRE (site 2) binding sites appear to give the most robust and consistent response across a broad range of tissue carcinoma cells when compared to the other HRE sequences tested. Dissecting the HRE and ChoRE did not improve performance, as neither domain appears to function independently. Replacing site 2 of each promoter with the 7bp ChoRE sequence found in LDH-A, demonstrated that it can function outside its natural context. When combined with the HIF-1 binding sites (site 1) from Epo and VEGF, both were dramatically "improved", showing significantly higher activity under hypoxia and anoxia. However, when LDH site 2 was placed in the context of the PGK enhancer a modest reduction in both the anoxic and hypoxic response was observed. Therefore, it appears that while the LDH-A ChoRE (site 2) can function outside its homologous context, it functions optimally in combination with its natural LDH-A core HIF-1 binding site. This sharply contrasted the site 2 of Epo HRE, which ablated all transcriptional activity outside its homologous HRE context.

Altering the LDH ChoRE (site 2) did not improve the hypoxic activity of the LDH HRE in either the MDA 468 or SQD9 human carcinoma cell lines, despite "optimising" the putative Myc/Max response element. However, the C→T mutation significantly reduced hypoxic function of the enhancer, possibly via a change in the

DNA binding activity of *trans*-acting factors, including Myc/Max, as previously described by Fisher et al. (1993). Results indicate that the natural ChoRE motif is optimal for function in the context of the LDH HRE enhancer sequence.

It has been demonstrated throughout this study that the expression of HREs may be consistent in relation to the ratio of expression between one another. However, the amplitude and induction of expression varies between cell lines. One contributing factor may be the tumourigenicity of individual cell lines. As suggested by Blancher et al. (2000), the more aggressive cell lines may have a greater normoxic gene expression than the less aggressive cell lines, which will have the greatest inducibility, eg. T47D. By expanding the characterisation of the optimal HREs into a larger cell line panel it was possible to demonstrate that hypoxia-inducible expression varies not only between human carcinoma cell lines from different tissues but also between cell lines from the same tissue origin, eg. T47D and MDA 468 are both breast carcinomas and HCT116 and WiDr originate from colon tissue. In each cell line tested, the activity of the LDH $(1+2)^{3-}$ HRE is superior to any of the PGK variations, which have previously been "optimised" in the early stages of commercial development (Binley et al., 1999; Boast et al., 1999; Griffith et al., 2000).

Results presented in this study suggest the LDH $(1+2)^{3-}$ HRE to have a superior activity compared with any of the PGK HRE variations in most cell lines tested. The following two chapters (6 and 7) aim to increase the hypoxic and anoxic activity further, hopefully without increasing the basal expression, resulting in higher HRE induction ratios. There are two ways in which this will be investigated. Firstly (chapter 6), by exploring the involvement of the PKA pathway in the hypoxic response. Secondly (chapter 7), previous research has indicated that it may be possible to develop a synthetic X-ray and hypoxia responsive promoter to transcriptionally target "genetic" radiotherapy.

Chapter 6

Co-operative interaction between the hypoxia and PKA response pathways

6.1 Introduction

A number of genes are upregulated in response to tissue hypoxia. The transcription of these genes is modulated by a universal transcription factor, HIF-1, which is post-transationally stabilised in hypoxic regions. HIF-1 is known to recognise a core 8bp sequence, which is essential for oxygen-regulated gene transcription. A cAMP-responsive element (CRE, site 3) overlaps the consensus HIF-1 site, with the core CRE motif overlapping the core HIF-1 motif, ACGT (figure 6.1; Kvietikova et al., 1995). This suggests that the HIF-1-mediated induction of gene expression may occur in concert with other transcription factors that serve to modulate.

HRE function may enhance the response to oxygen deprivation. A CRE oligonucleotide has been demonstrated to compete efficiently with a HRE oligonucleotide for binding at the HIF-1 site; CREB-1/ATF-1 homo- and heterodimers constitutively bind the HIF-1 recognition site, suggesting that the PKA-dependent phosphorylation of CREB may modulate HRE function. Both the human and mouse PGK HREs contain a variant of the asymmetrical CREB-binding site (figure 6.1), methylation interference assays suggest that HIF-1 and the constitutive bound species (CREB-1/ATF-1) contact the same G-residues (Wang and Semenza, 1993). This may suggest the exchange of factors upon hypoxic induction rather than co-occupancy (Kvietikova et al., 1995).

Specific co-operativity has been demonstrated between distinct HIF-1 and CRE binding sites in the LDH-A (Firth et al., 1995) and Glut-1 genes (Ebert et al., 1995).

Present observations suggest a level of integration between the secondary messenger cAMP and the oxygen sensor, via co-operative transcriptional activation (Firth et al., 1995; Kvietikova et al., 1995).

Figure 6.1: Comparative sequence homology of HIF-1 and CRE binding sites in various hypoxia-inducible genes.

(G/A)CGT(G/C)C	Consensus HRE
TGACGTCA	Consensus CRE
AGACGTGC	Human PGK
TCACGTCC	Mouse PGK
GGACGTGC	Mouse LDH-A
AGGCGTGC	Mouse GLUT-1
TACGTGCT	Human Epo
TACGTGCT	Mouse Epo
ATACGTGG	Rat VEGF

LDH-A and Glut-1 were co-stimulated by hypoxia and a PKA activator (forskolin or 8-Cl-cAMP) in order to evaluate the potential for co-operative gene induction across a panel of human carcinoma cell lines (breast, fibrosarcoma and colon).

6.2 Methods

DNA constructs encoding the firefly luciferase reporter gene under the transcriptional control of HRE chimeras, derived from either the Epo, PGK-1, LDH-A, Glut-1 or VEGF genes, were transiently transfected into a panel of human carcinoma cell lines (HT1080, MDA 468, SQD9). The capacity of each HRE sequence to regulate gene expression in response to hypoxia, +/- cAMP analogues, was quantified relative to the SV40 early gene promoter. Cells were all transfected by electroporation and the experimental procedure was as described in 2.6. However, transfected cells were incubated in normoxia for 8 hours in the presence or absence of either 8-cl-cAMP or forskolin (activators of the PKA pathway) prior to 16 hours exposure to anoxia. Control cells were incubated for 24 hours in normoxia, +/- the PKA analog. Those cells primed with either 8-cl-cAMP or forskolin were incubated for the full experiment with the drug.

6.3 Results

It was important to determine a dose of 8-cl-cAMP that would stimulate the cells, via the PKA pathway, but was non-toxic. Previous data suggest a dose between 10 and 30μM (Firth et al., 1995). The experiment described was initially performed with varying concentrations of 8-cl-cAMP, ranging from 0.3 to 100μM, in two cell lines, HT1080 and MDA 468. The results were calculated as previously described and the amplitudes plotted on the graphs below after normalisation to the aerobic pGL3.control value.

Figure 6.2: Effect of 8-cl-cAMP on the expression of a variety on PGL3 HRE vectors in the MDA 468 breast carcinoma cell line, n=3. (See appendix 28)

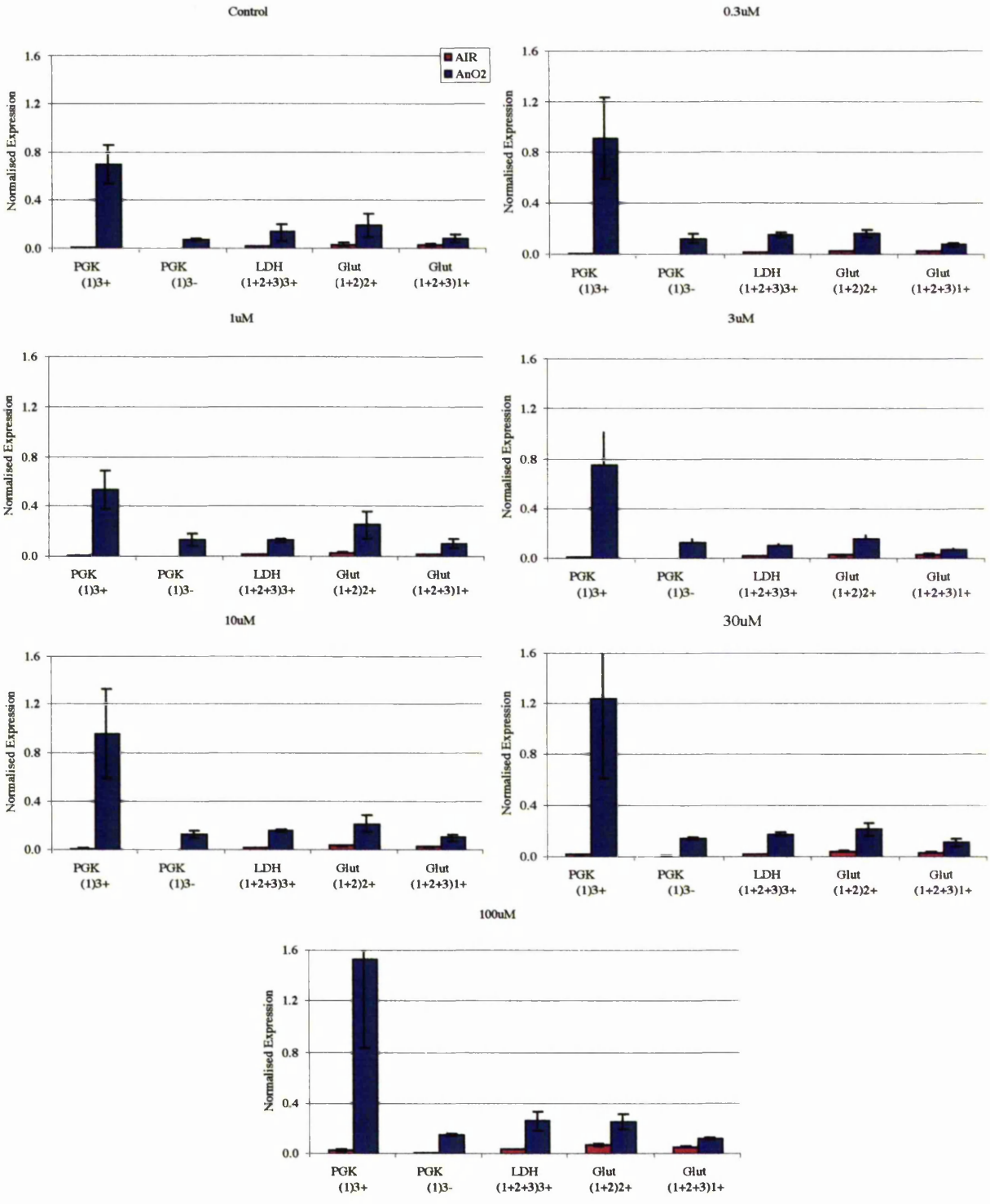

Figure 6.3: Effect of 8-cl-cAMP on the expression of a variety on PGL3 HRE vectors in the HT1080 fibrosarcoma carcinoma cell line, n=3. (See Appendix 29)

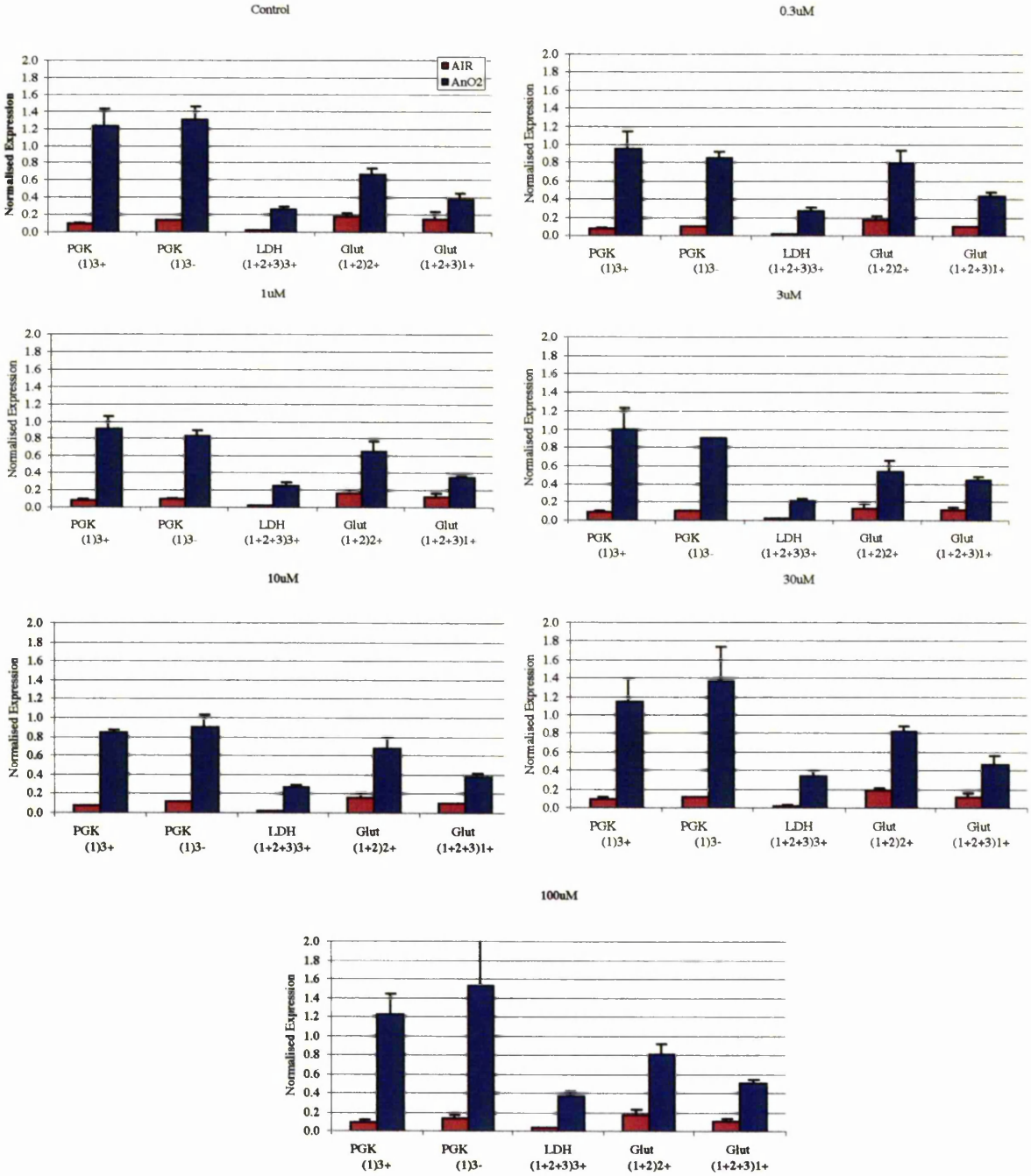

There was a minimal increase in anoxic HRE activity of cells primed with 8-cl-cAMP. A dose around 30μM appeared to have the greatest stimulatory effect although this was still small and was selected and applied to all cell lines as was in line with published data (Firth et al., 1995).

Any effect of the cAMP analogues on luciferase itself, was accounted for through the use of the pGL3.control vector being exposed to identical conditions as the test vectors and used for normalisation.

All experiments were performed in triplicate.

Figure 6.4: HRE activity after 8 hours +/- a PKA analog followed by 16 hours air or anoxia and 3 hours reoxygenation in the MDA 468 cell line, n=3.

(See appendix 30)

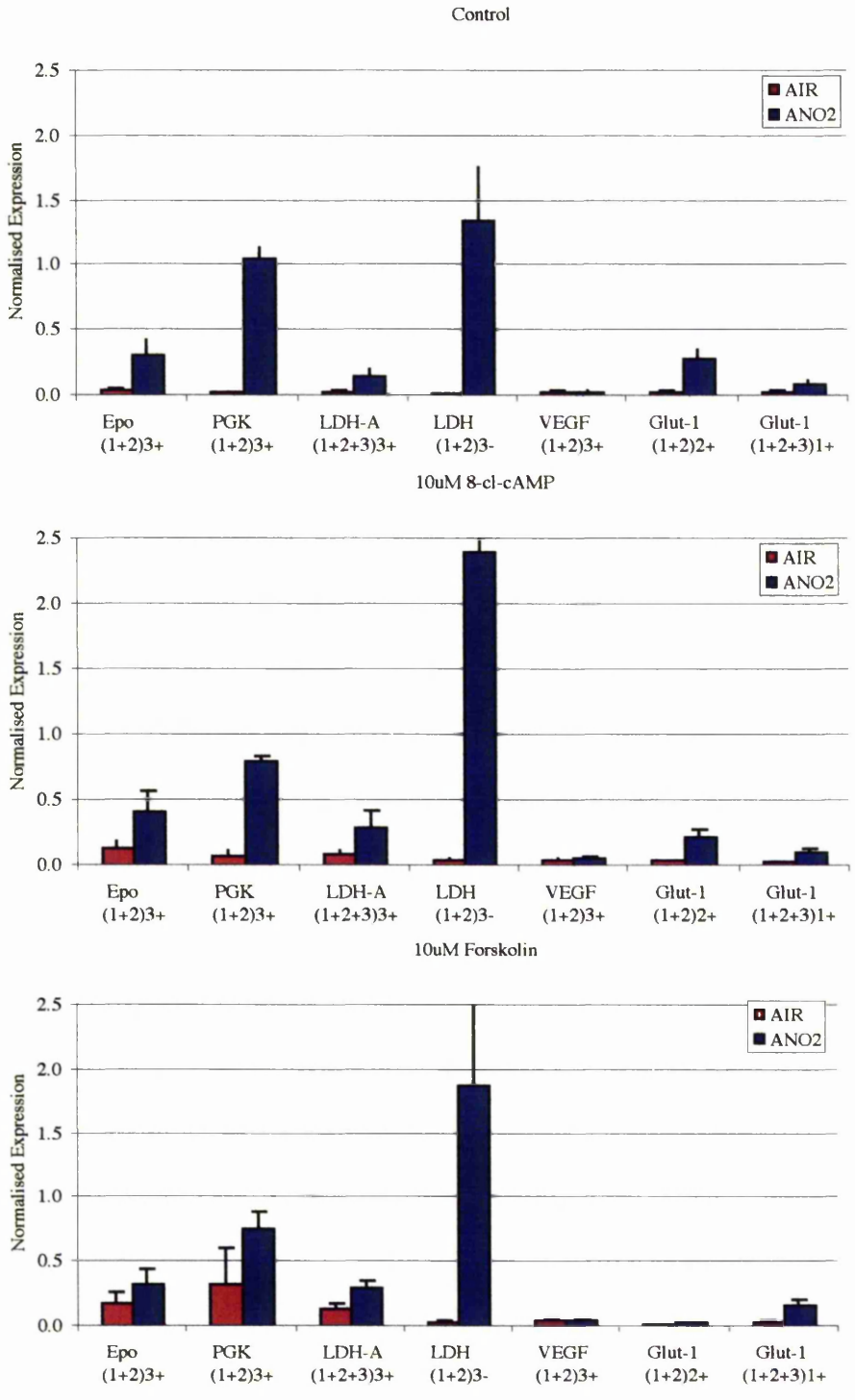

Figure 6.5: HRE activity after 8 hours +/- a PKA analog followed by 16 hours air or anoxia and 3 hours reoxygenation in the HT1080 cell line, n=3.

(See appendix 31)

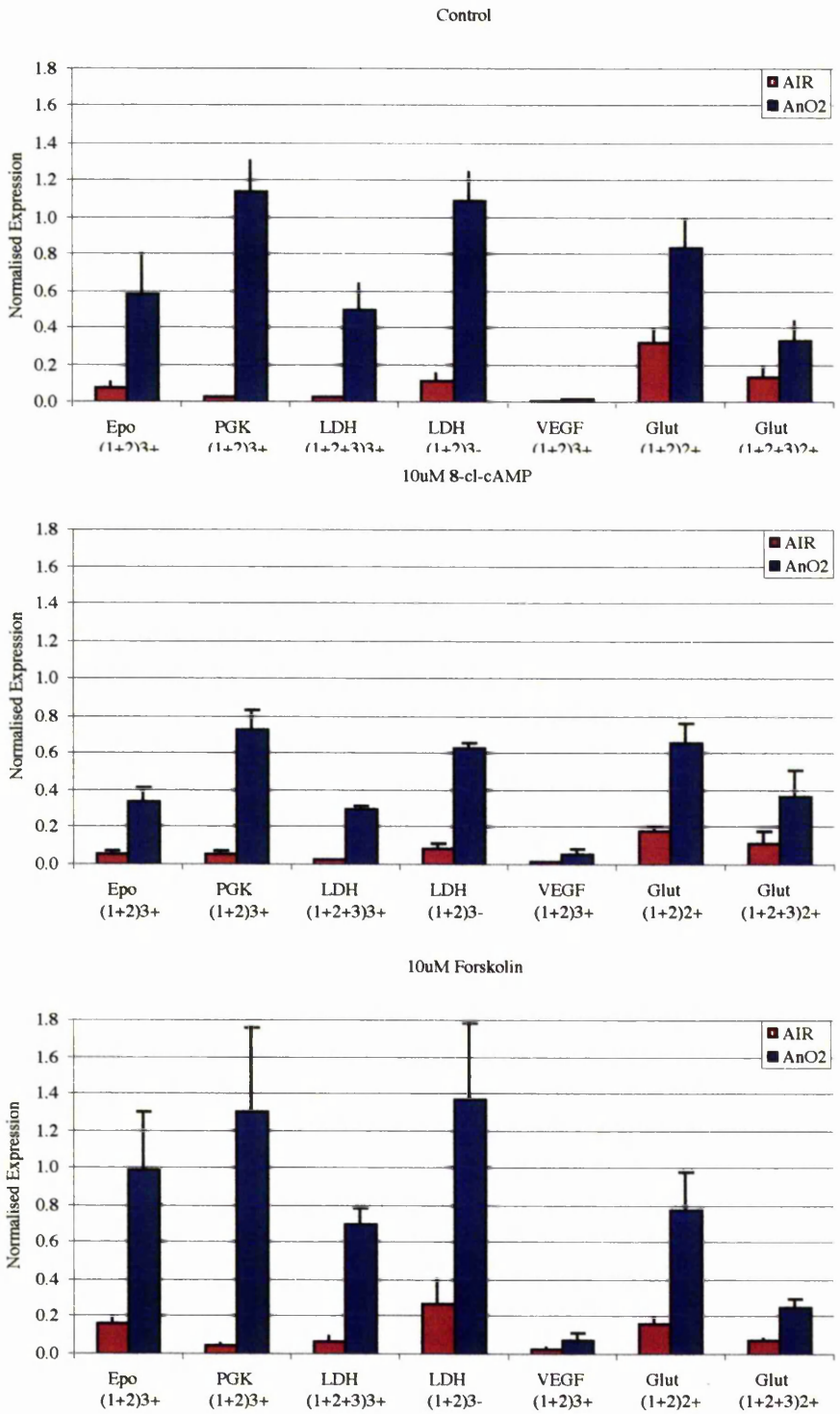

Figure 6.6: HRE activity after 8 hours +/- a PKA analog followed by 16 hours air or anoxia and 3 hours reoxygenation in the SQD9 cell line, n=3.

(See appendix 32)

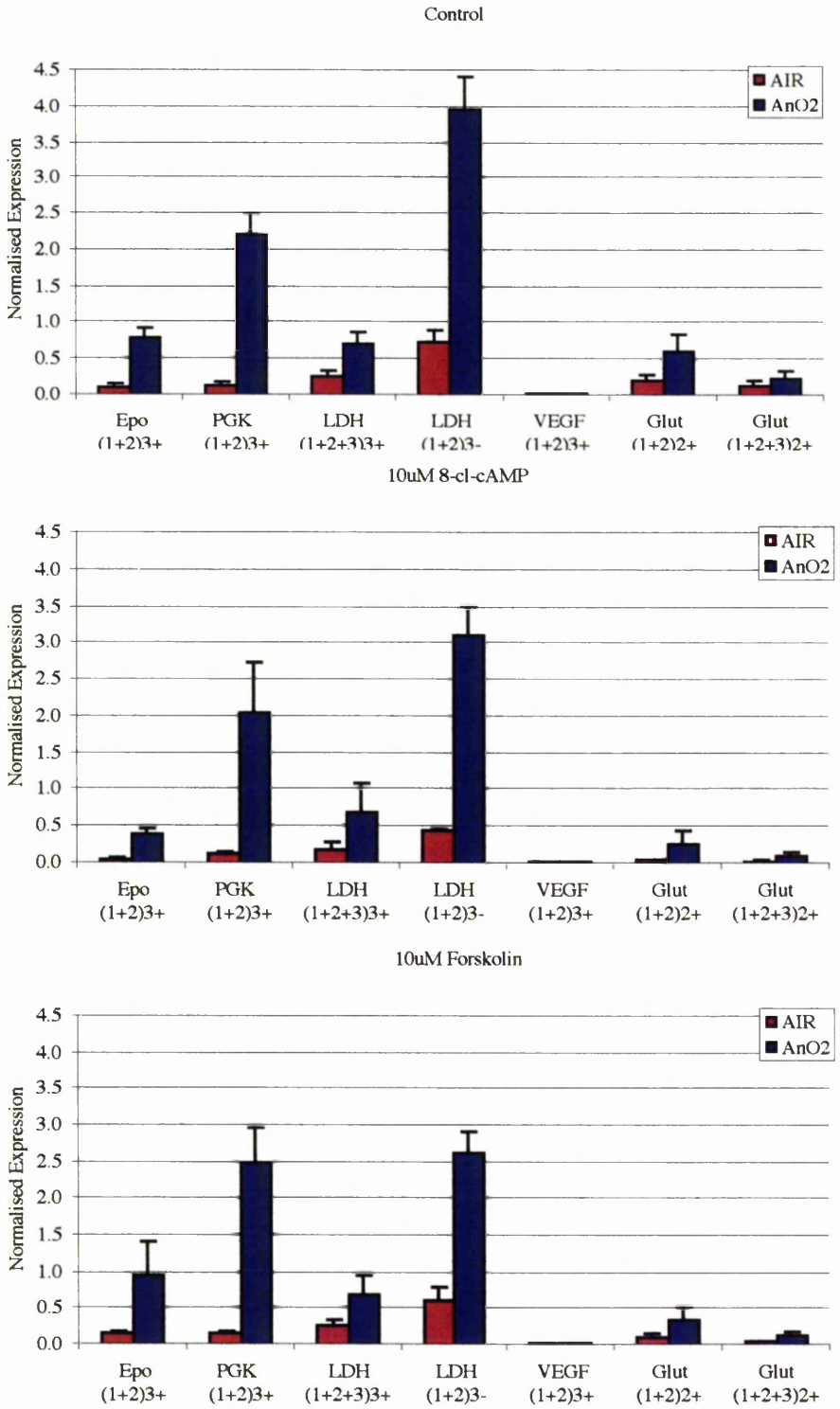

Table 6.1: HRE induction after 8 hours +/- a PKA analog followed by 16 hours air or anoxia and 3 hours reoxygenation

	HRE Induction								
	MDA 468			HT1080			SQD9		
	C	8-Cl	F	C	8-Cl	F	C	8-Cl	F
Epo $(1+2)^{3+}$	6.1	3.2	1.8	7.9	6.3	6.1	6.7	7.1	6.6
PGK $(1+2)^{3+}$	46.2	10.8	2.3	43.2	11.6	27.7	16.5	16.3	14.9
LDH-A $(1+2+3)^{3+}$	4.3	3.7	2.3	17.1	12.4	10.6	2.6	3.7	2.6
LDH-A $(1+2)^{3-}$	69.5	58.4	53.3	9.0	7.4	5.0	5.3	6.9	4.2
VEGF $(1+2)^{3+}$	1.1	1.4	1.0	2.7	4.1	3.1	0.9	1.5	1.4
Glut-1 $(1+2)^{2+}$	8.1	5.6	1.9	2.6	3.6	4.6	2.9	6.0	3.4
Glut-1 $(1+2+3)^{1+}$	2.8	3.8	5.3	2.4	3.1	3.5	1.9	3.3	2.8

C= Control, 8-Cl= 8-cl-cAMP, F= Forskolin

The LDH (1+2) HRE containing constructs showed the greatest induction under anoxia alone. Gene expression was upregulated 9-fold in the HT1080 cell line, 5-fold in SQD9 and 70-fold in the MDA 468. Addition of 8-cl-cAMP or foskolin prior to the 16 hours normoxic / anoxic incubation increased the amplitude of gene expression minimally in all cases. The greatest increases in activity were seen for LDH (1+2) plus 8-cl-cAMP in the MDA 468 cells and Epo and LDH (1+2) plus forskolin in the HT1080 cells. The oxic expression, +/- 8-cl-cAMP or forskolin, varied depending on the cell line. Therefore, the oxic / anoxic induction ratio was reduced due to an increased HRE stimulation under aerobic conditions, indicative of cross-talk between the cAMP-dependent signalling pathway and hypoxia-dependent signal transduction. The effect of 8-cl-cAMP and forskolin on the individual domain of LDH-A was then investigated, however, neither had any effect on their expression.

Figure 6.7: Expression of the dissected LDH-A elements 8 hours +/- a PKA analog followed by 16 hours air or anoxia and 3 hours reoxygenation in the HT1080 cell line, n=3. (See appendix 33)

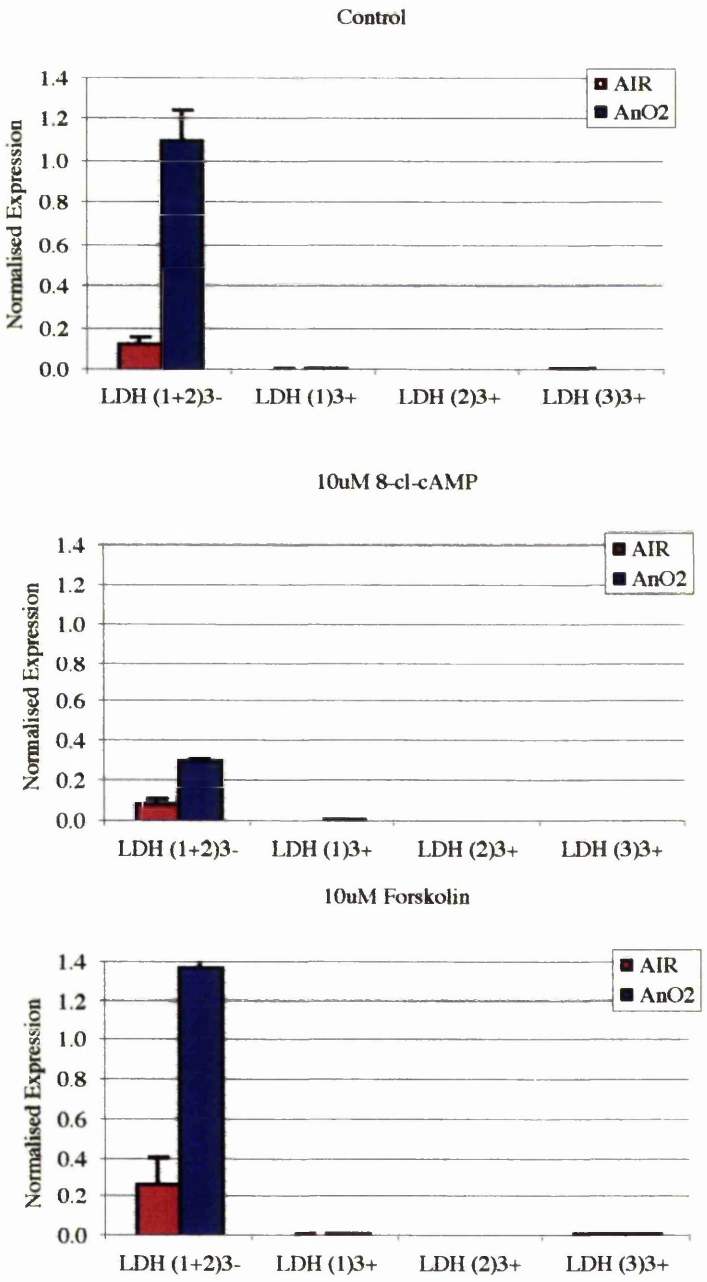

Figure 6.8: Expression of the dissected LDH-A elements 8 hours +/- a PKA analog followed by 16 hours air or anoxia and 3 hours reoxygenation in the SQD9 cell line, n=3. (See appendix 34)

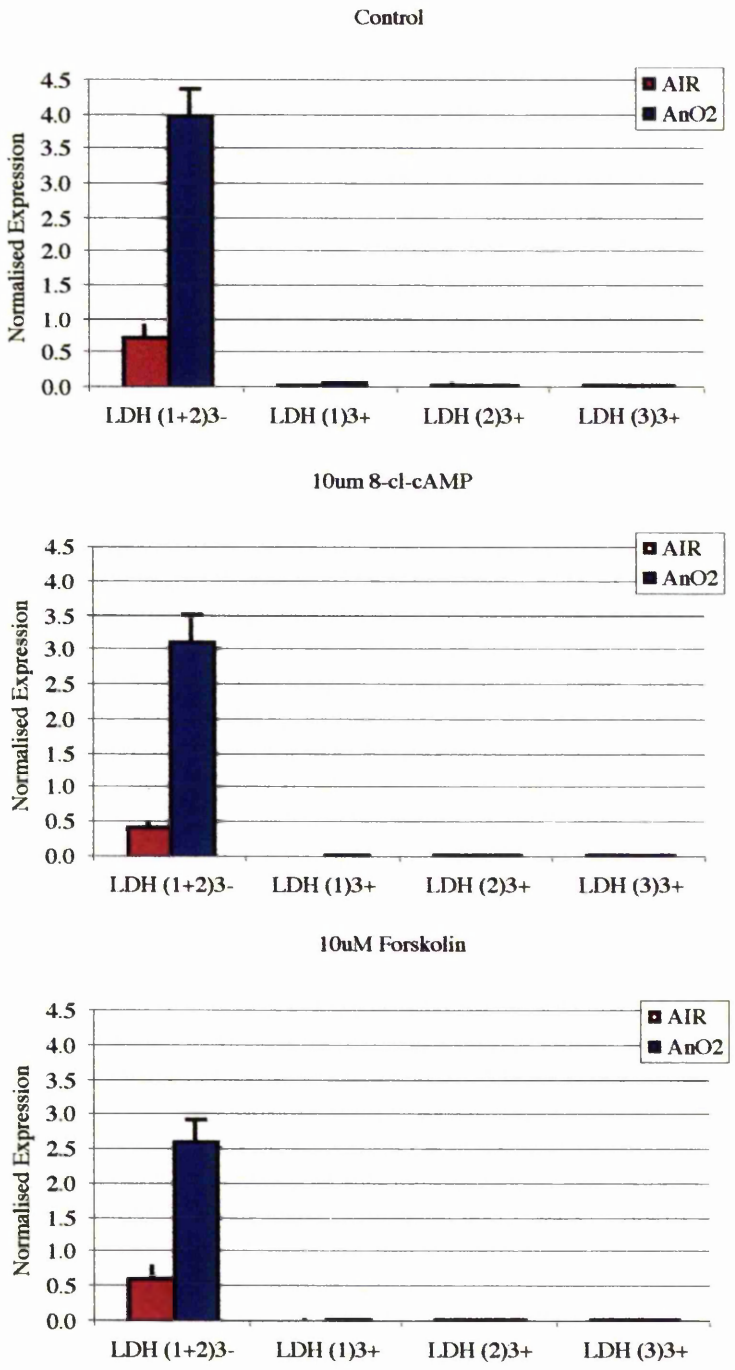

6.4 Discussion

The cAMP analogs, 8-cl-cAMP and forskolin, have been shown to increase LDH-A and Glut-1 HRE activity in Hela cells (Firth et al., 1995) These experiments tried to recpitulate these results, however, the cAMP PKA activators, 8-cl-cAMP and forskolin produced a minimal increase in HRE expression. The greatest effect was observed for the LDH (1+2) HRE. Firth et al. (1995), saw a decrease in HRE expression under normoxia when exposed to forskolin in the HeLa human cervical carcinoma cell line. Results appeared to be cell line specific with both positive and negative fluctuations in the oxic expression. The cAMP agonist, 8-Br-cAMP and forskolin have been shown to increase binding of CREB and ATF-1 to the constitutive HIF-1 binding site in a dose-dependent manner (Kvietikova et al., 1997). The PKA-dependent phsophorylation of CREB may enhance HRE function via the core CRE site which overlaps with the HIF-1 binding site. However, CREB does not appear to be essential to the hypoxia signal transduction pathway itself, with the CRE having a negative effect on the hypoxic inducibility of both the LDH-A and Glut-1 enhancers.

The cAMP analogues, 8-cl-cAMP and forskolin, bind to receptors on the regulatory subunits of PKA I and II with differing affinities. 8-cl-cAMP substitutes for endogenous cAMP. It has a high selectivity for PKA type II and preserves it in the holoenzyme form so preventing proteolysis, whilst downregulating PKA type I. 8-cl-cAMP restores a non-malignant pattern of PKA I:II in cancer cells, leading to differentiation and growth arrest in a wide variety of human cancer cell lines. In contrast, forskolin maximally stimulates both PKA types I and II non-specifically. Both of these analogs increase total CRE binding *in vitro*.

Each HRE vector contained a different set of response elements potentially involved in the hypoxia signal transduction pathway. By manipulating the levels of PKA types I and II (Table 6.2) it may be possible to manipulate the interplay between these distinct signalling pathways. However, these data suggest the influence of PKA pathway modulation on HRE function is too modest to be therapeutically useful.

Table 6.2: Pairs of cAMP analogs that preferentially activate PKAI/PKAII

Analog Pairs	Rel.Affinity for site A of PKA I	Rel.Affinity for site B of PKA I	Rel.Affinity for site A of PKA II	Rel.Affinity for site B of PKA II	Selectivity PKA I: PKA II
8-PIP-cAMP	2.3	0.065	0.046	3.2	5:1
8-AHA-cAMP	0.11	1.6	0.021	0.29	
6-Phe-cAMP	18.0	0.48	40.0	0.44	1:4
5,6-Cl-cBIMP	0.11	5.1	0.38	42.0	
6-MBC-cAMP	0.48	0.068	16.0	0.13	1:60
Sp-5,6-Cl-cBIMPS	0.022	0.13	0.034	14.0	
8-Cl-cAMP	2.7	2.0	0.051	4.6	1:3.3

Chapter 7

Integrating the Transcriptional Response to Hypoxia and Ionising Radiation

7.1 Introduction

Efforts have been made to optimise synthetic HRE chimeric promoters to generate robust and efficient vectors for gene therapeutics (Boast et al., 1999; Shibata et al., 2000). Rather than soley optimising the hypoxic response of chimeric HRE promoters, it may be possible to develop dual hypoxia and X-ray inducible promoters, such that the combination of both stimuli might provide a greater-than-additive effect upon transcriptional output.

A number of early response genes are induced in response to ionising irradiation (e.g. c-fos, Egr-1). This response is thought to be dependent upon the presence of serum response elements (SREs or CArGs; $CC[A/T]_6GG$) within the promoter regions (Datta et al., 1992). A natural example of the potential transcriptional relationship between HREs and SREs exists in the 5' enhancer of the glucose transporter-1 (Glut-1), where co-stimulation of the hypoxic-signalling pathway and the PKC signal transduction pathway result in significant transcriptional cooperativity (Ebert et al., 1995). In an attempt to recapitulate these observations using a chimeric promoter, a construct was generated, composed of the truncated X-ray responsive Egr-1 promoter (425bp) fused to a pentimer of the Epo gene minimal HRE (24bp) and a TNFa reporter gene (figure 7.1). This construct was responsive to both hypoxia (3.4-fold) and X-rays (3.3-fold), and the combination of both stimuli resulted in a synergistic output (11.7-fold) in the human colon carcinoma cell lines, HCT 116 and WiDr (Salloum et al., 1999; Saunders et al., 2000). Employing the now standardised reporter gene expression techniques, these initial observations were extended to a larger cell line panel.

Figure 7.1: Schematic representation of pGL3.Epo.Egr-1

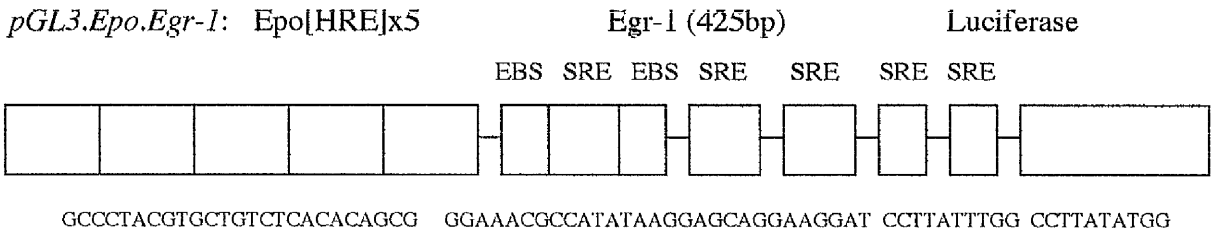

Further improvements to the chimeric promoter, Egr-1, have been explored by utilising the minimal CArG elements (figure 7.2). Marples et al. (2000), utilised the minimal CArG elements in the 5'-distal 'enhancer' region. They attached four directly repeated CArG elements to a green fluorescent protein (GFP) reporter and transiently transfected the construct into U87-MG glioma and MCF-7 breast human carcinoma cell lines. The CArG elements were able to function as radio-responsive transcriptional enhancers with an optimal dose of 3Gy, and were significantly more radiation inducible than the 425bp Egr-1 promoter in MCF-7 cells. This suggested that the CArG elements were able to function independently of other *cis*-acting element binding sites in the Egr-1 promoter regulated by various transcription factors e.g. SP-1, AP-1 and CREB. This was the first evidence demonstrating CArG elements functioning outside their natural context (Marples et al., 2000). The responsiveness of the 3'-proximal CArG elements alone and in combination with the Epo HRE used in the study by Salloum et al., (1999) were examined using the luciferase assay system. The final aim was to produce a novel combination of the best radiation-inducible enhancer with an optimal HRE.

Figure 7.2: Schematic representation of pGL3.CArG and pGL3.Epo.CArG

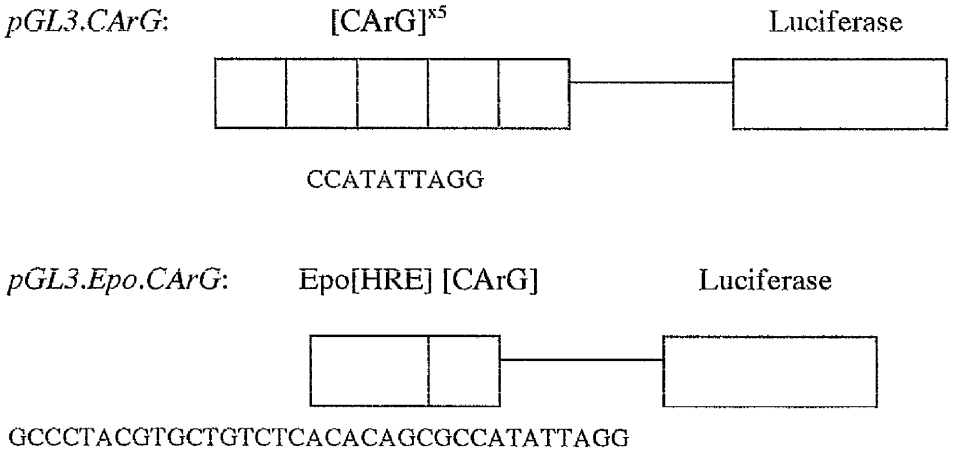

7.2 Methods

An oligonucleotide of the Epo 24bp HRE (chapter 4) containing the core HIF-1 binding site, had been multimerised to produce a pentimer (120bp; Pugh et al., 1993) and was kindly donated by Dr Peter Radcliffe, Institute of Molecular Medicine, Oxford. An Epo/Egr-TNFα vector (6.1 kb) was constructed by Dr Mark Saunders, which contained the five Epo HREs located 5' of the truncated Egr-1 promoter. The Egr-1 and Epo.Egr-1 fragments were isolated and cloned into the pGL3.basic vector (Promega). To facilitate this process, the multiple cloning region of the Sp72 (contaning the Glut-1 610bp sequence) vector was isolated Xho (5') and Xho (3') and subcloned into the Xho site in the muliple cloning region of pGL3.basic to provide a greater range of restriction sites into which Egr-1 and Epo.Egr-1 could be cloned (figure 7.3a). Egr-1 was isolated from Epo.Egr-1.TNFα at Sph I (5') and Bgl II (3') and ligated into pGL3.basic/Sp72 (Sph I/Bgl II) (figure 7.3b). Epo.Egr-1 was cut out of the same vector at Xho (5') and Bgl II (3') and cloned into pGL3.basic/sp72 at the respective sites (figure 7.3c). The Epo pentimer was isolated from the same plasmid Xho (5') and Xba (3') and cloned into the pGL3.promoter vector (Promega) at the corresponding sites (figure 7.3d).

Figure 7.3: Construction of pGL3.Egr-1 and pGL3.Epo.Egr-1 plasmids

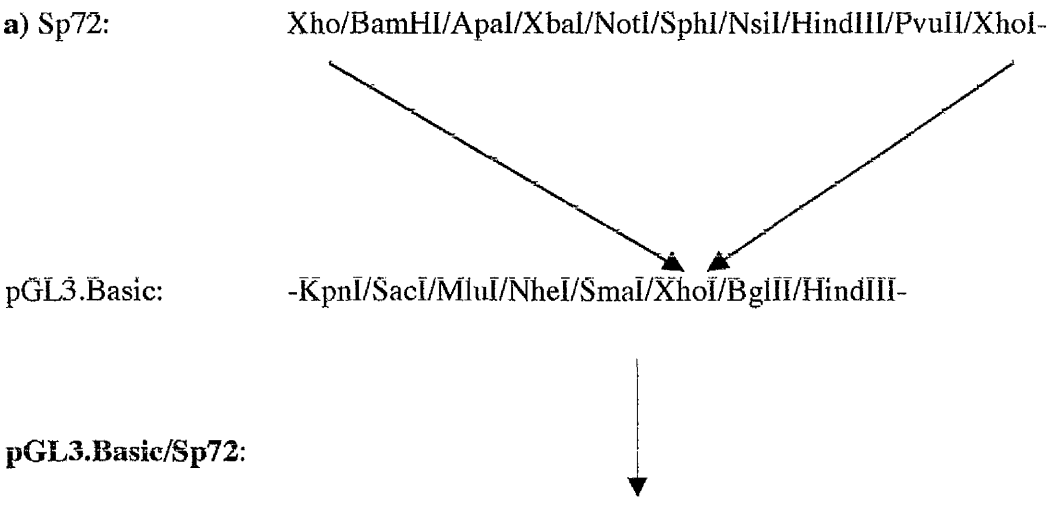

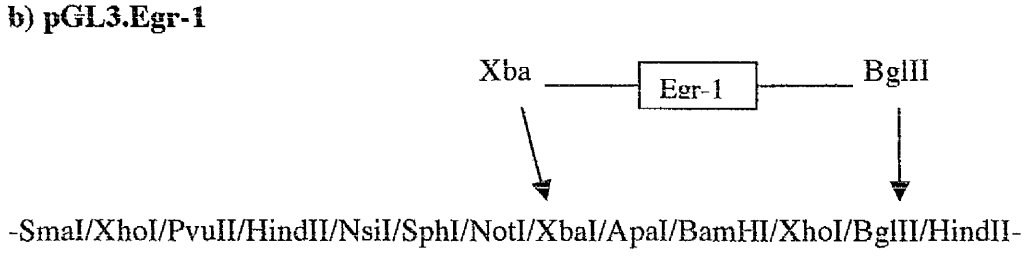

c) pGL3.Epo.Egr-1

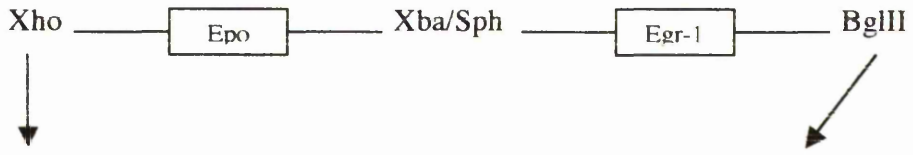

-SmaI/XhoI/PvuII/HindII/NsiI/SphI/NotI/XbaI/ApaI/BamHI/XhoI/BglII/HindII-

d) pGL3.Epo[5]

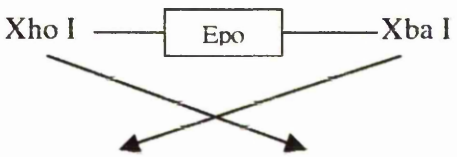

-SmaI/XhoI/PvuII/HindII/NsiI/SphI/NotI/XbaI/ApaI/BamHI/XhoI/BglII/HindII-

Oligonucleotides consisting of an Epo-CArG monomer or a CArG pentimer (figure 7.2) were made (SigmaGenosys) with Bgl II and Bam HI ends and cloned into the Bgl II site of pGL3.basic vector (Promega). The structure of all constructs was confirmed by restriction digests and sequencing (2.6).

The response of each vector in a panel of cell lines to either hypoxia (1% O_2), X-rays (5 Gy), or both stimuli, was tested. The experimental vectors were independently co-transfected with a CMV-driven renilla reporter plasmid by electroporation. 24 hours after transfection, cells were re-seeded into duplicate 24-well plates and exposed to air or 1% O_2 for 16 hours. Following the hypoxic exposure cells were irradiated with 5 Gy (250 kV X-ray source) under aerobic conditions and returned to normoxia for 1 to 6

hours reoxygenation. Subsequently cells were lysed and assayed for firefly and renilla luciferase activities (see section 2.6).

9.3 Results

All HREs used in this chapter were trimers as previously described. The exception being Epo, which was a pentimer (Pugh et al., 1993), identical to that used in the pGL3.Epo.Egr-1 vector in earlier studies (Salloum et al., 1999; Saunders et al., 2000).

7.3.1 pGL3.Epo.Egr-1: Transcriptional response to hypoxia and ionising radiation.

The effect of hypoxia, ionising radiation (5Gy) or the combination of both stimuli on Egr-1, Epo.Egr-1 and Epo[HRE]^5 was measured via the luciferase reporter system. Experiments were performed in human carcinoma cell line lines; fibrosarcoma (HT1080), breast (MDA 468), prostate (DU145), hepatocellular (HepG2) and colon (HCT 116 and WiDr) using the protocol described by Salloum et al. (1999). There have been a number of different reports as to the optimal length of reoxygenation after exposure to ionising radiation, therefore, cells were exposed to 1, 3 and 6 hours reoxygenation.

Figure 7.3: Expression of Egr-1, Epo.Egr-1 and Epo exposed to 16 hours air or hypoxia, +/- 5Gy and 1 to 6 hours reoxygenation in the HT1080 cell line, n=3.

(See appendix 35)

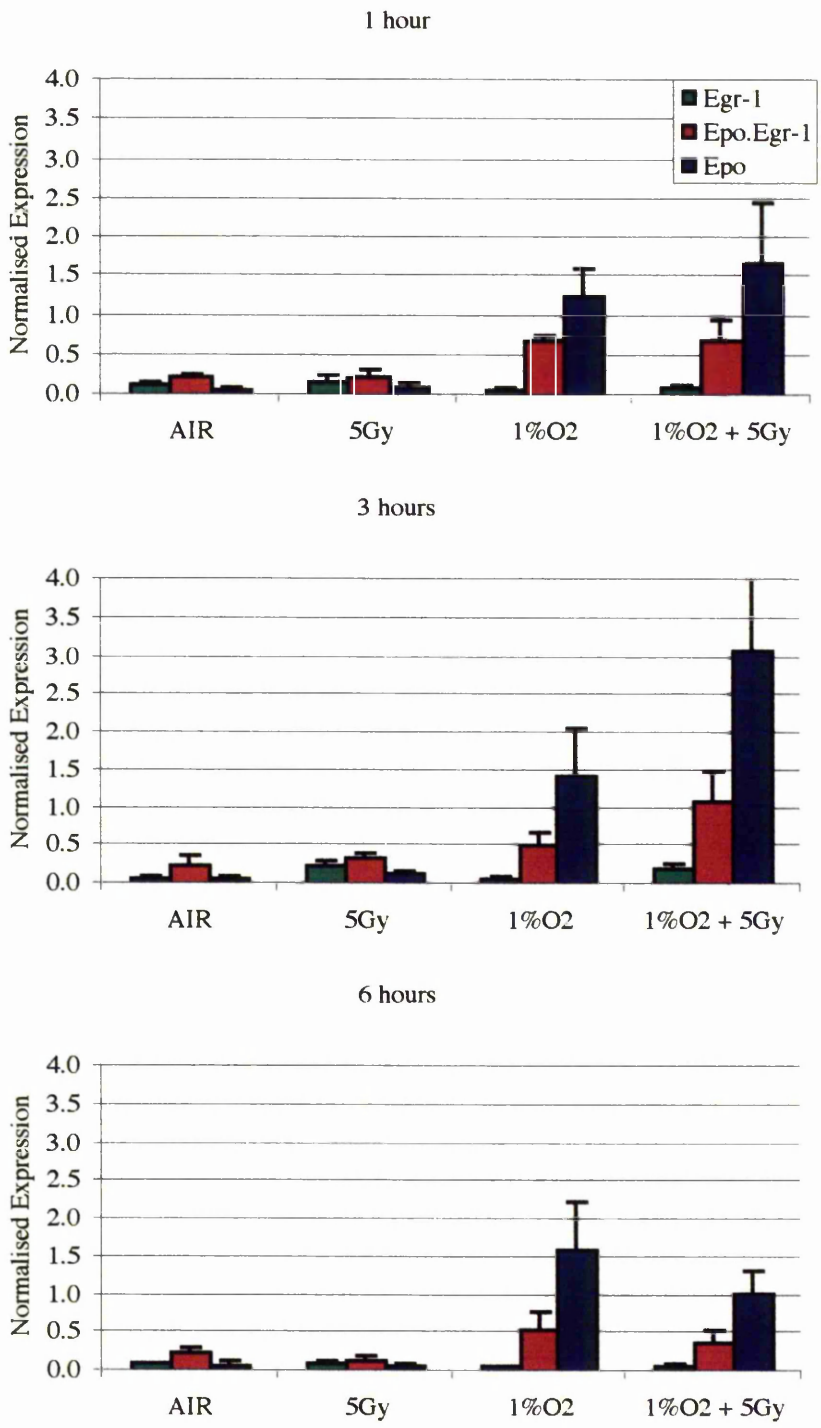

Table 7.1: Induction of Egr-1, Epo.Egr-1 and Epo exposed to 16 hours air or hypoxia, +/- 5Gy and 1 to 6 hours reoxygenation in the HT1080 cell line, n=3.

	1 hour			3 hours			6 hours		
	Egr-1	Epo.Egr-1	Epo	Egr-1	Epo.Egr-1	Epo	Egr-1	Epo.Egr-1	Epo
5Gy	1.13	0.97	1.15	2.72	1.46	1.84	1.09	0.63	0.65
$1\%O_2$	0.55	2.91	15.96	0.97	2.24	20.09	0.60	2.44	19.36
$1\%O_2$ + 5Gy	0.56	2.98	21.34	2.25	4.71	43.40	0.84	1.71	12.11

Optimal activity for each construct in the HT1080 cell line occurred at three hours reoxygenation. A modest Egr-1 promoter activity was observed in response to 5GY +/- $1\%O_2$, relative to air or $1\%O_2$ alone. A 1.5-fold and 11-fold increase was observed for Epo.Egr-1 and Epo respectively at $1\%O_2$ which rose by a further 2-fold for each plasmid when both stimuli were applied. However the Epo HRE was partially muted in the context of the Egr-1 promoter relative to the SV40 basal promoter.

Figure 7.4: Expression of Egr-1, Epo.Egr-1 and Epo exposed to 16 hours air or hypoxia, +/- 5Gy and 1 to 6 hours reoxygenation in the MDA 468 cell line, n=3.

(See appendix 36)

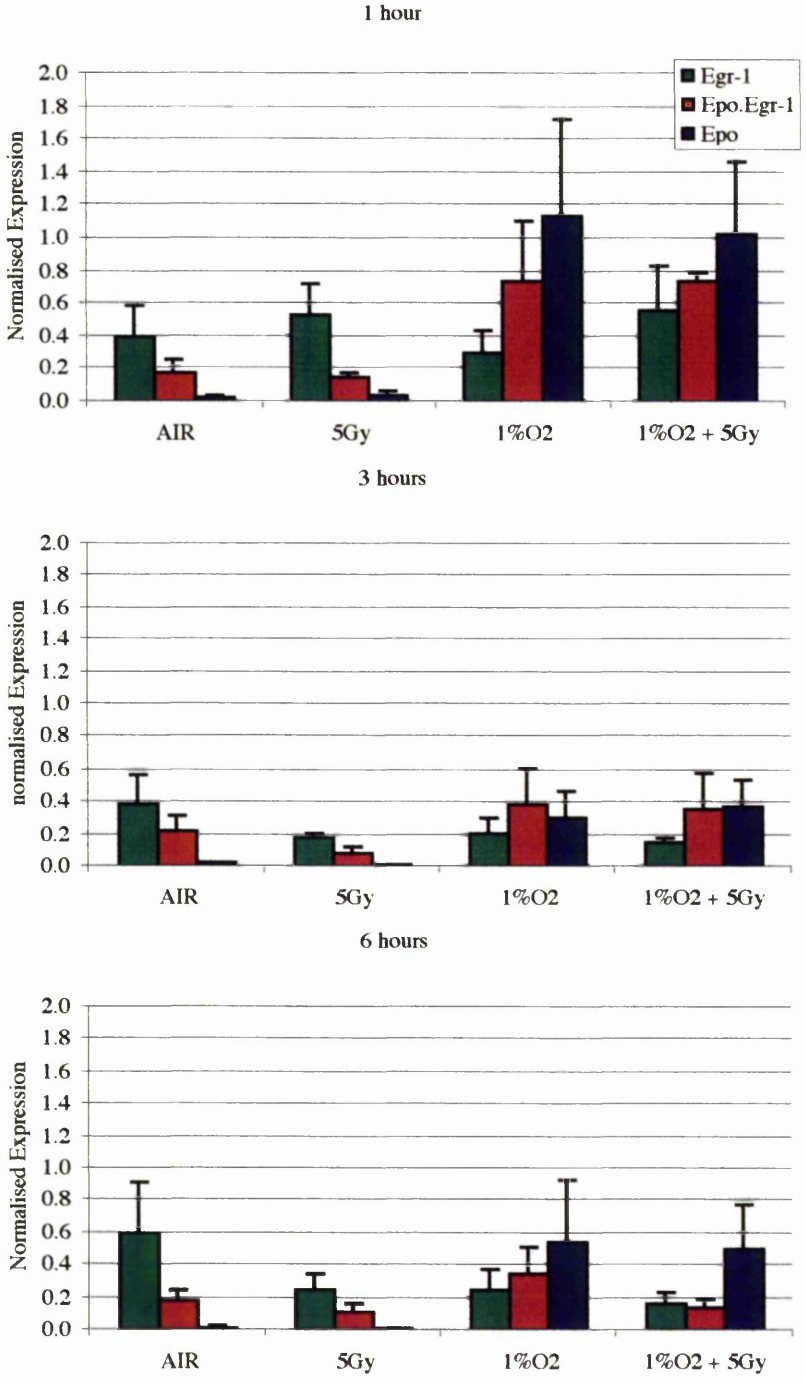

Table 7.2: Induction of Egr-1, Epo.Egr-1 and Epo exposed to 16 hours air or hypoxia, +/- 5Gy and 1 to 6 hours reoxygenation in the MDA 468cell line, n=3.

	1 hour			3 hours			6 hours		
	Egr-1	Epo.Egr-1	Epo	Egr-1	Epo.Egr-1	Epo	Egr-1	Epo.Egr-1	Epo
5Gy	1.35	0.82	2.18	0.46	0.39	0.51	0.42	0.59	0.71
$1\%O_2$	0.76	4.06	52.04	0.54	1.72	14.04	0.43	1.92	27.15
$1\%O_2$ + 5Gy	1.43	4.05	47.29	0.38	1.61	17.09	0.27	0.75	25.49

Both the Epo.Egr-1 and Epo constructs were responsive to hypoxia at the three time points examined. Egr-1 showed a marginal increase in activity in response to 5Gy radiation after one hour reoxygenation however, the activity had diminished by three hours. Niether Epo.Egr-1 nor Epo were responsive to radiation, instead a reduction in gene expression was noted. Thus the independent response elements within this chimeric promoter appeared not to cooperate in this cell line.

Figure 7.5: Expression of Egr-1, Epo.Egr-1 and Epo exposed to 16 hours air or hypoxia, +/- 5Gy and 1 to 6 hours reoxygenation in the DU145 cell line, n=3.

(See appendix 37)

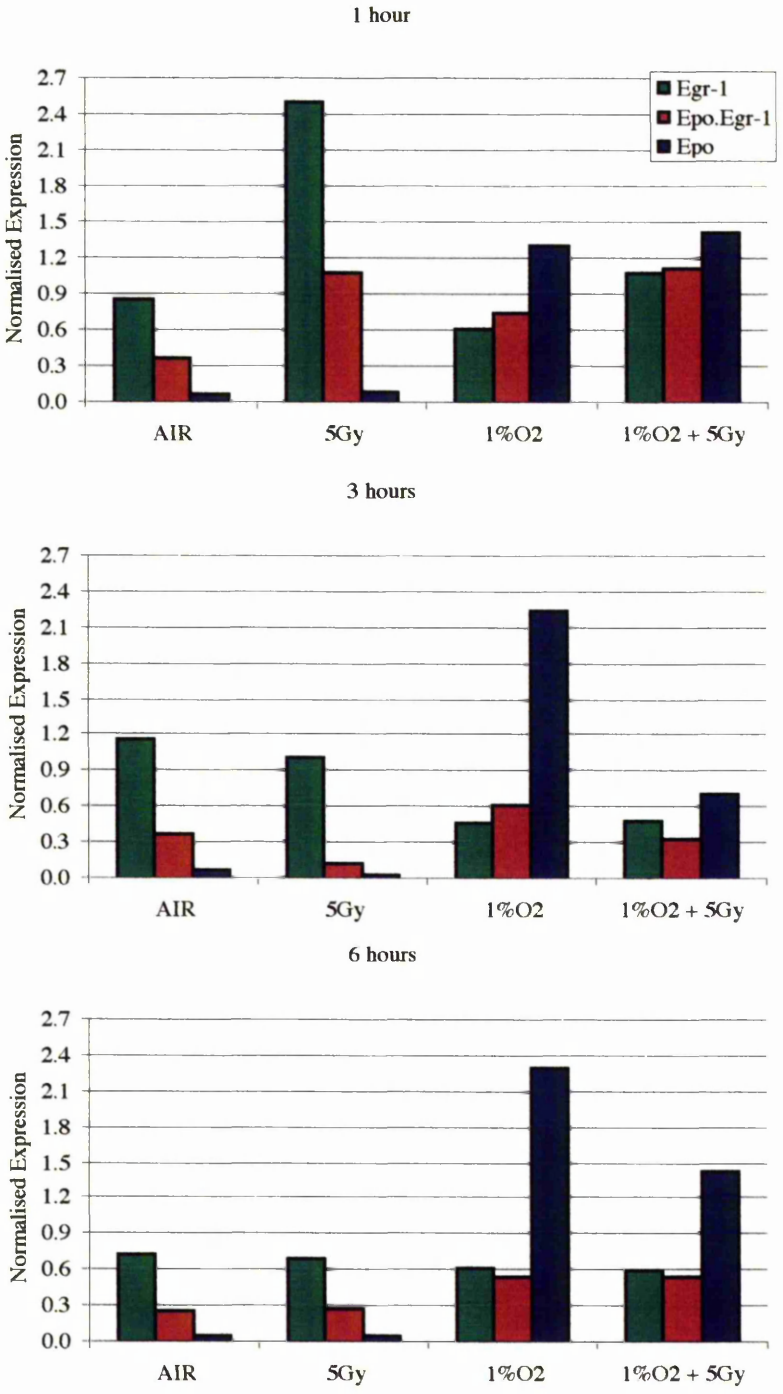

Table 7.3: Induction of Egr-1, Epo.Egr-1 and Epo exposed to 16 hours air or hypoxia, +/- 5Gy and 1 to 6 hours reoxygenation in the DU145 cell line, n=3.

	1 hour			3 hours			6 hours		
	Egr-1	Epo.Egr-1	Epo	Egr-1	Epo.Egr-1	Epo	Egr-1	Epo.Egr-1	Epo
5Gy	2.91	2.89	1.18	0.87	0.36	0.39	0.95	1.02	0.10
$1\%O_2$	0.71	1.99	18.17	0.40	1.66	30.31	0.85	2.02	3.49
$1\%O_2$ + 5Gy	1.25	3.00	19.60	0.42	0.89	9.61	0.82	2.00	2.18

The Egr-1 plasmid was responsive to 5 Gy after one hour reoxygenation, the activity of Egr-1 had diminished by three hours. The Epo HRE was responsive to hypoxia at each time point but not radiation. Only Epo.Egr-1 was marginally responsive to both independent stimuli, but this activity was not strictly additive upon co-stimulation. These data suggest that the the X-ray inducibility of the Egr-1 promoter *in vitro* is strongly cell line dependent.

Prelimary data of other cell lines tested with optimal reoxygenation times is shown below shown.

Figure 7.6: Expression of Egr-1, Epo.Egr-1 and Epo exposed to 16 hours air or hypoxia, +/- 5Gy and 6 hours reoxygenation in the HepG2 cell line, n=1.

(See appendix 38)

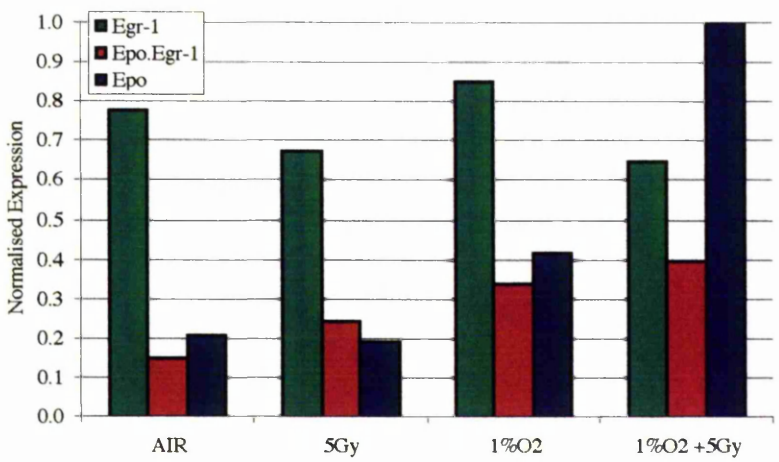

The Epo HRE-driven construct showed an increase in activity in response to hypoxia and, surprisingly, the combination of hypoxia and X-rays. In contrast Egr-1 displayed no hypoxic response and no increase in expression in response to radiation. In the HepG2 cell line the results of the Epo.Egr-1 construct suggested that the transcriptional response of the co-stimuli was additive. However the weak inducibility of the vector prevented any conclusions from being drawn.

Figure 7.7: Expression of Egr-1, Epo.Egr-1 and Epo exposed to 16 hours air or hypoxia, +/- 5Gy and 3 hours reoxygenation in the HCT116 cell line, n=1.

(See appendix 39)

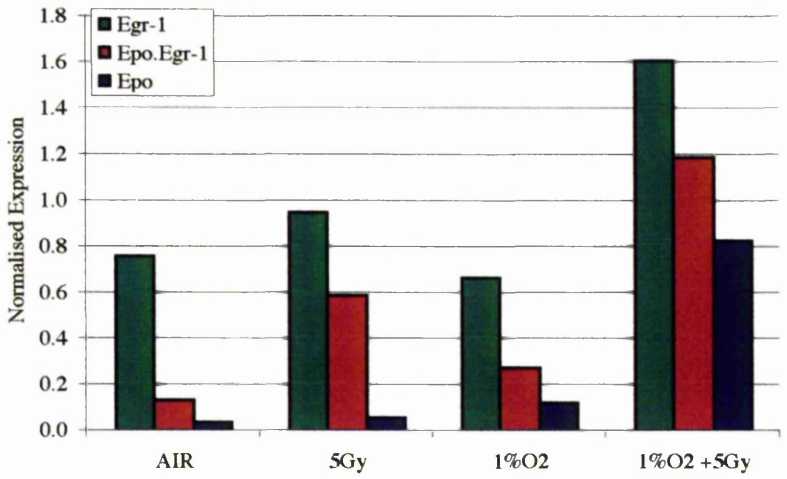

In the HCT-116 cell line, the Egr-1 promoter, in isolation, showed both a radiation and hypoxia inducible response, the combination of which was apparently additive. Luciferase activity peaked at three hours reoxygenation. Similarly, the Epo.Egr was responsive to the combination of hypoxia and X-rays, but the induction ratio to all stimuli was greater than that seen for Egr-1 due to a significant suppression of the non-irradiated oxic baseline. Thus the Epo HRE has a negative influence on the Egr-1 promoter activity under oxic conditions and consequently improved the 5Gy induction ratio from 1.2-fold to 5-fold. The Epo-driven reporter responded weakly to hypoxia, but again demonstrated a robust induction by co-stimulation. This appears to be the first cell line in which a cooperative response to both stimuli has been observed. However,

considering the cooperative nature of the co-stimuli upon the independent Egr-1 and Epo-driven reporter plasmids, it appears that the synergistic nature of the Epo.Egr-1 driven response to co-stimulation is unlikely to be due to any strict transcriptional cooperativity.

Figure 7.8: Expression of Egr-1, Epo.Egr-1 and Epo exposed to 16 hours air or hypoxia, +/- 5Gy and 3 hours reoxygenation in the WiDr cell line, n=1.

(See appendix 40)

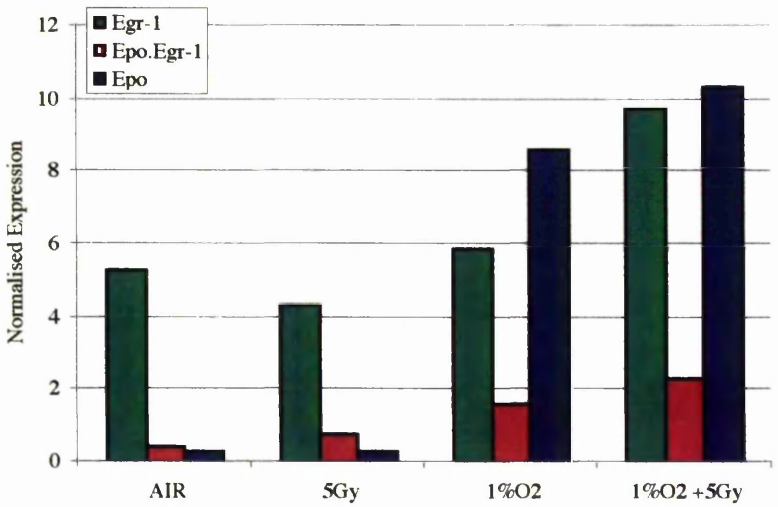

Both the Epo HRE, and to a lesser extent Egr-1 driven reporter plasmids, had an increased activity in response to hypoxia alone. Conversely Egr-1, and to a lesser extent Epo, had an additive response to the combination of hypoxia and 5Gy. The Epo.Egr-1 construct displays a hypoxia and X-ray responsiveness but it is distinctly muted, particularly when compared to the expression of the distinct elements. This further supports the suggestion that no specific cooperativity exists between the cognate transcription factors that bind the HREs and the Egr-1 promoter, but rather both components of the chimera are displaying an independently cooperative response to co-stimulation. Indeed, the weak nature of the Epo.Egr-1 chimeric promoter would suggest that the transcription factor interactions on this transcriptional control sequence are complex.

7.3.2 pGL3.Epo.CArG: Transcriptional response to hypoxia and ionising radiation.

Epo.CArG was made as an oligo containing a single copy of Epo and CArG. Attempts were made to multimerise the oligo but were unsuccessful. However, any response produced to hypoxia or X-rays should be visible with a single copy. Experiments in previous chapters indicate that multiple copies would increase the amplitude and induction of response rather than ablating it. The CArG oligonucleotide was prepared as a pentimer ($CArG^5$), when multimerised a single dimer was produced ($CArG^{10}$).

In each cell line tested, the CArG.Epo construct, despite being a single copy, was responsive to hypoxia and the combination of hypoxia and X-rays, with similar activities. The two CArG constructs appeared unresponsive to either stimulus.

Figure 7.9: Expression of CArG.Epo versus CArG multimers exposed to 16 hours air or hypoxia and 3 hours reoxygenation in the HT1080 cell line, n=2.

(See appendix 41)

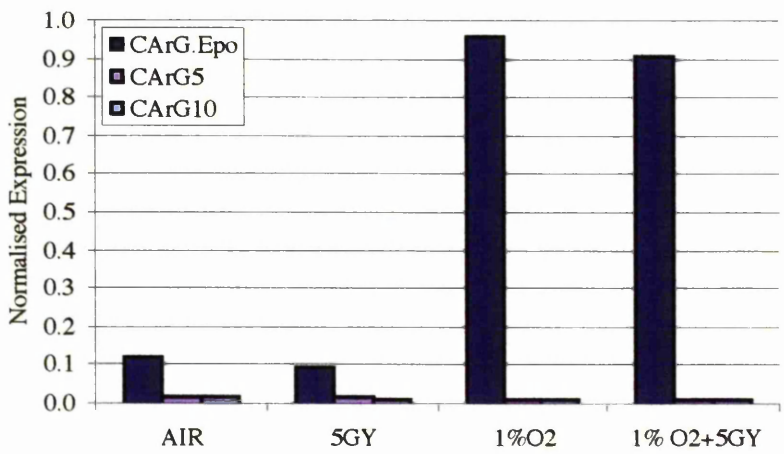

Figure 7.10: Expression of CArG.Epo versus CArG multimers exposed to 16 hours air or hypoxia and 1 hour reoxygenation in the MDA 468 cell line, n=2.

(See appendix 42)

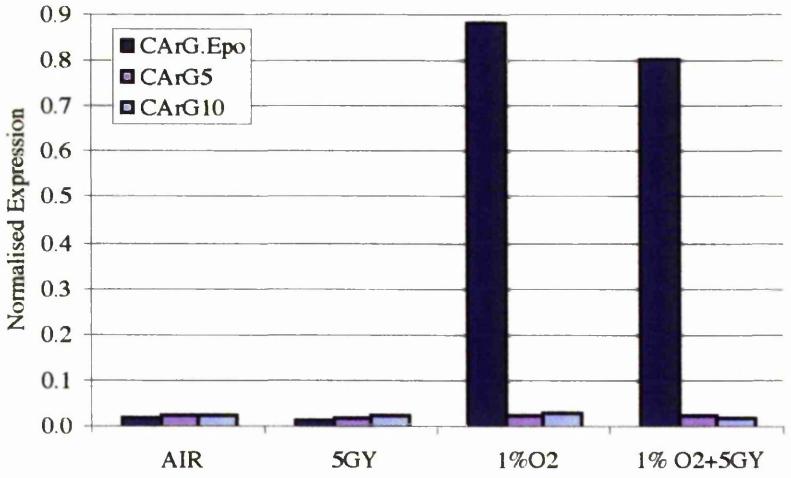

Figure 7.11: Expression of CArG.Epo versus CArG multimers exposed to 16 hours air or hypoxia and 3 hours reoxygenation in the DU145 cell line, n=2.

(See appendix 43)

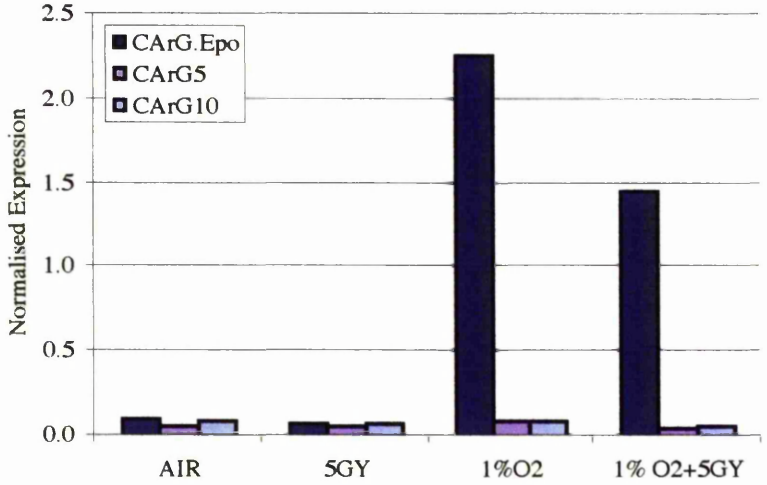

7.3.3 Synergistic response of HREs to hypoxia and ionising radiation

The observation that the Epo HRE pentimer, independent of the Egr-1 promoter, was responsive in an apparently cooperative fashion to the co-stimuli of 1% O_2 and 5 Gy, raised the question as to whether this was a property unique to the Epo construct, or common to HREs. Consequently a selection of the most robust HREs previously identified in this study, were examined for their response to the combined stimuli of hypoxia and radiation. Results were compared to that of the Epo pentimer. The experimental procedure was identical to that throughout this chapter: 16 hours air or hypoxia followed by exposure to 5Gy and 1 to 6 hours reoxygenation (only the optimal time points are show).

Figure 7.12: HRE activity when exposed to hypoxia and radiation with 3 hours reoxygenation, in the HT1080 cell line, =3 (except Epo n=4).

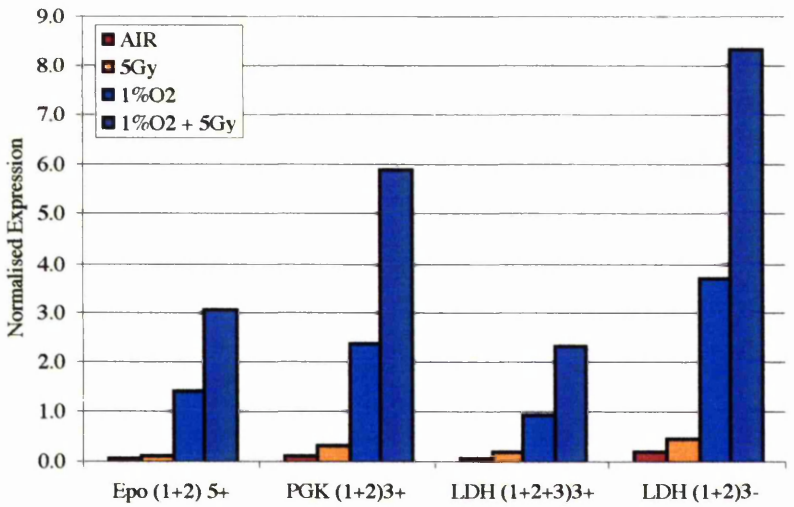

Table 7.14: Induction of HREs exposed to hypoxia and radiation in the HT1080 cell line.

	Epo (1+2) $^{5+}$	PGK (1+2)$^{3+}$	LDH (1+2+3)$^{3+}$	LDH (1+2)$^{3-}$
5Gy	1.84	3.06	2.52	2.07
1%O_2	20.09	20.79	10.46	16.33
1%O_2 + 5Gy	43.40	52.02	26.34	36.52

The HT1080 response was sustained at the time points measured, up to six hours post-reoxygentaion, with a peak in the combined response to hypoxia and X-rays at three hours reoxygenation, in a manner similar to hypoxia alone. There was a 10 to 20 fold increase in HRE activity when cells were exposed to 1%O_2. The combination of hypoxia and X-rays produced a 250% upregulation when compared to hypoxia alone for each HRE. This was not observed when the HT1080 cell line was irradiated but did not experience pre-hypoxia.

Figure 7.13: HRE activity when exposed to hypoxia and radiation with 1 hour reoxygenation in the MDA 468 cell line, n=3

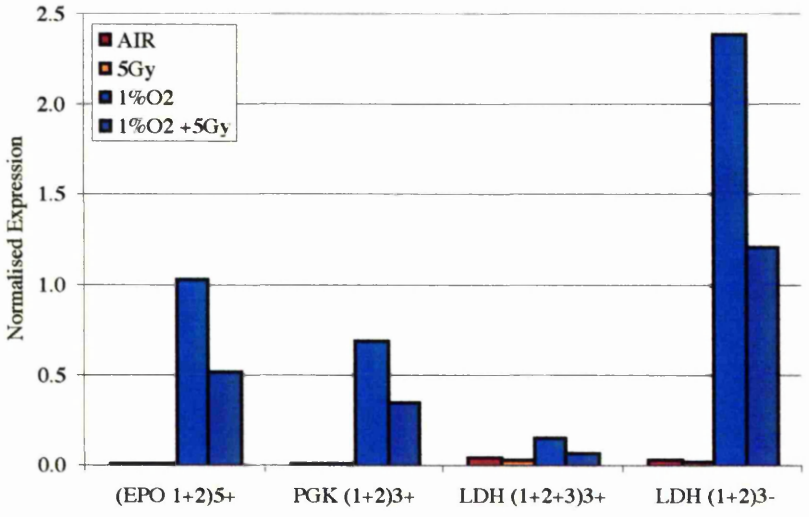

Table 7.15: Induction of HREs exposed to hypoxia and radiation in the MDA 468 cell line.

	Epo (1+2) $^{5+}$	PGK $(1+2)^{3+}$	LDH $(1+2+3)^{3+}$	LDH $(1+2)^{3-}$
5Gy	0.91	0.64	0.67	0.71
$1\%O_2$	58.36	41.22	3.26	72.32
$1\%O_2$ + 5Gy	29.96	20.65	1.55	36.80

At 3 hours reoxygenation the amplitude of response of each HRE at $1\%O_2$ equated to that seen at $1\%O_2$ + 5Gy, and at six hours reoxygenation the $1\%O_2$ amplitude had dropped below that of $1\%O_2$ + 5Gy. Therefore in this cell line the combination of hypoxia and X-rays produces a more durable response compared to $1\%O_2$ alone, when total light units were considered over all time points measured. This implies an extended HRE activity post-reoxygenation that is unrelated to hypoxic stabilisation of HIF-1. However, this response does not exceed that of the HRE activity to hypoxia alone, with radiation causing at least a 2-fold reduction in expression at one hour reoxygenation.

Figure 7.14: HRE activity when exposed to hypoxia and radiation with 1 hour reoxygenation in the DU145 cell line, n=2 (LDH (1+2); Epo[5]), n=1 (PGK (1+2); LDH (1+2+3)).

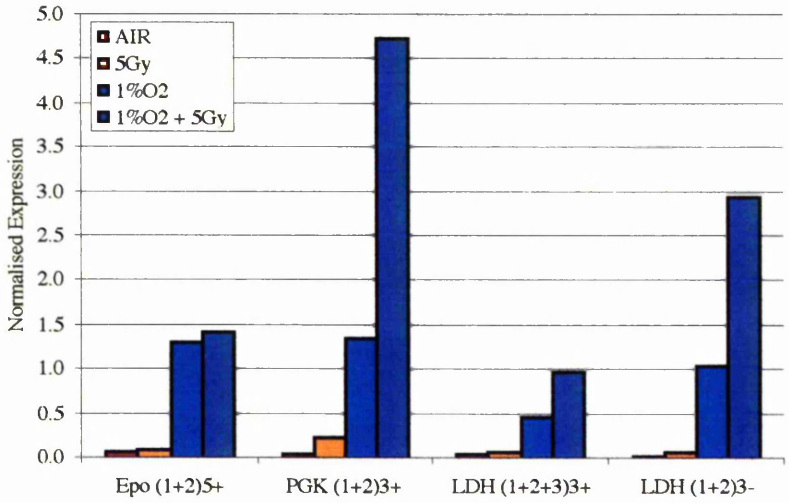

Table 7.17: Induction of HREs exposed to hypoxia and radiation in the DU145 cell line.

	Epo $(1+2)^{5+}$	PGK $(1+2)^{3+}$	LDH $(1+2+3)3+$	LDH $(1+2)^{3-}$
5Gy	1.18	4.28	1.44	2.49
$1\%O_2$	18.17	25.56	9.17	33.05
$1\%O_2$ + 5Gy	19.60	89.45	19.45	91.45

In the DU145 cell line the radiation inducibility of each HRE disappears by 3 hours reoxygenation. This suggests it is a transient response similar to that seen with Egr-1 and Epo.Egr-1 at one hour but not three hours post-hypoxia. All HREs respond to hypoxia, with a further 2-3-fold increase in activity on exposure to both stimuli, except for the Epo HRE.

Figure 7.15: HRE activity when exposed to hypoxia and radiation with 6 hours reoxygenation in the HepG2 cell line, n=1

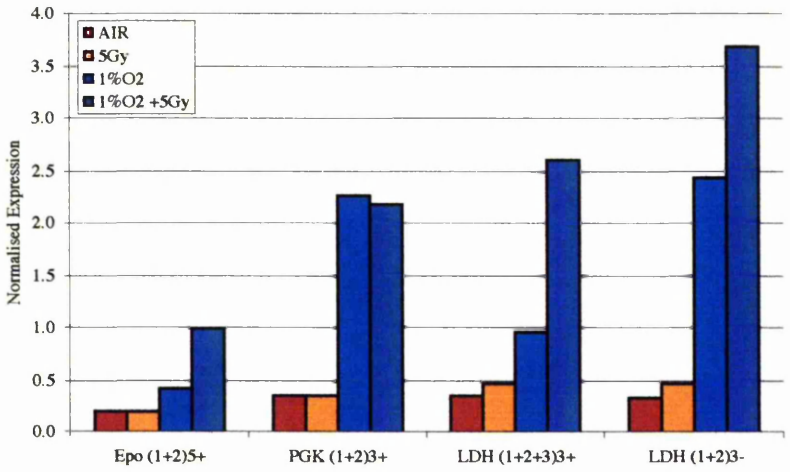

Table 7.19: Induction of HREs exposed to hypoxia and radiation in the HepG2 cell line.

	Epo (1+2) $^{5+}$	PGK (1+2)$^{3+}$	LDH (1+2+3)$^{3+}$	LDH (1+2)$^{3-}$
5Gy	0.94	0.99	1.30	1.38
1%O_2	2.00	6.28	2.71	7.23
1%O_2 + 5Gy	4.79	6.05	7.27	10.93

All of the HREs respond to hypoxia, and three of four (no PGK response) showed a further increase in activity on exposure to hypoxia and X-rays.

7.4 Discussion

As shown in Chapter 3, neither the CMV nor SV40 promoters are affected by changes in oxygen tension. These results are consistent with other published reports (Cheng and Iliakis, 1995; Boast et al., 1999). Cheng and Iliakis (1995), demonstrated that expression of the CMV and SV40 promoters also remained unchanged when exposed to 20Gy ionising radiation. In agreement no change in activity was observed for the pGL3.control vector, containing the SV40 promoter, or the pRL.CMV transfection control vector, containing the CMV promoter, in this set of experiments. Therefore, not only are both promoters used in the luciferase assay (SV40-Firefly and CMV-Renilla) unresponsive to hypoxia and radiation, but the post-transcriptional and post-translational activities of the reporter genes are not measurably influenced. Thus it is reasonable to conclude that all the changes in expression are a direct result of each enhancer element, rather than changes in promoter expression.

In four of the six cell lines (WiDr, HCT-116, HepG2, HT1080, but not DU145 and MDA468) there appears to be a combined response to hypoxia and radiation, which resulted in an additive or apparently super-additive increase in the activity of the Epo.Egr-1 chimeric promoter. However, in each case, there was a comparable or greater increase in the activity of Epo to the combined stimuli. The Egr-1 promoter only displayed this additive response to co-stimulation in the WiDr and HCT-116 cell lines. This implies that the increase in Epo.Egr-1 activity is as a result of the radiation responsiveness of Epo rather than Egr-1 For example there is 2–fold rise in Epo and Epo.Egr-1 expression in the HT1080 cell line exposed to both stimuli compared to hypoxia alone at three hours reoxygenation (figure7.3). A similar response was not observed for the Egr-1 construct.

The HCT116 colon carcinoma cell line appears to be the only cell line in this panel where an apparently synergistic response to hypoxia and X-rays was observed. However, the results are of a single preliminary experiment, so should be interpreted with caution. Egr-1 responded marginally to X-rays alone (1.2-fold), but not hypoxia,

yet produced a 2-fold increase in activity in response to hypoxia and X-rays. Epo responded 3-fold to hypoxia but had a dramatic 8-fold response to both stimuli. It appears that Epo.Egr-1 was responsive to the combination of both hypoxia and X-rays, producing a 4.5-fold response to X-rays alone but a 9-fold response to both stimuli. Even so, the absolute amplitude of reporter gene expression was less than that of Egr-1 alone (figure 7.7). This suggests that both the HREs and proximal Egr-1 promoter respond independently to co-stimulation and that the enhancement in induction ratios is not the result of any cooperativity between these regulatory elements, but rather a co-repression phenomenon. Thus both components of the chimeric promoter has a negative influence upon the other such that neither is able to drive transcription if the other is not occupied by appropriate inducible transcription factor(s). Indeed in the WiDr cell line the data would suggest that the combination of the Epo HRE with the Egr-1 promoter is antagonistic, whereby each component is inducible when utilised independently, but as a chimera the amplitude of co-induction is poor. This is predominantly a consequence of the negative influence of the Epo HREs on constitutive Egr-1 promoter activity.

Results suggest that the Egr-1 promoter may be hypoxia-responsive in the HepG2, HCT116 and WiDr cell lines. A number of studies (Soo-Kyung et al., 1999) have demonstrated an increased rate of Egr-1 transcription and protein, as well as DNA-binding activity in response to hypoxia. The mechanism for this response may be mediated by the Elk-1 binding sites in the 3'-proximal region of the Egr-1 promoter (see figure 7.1; Yan et al., 1999).

The HREs appeared to be radiation responsive in each of the cell lines tested (except the MDA 468s). It may be possible that the radiation response could be, in part, attributed to the status of other elements intrinsically expressed in each cell line, such as estrogen receptor or p53 status. The additional oxidative stress initiated by irradiating the cells immediately upon reoxygenation may contribute to the reperfusion insult. However proof that these observations are not artefacts of the reporter system will require more experimentation, including the analysis of HIF-1α protein levels and HRE binding affinity. In addition reporter gene (luciferase) protein and mRNA levels will

require analysis in order to establish that the phenomenon is genuinely the result of HRE transcriptional activation.

The synthetic CArG elements appeared to be unresponsive to both $1\%O_2$ and radiation in each of the cell lines tested and may even be having a negative regulatory effect on the activity of Epo. Combined with the data presented here and that of Datta et al. (1992) and Marples et al. (2000), it appears that only the 5'-distal CArG elements function independently of the Egr-1 promoter in response to X-rays and hypoxia.

The results presented here suggest that the Egr-1 promoter response to both hypoxia and X-rays is rapid and transient with optimal Egr-1 expression occurring in both a cell line and reoxygenation dependent manner. Bonventre et al. (1991), reported that reperfusion / reoxygenation was required for Egr-1 mRNA and protein accumulation to occur in the ischaemic rat kidney. Expression peaked at 1 hour following reperfusion, had decreased by 3 hours and was undetectable by 24 hours. Using the CArG enhancer element described by Marples et al. (2000), Scott et al. (2000) has developed a strategy utilising the cre/loxP recombination system of the bacteriophage PI to produce a more sustained response at lower radiation doses. It would be interesting to combine LDH $(1+2)^{3-}$ with the CArG elements optimised by Marples et al. (2000), combined with the natural Elk-1 binding sites of the 3'-proximal CArG elements. Along with the cre-LoxP site, this may produce a more prolonged response and increase the differential between basal and induced expression.

Chapter 8

Discussion

The disorganised and inadequate vasculature typical of most solid tumours results in regions of chronic (spatial) and acute (temporal) hypoxia. Cells in these hypoxic regions are considered to be resistant to radio- and chemotherapy. Beyond the diffusion distance of molecular oxygen, there are multiple indirect consequences of poor tissue perfusion. Since many antineoplastic agents act on the DNA of proliferating cells, the poor cell cycle kinetics of hypoxic cells affords some protection (Durand et al., 1999). In addition, hypoxia itself may induce multiple stress-related proteins that confer transient resistance to chemotherapeutic agents (Dachs et al., 1998). Further, these cells are often distal from functional tumour vasculature and may escape exposure to cytotoxic concentrations of agents, particularly if the tissue diffusion characteristics of the therapeutic agent are limited (e.g. DNA intercalators). Despite the multiple resistance mechanisms manifest by inadequate tumour perfusion, it represents a universal and exploitable difference between tumour and normal tissue. A major approach to exploiting this altered physiology of the tumour microenvironment is the use of bioreductive drugs, several of which are currently in clinical trials (tirapazamine, AQ4N; Brown and Giaccia, 1998).

As a consequence of reduced oxygen and nutrients, e.g. glucose, hypoxic cells alter the expression of multiple genes involved in cellular and physiological homeostasis in order to adapt and survive under these adverse conditions. There is an increase in the expression of genes involved in diverse functions such as angiogenesis, vascular homeostasis, pH regulation, glucose transport and glycolytic metabolism. Hypoxia responsive elements (HREs) regulate the expression of these genes and consequently they are over-expressed in hypoxic tumour cells compared to adequately oxygenated tissues. These HREs could be exploited in gene therapy strategies, to selectively drive

the expression of (various) therapeutic gene products within the hypoxic regions of tumour tissues. Putting aside the issue of which gene products are most appropriate in such an application, a key question that arises is which HRE(s), (in an optimised configuration), would provide the most robust, consistent and selective transcriptional response to hypoxia in multiple tumour cells of epithelial origin?

Thus the aim of this thesis was to evaluate the hypoxia-inducible transcription and amplitude of a variety of HRE sequences across a panel of human carcinoma cell lines of diverse tissue origin. The intention was to identify the most robust and consistently active HRE at physiologically relevant oxygen tensions (1% O_2) for use in gene therapeutic applications. A set of HREs derived from angiogenic, glucose transporter and glycolytic genes have been dissected and evaluated in order to obtain the maximal level of gene induction under hypoxia. A HRE involved in lactate metabolism was identified which, by these criteria, produced a superior response under hypoxia. This optimisation was found to involve the sequence identity of a constitutive transcription factor binding site adjacent to the well recognised core HIF-1 binding site.

Previously the HREs contained within the Epo, PGK, VEGF, Glut-1 and LDH-A HREs have been dissected and optimised for their hypoxic response by a variety of investigators (Maxwell et al., 1993; Firth et al., 1994; Semenza et al., 1994; Liu et al., 1995; Ebert et al., 1995; Firth et al., 1995; Boast et al., 1999; Shibata et al., 2000) However, the activities of each HRE have not been compared to one another under identical experimental conditions. Some studies were restricted to a single cell line, whilst in others, HREs with differing copy numbers were compared. This work began by comparing the previously optimised HRE sequences from the Epo, PGK, VEGF, Glut-1, and LDH-A oxygen-responsive genes. Each HRE was studied as a trimer using the now widely accepted Dual Luciferase Assay system designed by Promega, across a panel of three human carcinoma cell lines.

Each HRE was either isolated from its existing plasmid or constructed as an oligonucleotide and cloned into the pGL3.promoter vector (Promega) as a trimer in the

homologous (positive) orientation, 5' of the SV40 promoter. Using a standardised protocol, each HRE construct was independently co-transfected with a pRL.CMV reporter plasmid (to control for transfection efficieny) into a panel of human carcinoma cell lines (MDA 468, HT1080, SQD9) by electroporation. 24 hours after transfection, the cells were reseeded into triplicate 24-well plates and exposed to either 16 hours air, 1%O_2, or ≥0.002%O_2, followed by 3 hours reoxygention. The cells were then lysed and assayed for firefly and renilla luciferase activities.

Results (chapter 4) demonstrated that the PGK HRE (either 18 or 24bp sequence) had the greatest hypoxic and anoxic activity compared to other HREs tested. The low inducibility of the LDH-A and Glut-1 HREs was noted. Transcription of these HREs is governed by an array of transcription factor binding sites. Within each oxygen-regulated gene there is sequence conservation at the HIF-1 binding site, as well as precise spacings between adjacent sites, thought to have a co-operative role with HIF-1 in the hypoxic response. Adjacent transcription factors bound to promoters and enhancers and may form nucleoprotein complexes which are capable of integrating responses from multiple signal transduction pathways (Tjian and Maniatis, 1994).

Firth et al. (1995) and Ebert et al. (1995) both demonstrated the functional importance of HIF-1 and its co-operative enhancer sequences; specifically the CRE, in producing a synergistic interaction in response to hypoxia in the LDH-A enhancer and the SRE in facilitating a synergistic response to hypoxia and PKC co-activation in a truncated Glut-1 enhancer lacking its natural CRE, respectively. By dissecting the functional *cis*-acting enhancer sequences contained within the LDH-A and Glut-1 HREs it was demonstrated that the CRE had a negative regulatory effect on HRE-regulated transcription across the cell line panel. The activity of the modified LDH-A HRE lacking the CRE (site 3) was compared to each of the three PGK HRE variants. LDH (1+2) had a hypoxic and anoxic expression equalled to, or superior than, PGK across a panel of seven human carcinoma cell lines from various tissue origins (breast, colon, lung, head and neck, prostate). Further, maximal induction was nearly always observed at 1%O_2, whereas the PGK variants showed 40-90% activity when compared to

≥0.002% O_2. This observation is relevant to the application of hypoxia-directed gene therapy, with respect to the magnitude and therapeutic relevance of the target cell population.

Whilst hypoxic response of the PGK HRE in either the forward or reverse orientation appeared to be cell line specific, the LDH (1+2) had a consistent superior response in the negative orientation in all cell lines tested. Increasing the copy number of either PGK or LDH-A had no positive effect on inducibility, however, increasing the copy number of Epo produced a much greater level of transcription, but it was not superior to that of PGK or LDH-A.

The data (chapter 4) demonstrated that in the Epo, PGK and LDH-A HREs site 2 played an integral role in the hypoxic response. It did not function independently but rather appeared to function co-operatively with the core HIF-1 binding site in the context of LDH-A. In an attempt to achieve greater levels of oxygen-regulated gene transcription site 2 of each HRE was replaced with site 2 of LDH-A (chapter 5). In the context of Epo and VEGF this site dramatically improved the hypoxic response. However, the modified PGK HRE had a reduced activity, but a marginally greater induction in two of the cell lines (HT1080 and SQD9) caused by a reduction in the basal activity. The equivalent sequence motif (site 2) from the Epo HRE could not confer any transcriptional regulation when combined with the HIF-1 binding site from LDH-A. Thus the LDH-A ChoRE (site 2) seemed to function optimally in its natural context but was able to co-operatively increase gene transcription in other HREs. This observation has not previously been reported and suggests a new aspect to the functional optimisation of HREs for therapeutic applications.

The LDH-A ChoRE (site 2) is identical to the core sequence motif, CACGTG, for the Myc/Max response element. It was shown by Fisher et al., (1993), that altering the base immediately 5' to this sequence could increase or ablate functionality of this enhancer. The data (chapter 5) demonstrated a significant reduction in the LDH-A response when the critical cytosine residue, 5' of the core E-box motif was exchanged

for thymidine (C→T). However, the responses were significantly lower than that of the original LDH (1+2) sequence, when the 'C' was exchanged for an 'A', 'G' or the site altered to produce a consensus E-box binding site. Therefore the original ChoRE motif contained in the LDH-A proved to have the best co-operative transcriptional (hypoxic and anoxic) response with the HIF-1 binding site, suggesting that the sequence requirements for cooperative interactions of their cognate transcription factors are precise.

LDH (1+2) showed the most specific inducible response to HIF-1α expression compared to Epo, PGK, VEGF or Glut-1 in the Ka13 and C4.5 (wt) cells, suggesting it has the strongest affinity for binding HIF-1α. With the exception of VEGF, each HRE appears to respond in a HIF-1α-dependent manner. In contrast, VEGF appeared equally responsive to either HIF-1α or EPAS-1 with similar induction ratios. Whilst the pattern of expression of the HRE panel was similar in each cell line, the amplitude of response may be dependent, in part at least, on the aggressiveness of each carcinoma cell line to proliferate after exposure to hypoxia (Blancher et al., 2000).

The transcriptional co-activators p300/CBP have been demonstrated to interact with HIF-1α and CREB (Arany et al., 1996) suggesting a level of integration between the secondary messanger cAMP and the oxygen sensor via co-operative transcriptional activation. Most of the actions of cAMP are implicated in a variety of cellular functions related to protein phosphorylation through PKA activation. CREB has been shown to compete for binding at the HIF-1 site. Each of the HREs contain a variant of the asymmetrical CREB site. A number of studies have shown a level of integration between the HIF-1 and CRE binding sites contained within the LDH-A and Glut-1 enhancers (Ebert et al., 1995; Firth et al., 1995). Firth et al. (1995) showed it was possible to co-stimulate the LDH-A HRE with hypoxia and forskolin to produce a synergistic response. These observations were re-evaluated in the original cell line and HRE panel, with the addition of LDH $(1+2)^{3-}$ (MDA 468, HT1080, SQD9). The experiments were performed in a similar manner to those previously but with the addition of an 8 hour incubation of cells with either 8-cl-cAMP or forskolin prior to (and

during) aerobic and anoxic exposure. The synergistic response observed was not as great as that reported by Firth et al. (1995) and affected both the anoxic and basal HRE activities (chapter 6). Each of the HREs appeared marginally responsive to 8-cl-cAMP and forskolin, the combined response of either of these cAMP analogs with anoxia was similar to anoxia alone. The results suggested that the PKA-dependent phosphorylation of CREB may enhance HRE function but is not an essential component of the hypoxia signal transduction pathway. This is evidenced by results in chapter 4 showing the CRE to have a negative regulatory effect on HIF-1 activity.

Ebert et al. (1995), showed a synergistic interaction between the PKC-activated serum response element (SRE) and the HRE of the Glut-1 326bp enhancer. This SRE is identical to that believed to confer the X-ray responsive properties of the Egr-1 promoter (Datta et al., 1992). When cells are exposed to ionising radiation, reactive oxygen intermediates are generated which activate a number of early response genes, including Egr-1, by activation of CArG elements within the SRE of these genes (Datta et al., 1992). Salloum et al. (1999), showed it was possible to combine both ionising radiation and hypoxia as transcriptional stimuli on a hypoxia and X-ray responsive promoter (Epo.Egr-1.TNFα) to produce a synergistic output, which was greater than that produced from either hypoxia or irradiation alone in the HCT 116 colon carcinoma cell line. In an attempt to recapitulate these results we cloned the Epo.Egr-1 construct, as well as the Epo pentimer and Egr-1 alone, into the pGL3.basic vector (Promega) and expanded the cell line panel. Results in chapter 7 indicate that, in isolation, the Epo pentimer is not only transcriptionally activated by low pO_2, but is responsive to X-rays post-hypoxia. Similarly, the Egr-1 promoter in isolation was responsive to X-rays and hypoxia in 5 of 7 cell lines. This implies that the "synergistic" output seen by the Epo.Egr-1 promoter is a result of an Epo HRE -dependent response to both hypoxia and radiation, rather than any interactive response of the Epo HRE to hypoxia and the Egr-1 promoter to radiation. The PGK and LDH-A HREs were also shown to be stimulated by both hypoxia and X-rays, with the X-ray response being more marked post-hypoxia. Interestingly the induction of VEGF has been reported in both cell lines and xenograft models of diverse tumour cell types following ionising irradiation (Gorski et al., 1999),

This phenomenon that confers a survival advantage to tumour vasculature and combining anti-VEGF antibody and ionising radiation prevented endothelial cell preservation within the tumour and dramatically enhanced the therapeutic index of the therapy.

Marples, et al. (2000), demonstrated the CArG elements in the 5'-distal enhancer region of the Egr-1 gene to confer the radiation inducibility. We examined the response of the 3'-proximal CArG elements to radiation alone and in combination with the Epo pentimer. Only the Epo.CArG construct was responsive to either stimuli implying that it is only the 5' CArG elements that confer the radiation inducibility of the Egr-1 promoter. It would be interesting to see the response of the LDH $(1+2)^{3-}$ HRE optimised in this work in combination with the CArG elements isolated by Marples et al. (2000). It is possible to make a dual X-ray and hypoxia responsive promoter to utilise in transcriptionally targeted 'genetic radiotherapy'.

In conclusion, the inducible response of certain HREs, especially VEGF, is transcription factor and cell line specific. This observed variability may be the result of interactions between cooperative cis-acting enhancer sequences contained within particular genes (Ratcliffe et al., 1997).

The CRE (site 3) from the LDH-A does not appear to convey an inducible response to hypoxia. Removal of this site from the 52bp LDH-A HRE (homologous enhancer) is reported to abolish or severely reduce activity (Firth et al., 1995). However, multimers of the shorter 26bp sequence, omitting either site 2 or 3, but retaining the HIF-1 site produced a response (Firth et al., 1995; Ratcliffe et al., 1997). Thus a minimalised LDH HRE element that appear to have no functional activity could be restored by iteration. Similarly, the minimal PGK HRE (site 1 only) was inactive as a monomer but could be restored by multimerisation (Firth et al., 1994). This study demonstrates that the short LDH-A HRE sequence (site 1 and 2) has an activity greater than (or occasionally equal to) the PGK HRE and that the CRE has a negative regulatory effect on LDH-A activity. Thus while CREB phosphorylation may marginally enhance

HRE function if stimulated by a cAMP analog, the CRE has a negative regulatory effect on the hypoxia signal transduction pathway.

The ChoRE (site 2) from the LDH-A enhancer strongly modulates the HIF-1 binding site to produce a robust hypoxic and anoxic response. The ChoRE may be having a regulatory effect on the aerobic level of gene transcription as well as increasing hypoxic inducibility.

In my opinion, gene therapy strategies are providing promising new advances in the treatment of cancer by the design of drugs that are selective to the resistant hypoxic tumour cell population. The primary advantage of hypoxia-targeted gene therapy is that it exploits a physiological characteristic of most solid tumours irrespective of tissue type.

Bioreductive prodrugs are designed so that they are non-toxic to oxygenated cells but can be converted, intracellularly, to highly cytotoxic species as a result of reductive metabolism by a specific enzyme. Many prodrugs designed are activated by a one-electron reduction, which is inactivated or rapidly cycled back to parent / inactive metabolite in oxygenated cells. However, a number of these agents are activated by a two-electron reduction, a reaction that cannot be reversed by the presence of oxygen. By placing the gene for the enzyme under the transcriptional control of a HRE a second level of specificity is added.

There are a number of GDEPT models that have been tested however development is an ongoing process, as a number of factors must be considered when designing these compounds:

- The prodrug should have a high aqueous solubility.
- High differential toxicity between the parent compound and the active metabolite.
- If the enzyme is endogenous it should be expressed at very low levels in normal tissues compared to tumours.

- The active metabolite should be diffusible with a half-life sufficient for local killing, but short enough to prevent distant spread into potential healthy tissue.
- The activity of the metabolite should not be reliant on the proliferative state of the cells.

A significant advantage of GDEPT is the bystander effect produced by a number of compounds. The enzyme nitroreductase activates the prodrug CB1954, the active metabolite produced has been demonstrated to have a diffusible bystander effect. The bystander effect means that the prodrug does not need to be activated in all tumour cells within a population. This is a major advantage owing to the fact that individual cells within a tumour mass have been shown to continually flux between the aerobic and hypoxic state.

There are a number of different vector delivery systems currently under investigation, including retro- and adeno-viral vectors, encapsulation in liposomes or macrophages and electroporation. There are a number of issues pertaining to the use of delivering viral vectors, even though attenuated, into humans. Adenoviral delivery systems entered phase I clinical trials, which were subsequently aborted due to death of patients. Delivery appears to be the major obstacle in making GDEPT a successful strategy for the treatment of cancer.

It is important not to assume that GDEPT alone will be sufficient to eradicate tumour cells as this therapy is only effective against cells at low oxygen tensions and those within approximately a 200μm radius. There are always going to be populations of aerobic cells, particularly early in tumour growth and in vascularised regions. It will be the combination of GDEPT with existing strategies such as fractionated radiation and antivascular agents for example, that will increase the curability of all solid tumours.

Future Objectives

A key objective in the future evaluation of the optimised LDH HRE would be to demonstrate whether Myc heterodimers are specifically involved in the superior activity of this HRE relative to the others. Two constructs pMyc.luciferase and pCMV.Myc are commercially available from Clontech. It would be interesting to perform co-transfection experiments with each of these construct independently, ie. pGL3.HRE and pRL.CMV plus pCMV.Myc and pMyc.luciferase plus pRL.CMV. pMyc.luciferase would establish whether Myc itself is modulated in response to hypoxia and pCMV.Myc would demonstrate if Myc can influence the transcription of LDH HRE and its site 2 modified chimeric HREs.

Both the Epo and VEGF enhancers contain other sequences that do not convey a hypoxic response alone but have been shown to contribute to the overall activity of the response. The Epo enhancer has been shown to be functionally dependent on a steroid response element, HNF-4 (Blanchard et al., 1992; Galson et al., 1995), whilst an AP-1 site has been demonstrated to be essential for HRE function in the VEGF promoter (Levy et al, 1995). In addition, hypoxia can modulate mRNA stability. For example the 3' UTR of the VEGF enhancer contains an AU-rich element, hypoxia stability region (HSR), thought to mediate the posttranscriptional response through mRNA stability (Claffey et al., 1998). Boast et al. (1999) and Shibata et al. (2000) have demonstrated that if the HSR region from VEGF is combined with HRE-regulated transcription there was a 2-fold improvement in the inducible hypoxic response.

The successful application of hypoxia-directed gene therapeutics will neccesitate the efficient delivery of therapeutic constructs to hypoxic tumour cells. Dachs et al. (2000) have demonstrated the feasability of successfully transfecting hypoxic tumour cells using electroporation and lipofectin *in vitro* and *in vivo*. It would be worthwhile to determine HRE expression when cells are transfected under anoxic conditions.

References

Adams, G.E. and Stratford, I.J. (1994) Bioreductive drugs for cancer therapy: the search for tumour specificity. *Intl. J. Radiat. Oncol. Biol. Phys.* **29**: 231-238.

An, W.G., Kanekal, M., Simon, M.C., Maltepe, E., Blagosklonny, M.V., and Neckers, L.M. (1998) Stabilisation of wild-type p53 by hypoxia-inducible factor-1a. *Nature* **392**: 405-408.

Amati B, Dalton S, Brooks MW, et al. (1992) Transcriptional activation by the human c-Myc oncoptotein in yeast requires interaction with Max. *Nature* **359**: 423-426.

Amati, B., Littlewood, T.D., Evan, G.I., and Land, H. (1993) The c-Myc protein induces cell cycle progression and apoptosis through dimerization with Max. *EMBO* **12**: 5083-5087.

Arany, Z., Huang, L.E., Eckner, R., Bhattacharya, S., Jiang, C., Goldberg, M.A., Bunn, H.F., and Livingston, D.M. (1996) An essential role for p300/CBP in the cellular response to hypoxia. *Proc. Natl. Acad. Sci.* **93**: 12969-12973.

Atkinson, G. and Hall, S.H. (1999) Prodrug activation gene therapy and external beam irradiation in the treatment of prostate cancer. *Urology* **54**: 1098-1104.

Bachur, N.R., Gordon, S.L., Gee, M.V., and Kon, H. (1979) NADPH cytochrome P450 reductase activation of quinone anticancer agents to free radicals. *Proc. Natl. Acad. Sci. USA.* **76**: 954-957.

Bae, M-K., Kwon, Y-W., Kim, M.S., Bae, S-K., Bae, M-H., Lee, Y.M., Kim, Y-J., and Kim, K-W. (1998) Identification of genes differentially expressed by hypoxia in hepatocellular carcinoma cells. *Biochem. and Biophys. Res. Comm.* **243**: 158-162.

Bae, S-K., Bae, M-H., Ahn, M-Y., Son, M.J., Lee, Y.M., Bae, M-K., Lee, O-H., Park, B.C., and Kim, K-W. (1999) Egr-1 mediates transcriptional activation of IGF-II gene in response to hypoxia. *Cancer Res.* **59**: 5989-5994.

Baodo, R.J. and Pardrigde, W.M. (1999) Amplification of gene expression using both 5'- and 3'-untranslated regions of Glut-1 glucose transporter mRNA. *Mol. Brain Res.* **63**: 371-374.

Beato, M. (1989) Gene regulation by steroid hormones. *Cell.* **56**: 335-344.

Beck, I., Ramirez, S., Weinmann, R., and Caro, J. (1991) Enhancer element at the 3'-flanking region controls transcriptional response to hypoxia in the human erythropoietin gene. *J. Biol. Chem.* **266**: 15563-15566.

Beck, I., Weinmann, R. and Caro, J. (1993) Characterisation of hypoxia0responsive enhnancer in the human erythropoietin gene shows presence of hypoxia-inducible 120 Kd nuclear DNA-binding protein in erythropoietin-producing and nonproducing cells. *Blood* **82**: 704-711.

Berkman, R.A., Merrill, M.J., Reinhold, W.C., Monacci, W.T., Saxena, A., Clark, W.C., Robertson, J.T., Ali, I.U., and Oldfield, E.H. (1993) Expression of the vascular permeability factor / vascular endothelial growth factor gene in central nervous system neoplasms. *J. Clin. Invest.* **91**: 153-159.

Binley, K., Iqball, S., Kingsman, A., Kingsman, S., and Naylor, S. (1999) An adenoviral vector regulated by hypoxia for the treatment of ischaemic disease and cancer. *Gene Therapy.* **6**:1721-1727.

Blackwell TK, Kretzner L, Blackwood EM, et al. (1990) Sequence-specific DNA-binding by the c-Myc protein. *Science* **250**: 1149-1151.

Blackwood EM and Eisenman RN. (1991) Max: a helix-loop-helix zipper protein that forms a sequence-specific DNA binding complex with Myc. *Science* **251**: 1211-1217.

Blanchard, K.L., Acquaviva, A.M., Galson, D.L. and Bunn, H.F. (1992) Hypoxic induction of the human erythropoietin gene: Cooperation between the promotor and enhancer, each of which contains steroid receptor response elements. *Mol. and Cell. Biol.* **12**: 5373-5385.

Blancher, C. and Harris, A.L. (1998) The molecular basis of the hypoxia response pathway: tumour hypoxia as a therapy target. *Cancer and Metast. Rev.* **17**: 187-194.

Blancher, C., Moore, J.W., Talks, K.L., Houlbrook, S., and Harris, A.L. (2000) Relationship of HIF-1a and HIF-2a expression to vascular endothelial growth factor induction and hypoxia survival in human breast cancer cell lines. *Cancer Res.* **60**: 7106-7113.

Boast, K., Binley, K., Iqball, S., Price, T., Spearman, H., Kingsman, S., Kingsman, A., and Naylor, S. (1999) Characterisation of physiologically regulated vectors for the treatment of ischemic disease. *Hum. Gene Therapy* **10**: 2197-2208.

Bonventre, J.V., Sukhatme, V.P., Bamberger, M., Ouellette, A.J., and Brown, D. (1991) Localisation of the protein product of the immediate early growth response gene, Egr-1, in the kidney after ischemia and reperfusion. *Cell Regul.* **2**: 251-260.

Boothman, D.A., Majmadar, G., and Johnson, T. (1994) Immediate X-ray-inducible responses from mammalian cells. *Radiat. Res.* **138**: S44-S46.

Brady, L.W., Mackoe, A.M., Micaily, B., Fisher, S.A. and Lamm, F. (1990) Innovative techniques in radiation oncology. *Cancer.* **65**: 610-624.

Breitman, T.R., Selonick, S.E., and Collins, S.J. (1980) Induction of differentiation of the human promyelocytic leukemia cell line (HL-60) by retinoic acid. *Proc. Natl. Acad. Sci. USA.* **77**: 2936-2940.

Brizel, D.M., Scully, S.P., Harrelson, J.M., Layfield, L.J., Bean, J.M., Prosnitz, L.R., and Dewhirst, M.W. (1996) Tumour oxygenation predicts the likelihood of distant metastases in human soft tissue sarcoma. *Cancer Res.* **56**: 941-943.

Brown, J.M. (1993) SR 4233 (Tirapazamine): a new anticancer drug exploiting hypoxia in solid tumours. *Br. J. Cancer* **67**: 1163-1170.

Brown, J.M. and Siim, B.G. (1994) Tumour hypoxia: the picture has changed in the 1990s. *Intl. J. Radiat. Biol.* **65**: 95-102.

Brown, J.M. and Siim, B.G. (1996) Hypoxia-specific cytotoxins in cancer therapy. *Sems. Radiat. Oncol.* **6**: 22-36.

Brown, M.J. and Giaccia, A.J. (1998) The unique physiology of solid tumours: Opportunities (and problems) for cancer therapy. *Cancer Res.* **58**: 1408-1416.

Brown, L.F., Berse, B., Jackman, R.W., Tognazzi, K., Manseau, E.J., Dvorak, H.F. and Senger, D.R. (1993a) Increased expression of vascular permeability factor (VEGF) and its receptors in kidney and bladder carcinomas. *Am. J. Pathol.* **143**:1255-1262.

Brown, L.F., Berse, B., Jackman, R.W., Tognazzi, K., Manseau, E.J., Senger, D.R., and Dvorak, H.F. (1993b) Expression of vascular permeability factor (VEGF) and its receptors in adenocarcinomas of the gastrointestinal tract. *Cancer Res.* **54**: 4727-4735.

Brown, L.F., Berse, B., Jackman, R.W., Tognazzi, K., Guidi, A.J., Dvorak, H.F., Senger, D.R., Connolly, J.L. and Schnitt, S.J. (1995) Expression of vascular permeability factor (VEGF) and its receptors in breast cancer. *Hum. Pathol.* **26**: 86-91.

Bunn, H.F., and Poynton, R.O. (1996) Oxygen sensing and molecular adaption to hypoxia. *Physiol. Rev.* **76**: 839-878.

Carmeliet, P., Dor, Y., Herbert, J-M., Fukumura, D., Brusselmans, K., Dewerchin, M., Neeman, M., Bono, F., Abramovitch, R., Maxwell, P., Koch, C.J., Ratcliffe, P., Moons, L., Jain, R.K., Collen, D., and Keshet, E. (1998) Role of HIF-1a in hypoxia-mediated apoptosis, cell proliferation and tumour angiogenesis. *Nature* **394**: 485-490.
Chambon, P. (1994) The signalling pathway: Molecular and genetic analysis. *Sem. Cell Biol.* **5**: 115-125.

Chaplin, D.J., Durand, R.E., and Olive, P.L. (1985) Cell selection from a murine tumour using the fluorescent probe Hoechst 33342. *Br. J. Cancer* **51**: 569-572.

Chaplin, D.J., Olive, P.L., and Durand, R.E. (1987) Intermittent blood flow in a murine tumour: radiobiological effects. *Cancer Res.* **47**: 597-601.

Chaplin, D.J. (1989) Hydralazine-induced tumour hypoxia: a potential target for cancer chemotherapy. *J. Natl. Cancer Inst.* **81**: 618-622.

Chaplin, D.J., and Hill, S.A. (1995) Temporal heterogeneity in microregional erythrocyte flux in experimental solid tumours. *Br. J. Cancer.* **71**: 1210-1213.

Chaplin, D.J., Pettit, G.R., and Hill, S.A. (1999) Anti-vascular approaches to solid tumour therapy: evaluation of combretastatin A4 phosphate. *Anticancer Res.* **19**: 189-195.

Cheng, X. and Iliakis, G. (1995) Effect of ionising radiation on the expression of chloramphenicol acetyltransferase gene under the control of commonly used constitiutive or inducible promoters. *Int. J. Radiat.* **67**: 261-267.

Chmura, S.J., Advani, S.J., Kufe, D.W., and Weichselbaum, R.R. (1999) Strategies for enhancing viral-based gene therapy using ionising radiation. *Rad. Oncol. Invest.* **7**: 261-269.

Cho-Chung, Y.S. (1990) Role of cAMP receptor proteins in growth, differentiation and suppression of malignancy: New approaches to therapy. *Canc. Res.* **50**: 7093-7100.

Christy, B.A. and Nathans, D. (1989) Functional serum response elements upstream of the growth factor-inducible gene *zif*268. *Mol. Cell Biol.* **9**: 4889-4895.

Chun, Y-S., Choi, E., Kim, G-T., Lee, M-J., Lee, M-J., Lee, S-E., Kim, M-S., and Park, J-W. (2000) Zinc induces the accumulation of hypoxia-inducible factor (HIF)-1a, but inhibits the nuclear translocation of HIF-1b, causing HIF-1 inactivation. *Biochem. and Biophys. Res. Comm.* **268**: 652-656.

Chung, T.D.K., Mauceri, H.J., Hallahan, D.E., Yu, J.J., Chung, S., Grdina, W.L., Yajnik, S., Kufe, D.W., and Weichselbaum, R.R. (1998) Tumour necrosis factor-a-based gene therapy enhances radiation cytotoxicity in human prostate cancer. *Cancer Gene Therapy* **5**: 344-349.

Claffey, K.P., Shih, S.C., Mullen, A., Dziennis, S., Cusick, J.L., Abrams, K.R., Lee, S.W., and Detmar, M. (1998) Identification of a human VPF/VEGF 3' untranslated region mediating hypoxia-induced mRNA stability. *Mol. Biol. Cell* **9**:469-481.

Connors, T.A. (1995) The choice of prodrugs for gene directed enzyme prodrug therapy of cancer. *Gene Therapy* **2**: 702-709.

Coumailleau, P., Poellinger, L., Gustafsson, J-A., and Whitelaw, M.J. (1995) Definition of a minimal domain of the dioxin receptor that is associated with Hsp90 and maintains wild type ligand binding affinity and specificity. *J. Biol. Chem.* **270**: 25291-25300.

Dachs, G.U. and Stratfors, I.J. (1996) The molecular response of mammalian cells to hypoxia and the potential for exploitation in cancer therapy. *Br. J. Cancer* **74**: S126-S132.

Dachs, G.U., Patterson, A.V., Firth, J.D., Ratcliffe, P.J., Townsend, S.K.M., Stratford, I.J., and Harris, A.J. (1997) Targeting gene expression to hypoxic tumour cells. *Nature Medicine* **3**: 515-520.

Dachs, G.U. and Chapli, D.J. (1998) Microenvironmental control of gene expression: implications for tumour angiogenesis, progression and metastasis. *Sems. Radiat. Oncol.* **8**: 208-216.

Dachs, G.U., Cemazar, M., Wilson, I., Heller, R., Heller, L.C., Jaroszeski, M.J., Sersa, G., and Tozer, G.M. (2000) A comparison of gene delivery methods using electroporation and lipofectin-based techniques *in vitro* and *in vivo*. *Tumour Physiol. Cancer Treat.* **11**: 79-80.

Dang, C.V., Lewis, B.C., Dolde, C., Dang, G., and Shim, H. (1997) Oncogenes in tumour metabolism, tumourigenesis and apoptosis. *J. Bioenerg. and Biomem.* **29**: 345-354.

Dang, C.V. and Semenza, G.L. (1999) Oncogenic alterations of metabolism. *TIBS* **24**: 68-72.

Danielsen, T., Hvidsten, M., Stokke, T., Solberg, K., and Rofstad, E.K. (1998) Hypoxia induces p53 accumulation in the S-phase and accumulation of hypophosphorylated retinoblastoma protein in all cell cycle phases of human melanoma cells. *Br. J. Cancer* **78**: 1547-1558.

Datta, R., Rubin, E., Sukhatme, V., Qureshi, S., Hallahan, D., Weichselbaum, R.R., and Kufe, D.W. (1992) Ionising radiation activates transcription of the Egr-1 gene via CArG elements. *Proc. Natl. Acad. Sci.* **89**: 10149-10153.

Demirpence, E., Pons, M., Balaguer, P. and Gagne, D. (1992) Study of antiestrogenic effect of retinoic acid in MCF-7 cells. *Biochem. Biophys. Res. Commun.* **183**: 100-106.

Denny, W.A., Wilson, W.R., and Hay, M.P. (1996) Recent developments in the design of bioreductive drugs. *Br. J. Cancer.* **74**: Suppl. xxvii, S32-S38.

Dibbens, J.A., Miller, D.L., Damert, A., Risau, W., Vadas, M.A., and Goodall, G.J. (1999) Hypoxic regulation of vascular endothelial growth factor mRNA stability requires the cooperation of multiple RNA elements. *Mol. Biol. Cell* **10**: 907-919.

Dolle, P., Ruberte, E., Leroy, P., Morriss-Kay, G, and Chambon, P. (1990) Retinoic acid receptors and cellular binding proteins. I A systemic study of the differential pattern of transcription during mouse organogenesis. *Development.* **110**: 1133-1151.

Durand, R.E. and Raleigh, J.A. (1998) Identification of nonproliferating but viable hypoxic tumour cells *in vivo*. *Cancer Res.* **58**: 3547-3550.

Durand, R.E. and Sham, E. (1998) The lifetime of hypoxic human tumour cells. *Intl. J. Radiat. Oncol. Biol. Phys.* **42**: 711-715.

Dvorak, H.F., Sioussat, T.M., Brown, L.F., Berse, B., Nagy, J.A., Sotrel, A., Manseau, E.J., Van De Water, L., and Senger, D.R. (1991) Distribution of vascular permeability factor (VEGF) in tumours: concentration in tumour blood vessels. *J. Exp. Med.* **174**: 1275-1278.

Ebert, B.L., Firth, J.D., and Ratcliffe, P.J. (1995) Hypoxia and mitochondrial inhibtors regulate expression of glucose transporter-1 via distinct cis-acting sequences. *J. Biol. Chem.* **270**: 29083-29089.

Ebert, B.L., Gleadle, J.M., O'Rourke, J.F., Bartlett, S.M., Poulton, J., and Ratcliffe, P.J. (1996) Isoenzyme-specific regulation of genes involved in energy metabolism by hypoxia: similarities with the regulation of erythropoietin. *J. Biochem.* **313**: 809-814.

Ehleben, W., Porwol, T., Fandrey, J., Kummer, W., and Acker, H. (1997) Cobalt and desferrioxamine reveal crucial members of the oxygen sensing pathway in HepG2 cells. *Kidney Intl.* **51**: 483-491.

Evans, R. (1988) The steroid and thyroid receptor superfamily. *Science.* **240**: 889-895.

Finlay, G.J., Wilson, W.R., and baguley, B.C. (1987) Cytokinetic factors in drug resistance of lewis lung carcinoma: Comparison of cells freshly isolated from tumours with cells from exponentially and plateau-phase cultures. *Br. J. Cancer.* **56**: 755-762.

Fandrey, J., Seydel, F.P., Siegers, C-P., and Jelkman, W. (1990) Role of cytochrome P450 in the control of the production of erythropoietin. *Life Sci.* **47**: 127-134.

Fandrey, J., Frede, S., Ehleben, W., Porwol, T., Acker, H., and Jelkmann, W. (1997) Cobalt chloride and desferrioxamine antagonise the inhibition of erythropoietin production by reactive oxygen species. *Kidney Intl.* **51**: 492-496.

Fenton, B.M., Paoni, S.F., Lee, J., Koch, C.J., and Lord, E.M. (1999) Quantification of tumour vasculature and hypoxia by immunohistochemical staining and HbO_2 saturation measurements. *Br. J. Cancer* **79**: 464-471.

Firth, J.D., Ebert, B.L., Pugh, C.W., and Ratcliffe, P.J. (1994) Oxygen regulated control elements in the phosphoglycerate kinase 1 and lactate dehydrogenase A genes:

Similarities with the erythropoietin 3' enhancer. *Proc. Natl. Acad. Sci. USA.* **91**: 6496-6500.

Firth, J.D., Ebert, B.L., and Ratcliffe, P.J. (1995) Hypoxic regulation of lactate dehydrogenase. *J. Biol. Chem.* **270**: 21021-21027.

Finkenzeller, G., Sparacio, A., Technau, A., Marme, D., and Siemeister, G. (1997) Sp1 recognition sites in the proximal promoter of the human vascular endothelial growth factor gene are essential for platelet-derived growth factor-induced gene expression. *Oncogene* **15**: 669-676.

Fisher, F., Crouch, D.H., Jayaraman, P.S., Clark, W., Gillespie, D.A.F., and Goding, C.R. (1993) Transcription activation of Myc and Max: flanking sequences target activation to a subset of CACGTG motifs *in vivo*. *EMBO* **12**: 5075-5082.

Folkman, J. (1990) What is the evidence that tumours are angiogenesis dependent? *J. Natl. Cancer Inst.* **82**: 4-6.

Folkman, J. (1995) Angiogenesis in cancer, vascular rheumatoid and other diseases. *Nature Medicine* **1**: 27_31.

Fontana, J.A. (1987) Interaction of retinoids and tamoxifen on the inhibition of human mammary carcinoma cell proliferation. *Exp. Cell Biol.* **55**: 136-144.

Fontana, J.A., Miksis, G., Miranda, D.M. and Durham, J.P. (1987) Inhibiton of human mammary carcinoma cell proliferation by retinoids and intracellular cAMP-elevating compounds. *J. Natl. Canc. Inst.* **78**: 1107-1112.

Fox, S.B. (1997) Tumour angiogenesis and prognosis. *Histopath.* **30**: 294-301.

Fraker, L.D., Halter, S., and Forbes, J.T. (1984) Growth inhibition by retinol of a human breast carcinoma cell line *in vitro* and in athymic mice. *Cancer Res.* **44**: 5757-5763.

Galson, D.L., Tsuchiya, T., Tendler, D.S., Huang, E., Ren, Y., Ogura, T., and Bunn, H.F. (1995) The orphan receptor hepatic nuclear factor-4 functions as a transcriptional activator for tissue-specific and hypoxia-specific erythropoietin gene expression an is antagonised by EAR3/COUP-TF1. *Mol. and Cell. Biol.* **15**: 2135-2144.

Gassmann, M., Wenger, R.H. (1997a) HIF-1, a mediator of the molecular response to hypoxia. *News Physiol. Sci.* **12**: 214-218.

Gassmann, M., Kvietikova, I., Rolfs, A., and Wenger, R.H. (1997b) Oxygen- and dioxin-regulated gene expression in mouse hepatoma cells. *Kid. Intl.* **51**: 567-574.

Gatenby, R.A., Kessler, H.B., Rosenblum, J.S., Coia, L.A., Moldofski, P.J., Hartz, W.H., and Broder, G.J. (1987) Oxygen distribution in squamous cell carcinoma

metastases and its relationship to outcome of radiation therapy. *Int. J. Radiat. Oncol. Biol. Phys.* **14**: 831-838.

Gerweek, L.E. and Seetharaman, K. (1996) Cellular pH gradient in tumour versus normal tissue: potential exploitation for the treatment of cancer. *Cancer Res.* **56**: 1194-1198.

Giaccia, A.J. (1996) Hypoxic stress proteins: Survival of the fittest. *Sem. Rad. Oncol.* **6**: 46-58.

Giguere, V., Lyn, S., and Yip, P. (1990a) Molecular cloning of cDNA encoding a second cellular retinoic acid-binding protein. *Proc. Natl. Acad. Sci. USA.* **87**: 6233-6237.

Giguere, V., Shago, M., and Zirngibl, R. (1990b) Identification of the novel isoform of the retinoic acid receptor-g expressed in the mouse embryo. *Mol. Cell Biol.* **10**: 2335-2340.

Goldberg, M.A., Dunning, S.P., and Bunn, H.F. (1988) Regulation of the erythropoeitin gene: Evidence that the oxygen sensor is a heme protein. *Science.* **242**: 1412-1415.

Goldberg, M.A., Gaut, C.C., and Bunn, H.F. (1991) Erythropoietin mRNA levels are governed by both the rate of transcription and posttranscriptional events. *Blood* **77**: 271-277.

Goldberg, M.A. and Schneider, T.J. (1994) Similarities between the oxygen sensing mechanisms regulating the expression of vascular endothelial growth factor and erythropoietin. *J. Biol. Chem.* **269**: 4355-4359.

Gopfert, T., Gess, B., Eckardt, K-U., and Kurtz, A. (1996) Hypoxia signalling in the control of erythropoietin gene expression in rat hepatocytes. *J. Cell. Physiol.* **168**: 354-361.

Gorski, D.H., Beckett, M.A., Jaskowiak, N.T., Calvin, D.P., Mauceri, H.J., Salloum, R.M., Seetharam, S., Koons, A., Kufe, D.W., and Weichselbaum, R.R. (1999) Blockage of the vascular endothelial growth factor stress response increases the anti-tumour effects of ionising radiation. *Cancer Res.* **59**: 3374-3378.

Gradin, K., McGuire, J., Wenger, R.H., Kvietikova, I., Whitelaw, M.L., Toftgard, R., Tora, L., Gassmann, M., and Poellinger, L. (1996) Functional interference between hypoxia and dioxin signal transduction pathways: competition for recruitment of the ARNT transcription factor. *Mol. and Cell. Biol.* **16**: 5221-5231.

Graeber, T.G., Peterson, J.F., Tsai, M., Monica, K., Fornace, A.J., and Giaccia, A.J. (1994) Hypoxia induces accumulation of p53 protein, but activation of a G_1-phase checkpoint by low-oxygen conditions is independent of p53 status. *Mol. and Cell. Biol.* **14**: 6264-6277.

Graeber, T.G., Osmanian, C., Jacks, T., Housman, D.E., Koch, C.J., Lowe, S.W., and Giaccia, A.J. (1996) Hypoxia-mediated selection of cells with diminished apoptotic potential in solid tumours. *Nature* **379**: 88-91.

Green, S., and Chambon, P. (1988) Nuclear receptors enhance our understanding of transcription regulation. *Trends Genet.* **4**: 309.

Griffiths, L., Binley, K., Iqball, S., Kan, O., Maxwell, P., Ratcliffe , P., Lewis, C., Harris, A., Kingsman , S. and Naylor, S. (2000) The macrophage - a novel system to deliver gene therapy to pathological
hypoxia. *Gene Therapy.* **7**: 255-62.

Hallahan, D.E., Virudachalam, S., Beckett, M., Sherman, M.L., Kufe, D., and Weichselbaum, R.R. (1991) Mechanisms of X-ray-mediated protooncogene c-jun expression in radiation-induced human sarcoma cell lines. *J. Radiat. Oncol. Biol. Phys.* **21**: 1677-1681.

Hallahan, D.E., Dunphy, E., Virudachalam, S., Sukhatme, V.P., Kufe, D.W., and Weichselbaum, R.R. (1995) c-jun and Egr-1 participate in DNA synthesis and cell survival in response to ionising radiation exposure. *J. Biol. Chem.* **270**: 30303-30309.

Hamada, K., Gleason, S.L., Levi, B-Z., Hirchfeld, S., Appella, E., and Ozato, K. (1989) H-2RIIBP, a member of the nuclear hormone receptor superfamily that binds to both the regulatory element of major histocompatibility class I genes and the estrogen response element. *Proc. Natl. Acad. Sci. USA.* **86**: 8289-8293.

Haq, R.U., Pfahl, M., and Chytil, F. (1991) Retinoic acid affects the expression of nuclear retinoic acid receptors in tissues of retinol-deficient rats. *Proc. Natl. Acad. Sci. USA.* **88**: 8272-8276.

Harris, A.L., Fox, S., Bicknell, R., Leek, R., Relf, M., LeJeune, S., and Kaklamanis, L. (1994) Gene therapy through signal transduction pathways and angiogenic growth factors as therapeutic targets in breast cancer. *Cancer* **74**: 1021-1025.

Hashimoto, K., Kishimoto, A., Aihara, H., Yasuda, I., Mikawa, K., and Nishizuka, Y. (1990) Protein kinase C during differentiation of human promyelocytic leukemia cell line, HL-60. *FEBS Lett.* **263**: 31-34.

Hejmadi, M.V., McKeown, S.R., Friery, O.P., McIntyre, I.A., Patterson, L.H., and Hirst, D.G. (1996) DNA damage following combination toxicity of radiation with the bioreductive drug A4QN: possible selective toxicity to oxic and hypoxic tumour cells. *Br. J. Cancer* **73**: 499-505.

Hill, S., Williams, K.B., and Denekamp, J. (1989) Vascular collapse after flavone acetic acid: a possible mechanism of its anti-tumour action. *Eur. J. Clin. Oncol.* **25**: 1419-1424.

Hipskind, R.A., Baccarini, M., and Nordheim, A. (1994) Transient activation of RAF-1, MEK and ERK2 coincides kinetically with ternary complex factor phosphorylation and immediate-early gene promoter activity *in vivo*. *Molec. and Cellul. Biol.* **14**: 6219-6231.

Hlatky, L., Tsionou, C., Hahnfeldt, P., and Coleman, C.N. (1994) Mammary fibroblasts may influence breast tumour angiogenesis via hypoxia-induced vascular endothelial growth factor up-regulation and protein expression. *Cancer Res.* **54**: 6083-6086.

Hong, A., Rojas, A., and Dische, S. (1989) Normobaric oxygen a s a sensitiser of hypoxic tumour cells. *Intl. J. Radiat. oncol. Biol. Phys.* **15**: 1097-1099.

Horsman, M.R., Khalil, A.A., Nordsmark, M., Grau, C., and Overgaard, J. (1994) Measurement of pO_2 in a murine tumour and its correlation with hypoxic fraction. In: *Oxygen transport to tissues XV* (Eds Vaupel, P.) Plenum Press, New York.

Hockel, M., Schlenger, K., Knoop, C., and Vaupel, P. (1991) Oxygenation of carcinomas of the uterine cervix: evaluation by computerised O_2 tension measurements. *Cancer Res.* **51**: 6098-6102.

Hockel, M., Knoop, C., Schlenger, K., Vorndran, B., Baubmann, E., Mitze, M., Knapstein, P.G., and Vaupel, P. (1993) Intratumoural pO_2 predicts survival in advanced cancer of the uterine cervix. *Radiot. and Oncol.* **26**: 45-50.

Hockel, M., Schlenger, K., Aral, B., Mitze, M., Schaffer, U., and Vaupel, P. (1996a) Association between tumour hypoxia and malignant progression in advanced cancer of the uterine cervix. *Cancer Res.* **56**: 4509-4515.

Hockel, M., Schlenger, K., Mitze, M., Schaffer, U., and Vaupel. P. (1996b) Hypoxia and radiation response in human tumours. *Sems. Radiat. Oncol.* **6**: 3-9.

Huang, R-P., Liu, C., Fan, Y., Mercola, D., and Adamson, E.D. (1995) Egr-1 negatively regulates human tumour cell growth via the DNA-binding domain. *Cancer Res.* **55**: 5054-5062.

Huang, L.E., Arany, Z., Livingston, D.M., and Bunn, F.H. (1996) Activation of hypoxia-inducible transcription factor depends primarily upon redox-sensitive stabilization of its a subunit. *J. Biol. Chem.* **50**: 32253-32259.

Huang, L.E., Ho, V., Arany, Z., Krainc, D., Galson, D., Tendler, D., Livingston, D.M., and Bunn, H.F. (1997) Erythropoietin gene regulation depends on heme-dependent oxygen sensing and assembly of interacting transcription factors. *Kid. Intl.* **51**: 548-552.

Hyunsung, H.L., Ko, P., and Whitlock, J.P. (1996) Induction of phosphoglycerate kinase-1 gene expression by hypoxia. *J. Biol. Chem.* **271**: 21262-21267.

Iliopoulos, C., Levy, A.P., Jiang, C., Kaelin, W.G., and Goldberg, M.A. (1996) Negative regulation of hypoxia-inducible genes by the von Hippel-Lindau protein. *Biochem.* **93**: 10595-10599.

Jain, S., Dolwick, M., Schmidt, J.V., and Bradfield, C.A. (1994) Potent transactivation domains of the Ah receptor and the ARNT map to their carboxyl termini. *J. Biol. Chem.* **269**: 31518-31524.

Janknecht, R., Ernst, W.H., Pingoud, V., and Nordheim, A. (1993) Activation of ternary complex factor ELK-1 by MAP kinases. *EMBO* **12**: 5097-5104.

Jelkmann, W. (1992) Eryhtropoietin: structure, control of production and function. *Phys. Rev.* **72**: 449-471.

Jiang, B., Semenza, G.L., Bauer, C., and Marti, H.H. (1996) Hypoxia-inducible factor-1 levels vary exponentially over a physiologically relevant range of O2 tension. *Am. J. Physiol.* **271**: C1172-C1180.

Jiang, B., Rue, E., Wang, G.L., Roe, R., and Semenza, G.L. (1996) Dimerisation, DNA binding, and transactivation properties of HIF-1. *J. Biol. Chem.* **271**: 17771-17778.

Jiang, B., Zheng, J.Z., Leung, S.W., Roe, R., and Semenza, G. (1997) Transactivation and inhibitory domains of hypoxia-inducible factor-1a. *J. Biol. Chem.* **31**: 19253-19260.

Joannidis, M., Cantley, L.G., Spokes, K., Stuart-Tilley, A.K., Alper, S.L., and Epstein, F.H. (1997) Modulation of c-fos and Egr-1 expression in the isolated perfused kidney by agents that alter tubular work. *Kidney Intl.* **52**: 130-139.

Jungmann, R.A., Huang, D. and Tian, D. Regualtion of LDH-A gene expression by transcriptional and posttranscriptional signal transduction mechanisms. *J. Exp. Zoo.* **282**: 188-195.

Kallinowski, F., Schlenger, K.H., Kloes, M., Stohrer, M., and Vaupel, P. (1989a) Tmour blood flow: The principle modulator of oxidative and glycolytic metabolism and of the metabolic micromilieu of human tumour xenografts *in vivo*. *Int. J. Cancer* **44**: 266-272.

Kallinowski, F., Schlenger, K.H., Runkel, S., Kloes, M., Stohrer, M., Okunieff, P., and Vaupel, P. (1989b) Blood flow, metabolism, cellular microenvironment and growth rate of human tumour xenografts. *Cancer Res.* **49**: 3759-3764.

Kallinowski, F. (1996) The role of tumour hypoxia for the development of future treatment concepts for locally advanced cancer. *Cancer J.* **9**: 37-40.

Kappus, H. (1986) Overview of enzyme systems involved in bioreduction of drugs and in redox cycling. *Biochem. Pharm.* **35**: 1-6.

Kawashita, Y., Ohtsuru, A., Kaneda, Y., Nagayama, Y., Kawazoe, Y., Eguchi, S., Kuroda, H., Fujioka, H., Ito, M., Kanematsu, T., and Yamashita, S. (1999) Regression of hepatocellular carcinoma in vitro and in vivo by radiosensitizing suicide gene therapy under the inducible and spatial control of radiation. *Human Gene Therapy* **10**: 1509-1519.

Kim, K.J., Li, B., Winer, J., Armanini, M., Gillet, N., Phillips, H.S., and Ferrara, N. (1993) Inhibition of vascular endothelial growth factor-induced angiogenesis suppresses tumour growth *in vivo*. *Nature* **362**: 841-844.

Kimura, H., Weisz, A., Kurashima, Y., Hashimoto, K., Ogura, T., D'Acquisto, F., Addeo, R., Makuuchi, M., and Esumi, H. (2000) Hypoxia response element of the human VEGF gene mediates transcriptional regulation by nitric oxide: control of HIF-1 activity by nitric oxide. *Blood* **95**: 189-197.

Kobayashi, A., Sogawa, K., and Fujii-Kuriyama, Y. (1996) Cooperative interaction between AhR.ARNT and Sp1 for the drug-inducible expression of CYP1A1 gene. *J. Biol. Chem.* **271**: 12310-12316.

Koong, A.C., Chen, E.Y., and Giaccia, A.J. (1994) Hypoxia causes the activation of nuclear factor kB through the phosphorylation of IkBa on tyrosine residues. *Cancer Res.* **54**: 1425-1430.

Kretzner L, Blackwood EM and Eisenman RN. (1992) Myc and Max proteins possess distinct transcriptional activities. *Nature* **359**: 426-429.

Kvietikova, I., Wenger, R.H., Marti, R.H., and Gassman, M. (1995) The transcription factors AFT-1 and CREB-1 bind constitutively to the HIF-1 DNA recognition site. *Nucleic Acids Res.* **23**: 4542-4550.

Kvietikova, I., Wenger, R.H., Marti, H.H., and Gassman, M. (1997) The hypoxia-inducible factor-1 DNA recognition site is cAMP-responsive. *Kidney Intl.* **51**: 564-566.

Lee, J., Gray, A., Yuan, J., Luoh, S-M., Avraham, H., and Wood, W.I. (1996) Vascular endothelial growth-factor related protein: a ligand and specific activator of the tyrosine kinase receptor Flt4. *Proc. Natl. Acad. Sci.* **93**: 1988-1992.

Lee, P.J., Jiang, B-H., Chin, B.Y., Iyer, N.V., Alam, J., Semenza, G.L., and Choi, A.M.K. (1997) Hypoxia-inducible factor-1 mediates transcriptional activation of the heme oxygenase-1 gene in response to hypoxia. *J. Biol. Chem.* **272**: 5375-5381.

Lee, M.Y., Hwang, E.S., and Lee, S.K. (1998) Novel CRE-binding proteins of 11-16 kDa bind to the LDH-A gene CRE in a sequence specific and hepatocyte-growth dependent manner in partially hepatectomised rat liver. *Biochem. and Biophys. Res. Comm.* **246**: 50-54.

Levy, A.P., Levy, N.S., Wegner, S., and Goldberg, M. (1995) Transcriptional regulation of the rat vascular endothelial growth factor gene by hypoxia. *J. Biol. Chem.* **270**: 13333-13340.

Li, H., Ko, H.P., and Whitlock, J.P. (1996) Induction of phosphoglycerate kinase 1 gene expression by hypoxia: roles of ARNT and HIF-1a. *J. Biol. Chem.* **271**: 21262-21267.

Liu, Y., Cox, S.R., Morita, T., and Kourembanas, S. (1995) Hypoxia regulates vascular endothelial growth factor gene expression in endothelial cells. *Circ. Res.* **77**: 638-643.

Loike, J.D., Brett, C.J., Ogawa, S., Silverstein, S.C., and Stern, D. (1992) Hypoxia induces glucose transporter expression in endothelial cells. *Am. Physiol. Soc.* C326-C333.

Lowe, S.W., Schmitt, E.M., Smith, S.W., Osborne, B.A., and Jacks, T. (1993) p53 is required for radiation-induced apoptosis in mouse thermocytes. *Nature* **362**: 847-849.

Mace, K.F., Hornung, R.L., Wiltrout, R.H., and Young, H.A. (1990) Correlation between *in vivo* induction of cytokine gene expression by flavone acetic acid and strict dose dependency and therapeutic efficacy against murine renal cancer. *Cancer Res.* **50**: 1742-1747.

Madan, A., and Curtin, P.T. (1993) A 24-base-pair sequence 3' to the human erythropoeitin gene contains a hypoxia-responsive transcriptional enhancer. *Proc. Natl. Acad. Sci.* **90**: 3928-3932.

Madan, A., Lin, C., Hatch, S.L., and Curtin, P.T. (1995) Regulated basal, inducible and tissue-specific human erythropoietin gene expression in transgenic mice requires multiple *cis* DNA sequences. *Blood* **85**: 2735-2741.

Madan, A., Varma, S., and Cohen, H.J. (1997) Co-transactivation of the 3' erythropoeitin hypoxia inducible enhancer by the HIF-1 protein. *Blood, Cells, Mol. and Diseases.* **23**: 169-176.

Maltepe, E., Schmidt, J.V., Baunoch, D., Bradfield, C.A., and Simon, M.C. (1997) Abnormal angiogenesis and responses to glucose deprivation in mice lacking the protein ARNT. *Nature* **386**: 403-404.

Manome, Y., Kunieda, T., Wen, P.Y., Koga, T., Kufe, D.W., and Ohno, T. (1998) Transgene expression in malignant glioma using a replication-defective adenoviral vector containing the Egr-1 promoter: Activation by ionising radiation or uptake of radioactive iododeoxyuridine. *Human Gene Therapy* **9**: 1409-1417.

Marples, B., Scott, S.D., Hendry, J.H., Embleton, M.J., Lashford, L.S., and Margison, G.P. (2000) Development of synthetic promoters for radiation-mediated gene therapy. *Gene Therapy.* **7**: 511-517.

Matsushita, S., Nitanda, T., Furukawa, T., Sumizawa, T., Tani, A., Nishimoto, K., Akoba, S., Miyadera, K., Fukushima, M., Yamada, Y., Yoshida, H., Kanzaki, T., and Akiyama, S. (1999) The effect of thymidine phosphorylase inhibitor on angiogenesis and apoptosis in tumours. *Cancer Res.* **59**: 1911-1916.

Marti, H.H., Jung, H.H., Pfeilschifter, J. and Bauer, C. (1994) Hypoxia and cobalt stimulate LDH activity in vascular smooth muscle cells. *Eur. J. Physiol.* **429**: 216-222.

Mattei, M., de The, H., and Mattei, J. (1988a) Assignment of the human hap retinoic acid receptor RAR-b gene to the p24 band of chromosome 3. *Hum. Genet.* **80**: 189-190.
Mattei, M., Petkovich, M., Mattei, J., Brand, M., and Chambon, P. (1988b) Mapping of the human retinoic acid receptor to the q21 band of chromosome 17. *Hum. Genet.* **80**: 186-188.

Maxwell, P.H., Dach, G.U., Gleadle, J.M., Nichiolls, L.G., Harris, A.L., Stratford, I.J., Hankinson, O., Pugh, C.W. and Ratcliffe, P.J. (1997). Hypoxia-inducible factor-1 modulates gene expression in solid tumours and influences both angiogenesis and tumour growth. *Proc. Natl. Acad. Sci. USA.* **94**: 8104-8109.

Maxwell, P.H., Weisener, M.S., Chang, G-W., Clifford, S.C., Vaux, E.C., Cockman, M.E., Wykoff, C.C., Pugh, C.W., Maher, E.R., and Ratcliffe, P.J. *Nature* **399**: 271-275.
McBride, W.H., and Dougherty, G.J. (1995) Radiotherapy for genes that cause cancer. *Nature Medicine* **1**: 1215-1217.

McGuire, J., Coumailleau, P., Whitelaw, M.L., Gustafsson, J-A., and Poellinger, L. (1996) The basic helix-loop-helix/PAS factor Sim is associated with Hsp90. *J. Biol. Chem.* **270**: 31353-31357.

Mednieks, M.I., Yokozaki, H., Merlo, G.R., Tortora, G., Clair, T., Ally, S., Tahara, E. and Cho-Chung, Y.S. (1989) Site-selective 8-Cl-cAMP which causes growth inhibition and differentiation increases DNA (CRE)-binding activity in cancer cells. *FEBS Lett.* **254**: 83-88.

Minet, E., Mottet, D., Michel, G., Roland, I., Raes, M., Remacle, J., and Michiels, C. (1999) Hypoxia-induced activation of HIF-1: role of HIF-1a-Hsp-90 interaction. *FEBS* **460**: 251-256.

Monaghan, J.E. The synergistic interaction between cisplatin and the bioreductive drug tirapazamine. A thesis submitted to the University of Manchester for the degree of Doctor of Philosophy (Ph.D.) in the faculty of Science, 2000.

Mueller-Klieser, W., Vaupel, P.W., Manz, R. and Schmidseder, R. (1981) Intracapillary oxyhaemaglobin saturation of malignant tumours in humans. *Int. J. Radiat. Oncol. Biol. Phys.* **7**: 1397-1404.

Muller, J.M., Krauss, B., Kaltschmidt, C., Baeuerle, P.A., and Rupec, R.A. (1997) Hypoxia induces c-fos transcription via a mitogen-activated protein kinase-dependent pathway. *J. Biol. Chem.* **272**: 23435-23439.

Murray, J.C., Smith, K.A., and Thurston, G. (1989) Flavone acetic acid induces a coagulopathy in mice. *Br. J. Cancer.* **60**: 729-733.

Nagpal, S., Saunders, M., Kastner, P., Durand, P., Nakshatri, H., and Chambon, P. (1992) Promotor context- and response element- dependent specificity of the transcriptional activation and modulating functions of retinoic acid receptors. *Cell.* **70**: 1007-1019.

Nass SJ and Dickson RB. (1997) Defining a role for c-Myc in breast tumorgenesis. *Breast Cancer Res. Treat.* **44**: 1-22.

Neeman, M., Abramovitch, A., Schiffenbauer, Y.S., and Tempel, C. (1997) Regulation of angiogenesis by hypoxic stress: from solid tumours to the ovarian follicle. *Int. J. Exp. Path.* **78**: 57-70.

Nichols, M., Weih, F., Schmid, W., DeVack, C., Kowenz-Leutz, E., Luckow, B., Boshart, M., and Schutz, G. (1992) Phosphorylation of CREB affects its binding to high and low affinity sites: implications for cAMP induced gene transcription. *EMBO* **11**: 3337-3346.

Ogreid, D., Ekanger, R., Suva, R.H., Miller, J.P., and Doskeland, S.O. (1989) Comparison of the two classes of binding sites (A and B) of type I and type II cyclic-AMP-dependent protein kinases by using cyclic nucleotide analogs. *Eur. J. Biochem.* **181**: 19-31.

Okano, M., Masuda, S., Narita, H., Masushige, S., Kato, S., Imagawa, S. and Sasaki, R. (1994) Retinoic acid upregulates erythropoietin production in hepatoma cells and in vitamin A-depleted rats. *FEBS Lett.* **349**: 229-233.

Okunieff, P., Hoeckel, M., Dunphy, E.P., Schlenger, K., Knoop, C., and Vaupel, P. (1993) Oxygen tension distributions are sufficient to explain the local response of human breast tumours treated with radiation alone. *Int. J. Radiat. Oncol. Biol. Phys.* **26**: 631-636.

Olson, T.A., Mohanraj, D., Carson, L.F. and Ramakrishnan, S. (1994) Vascular permeability factor gene expression in normal and neoplastic human ovaries. *Cancer Res.* **54**: 276-280.

O'Reilly, M.S., Holmgren, L., Shing, Y., Chen, C., Rosenthal, R.A., Moses, M., Lane, W.S., Cao, Y., Sage, E.H., and Folkman, J. (1994) Angiostatin: a novel angiogensis inhibitor that mediates the suppression of metastases by a lewis lung carcinoma. *Cell* **79**: 315-328.

O'Rouke, J.F., Pugh, C.W., Bartlett, S.M., and Ratcliffe, P.J. (1996) Identification of hypoxically inducible mRNAs in HeLa cells using differential-display PCR. *Eur. J. Biochem.* **241**: 403-410.

O'Rourke, J.F., Dachs, G.U., Gleadle, J.M., Maxwell, P.H., Pugh, C.W., Stratford, I.J., Wood, S.M., and Ratcliffe, P.J. (1997) Hypoxia response elements. *Oncol. Res.* **9**: 327-332.

Overgaard, J. and Horsman, M.R. (1996) Modification of hypoxia-induced radioresistance in tumours by the use of oxygen and sensitisers. *Sems Radiat. Oncol.* **6**: 10-21.

Patterson, A.V. Rational enzyme-directed prodrug development: Exploiting tumour hypoxia to target the bioactivation of cytotoxic prodrugs. A thesis submitted in partial fulfilment of the requirements of Oxford Brooks University for the degree of Doctor of Philosophy (Ph.D.) in the faculty of Science, 1998.

Peng, J., Zhang, L., Drysdale, L., and Fong, G-H. (2000) The transcription factor EPAS-1/hypoxia inducible factor-2a plays an important role in vascular remodelling. *PNAS* **97**: 8386-8391.

Petkovich, M., Brand, N., and Krust, A. (1987) A human retinoic acid receptor which belongs to the family of receptors. *Nature.* **330**: 444-450.

Petterson, E.O., Juul, N.O., and Ronning, O.W. (1986) Regulation of protein metabolism of human cells during and after acute hypoxia. *Cancer Res.* **46**: 4346-4351.

Pfahl, M. (1994) Vertebrate receptors: Molecular biology, dimerization and response elemnts. *Cell Biol.* **5**: 95-103.

Plate, K.H., Breier, G., Weich, H.A., and Risau, W. (1992) Vascular endothelail growth factor is a potential tumour angiogenesis factor in human gliomas *in vivo*. *Nature* **359**: 845-848.

Powell, M.E.B., Hill, S.A., Saunders, M.I., Hoskin, P.J., and Chaplin, D.J. (1997) Human tumour blood flow is enhanced by nicotinamide and carbogen breathing. *Cancer Res.* **57**: 5261-5264.

Powis, G., and Appel, P.L. (1980) Relationship of the single electron reduction potential of quinones to their reduction by flavoproteins. *Biochem. Pharm.* **29**: 2567-2572.

Pugh, C.W., Tan, C.C., Jones, R.W., and Ratcliffe, P.J. (1991) Functional analysis of an oxygen-regulated transcriptional enhancer lying 3' to the mouse erythropoietin gene. *Proc. Natl. Acad. Sci.* **88**: 10553-10557.

Pugh, C.W., Ebert, B.L., Ebrahim, O., and Ratcliffe, P.J. (1994) Characterisation of functional domains within the mouse erythropoietin 3' enhancer conveying oxygen-regulated responses in different cell lines. *Bioch. and Biophys.* **1217**: 297-306.

Pugh, C.W., O'Rourke, J.F., Nagos, M., Gleadle, J.M., and Ratcliffe, P.J. (1997) Activation of hypoxia-inducible factor-1, Definition of the regulatory domains within the a subunit. *J. Biol. Chem.* **17**: 11205-11214.

Qureshi, S.A., Rim, M., Bruder, J., Kolch, W., Rapp, U., Sukhatme, V.P., and Foster, D.A. (1991b) An inhibitory mutant of c-Raf-1 blocks v-Src-induced activation of the Egr-1 promoter. *J. Biol. Chem.* **266**: 20594-20597.

Raleigh, J.A., Dewhirst, M.W., and Thrall, D.E. (1996) Measuring tumour hypoxia. *Sem. Rad. Oncol.* **6**: 37-45.

Raleigh, J.A., Chou, S-C., Calkins-Adams, D.P., Ballenger, C.A., Novotny, D.B., and Varia, M.A. (2000) A clinical study of hypoxia and metallothionein protein expression in squamous cell carcinomas. *Clin. Cancer Res.* **6**: 855-862.

Rastinejad, F., Polverini, P.J., and Bouck, N.P. (1989) Regulation of the activity of a new inhibitor of angiogenesis by a cancer suppressor gene. *Cell* **56**: 345-355.

Ratcliffe, P.J., Ebert, B.L., Firth, J.D., Gleadle, J.M., Maxwell, P.H., Nagao, M., O'Rourke, J.F., Pugh, C.W., and Wood, S.M. (1997) Oxygen regulated gene expression: Erythropoeitin as a model system. *Kidney Intl.* **51**: 514-526.

Reinhold, H.S., Blachiwiecz, B., and Blok, A. (1977) Oxygenation and reoxygenation in 'sandwich' tumours. *Bibl. Anat.* **15**: 270-272.

Reynolds, T.Y., Rockwell, S., and Glazer, P.M. (1996) Genetic instability induced by the tumour microenvironment. *Cancer Res.* **56**: 5754-5757.

Richard, D.E., Berra, E., Gothie, E., Roux, D., and Pouyssegur, J. (1999) p42/44 mitogen-activated protein kinases phosphorylate HIF-1a and enhance the transcriptional activity of HIF-1. *J. Biol. Chem.* **274**: 32631-32637.

Richard, D.E., Berra, E., and Pouyssegur, J. (1999) Angiogenesis: How a tumour adapts to hypoxia. *Biochem. and Biophys. Res. Comm.* **266**: 718-722.

Riley, P.A. (1994) Free radicals in biology: oxidative stress and the effects of ionising radiation. *Intl. J. Radiat. Biol.* **65**: 27-33.

Rofstad, E.K. and Danielsen, T. (1999) Hypoxia-induced metastasis of human melanoma cells: involvement of vascular endothelial growth factor-mediated angiogenesis. *Br. J. Cancer* **80**: 1697-1707.

Rohlff, C., and Glazer, R.I. (1995) Regulation of multidrug resistance through the cAMP and EGF signalling pathways. *Cellular signalling*. **5**: 431-443.

Ryan, H.E., Lo, J., and Johnson, R.S. (1998) HIF-1a is required for solid tumour formation and embryonic vascularisation. *EMBO* **17**: 3005-3015.

Sakamoto, K.M., Bardeleben, C., Yates, K.E., Raines, M.A., Golde, D.W., and Gasson, J.C. (1991) 5' upstream sequence and genomic structure of the human primary response gene, Egr-1/TIS8. *Oncogene* **6**: 867-871.

Salceda, S., Beck, I., and Caro, J. (1996) Absolute requirement of the aryl hydrocarbon receptor nuclear translocator for gene activation by hypoxia. *Biochem. and Biophys.* **334**: 389-394.

Salceda, S. and Caro, J. (1997) Hypoxia-inducible factor-1a (HIF-1a) is rapidly degraded by the ubiquitin-proteasome system under normoxic conditions. *J. Biol. Chem.* **272**: 22642-22647.

Salceda, S., Beck, I., Srinivas, V., Caro, J. (1997) Complex role of protein phosphorylation in gene activation by hypoxia. *Kidney Intl.* **51**: 556-559.

Salloum, R.M., Saunders, M., Mauceri, H.J., Hanna, N., Jaskowiak, N., Posner, M., Beckett, M., Kufe, D., and Weichselbaum, R.R. () Dual induction of the Epo.Egr.TNFa plasmid in hypoxic tumours produces tumour growth delay.

Salnikow, K., Blagosklonny, M.V., Ryan, H., Johnson, R., and Costa, M. (2000) Carcinogenic nickel induces genes involved with hypoxic stress. *Cancer Res.* **60**: 38-41.

Samoto, K., Ikezaki, K., Ono, M., Shono, T., Kohno, K., Kuwano, M., and Fukui, M. (1995) Expression of vascular endothelial growth factor and its possible relation with neovascularisation in human brain tumours. *Cancer Res.* **55**: 1189-1193.

Sandner, P., Gess, B., and Wolf, K. (1996) Divergent regulation of vascular endothelial growth and erythropoietin gene expression *in vivo*. *Eur. J. Physiol.* **431**: 905-912.

Sasaki, I., Ueyama, H., and Ueda, K. (1990) Increase of 63kDa protein kinase in the nuclear matrix of HL-60 cells during differentiation by retinoic acid. *J. Nutr. Sci. Vitaminol. (Tokyo)* **36**: 1-10.

Saunders, M.P. The use of gene therapy to selectively activate bioreductive drugs in tumour cell lines. A thesis submitted to the University of Manchester for the degree of Doctor of Philosophy (Ph.D.) in the faculty of Science, 1999.

Scandurro, A.B., Rondon, I.J., Wilson, R.B., Tenenbaum, S.A., Garry, R.F., and Beckman, B.S. (1997) Interaction of erythropoietin RNA binding protein with erythropoietin RNA requires an association with HSP 70. *Kid. Intl.* **51**: 579-584.

Schmidt-Ullrich, R.K., Dent, P., Grant, S., Mikkelsen, R.B. and Valerie, K. (2000) Signal transduction and cellular radiation responses. *Rad. Res.* **153**: 245-257.

Schule, R., Rangarajan, P., Yang, N., Kliewer, S., Ransone, L.J., Bolado, J., Verma, I.M. and Evans, R.M. (1991) Retinoic acid is a negative regulator of AP-1 responsive genes. *Proc. Natl. Acad. Sci. USA.* **88**: 6092-6096.

Schuster, S.J., Badiavas, E.V., Costa-Giomi, P., Weinmann, R., Erslev, A.J., and Caro, J. (1989) Stimulation of erythropoietin gene transcription during hypoxia and cobalt exposure. *Blood* **73**: 13-16.

Scott, S.D., Marples, B., Hendry, J.H., Lashford, L.S., Embleton, M.J., Hunter, R.D., Howell, A., and Margison, G.P. (2000) A radiation-controlled molecular switch for use in gene therapy of cancer. *Gene Therapy* **7**: 1121-1125.

Semenza, G.L., Nejfelt, M.K., Chi, S.M., and Antonarakis, S.E. (1991) Hypoxia-inducible nuclear factors bind to an enhancer element located 3' to the human erythropoietin gene. *Proc. Natl. Acad. Sci.* **88**: 5680-5684.

Semenza, G.L. and Wang, G.L. (1992) A nuclear factor induced by hypoxia via de novo protein synthesis binds to the human erythropoietin gene enhancer at a site required for transcriptional activation. *Mol. and Cell. Biol.* **12**: 5447-5454.

Semenza, G.L., Roth, P.H., Fang, H., and Wang, G.L. (1994) Transcriptional regulation of genes encoding glycolytic enzymes by hypoxia-inducible factor-1. *J. Biol. Chem. 269*: 23757-23763.

Semenza, G.L. (1996a) Transcriptional regulation by hypoxia-inducible factor-1. *Trends in Cardiovasc. Med.* **6**: 151-157.

Semenza, G.L., Jiang, B., Leung, S.W., Passantino, R., Concordet, J., Maire, P., and Giallongo, A. (1996b) Hypoxia response elements in the aldolase A, Enolase 1, and lactate dehydrogenase A gene promotors contain essential binding sites for hypoxia-inducible factor-1. *J. Biol. Chem.* **271**: 32529-32537.

Semenza, G.L., Agani, F., Booth, G., Forsythe, J., Iyer, N., Jiang, B., Leung, S., Roe, R., Wiener, C., and Yu, A. (1997) Structural and functional analysis of hypoxia-inducible factor-1. *Kidney Intl.* **51**: 553-555.

Semenza, G.L. (2000a) Hypoxia, clonal selection, and the role of HIF-1 in tumour progression. *Crit. Rev. in Biochem. and Mol. Biol.* **35**: 71-103.

Semenza, G.L. (2000b) HIF-1: a mediator of physiological and pathophysiological responses to hypoxia. *J. Appl. Physiol.* **88**: 1474-1480.

Semenza, G.L. (2000c) HIF-1 and human disease: one highly involved factor. *Genes and Devel.* **14**: 1983-1991.

Semenza, G.L. (2000d) Expression of hypoxia-inducible factor-1: Mechanisms and consequences. *Biochem. Pharm.* **59**: 47-53.

Seung, L.P., Mauceri, H.J., Beckett, M.A., Hallahan, D.E., Hellman, S. and Weichselbaum, R.R. (1995) Genetic radiotherapy overcomes tumour resistance to cytotoxic agents. *Cancer Res.* **55**: 5561-5565.

Shibata, T., Giaccia, A.J., and Brown, J.M. (2000) Development of a hypoxia-responsive vector for tumour-specific gene therapy. *Gene Therapy* **7**: 493-498.

Shweiki, D., Itin, A., Soffer, D., and Keshet, E. (1992) Vascular endothelial growth factor induced by hypoxia may mediate hypoxia-initiated angiogenesis. *Nature* **359**: 843-845.

Shweiki, D., Itin, A., Neufeld, G., Gitay-Goren, H., and Keshet, E. (1993) Patterns of expression of vascular endothelial growth factor (VEGF) and VEGF receptors in mice suggests a role in hormonally regulated angiogenesis. *J. Clin. Invest.* **91**: 2235-2243.

Shweiki, D., Neeman, M., Itin, A., and Keshet, E. (1994) Induction of vascular endothelial growth factor expression by hypoxia and by glucose deficiency in multicell spheroids: implications for tumour angiogenesis. *Proc. Natl. Acad. Sci.* **92**: 768-772.

Siim, B.G., Denny, W.A., and Wilson, W.R. (1997) Nitro reduction as an electronic switch for bioreductive prodrug activation. *Oncol. Res.* **9**: 357-369.

Silins, G., Grimmond, S., Egerton, M., and Hayward, N. (1997) Analysis of the promoter region of the human VEGF-related factor gene. *Biochem. and Biophys. Res. Comm.* **230**: 413-418.

Smitskamp-Wilmw, E., Giaccone, G., Pinedo, H.M., van der Laan, B.F.A.M., and Peters, G.J. (1995) DT-diaphorase activity in normal and neoplastic human tissues: an indicator for sensitivity to bioreductive agents. *Br. J. Cancer.* **72**: 917-921.

Springer, C.J. and Niculescu-Duvaz, I. (2000) Approaches to gene-directed enzyme prodrug therapy (GDEPT). *Cancer Gene Therapy* **35**: 403-409

Stern, S. and Guichard, M. (1996) Efficacy of agents counteracting hypoxia in fractionated radiation regimes. *Radiat. and Oncol.* **41**: 143-149.

Stone, H.B., Brown, J.M., Phillips, T.L., and Sutherland, R.M. (1993) Oxygen in human tumours: correlation between methods of measurement and response to therapy. *Rad. Res.* **136**: 422-434.

Stratford, I.J., Adams, G.E., Bremner, J.C.M., Cole, S., Edwards, H.S., Robertson, N., and Wood, P.J. (1994) Manipulation and exploitation of the tumour enviroment for therapeutic benefit. *Int. J. Radiat. Biol.* **65**: 85-94.

Smith, M.A., and Eichele, G. (1991) Temporal and regional differences in the expression pattern of distinct retinoic acid receptor-b transcripts in the chick embryo. *Development.* **111**: 245-252.

Smith, M.A., Parkinson, D.R., Cheson, B.D., and Friedman, M.A. (1992) Retinoids in cancer therapy. *J. Clin. Onc.* **10**: 839-864.

Srinivas, V., Zhu, X., Salceda, S., Nakamura, R., and Caro, J. (1998) Hypoxia-inducible factor-1a (HIF-1a) is a non-heme iron protein. *J. Biol. Chem.* **273**: 18019-18022.

Sukhatme, V.P. (1990) Early transcription events in cell growth: the Egr family. *J. Am. Soc. Neph.* **1**: 859-866.

Sukhatme, V.P. (1991) The Egr family of nuclear signal transducers. *Am. J. Kid. Dis.* **17**: 615-618.

Sutter, C.H., Laughner, E., and Semenza, G.L. (2000) Hypoxia-inducible factor-1a protein expression is controlled by oxygen-regulated ubiquitiniation that is disrupted by deletions and missense mutations. *Proc. Natl. Acad. Sci.* **80**: 2519-2523.

Sunderland, R.M., Eddy, H.A., Bareham, B., Reich, K., and Vanantwerp, D. (1979) Resistance to adriamycin in multicellular spheroids. *Intl. J. Radiat. Oncol. Biol. Phys.* **5**: 1225-1230.

Sutherland, R.M., Ausserer, W.A. and Murphy, B.J. (1996) Tumour hypoxia and heterogeneity: Challenges and opportunities for the future. *Sem. Rad. Oncol.* **6**:59-70.

Symonds, H., Krall, L., Remington, L., Saenz-Robies, M., Lowe, S., Jacks, T., and Van Dyke, T. p53-dependent apoptosis suppresses tumour growth and progression *in vivo*. *Cell* **78**: 703-711.

Takagi, H., King, G.L., Robinson, G.S., Ferrara, N., and Aiello, L.P. (1996) Adenosine mediates hypoxic induction of vascular endothelial growth factor in retinal pericytes and endothelial cells. *Opthal. and Vis. Sci.* **37**: 2165-2176.

Takahashi, Y., Sasaki, H., Kim, S.J., Tobisu, K., Tsukamoto, T., Kumamoto, Y., Sugimura, T., and Terada, M. (1994) Markedly increased amounts of messenger RNAs for vascular endothelial growth factor and placenta growth factor in renal cell carcinoma associated with angiogenesis. *Cancer Res.* **54**: 4233-4237.

Takahashi, Y., Kitadai, Y., Bucana, C.D., Cleary, K.R., and Ellis, L.M. (1995) Expression of vascular endothelial growth factor and its receptor, KDR, correlates with

vascularity, metastasis and proliferation of human colon cancer. *Cancer Res.* **55**: 3964-2968.

Talks, K.L., Turley, H., Gatter, K.C., Maxwell, P.H., Pugh, C.W., Ratcliffe, P.J., and Harris, A.L. (2000) The expression and distribution of HIF-1a and HIF-2a in normal human tissues, cancers and tumour-associated macrophages. *Am. J. Path.* **157**: 411-421.

Tannock, I. (1982) Response of aerobic and hypoxic cells in a solid tumour to adriamycin and cyclophosphamide and interaction of the drugs with radiation. *Cancer Res.* **42**: 4921-4926.

Taraboletti, G., Roberts, D., Liotta, L.A., and Giavazzi, R. (1990) Platelet thrombospondin modulates endothelial cell adhesion, motility and growth: a potential angiogenesis regulatory factor. *J. Cell Biol.* **111**: 765-772.

Teicher, B.A. (1994) Hypoxia and drug resistance. *Cancer and Met. Rev.* **13**: 139-168.

Teicher, B.A. (1995) Physiologic mechanisms of therapeutic resistance. *Oncology* **9**: 475-506.

Thomlinson and Gray (1955) The histological structure of some human lung cancers and the possible implications for radiotherapy. *Br. J. Cancer* **9**:539-549

Tortora, G., and Cho-Chung, Y.S. (1990) Type II regulatory subunit of protein kinase restores cAMP-dependent transcription in a cAMP-unresponsive cell line. *J. Biol. Chem.* **265**: 18067-18070.

Tsai-Morris, C-H., Cao, X., and Sukhatme, V.P. (1988) 5' flanking sequence and genomic structure of Egr-1, a murine mitogen inducible zinc finger encoding gene. *Nucl. Acids Res.* **16**: 8835-8846.

Treisman, R. (1992) The serum response element. *TIBS* **17**: 423-426.

Vaupel, P., Kallinowski, F., and Okuneiff, P. (1989) Blood flow, oxygen and nutrient supply, and metabolic microenviroment of human tumours: A review. *Cancer Res.* **49**: 6449-6465.

Vaupel, P.W. (1990) Oxygenation of human tumours. *Strahlenther. Onkol.* **166**: 361-386.

Vaupel, P., Schlenger, K., Knoop, C., and Hockel, M. (1991) Oxygenation of human tumours: Evaluation of tissue oxygen distribution in breast cancers by computerised oxygen tension measurements. *Cancer Res.* **51**: 3316-3322.

Vaupel, P.W. (1993) Oxygenation of solid tumours. In: *Drug Resistance in Oncology*, Teicher B.A., (ed) pp. 53-85 Marcel Dekker: New York.

Volm, M. and Koomagi, R. (2000) *Anticancer Res.* **20**: 1527-1534.

Wang, G.L., and Semenza, G.L. (1993a) Characterisation of hypoxia-inducible factor-1 and regulation of DNA binding activity by hypoxia. *J. Biol. Chem.* **29**: 21513-21518.

Wang, G.L., and Semenza, G.L. (1993b) Desferrioxamine induces erythropoeitin gene expression and hypoxia-inducible factor-1 DNA binding activity: Implications for models of hypoxia signal transduction. *Blood.* **82**: 3610-3615.

Wang, G.L. and Semenza , G.L. (1993c) General involvement of hypoxia-inducible factor-1 in transcriptional response to hypoxia. *Proc. Natl. Acad. Sci.* **90**: 4304-4308.

Wang, G.L., and Semenza, G.L. (1995a) Purification and characterisation of hypoxia-inducible factor-1. *J. Biol. Chem.* **270**: 1230-1237.

Wang, G.L., Jiang, B., Rue, E.A., and Semenza, G.L. (1995b) Hypoxia-inducible factor-1 is a basic-helix-loop-helix-PAS heterodimer regulated by Cellular O2 tension. *Proc. Natl. Acad. Sci.* **92**: 5510-5514.

Wang, G.L., and Semenza, G.L. (1996) Oxygen sensing and response to hypoxia by mammalian cells. *Redox Report* **2**: 89-96.

Watson PH, Singh R and Hole AK. (1996) Influence of c-Myc on the progression of human breast cancer. *Curr. Top. Microbiol. Immunol.* **213**: 267-283.

Weichselbaum, R.R., Hallahan, D., Fuks, Z., and Kufe, D. (1994) Radiation induction of immediate early genes: effectors of the radiation-stress response. *Int. J. Radiat. Oncol. Biol Phys.* **30**: 229-234.

Weinstat-Saslow, D.L., Zabrenetzky, V.S., Van Houtte, K., Frazier, W.A., Roberts, D.D., and Steeg, P.S. Transfection of thrombospondin-1 complementary DNA into a human breast carcinoma cell line reduces primary tumour growth, metastatic potential and angiogenesis. *Cancer Res.* **54**: 6504-6511.

Weisener, M.S., Turley, H., Allen, W.E., William, C., Eckardt, K-U., Talks, K.L., Wood, S.M., Gatter, K.C., Harris, A.L., Pugh, C.W., Tatcliffe, P.J., and Maxwell, P.H. (1998) Induction of endothelial PAS domain protein-1 by hypoxia: characterisation and comparison with HIF-1a. *Blood* **92**: 2260-2268.

Wenger, R.H., Kvietikova, I., Rolfs, A., Gassman, M., and Marti, H.H. (1997a) Hypoxia-inducible factor-1a is regulated at the post-mRNA level. *Kidney Intl.* **51**: 560-563.

Wenger, R.H., and Gassman, M. (1997b) Oxygen(es) and the Hypoxia-inducible factor-1. *Biol. Chem.* **378**: 609-616.

Wetherall, N.T. and Taylor, C.M. (1986) The effects of retinoid treatment and antiestrogens on the growth of T47D human breast cancer cells. *Eur. J. Clin. Oncol.* **22**: 53-59.

Wilson, W.R. (1996) Tumour hypoxia: Challenges for cancer chemotherapy.

Wood, M.S., Weisener, M.S., Yeates, K.M., Okaca, N., Pugh, C.W., Maxwell, P.H., and Ratcliffe, P.J. (1995) Selection and analysis of a mutant cell line defective in the HIF-1α subunit. *J. Biol. Chem.* **274**: 8360-8368.

Wood, M.S., Gleadle, J.M., Pugh, C.W., Hankinson, O., and Ratcliffe, P.J. (1996) The role of the aryl hydrocarbon receptor nuclear translocator (ARNT) in hypoxic induction of gene expression. *J. Biol. Chem.* **271**: 15117-15123.

Workman, P., and Stratford, I.J. (1993) The experimental development of bioreductive drugs and their role in cancer therapy. *Cancer and Metast. Rev.* **12**: 73-82.

Wouters, B.G. and Brown, J.M. (1997) Cells at intermediate oxygen levels can be more important than the "hypoxic fraction" in determining tumour response to fractionated radiotherapy. *Rad. Res.* **147**: 541-550.

Wykoff, C.C., Beasley, N.J.P., Watson, P.H., Turner, K.J., Pastorek, J., Sibtain, A., Wilson, G.D., Turley, H., Talks, K.L., Maxwell, P.H., Pugh, C.W., Ratcliffe, P.J., and Harris, A.L. (2000) Hypoxia-inducible expression of tumour associated carbonic anhydrases. *Cancer Res.* **60**: 7075-7083.

Yan, S., Zou, Y.S., Gao, Y., Mackman, N., Lee, S.L., Milbrandt, J., Pinsky, D., Kisiel, W., and Stern, D. (1998) Tissue factor transcription driven by Egr-1 is a critical mechanism of murine pulmonary fibrin deposition in hypoxia. *Proc. Natl. Acad. Sci.* **95**: 8298-8303.

Yan, S., Lu, J.L., Zou, Y.S., Soh-Won, J., Cohen, D.M., Buttrick, P.M., Cooper, D.R., Steinberg, S.F., Mackman, N., Pinsky, D.J., and Stern, D.M. (1999) Hypoxia-associated induction of early growth response-1 gene expression. *J. Biol. Chem.* **274**: 15030-15040.

Yang-Yen, H.F., Zhang, X.K., Graupner, G., Tzukerman, M., Sakamoto, B., Karin, M. and Pfahl, M. (1991) Antagonism between retinoic acid receptors and AP-1: Implications for tumour promotion and inflammation. *New Biol.* **3**: 1206-1219.

Young, S.D., Marshall, R.S., and Hill, R.P. (1988) Hypoxia induces DNA overreplication and enhances metastatic potential of murine tumour cells. *Proc. Natl. Acad. Sci.* **85**: 9533-9537.

Yuan, J., Narayanan, L., Rockwell, S., and Glazer, P.M. (2000) Diminished DNA repair and elevated mutagenesis in mammalian cells exposed to hypoxia and low pH. *Cancer Res.* **60**: 4372-4376.

ZagZag, D., Scalzitti, J.M., Laughner, E., Sinons, J.W., and Semenza, G.L. (2000) Expression of HIF-1a in human brain tumours: association with angiogenesis, invasion and progression. *Cancer*, in press.

Zaman, K., Ryu, H., Hall, D., O'Donovon, K., Lin, K-I., Miller, M.P., Marquis, J.C., Baraban, J.M., Semenza, G.L., and Ratan, R.R. (1999) Protection from oxidative stress-induced apoptosis in cortical neuronal cultures by iron chelators is associated with enhanced DNA binding of hypoxia-inducible factor-1 and ATF-1/CREB and increased expression of glycolytic enzymes, $p21^{waf1/cip1}$ and erythropoietin. *J. Neurosci.* **15**: 9821-9830.

Zeman, E.M., Lemmon, M.J., and Brown, J.M. (1990) Aerobic radiosensitization by SR 4233 in vitro and in vivo. *Int. J. Radiat. Biol. Phys.* **18**: 125-132.

Zhang, W., Tsuchiya, T. and Yasukochi, Y. (1999) Transitional change in interaction between HIF-1 and HNF-4 in response to hypoxia. *J. Hum. Genet.* **44**: 293-299.

Zhong, H., De Marzo, A.M., Laughner, E., Lim, M., Hilton, D.A., ZagZag, D., Buechler, P., Isaacs, W.B., Semenza, G.L., and Simons, J.W. (1999) Overexpression of HIF-1α in common human cancers and their matastases. *Cancer res.* **59**: 5830-5835.

Appendices

In each of the tables shown, mean values are in italics. It is these values which are shown graphically in the appropriate chapters.

Appendix 1

Normalised expression of pGL3.Control, pGL3.PGK^{+++} and pGL3.PGK^{---} in the human fibrosarcoma cell line HT1080, exposed to 16 hours air or anoxia.

10;1

15ug

	AIR	AIR	AIR	*AIR*	sdev	SE
Control	1.0000	1.0000	1.0000	*1.0000*	0.0000	0.0000
PGK+++	0.1024	0.0321	0.0667	*0.0671*	0.0351	0.0203
PGK---	0.1087	0.0479	0.0942	*0.0836*	0.0317	0.0183

	AnO_2	AnO_2	AnO_2	*AnO 2*	sdev	SE
Control	1.0807	0.8301	2.2187	*1.3765*	0.7400	0.4278
PGK+++	1.2737	0.6402	0.4292	*0.7810*	0.4395	0.2540
PGK---	1.0562	0.9610	1.0451	*1.0208*	0.0520	0.0301

10ug

	AIR	AIR	AIR	*AIR*	sdev	SE
Control	1.0000	1.0000	1.0000	*1.0000*	0.0000	0.0000
PGK+++	0.0728	0.0329	0.1579	*0.0879*	0.0638	0.0369
PGK---	0.0705	0.0225	0.0621	*0.0517*	0.0257	0.0148

	AnO_2	AnO_2	AnO_2	*AnO 2*	sdev	SE
Control	1.0099	1.2231	0.9493	*1.0608*	0.1438	0.0831
PGK+++	0.6209	1.4033	0.8113	*0.9452*	0.4080	0.2358
PGK---	0.6462	1.2239	0.5672	*0.8124*	0.3585	0.2072

5ug

	AIR	AIR	AIR	*AIR*	sdev	SE
Control	1.0000	1.0000	1.0000	*1.0000*	0.0000	0.0000
PGK+++	0.0132	0.0743	0.0590	*0.0488*	0.0318	0.0184
PGK---	0.0141	0.0756	0.0945	*0.0614*	0.0420	0.0243

	AnO_2	AnO_2	AnO_2	*AnO 2*	sdev	SE
Control	0.5280	1.2262	0.9396	*0.8979*	0.3510	0.2029
PGK+++	0.3160	0.7535	0.8595	*0.6430*	0.2882	0.1666
PGK---	0.2816	0.6613	1.1193	*0.6874*	0.4194	0.2425

40;1

15ug

	AIR	AIR	AIR	*AIR*	sdev	SE
Control	1.0000	1.0000	1.0000	*1.0000*	0.0000	0.0000
PGK+++	0.0766	0.0100	0.1580	*0.0816*	0.0741	0.0428
PGK---	0.0809	0.0234	0.2895	*0.1313*	0.1400	0.0809

	AnO_2	AnO_2	AnO_2	*AnO 2*	sdev	SE
Control	1.8396	1.2086	0.2956	*1.1146*	0.7763	0.4487
PGK+++	1.2636	0.2801	0.4579	*0.6672*	0.5241	0.3029
PGK---	1.4954	0.7590	0.0445	*0.7663*	0.7255	0.4194

10ug

	AIR	AIR	AIR	*AIR*	sdev	SE
Control	1.0000	1.0000	1.0000	*1.0000*	0.0000	0.0000
PGK+++	0.9040	0.0368	0.0206	*0.3204*	0.5054	0.2922
PGK---	1.4961	0.0465	0.0320	*0.5249*	0.8411	0.4862

	AnO_2	AnO_2	AnO_2	*AnO 2*	sdev	SE
Control	0.8248	1.4509	1.2302	*1.1687*	0.3175	0.1835
PGK+++	2.7039	1.3340	0.9876	*1.6752*	0.9076	0.5246
PGK---	2.4458	0.6568	5.3681	*2.8236*	2.3783	1.3747

5ug

	AIR	AIR	AIR	*AIR*	sdev	SE
Control	1.0000	1.0000	1.0000	*1.0000*	0.0000	0.0000
PGK+++	0.0099	0.0266	0.3796	*0.1387*	0.2088	0.1207
PGK---	0.0209	0.0501	0.3578	*0.1429*	0.1867	0.1079

	AnO_2	AnO_2	AnO_2	*AnO 2*	sdev	SE
Control	1.0211	1.4374	0.9389	*1.1325*	0.2673	0.1545
PGK+++	0.6164	1.2491	2.2269	*1.3641*	0.8114	0.4690
PGK---	0.8914	1.5320	1.7203	*1.3813*	0.4345	0.2512

Appendix 2

Normalised expression of pGL3.Control, pGL3.PGK^{+++} in the human head and neck carcinoma cell line, SQ20B, exposed to 16 hours air or anoxia.

10;1

15ug

	AIR	AIR	*AIR*	sdev
Control	1.0000	1.0000	*1.0000*	0
PGK^{+++}	0.1532	0.0724	*0.1128*	0.0571

	AnO_2	AnO_2	*AnO $_2$*	sdev
Control	1.0039	2.0488	*1.5264*	0.7389
PGK^{+++}	1.2694	2.6504	*1.9599*	0.9765

10ug

	AIR	AIR	*AIR*	sdev
Control	1.0000	1.0000	*1.0000*	0.0000
PGK^{+++}	0.2328	0.1050	*0.1689*	0.0904

	AnO_2	AnO_2	*AnO $_2$*	sdev
Control	0.9628	2.6471	*1.8050*	1.1910
PGK^{+++}	1.7306	3.5358	*2.6332*	1.2764

5ug

	AIR	AIR	*AIR*	sdev
Control	1.0000	1.0000	*1.0000*	0.0000
PGK^{+++}	0.1689	0.0922	*0.1305*	0.0542

	AnO_2	AnO_2	*AnO $_2$*	sdev
Control	0.4877	1.8276	*1.1576*	0.9475
PGK^{+++}	1.7041	3.0501	*2.3771*	0.9517

Appendix 3

Table 3.8: Normalised expression of pGL3.PGK^{+++} and pGL3.PGK^{---} in the human fibrosarcoma cell line HT1080, exposed to 16 hours air or anoxia.

PGK+++				MEAN						MEAN						MEAN		
	AIR	AIR	AIR	AIR	Sdev	SE	1%O2	1%O2	1%O2	1%O2	sdev	SE	AnO2	AnO2	AnO2	AnO2	sdev	SE
0 hr	0.0125	0.9532	0.0682	0.3446	0.5278	0.3051	0.6310	0.0904	0.3678	0.3631	0.2704	0.1563	0.2231	1.3125	0.1690	0.5682	0.6451	0.3729
1 hr	0.0126	0.1859	0.0409	0.0798	0.0930	0.0538	0.7843	1.7468	0.3773	0.9695	0.7033	0.4065	0.2607	1.6223	0.2051	0.6960	0.8026	0.4640
2 hr	0.0060	0.0687	0.0481	0.0409	0.0319	0.0185	0.2048	0.7474	0.5133	0.4885	0.2722	0.1573	0.1061	0.2877	0.2053	0.1997	0.0909	0.0525
3 hr	0.0191	0.2262	0.0361	0.0938	0.1150	0.0665	0.4112	1.5491	0.6641	0.8748	0.5975	0.3454	0.5620	2.0462	0.2921	0.9668	0.9446	0.5460
4 hr	0.0070	0.0947	0.0390	0.0469	0.0444	0.0257	0.2886	0.9393	0.3762	0.5347	0.3531	0.2041	0.3568	0.3519	0.5571	0.4219	0.1171	0.0677
6 hr	0.0025	0.0992	0.0299	0.0439	0.0498	0.0288	0.1306	1.0348	0.3081	0.4912	0.4791	0.2769	0.0617	0.4850	0.8414	0.4627	0.3903	0.2256

PGK---				MEAN						MEAN						MEAN		
	AIR	AIR	AIR	AIR	Sdev	SE	1%O2	1%O2	1%O2	1%O2	sdev	SE	AnO2	AnO2	AnO2	AnO2	sdev	SE
0 hr	0.0156	0.8601	0.0564	0.3107	0.4762	0.2753	0.8113	0.1820	0.4202	0.4711	0.3177	0.1837	0.2854	1.0414	0.1853	0.5040	0.4680	0.2705
1 hr	0.0145	0.1225	0.0488	0.0619	0.0552	0.0319	0.8858	1.0342	0.3804	0.7668	0.3427	0.1981	0.2683	1.3165	0.2151	0.5999	0.6211	0.3590
2 hr	0.0055	0.0194	0.0501	0.0250	0.0228	0.0132	0.2130	0.5112	0.6104	0.4448	0.2068	0.1196	0.1633	0.4864	0.2410	0.2969	0.1687	0.0975
3 hr	0.0192	0.2660	0.0331	0.1061	0.1386	0.0801	0.5372	2.1037	0.6840	1.1083	0.8651	0.5001	0.4609	1.1173	0.3342	0.6374	0.4203	0.2430
4 hr	0.0081	0.1142	0.0392	0.0538	0.0545	0.0315	0.2876	0.8352	0.2586	0.4605	0.3248	0.1878	0.3675	0.4384	0.5390	0.4483	0.0862	0.0498
6 hr	0.0024	0.1710	0.0342	0.0692	0.0896	0.0518	0.1236	1.4633	0.2672	0.6180	0.7355	0.4252	0.1058	0.6959	0.6452	0.4823	0.3271	0.1890

Appendix 4

Normalised expression of pGL3.PGK^{+++} and pGL3.PGK^{---} in the human head and neck carcinoma cell line SQD9, exposed to 16 hours air or anoxia.

PGK+++				MEAN						MEAN						MEAN		
	AIR	AIR	AIR	AIR	Sdev	SE	1%O_2	1%O_2	1%O_2	1%O_2	sdev	SE	AnO_2	AnO_2	AnO_2	AnO_2	sdev	SE
0 hr	0.3536	0.4740	0.3496	0.3924	0.0707	0.0408	2.3452	2.2098	2.5961	2.3837	0.1960	0.1133	2.7786	1.7566	3.1486	2.5613	0.7210	0.4168
1 hr	0.3942	0.2794	0.1987	0.2908	0.0982	0.0568	2.1116	1.5324	1.0215	1.5552	0.5454	0.3153	1.0279	1.0706	1.1489	1.0824	0.0614	0.0355
2 hr	0.3659	0.3392	0.4208	0.3753	0.0416	0.0240	2.5426	1.6419	2.0532	2.0793	0.4509	0.2606	2.5715	0.9177	1.3731	1.6208	0.8543	0.4938
3 hr	0.3195	0.2818	0.2878	0.2964	0.0202	0.0117	2.6958	1.9111	1.6167	2.0746	0.5578	0.3224	1.1048	3.5627	3.5947	2.7540	1.4284	0.8257
4 hr	0.3331	0.2842	0.3692	0.3288	0.0427	0.0247	2.2200	1.4702	2.0929	1.9277	0.4013	0.2319	1.4463	1.5897	2.8516	1.9625	0.7733	0.4470
6 hr	0.2415	0.3128	0.3125	0.2889	0.0411	0.0237	1.8645	1.6647	2.7557	2.0950	0.5808	0.3357	1.0031	1.1599	2.5745	1.5792	0.8656	0.5003

PGK---				MEAN						MEAN						MEAN		
	AIR	AIR	AIR	AIR	Sdev	SE	1%O_2	1%O_2	1%O_2	1%O_2	sdev	SE	AnO_2	AnO_2	AnO_2	AnO_2	sdev	SE
0 hr	0.0723	0.1515	0.0850	0.1029	0.0425	0.0246	0.4701	0.7684	0.5230	0.5872	0.1591	0.0920	0.4000	0.3814	0.4749	0.4188	0.0495	0.0286
1 hr	0.0578	0.0700	0.0739	0.0672	0.0084	0.0049	0.3008	0.3142	0.2824	0.2991	0.0160	0.0092	0.1137	0.1447	0.1661	0.1415	0.0263	0.0152
2 hr	0.0529	0.0787	0.1482	0.0933	0.0493	0.0285	0.4509	0.3534	0.6724	0.4922	0.1635	0.0945	0.5570	0.1087	0.2497	0.3051	0.2293	0.1325
3 hr	0.0685	0.0906	0.0872	0.0821	0.0119	0.0069	1.6781	0.9439	0.7568	1.1263	0.4870	0.2815	0.0829	1.5317	1.4067	1.0071	0.8028	0.4641
4 hr	0.0478	0.0702	0.1147	0.0776	0.0340	0.0197	0.4063	0.3661	0.5685	0.4469	0.1072	0.0619	0.1604	0.4457	0.8593	0.4885	0.3514	0.2031
6 hr	0.0651	0.0970	0.1498	0.1040	0.0428	0.0247	0.4500	0.4236	0.7362	0.5366	0.1734	0.1002	0.0610	0.2606	0.5082	0.2766	0.2240	0.1295

Appendix 5

Normalised expression of HRE-luciferase vectors exposed to 16 hours air, hypoxia or anoxia and three hours reoxygenation in the MDA 468 human breast carcinoma cell line.

				MEAN		
	AIR	AIR	AIR	AIR	Sdev	SE
LDH-A (1+2+3) $^{3+}$	0.0178	0.1021	0.0316	0.0505	0.0452	0.0261
Epo (1+2) $^{3+}$	0.0301	0.0456	0.0237	0.0332	0.0113	0.0065
PGK (1+2) $^{3+}$	0.0339	0.0522	0.0127	0.0329	0.0197	0.0114
VEGF (1+2) $^{3+}$	0.0210	0.0655	0.0128	0.0331	0.0283	0.0164
Glut-1 (1+2+3) $^{1+}$	0.0503	0.0194	0.0229	0.0309	0.0169	0.0098

	$1\%O_2$	$1\%O_2$	$1\%O_2$	$1\%O_2$	Sdev	SE
LDH-A (1+2+3) $^{3+}$	0.1524	0.0858	0.0681	0.1021	0.0444	0.0257
Epo (1+2) $^{3+}$	0.0913	0.1043	0.0784	0.0913	0.0129	0.0075
PGK (1+2) $^{3+}$	0.5911	0.7666	0.3220	0.5599	0.2240	0.1295
VEGF (1+2) $^{3+}$	0.0265	0.0629	0.0219	0.0371	0.0225	0.0130
Glut-1 (1+2+3) $^{1+}$	0.0176	0.0668	0.0967	0.0604	0.0400	0.0231

	AnO_2	AnO2	AnO2	AnO2	Sdev	SE
LDH-A (1+2+3) $^{3+}$	0.0598	0.2712	0.2787	0.2032	0.1243	0.0718
Epo (1+2) $^{3+}$	0.1591	0.2826	0.1470	0.1962	0.0750	0.0434
PGK (1+2) $^{3+}$	1.2301	1.6793	0.4263	1.1119	0.6348	0.3669
VEGF (1+2) $^{3+}$	0.0536	0.0229	0.0274	0.0346	0.0166	0.0096
Glut-1 (1+2+3) $^{1+}$	0.1545	0.0714	0.0341	0.0866	0.0617	0.0356

Appendix 6

Normalised expression of HRE-luciferase vectors exposed to 16 hours air, hypoxia or anoxia and three hours reoxygenation in the HT1080 human fibrosarcoma cell line.

				MEAN		
	AIR	AIR	AIR	AIR	Sdev	SE
LDH-A (1+2+3) $^{3+}$	0.0250	0.0343	0.0310	0.0301	0.0047	0.0027
Epo (1+2) $^{3+}$	0.0336	0.0663	0.0494	0.0498	0.0163	0.0095
PGK (1+2) $^{3+}$	0.1392	0.1039	0.0864	0.1098	0.0249	0.0144
VEGF (1+2) $^{3+}$	0.0075	0.0070	0.0063	0.0069	0.0005	0.0003
Glut-1 (1+2+3) $^{1+}$	0.1133	0.0388	0.0570	0.0697	0.0388	0.0225
				MEAN		
	$1\%O_2$	$1\%O_2$	$1\%O_2$	$1\%O_2$	Sdev	SE
LDH-A (1+2+3) $^{3+}$	0.7098	0.7552	0.5840	0.6830	0.0887	0.0513
Epo (1+2) $^{3+}$	0.1766	0.1641	0.1586	0.1664	0.0093	0.0054
PGK (1+2) $^{3+}$	1.2980	1.0609	0.8819	1.0802	0.1677	0.0969
VEGF (1+2) $^{3+}$	0.0197	0.0130	0.0120	0.0149	0.0057	0.0033
Glut-1 (1+2+3) $^{1+}$	0.0997	0.2550	0.3120	0.2222	0.1099	0.0635
				MEAN		
	AnO_2	AnO2	AnO2	AnO2	Sdev	SE
LDH-A (1+2+3) $^{3+}$	0.3150	0.2250	0.2808	0.2736	0.0454	0.0263
Epo (1+2) $^{3+}$	0.2170	0.4072	0.4641	0.3628	0.1294	0.0748
PGK (1+2) $^{3+}$	1.7111	1.6827	1.3987	1.5975	0.0201	0.0116
VEGF (1+2) $^{3+}$	0.0258	0.0154	0.0143	0.0185	0.0081	0.0047
Glut-1 (1+2+3) $^{1+}$	0.5324	0.2819	0.3438	0.3860	0.1305	0.0754

Appendix 7

Normalised expression of HRE-luciferase vectors exposed to 16 hours air, hypoxia or anoxia and three hours reoxygenation in the SQD9 human head and neck sarcoma cell line.

				MEAN		
	AIR	AIR	AIR	AIR	Sdev	SE
LDH-A (1+2+3) $^{3+}$	0.3567	0.3079	0.5482	0.4043	0.1270	0.0734
Epo (1+2) $^{3+}$	0.3087	0.1580	0.0514	0.1727	0.1293	0.0748
PGK (1+2) $^{3+}$	0.2168	0.3671	0.1433	0.2424	0.1141	0.0660
VEGF (1+2) $^{3+}$	0.0291	0.0428	0.0164	0.0294	0.0132	0.0076
Glut-1 (1+2+3) $^{1+}$	0.0715	0.0481	0.2702	0.1299	0.1220	0.0705
				MEAN		
	$1\%O_2$	$1\%O_2$	$1\%O_2$	$1\%O_2$	Sdev	SE
LDH-A (1+2+3) $^{3+}$	1.6206	0.7475	1.4611	1.2764	0.4649	0.2687
Epo (1+2) $^{3+}$	2.7667	1.3472	0.6276	1.5805	1.0885	0.6292
PGK (1+2) $^{3+}$	4.7031	1.8790	2.2137	2.9319	1.5430	0.8919
VEGF (1+2) $^{3+}$	0.0393	0.3297	0.0226	0.1305	0.1727	0.0998
Glut-1 (1+2+3) $^{1+}$	0.4172	0.1273	1.0634	0.5360	0.4792	0.2770
				MEAN		
	AnO_2	AnO2	AnO2	AnO2	Sdev	SE
LDH-A (1+2+3) $^{3+}$	1.0407	0.6015	1.0744	0.9055	0.2638	0.1525
Epo (1+2) $^{3+}$	1.7068	0.7834	0.5516	1.0140	0.6111	0.3533
PGK (1+2) $^{3+}$	1.7347	3.0201	1.3460	2.0336	0.8762	0.5065
VEGF (1+2) $^{3+}$	0.0209	0.4548	0.0208	0.1655	0.2506	0.1448
Glut-1 (1+2+3) $^{1+}$	0.2901	0.0690	0.3983	0.2525	0.1678	0.0970

Appendix 8

Comparative inducibility of LDH-A 1 v 2 v 3 in the HT1080 cell line exposed to 16 hours air or anoxia.

				MEAN		
	AIR	AIR	AIR	AIR	Sdev	SE
LDH (1+2+3) $^{1+}$	0.0061	0.0343	0.0310	0.0238	0.0154	0.0089
LDH (1+2+3) $^{2+}$	0.0025	0.0027	0.0040	0.0031	0.0008	0.0005
LDH (1+2+3) $^{3+}$	0.0351	0.0493	0.0487	0.0443	0.0080	0.0046
				MEAN		
	AnO_2	AnO_2	AnO_2	AnO_2	Sdev	SE
LDH (1+2+3) $^{1+}$	0.1780	0.2250	0.2808	0.2279	0.0514	0.0297
LDH (1+2+3) $^{2+}$	0.0394	0.0327	0.0810	0.0510	0.0261	0.0151
LDH (1+2+3) $^{3+}$	1.1141	1.3281	1.3782	1.2734	0.1403	0.0811

Appendix 9

Dissection of the functional elements of the LDH-A and Glut-1 enhancers in the MDA 468 human cancer cell line(n=3).

					MEAN		
		AIR	AIR	AIR	AIR	Sdev	SE
LDH-A	(1+2+3) $^{3+}$	0.0178	0.1021	0.0316	0.0505	0.0452	0.0261
LDH-A	(1+2) $^{3-}$	0.0190	0.0245	0.0239	0.0225	0.0030	0.0017
LDH-A	(1) $^{3+}$	0.0257	0.0474	0.0344	0.0358	0.0110	0.0063
LDH-A	(2) $^{3+}$	0.0593	0.0815	0.0067	0.0492	0.0384	0.0222
LDH-A	(3) $^{3+}$	0.0168	0.1443	0.0393	0.0668	0.0680	0.0393
Glut-1	(1+2+3) $^{1+}$	0.0503	0.0194	0.0229	0.0309	0.0169	0.0098
Glut-1	(1+2) $^{2+}$	0.0627	0.0268	0.0166	0.0354	0.0242	0.0140
					MEAN		
		$1\%O_2$	$1\%O_2$	$1\%O_2$	$1\%O_2$	Sdev	SE
LDH-A	(1+2+3) $^{3+}$	0.1524	0.0858	0.0681	0.1021	0.0444	0.0257
LDH-A	(1+2) $^{3-}$	1.6459	1.9978	1.4228	1.6888	0.2899	0.1675
LDH-A	(1) $^{3+}$	0.1440	0.1400	0.1308	0.1383	0.0067	0.0039
LDH-A	(2) $^{3+}$	0.0564	0.0787	0.0104	0.0485	0.0349	0.0201
LDH-A	(3) $^{3+}$	0.2179	0.1125	0.1901	0.1735	0.0546	0.0316
Glut-1	(1+2+3) $^{1+}$	0.0476	0.0768	0.0967	0.0737	0.0247	0.0143
Glut-1	(1+2) $^{2+}$	0.0681	0.0715	0.0944	0.0780	0.0143	0.0082
					MEAN		
		AnO_2	AnO_2	AnO_2	AnO_2	Sdev	SE
LDH-A	(1+2+3) $^{3+}$	0.0598	0.2712	0.2787	0.2032	0.1243	0.0718
LDH-A	(1+2) $^{3-}$	1.1956	2.2447	1.7939	1.7447	0.5262	0.3042
LDH-A	(1) $^{3+}$	0.1069	0.1097	0.0338	0.0835	0.0430	0.0249
LDH-A	(2) $^{3+}$	0.0620	0.0917	0.0224	0.0587	0.0348	0.0201
LDH-A	(3) $^{3+}$	0.0153	0.1329	0.0159	0.0547	0.0678	0.0392
Glut-1	(1+2+3) $^{1+}$	0.1545	0.0714	0.0341	0.0866	0.0617	0.0356
Glut-1	(1+2) $^{2+}$	0.3754	0.1512	0.3289	0.2852	0.1183	0.0684

Appendix 10

Dissection of the functional elements of the LDH-A and Glut-1 enhancers in the HT1080 human cancer cell line (n=3).

					MEAN		
		AIR	AIR	AIR	AIR	Sdev	SE
LDH-A	(1+2+3) $^{3+}$	0.0250	0.0343	0.0310	0.0301	0.0047	0.0027
LDH-A	(1+2) $^{3-}$	0.0314	0.1583	0.1169	0.1022	0.0647	0.0374
LDH-A	(1) $^{3+}$	0.0029	0.0074	0.0064	0.0056	0.0023	0.0014
LDH-A	(2) $^{3+}$	0.0028	0.0079	0.0044	0.0050	0.0026	0.0015
LDH-A	(3) $^{3+}$	0.0084	0.0059	0.0089	0.0077	0.0016	0.0009
Glut-1	(1+2+3) $^{1+}$	0.1133	0.0388	0.0570	0.0697	0.0388	0.0225
Glut-1	(1+2) $^{2+}$	0.2590	0.2014	0.1275	0.1960	0.0659	0.0381
					MEAN		
		1%O2	1%O2	1%O2	$1\%O_2$	Sdev	SE
LDH-A	(1+2+3) $^{3+}$	0.7098	0.7552	0.5840	0.6830	0.0887	0.0513
LDH-A	(1+2) $^{3-}$	0.6951	0.9044	0.8937	0.8311	0.1179	0.0682
LDH-A	(1) $^{3+}$	0.0026	0.0048	0.0045	0.0040	0.0012	0.0007
LDH-A	(2) $^{3+}$	0.0021	0.0032	0.0029	0.0027	0.0006	0.0003
LDH-A	(3) $^{3+}$	0.0082	0.0039	0.0052	0.0058	0.0022	0.0013
Glut-1	(1+2+3) $^{1+}$	0.0997	0.2550	0.3120	0.2222	0.1099	0.0635
Glut-1	(1+2) $^{2+}$	0.1882	0.5124	0.5001	0.4002	0.1837	0.1062
					MEAN		
		AnO2	AnO2	AnO2	AnO_2	Sdev	SE
LDH-A	(1+2+3) $^{3+}$	0.3150	0.2250	0.2808	0.2736	0.0454	0.0263
LDH-A	(1+2) $^{3-}$	1.3820	0.9897	1.1920	1.1879	0.1962	0.1134
LDH-A	(1) $^{3+}$	0.0055	0.0090	0.0073	0.0073	0.0018	0.0010
LDH-A	(2) $^{3+}$	0.0021	0.0073	0.0050	0.0048	0.0026	0.0015
LDH-A	(3) $^{3+}$	0.0092	0.0051	0.0073	0.0072	0.0020	0.0012
Glut-1	(1+2+3) $^{1+}$	0.5324	0.2819	0.3438	0.3860	0.1305	0.0754
Glut-1	(1+2) $^{2+}$	0.8030	0.6286	0.6056	0.6791	0.1079	0.0624

Appendix 11

Dissection of the functional elements of the LDH-A and Glut-1 enhancers in the SQD9 human cancer cell line (n=3).

					MEAN		
		AIR	AIR	AIR	AIR	Sdev	SE
LDH-A	(1+2+3) $^{3+}$	0.3079	0.3567	0.5482	0.4043	0.1270	0.0734
LDH-A	(1+2) $^{3-}$	1.0817	0.6052	0.5538	0.7469	0.2911	0.1682
LDH-A	(1) $^{3+}$	0.0472	0.0380	0.0144	0.0332	0.0169	0.0098
LDH-A	(2) $^{3+}$	0.0452	0.0648	0.0183	0.0427	0.0233	0.0135
LDH-A	(3) $^{3+}$	0.0425	0.0220	0.0172	0.0272	0.0134	0.0077
Glut-1	(1+2+3) $^{1+}$	0.0715	0.0481	0.2702	0.1299	0.1220	0.0705
Glut-1	(1+2) $^{2+}$	0.2209	0.3485	0.1312	0.2335	0.1092	0.0631
					MEAN		
		$1\%O_2$	$1\%O_2$	$1\%O_2$	$1\%O_2$	Sdev	SE
LDH-A	(1+2+3) $^{3+}$	0.7475	1.6206	1.4611	1.2764	0.4649	0.2687
LDH-A	(1+2) $^{3-}$	4.0672	4.6064	5.0160	4.5632	0.4759	0.2751
LDH-A	(1) $^{3+}$	0.0957	0.0691	0.0308	0.0652	0.0326	0.0189
LDH-A	(2) $^{3+}$	0.0534	0.0638	0.0168	0.0446	0.0247	0.0143
LDH-A	(3) $^{3+}$	0.0344	0.0386	0.0188	0.0306	0.0104	0.0060
Glut-1	(1+2+3) $^{1+}$	0.4172	0.1273	1.0634	0.5360	0.4792	0.2770
Glut-1	(1+2) $^{2+}$	0.5847	0.7273	0.6754	0.6625	0.0722	0.0417
					MEAN		
		AnO_2	AnO_2	AnO_2	AnO_2	Sdev	SE
LDH-A	(1+2+3) $^{3+}$	0.6015	1.0407	1.0744	0.9055	0.2638	0.1525
LDH-A	(1+2) $^{3-}$	3.1646	4.6193	4.1510	3.9783	0.7426	0.4292
LDH-A	(1) $^{3+}$	0.0761	0.0657	0.0224	0.0547	0.0284	0.0164
LDH-A	(2) $^{3+}$	0.0431	0.0260	0.0191	0.0294	0.0123	0.0071
LDH-A	(3) $^{3+}$	0.0373	0.0238	0.0197	0.0269	0.0092	0.0053
Glut-1	(1+2+3) $^{1+}$	0.2901	0.0690	0.3983	0.2525	0.1678	0.0970
Glut-1	(1+2) $^{2+}$	0.7585	0.9398	0.5545	0.7509	0.1927	0.1114

Appendix 12

Expression of LDH $(1+2)^3$ in the forward and reverse orientation versus LDH $(1+2)^6$ in the reverse orientation in three human carcinoma cell lines, n=3.

MDA468				MEAN		
	AIR	AIR	AIR	AIR	Sdev	SE
LDH $(1+2)^{3-}$	0.0190	0.0245	0.0239	0.0225	0.0030	0.0017
LDH-A $(1+2)^{3+}$	0.0152	0.0442	0.0563	0.0386	0.0211	0.0122
LDH $(1+2)^{6-}$	0.0128	0.0408	0.0555	0.0363	0.0217	0.0125
				MEAN		
	$1\%O_2$	$1\%O_2$	$1\%O_2$	$1\%O_2$	Sdev	SE
LDH $(1+2)^{3-}$	1.6459	1.9978	1.4228	1.6888	0.2899	0.1675
LDH-A $(1+2)^{3+}$	0.2260	0.2168	0.4761	0.3063	0.1471	0.0850
LDH $(1+2)^{6-}$	1.1749	1.3517	1.6883	1.4050	0.2608	0.1508
				MEAN		
	AnO_2	AnO_2	AnO_2	AnO_2	Sdev	SE
LDH $(1+2)^{3-}$	1.1956	2.2447	1.7939	1.7447	0.5262	0.3042
LDH-A $(1+2)^{3+}$	0.2277	0.7155	0.7516	0.5649	0.2926	0.1692
LDH $(1+2)^{6-}$	1.3417	4.8142	2.5170	2.8910	1.7662	1.0209

HT1080				MEAN		
	AIR	AIR	AIR	AIR	Sdev	SE
LDH $(1+2)^{3-}$	0.0314	0.1583	0.1169	0.1022	0.0647	0.0374
LDH-A $(1+2)^{3+}$	0.0986	0.0606	0.0645	0.0746	0.0209	0.0121
LDH $(1+2)^{6-}$	0.1816	0.1971	0.1736	0.1841	0.0119	0.0069
				MEAN		
	$1\%O_2$	$1\%O_2$	$1\%O_2$	$1\%O_2$	Sdev	SE
LDH $(1+2)^{3-}$	0.6951	0.9044	0.8937	0.8311	0.1179	0.0682
LDH-A $(1+2)^{3+}$	0.7371	0.9547	1.0291	0.9070	0.1518	0.0877
LDH $(1+2)^{6-}$	1.1991	1.9106	1.6107	1.5734	0.3572	0.2065
				MEAN		
	AnO_2	AnO_2	AnO_2	AnO_2	Sdev	SE
LDH $(1+2)^{3-}$	1.3820	0.9897	1.1920	1.1879	0.1962	0.1134
LDH-A $(1+2)^{3+}$	1.1619	0.8200	0.8059	0.9293	0.2016	0.1165
LDH $(1+2)^{6-}$	1.6475	1.6026	1.3756	1.5419	0.1457	0.0842

SQD9				MEAN		
	AIR	AIR	AIR	AIR	Sdev	SE
LDH $(1+2)^{3-}$	0.6052	0.5538	1.0817	0.7469	0.2911	0.1682
LDH-A $(1+2)^{3+}$	0.3209	0.2235	0.2483	0.2642	0.0507	0.0293
LDH $(1+2)^{6-}$	1.0379	2.4921	1.0233	1.5178	0.8438	0.4878
				MEAN		
	$1\%O_2$	$1\%O_2$	$1\%O_2$	$1\%O_2$	Sdev	SE
LDH $(1+2)^{3-}$	4.6064	5.0160	4.0672	4.5632	0.4759	0.2751
LDH-A $(1+2)^{3+}$	2.4289	1.4506	2.1509	2.0101	0.5041	0.2914
LDH $(1+2)^{6-}$	2.0280	5.0640	4.9391	4.0104	1.7179	0.9930
				MEAN		
	AnO_2	AnO_2	AnO_2	AnO_2	Sdev	SE
LDH $(1+2)^{3-}$	4.6193	4.1510	3.1646	3.9783	0.7426	0.4292
LDH-A $(1+2)^{3+}$	2.4277	0.9765	2.0114	1.8052	0.7473	0.4320
LDH $(1+2)^{6-}$	2.9544	4.8846	5.3104	4.3831	1.2555	0.7257

Appendix 13

Expression of PGK $(1+2)^3$ in the forward orientation versus PGK $(1+2)^6$ in the positive orientation in three human carcinoma cell lines, n=3.

MDA 468

	AIR	AIR	AIR	MEAN AIR	Sdev	SE
PGK $(1+2)^{3fwd}$	0.0339	0.0522	0.0127	0.0329	0.0197	0.0114
PGK $(1+2)^{6+}$	0.0152	0.0108	0.0160	0.0140	0.0028	0.0016

	$1\%O_2$	$1\%O_2$	$1\%O_2$	MEAN $1\%O_2$	Sdev	SE
PGK $(1+2)^{3+}$	0.5911	0.7666	0.3220	0.5599	0.2240	0.1295
PGK $(1+2)^{6+}$	0.1292	0.0865	0.2705	0.1621	0.0963	0.0557

	AnO_2	AnO_2	AnO_2	MEAN AnO_2	Sdev	SE
PGK $(1+2)^{3+}$	1.2301	1.6793	0.4263	1.1119	0.6348	0.3669
PGK $(1+2)^{6+}$	0.4678	0.0892	0.2937	0.2836	0.1895	0.1095

HT1080

	AIR	AIR	AIR	MEAN AIR	Sdev	SE
PGK $(1+2)^{3+}$	0.0864	0.1392	0.1039	0.1098	0.0269	0.0155
PGK $(1+2)^{6+}$	0.0911	0.0337	0.0216	0.0488	0.0371	0.0215

	$1\%O_2$	$1\%O_2$	$1\%O_2$	MEAN $1\%O_2$	Sdev	SE
PGK $(1+2)^{3+}$	0.8819	1.2980	1.0609	1.0802	0.2088	0.1207
PGK $(1+2)^{6+}$	0.7200	0.2667	0.1644	0.3837	0.2957	0.1709

	AnO_2	AnO_2	AnO_2	MEAN AnO_2	SDEV	SE
PGK $(1+2)^{3+}$	1.3987	1.7111	1.6827	1.5975	0.1727	0.0998
PGK $(1+2)^{6+}$	0.9141	0.4596	0.6840	0.6859	0.2273	0.1314

SQD9

	AIR	AIR	AIR	MEAN AIR	Sdev	SE
PGK $(1+2)^{3+}$	0.2168	0.3671	0.1433	0.2424	0.1141	0.0660
PGK $(1+2)^{6+}$	0.1907	0.0864	0.0764	0.1179	0.0633	0.0366

	$1\%O_2$	$1\%O_2$	$1\%O_2$	MEAN $1\%O_2$	Sdev	SE
PGK $(1+2)^{3+}$	4.7031	1.8790	2.2137	2.9319	1.5430	0.8919
PGK $(1+2)^{6+}$	0.4221	0.6324	0.5304	0.5283	0.1052	0.0608

	AnO_2	AnO_2	AnO_2	MEAN AnO_2	Sdev	SE
PGK $(1+2)^{3+}$	1.7347	3.0201	1.3460	2.0336	0.8762	0.5065
PGK $(1+2)^{6+}$	0.4785	0.4733	0.4378	0.4632	0.0222	0.0128

Appendix 14

Expression of Epo $(1+2)^3$ in the forward orientation versus Epo $(1+2)^5$ in the positive orientation in three human carcinoma cell lines, n=3.

MDA 468				MEAN		
	AIR	AIR	AIR	AIR	Sdev	SE
Epo $(1+2)^{3+}$	0.0301	0.0456	0.0237	0.0332	0.0113	0.0065
Epo $(1+2)^{5+}$	0.0092	0.0436	0.0119	0.0216	0.0192	0.0111
				MEAN		
	$1\%O_2$	$1\%O_2$	$1\%O_2$	$1\%O_2$	Sdev	SE
Epo $(1+2)^{3+}$	0.0913	0.1043	0.0784	0.0913	0.0129	0.0075
Epo $(1+2)^{5+}$	0.1836	0.0869	0.6394	0.3033	0.2951	0.1706

HT1080				MEAN		
	AIR	AIR	AIR	AIR	Sdev	SE
Epo $(1+2)^{3+}$	0.0336	0.0663	0.0494	0.0498	0.0163	0.0095
Epo $(1+2)^{5+}$	0.0155	0.0483	0.0574	0.0404	0.0220	0.0127
				MEAN		
	$1\%O_2$	$1\%O_2$	$1\%O_2$	$1\%O_2$	Sdev	SE
Epo $(1+2)^{3+}$	0.1766	0.1641	0.1586	0.1664	0.0093	0.0054
Epo $(1+2)^{5+}$	0.5743	1.4335	0.4691	0.8256	0.5291	0.3058

SQD9				MEAN		
	AIR	AIR	AIR	AIR	Sdev	SE
Epo $(1+2)^{3+}$	0.3087	0.1580	0.0514	0.1727	0.1293	0.0748
Epo $(1+2)^{5+}$	0.0683	0.0510		0.0597	0.0122	0.0070
				MEAN		
	$1\%O_2$	$1\%O_2$	$1\%O_2$	$1\%O_2$	Sdev	SE
Epo $(1+2)^{3+}$	2.7667	1.3472	0.6276	1.5805	1.0885	0.6292
Epo $(1+2)^{5+}$	1.1230	1.5968		0.2354	0.0760	0.0440

Appendix 15

HRE expression transiently transfected into the C4.5 CHO cell line, exposed to 16 hours air, hypoxia or anoxia and 3 hours reoxygenation, n=3 (except @ 1%O_2 n=2)

				C4.5	Sdev	SE
Epo (1+2)/AIR	0.2819	0.3919	0.0995	0.2578	1.48E-01	8.54E-02
1% O_2		1.2272	0.4289	0.8280	5.64E-01	3.26E-01
AnO_2	0.5891	1.2674	0.4028	0.7531	4.55E-01	2.63E-01
PGK (1+2)/AIR	0.1387	0.1150	0.0667	0.1068	3.67E-02	2.12E-02
1% O_2		1.3254	1.3085	1.3170	1.19E-02	6.90E-03
AnO_2	1.2729	1.4926	1.2343	1.3332	1.39E-01	8.05E-02
LDH (1+2+3)/AIR	0.2103	0.1995	0.0955	0.1684	6.34E-02	3.67E-02
1% O_2		0.7449	0.7410	0.7430	2.72E-03	1.57E-03
AnO_2	0.8458	0.5625	0.6601	0.6895	1.44E-01	8.32E-02
LDH Site (1+2)/AIR	0.2164	0.1539	0.0765	0.1489	7.01E-02	4.05E-02
1% O_2		1.9401	2.6801	2.3101	5.23E-01	3.02E-01
AnO_2	1.8643	2.3089	2.4856	2.2196	3.20E-01	1.85E-01
G326 (1+2)/AIR	0.1501	0.1516	0.0561	0.1193	5.47E-02	3.16E-02
1% O_2		0.4928	0.2548	0.3738	1.68E-01	9.73E-02
AnO_2	0.5399	0.4415	0.2425	0.4079	1.51E-01	8.76E-02
G610 (1+2+3)/AIR	0.2338	0.2036	0.0726	0.1700	8.57E-02	4.95E-02
1% O_2		0.3951	0.2571	0.3261	9.76E-02	5.64E-02
AnO_2	0.4474	0.1683	0.1607	0.2588	1.63E-01	9.44E-02
VEGF (1+2)/AIR	0.4994	0.1944	0.0591	0.2510	2.26E-01	1.30E-01
1% O_2		0.2624	0.1818	0.2221	5.70E-02	3.29E-02
AnO_2	0.6600	0.5000	0.1097	0.4232	2.83E-01	1.64E-01

Appendix 16

HRE expression transiently transfected into the Ka13 CHO cell line plus 5μg HIF-1a, exposed to 16 hours air, hypoxia or anoxia and 3 hours reoxygenation, n=3.

				HIF-1α	Sdev	SE
Epo (1+2)/AIR	0.3540	0.1726	0.2121	0.2462	9.54E-02	5.51E-02
1% O_2	0.1974	0.4872	0.2896	0.3248	1.48E-01	8.56E-02
AnO_2	0.6745	0.4466	0.9651	0.6954	2.60E-01	1.50E-01
PGK (1+2)/AIR	0.4550	0.1930	0.1288	0.2589	1.73E-01	9.99E-02
1% O_2	0.2762	0.5126	0.3621	0.3836	1.20E-01	6.92E-02
AnO_2	1.0390	0.5048	0.4082	0.6507	3.40E-01	1.96E-01
LDH (1+2+3)/AIR	0.3790	0.1709	0.3032	0.2843	1.05E-01	6.09E-02
1% O_2	0.2008	0.5176	0.3753	0.3645	1.59E-01	9.17E-02
AnO_2	0.8824	0.3986	1.0988	0.7933	3.59E-01	2.07E-01
LDH Site (1+2)/AIR	0.6914	0.5136	0.8305	0.6785	1.59E-01	9.18E-02
1% O_2	0.7523	1.0657	1.2504	1.0228	2.52E-01	1.46E-01
AnO_2	1.8329	0.9867	2.6352	1.8183	8.24E-01	4.76E-01
G326 (1+2)/AIR	0.1478	0.1123	0.0397	0.0999	5.51E-02	3.18E-02
1% O_2	0.0876	0.2946	0.1006	0.1609	1.16E-01	6.70E-02
AnO_2	0.3271	0.2211	0.1171	0.2218	1.05E-01	6.07E-02
G610 (1+2+3)/AIR	0.2153	0.1009	0.0275	0.1145	9.46E-02	5.47E-02
1% O_2	0.0449	0.2099	0.0565	0.1038	9.21E-02	5.32E-02
AnO_2	0.3181	0.1132	0.0501	0.1605	1.40E-01	8.10E-02
VEGF (1+2)/AIR	0.1392	0.0694	0.2706	0.1597	1.02E-01	5.90E-02
1% O_2	0.0279	0.1041	0.0431	0.0584	4.04E-02	2.33E-02
AnO_2	0.4431	0.0748	0.4505	0.3228	2.15E-01	1.24E-01

Appendix 17

HRE expression transiently transfected into the Ka13 CHO cell line plus 5μg EPAS-1, exposed to 16 hours air, hypoxia or anoxia and 3 hours reoxygenation, n=3.

				EPAS-1	Sdev	SE
Epo (1+2)/AIR	0.0312	0.1316	0.1363	0.0997	5.94E-02	3.43E-02
1% O_2	0.1640	0.3110	0.2071	0.2274	7.56E-02	4.37E-02
AnO_2	0.0316	0.2497	0.3814	0.2209	1.77E-01	1.02E-01
PGK (1+2)/AIR	0.0384	0.1149	0.0491	0.0675	4.14E-02	2.39E-02
1% O_2	0.1101	0.2606	0.0810	0.1506	9.64E-02	5.57E-02
AnO_2	0.0335	0.2228	0.1839	0.1467	1.00E-01	5.78E-02
LDH (1+2+3)/AIR	0.0436	0.1337	0.0900	0.0891	4.51E-02	2.60E-02
1% O_2	0.1560	0.2399	0.1575	0.1845	4.80E-02	2.77E-02
AnO_2	0.0465	0.1600	0.2414	0.1493	9.79E-02	5.66E-02
LDH Site (1+2)/AIR	0.0289	0.1509	0.0569	0.0789	6.39E-02	3.69E-02
1% O_2	0.0908	0.1967	0.0751	0.1209	6.61E-02	3.82E-02
AnO_2	0.0215	0.2504	0.0803	0.1174	1.19E-01	6.87E-02
G326 (1+2)/AIR	0.0366	0.1198	0.0541	0.0702	4.39E-02	2.54E-02
1% O_2	0.1168	0.1879	0.0982	0.1343	4.74E-02	2.74E-02
AnO_2	0.0375	0.1955	0.0877	0.1069	8.07E-02	4.67E-02
G610 (1+2+3)/AIR	0.0492	0.1609	0.0891	0.0997	5.66E-02	3.27E-02
1% O_2	0.1309	0.2712	0.1109	0.1710	8.73E-02	5.05E-02
AnO_2	0.0492	0.1833	0.1559	0.1295	7.09E-02	4.10E-02
VEGF (1+2)/AIR	0.0250	0.0541	0.0927	0.0573	3.40E-02	1.96E-02
1% O_2	0.0974	0.2584	0.1716	0.1758	8.06E-02	4.66E-02
AnO_2	0.2924	0.1545	0.2834	0.2434	7.72E-02	4.46E-02

Appendix 18

Comparitive expression of HREs containing either their natural site 2 or that from LDH-A in the MDA 468 cell line, n=3.

				MEAN		
	AIR	AIR	AIR	AIR	Sdev	SE
LDH (1+2) $^{3-}$	0.0190	0.0245	0.0239	0.0225	0.0030	0.0017
Epo (1+2) $^{3+}$	0.0301	0.0456	0.0237	0.0332	0.0113	0.0065
[Epo 1 + LDH 2] $^{3+}$	0.0406	0.0342	0.0347	0.0365	0.0036	0.0021
PGK (1+2) $^{3+}$	0.0339	0.0522	0.0127	0.0329	0.0197	0.0114
[PGK 1 + LDH 2] $^{3+}$	0.0566	0.0753	0.0212	0.0510	0.0275	0.0159
VEGF (1+2) $^{3+}$	0.0210	0.0655	0.0128	0.0331	0.0283	0.0164
[VEGF 1 + LDH 2] $^{3+}$	0.0371	0.0576	0.0233	0.0393	0.0172	0.0100
				MEAN		
	$1\%O_2$	$1\%O_2$	$1\%O_2$	$1\%O_2$	Sdev	SE
LDH (1+2) $^{3-}$	1.6459	1.9978	1.4228	1.6888	0.2899	0.1675
Epo (1+2) $^{3+}$	0.0913	0.1043	0.0784	0.0913	0.0129	0.0075
[Epo 1 + LDH 2] $^{3+}$	0.3428	0.5269	0.2440	0.3712	0.1436	0.0830
PGK (1+2) $^{3+}$	0.5911	0.7666	0.3220	0.5599	0.2240	0.1295
[PGK 1 + LDH 2] $^{3+}$	0.2586	0.2683	0.0562	0.1943	0.1197	0.0692
VEGF (1+2) $^{3+}$	0.0265	0.0629	0.0219	0.0371	0.0225	0.0130
[VEGF 1 + LDH 2] $^{3+}$	0.1070	0.1445	0.0680	0.1065	0.0382	0.0221
				MEAN		
	AnO_2	AnO_2	AnO_2	AnO_2	Sdev	SE
LDH (1+2) $^{3-}$	1.1956	2.2447	1.7939	1.7447	0.5262	0.3042
Epo (1+2) $^{3+}$	0.1591	0.2826	0.1470	0.1962	0.0750	0.0434
[Epo 1 + LDH 2] $^{3+}$	0.3076	0.7276	0.4096	0.4816	0.2191	0.1266
PGK (1+2) $^{3+}$	1.2301	1.6793	0.4263	1.1119	0.6348	0.3669
[PGK 1 + LDH 2] $^{3+}$	0.7245	1.0298	0.1575	0.6373	0.4426	0.2559
VEGF (1+2) $^{3+}$	0.0536	0.0229	0.0274	0.0346	0.0166	0.0096
[VEGF 1 + LDH 2] $^{3+}$	0.1691	0.4294	0.0480	0.2155	0.1949	0.1126

Appendix 19

Comparitive expression of HREs containing either their natural site 2 or that from LDH-A in the HT1080 cell line, n=3.

	AIR	AIR	AIR	MEAN AIR	Sdev	SE
LDH (1+2) $^{3-}$	0.0583	0.1583	0.1169	0.1112	0.0503	0.0291
Epo (1+2) $^{3+}$	0.0336	0.0663	0.0494	0.0498	0.0163	0.0095
[Epo 1 + LDH 2] $^{3+}$	0.0216	0.0478	0.0410	0.0368	0.0136	0.0079
PGK (1+2) $^{3+}$	0.0864	0.1392	0.1039	0.1098	0.0269	0.0155
[PGK 1 + LDH 2] $^{3+}$	0.0117	0.0777	0.0501	0.0465	0.0332	0.0192
VEGF (1+2) $^{3+}$	0.0075	0.0070	0.0063	0.0069	0.0006	0.0003
[VEGF 1 + LDH 2] $^{3+}$	0.0127	0.0595	0.0415	0.0379	0.0236	0.0137

	$1\%O_2$	$1\%O_2$	$1\%O_2$	MEAN $1\%O_2$	Sdev	SE
LDH (1+2) $^{3-}$	0.5972	0.9044	0.8937	0.7985	0.1744	0.1008
Epo (1+2) $^{3+}$	0.1766	0.1641	0.1586	0.1664	0.0093	0.0054
[Epo 1 + LDH 2] $^{3+}$	0.3232	0.3280	0.3732	0.3415	0.0276	0.0159
PGK (1+2) $^{3+}$	0.8819	1.2980	1.0609	1.0802	0.2088	0.1207
[PGK 1 + LDH 2] $^{3+}$	0.4247	0.8360	0.8560	0.7055	0.2434	0.1407
VEGF (1+2) $^{3+}$	0.0197	0.0130	0.0120	0.0149	0.0042	0.0024
[VEGF 1 + LDH 2] $^{3+}$	0.2033	0.5799	0.5108	0.4313	0.2005	0.1159

	AnO_2	AnO_2	AnO_2	MEAN AnO_2	Sdev	SE
LDH (1+2) $^{3-}$	0.3955	0.9897	1.1920	0.8591	0.4140	0.2393
Epo (1+2) $^{3+}$	0.2170	0.4072	0.4641	0.3628	0.1294	0.0748
[Epo 1 + LDH 2] $^{3+}$	0.2325	0.4872	0.3414	0.3537	0.1278	0.0739
PGK (1+2) $^{3+}$	1.3987	1.7111	1.6827	1.5975	0.1727	0.0998
[PGK 1 + LDH 2] $^{3+}$	0.1925	1.2391	1.3396	0.9237	0.6353	0.3672
VEGF (1+2) $^{3+}$	0.0258	0.0154	0.0143	0.0185	0.0063	0.0037
[VEGF 1 + LDH 2] $^{3+}$	0.1150	0.9323	1.0414	0.6962	0.5063	0.2927

Appendix 20

Comparitive expression of HREs containing either their natural site 2 or that from LDH-A in the SQD9 cell line, n=3.

	AIR	AIR	AIR	MEAN AIR	Sdev	SE
LDH (1+2) $^{3-}$	1.0817	0.6052	0.5538	0.7469	0.2911	0.1682
Epo (1+2) $^{3+}$	0.3087	0.1580	0.0514	0.1727	0.1293	0.0748
[Epo 1 + LDH 2] $^{3+}$	0.5762	0.2166	0.2865	0.3598	0.1907	0.1102
PGK (1+2) $^{3+}$	0.2168	0.3671	0.1433	0.2424	0.1141	0.0660
[PGK 1 + LDH 2] $^{3+}$	0.1439	0.0755	0.1439	0.1211	0.0395	0.0228
VEGF (1+2) $^{3+}$	0.0291	0.0428	0.0164	0.0294	0.0132	0.0076
[VEGF 1 + LDH 2] $^{3+}$	0.1625	0.0845	0.67136	0.3061	0.3187	0.1842

	$1\%O_2$	$1\%O_2$	$1\%O_2$	MEAN $1\%O_2$	Sdev	SE
LDH (1+2) $^{3-}$	4.0672	4.6064	5.0160	4.5632	0.4759	0.2751
Epo (1+2) $^{3+}$	2.7667	1.3472	0.6276	1.5805	1.0885	0.6292
[Epo 1 + LDH 2] $^{3+}$	6.6345	4.0329	2.5943	4.4206	2.0478	1.1837
PGK (1+2) $^{3+}$	4.7031	2.8790	2.2137	3.2653	1.2889	0.7450
[PGK 1 + LDH 2] $^{3+}$	1.0888	1.8975	1.0888	1.3584	0.4669	0.2699
VEGF (1+2) $^{3+}$	0.0393	0.3297	0.0226	0.1305	0.1727	0.0998
[VEGF 1 + LDH 2] $^{3+}$	4.3661	2.0971	1.74536	2.7362	1.4225	0.8222

	AnO_2	AnO_2	AnO_2	MEAN AnO_2	Sdev	SE
LDH (1+2) $^{3-}$	3.1646	4.6193	4.1510	3.9783	0.7426	0.4292
Epo (1+2) $^{3+}$	1.7068	0.7834	0.5516	1.0140	0.6111	0.3533
[Epo 1 + LDH 2] $^{3+}$	3.5763	2.8437	1.7656	2.7285	0.9108	0.5265
PGK (1+2) $^{3+}$	1.7347	3.0201	1.3460	2.0336	0.8762	0.5065
[PGK 1 + LDH 2] $^{3+}$	1.6493	1.3785	1.6493	1.5590	0.1564	0.0904
VEGF (1+2) $^{3+}$	0.0209	0.4548	0.0208	0.1655	0.2506	0.1448
[VEGF 1 + LDH 2] $^{3+}$	1.9605	1.0911	0.93083	1.3275	0.5541	0.3203

Appendix 21

Comparitive expression of the LDH HREs containing either its natural site 2 or that from Epo in the 3 human carcinoma cell lines, n=3.

MDA 468				MEAN		
	AIR	AIR	AIR	AIR	Sdev	SE
LDH $(1+2)^{3-}$	0.0190	0.0245	0.0239	0.0225	0.0030	0.0017
$[LDH\ 1 + Epo\ 2]^{3+}$	0.0205	0.0107	0.0127	0.0146	0.0052	0.0030
				MEAN		
	$1\%O_2$	$1\%O_2$	$1\%O_2$	$1\%O_2$	Sdev	SE
LDH $(1+2)^{3-}$	1.6459	1.9978	1.4228	1.6888	0.2899	0.1675
$[LDH\ 1 + Epo\ 2]^{3+}$	0.0203	0.0206	0.0147	0.0186	0.0033	0.0019
				MEAN		
	AnO_2	AnO_2	AnO_2	AnO_2	Sdev	SE
LDH $(1+2)^{3-}$	1.1956	2.2447	1.7939	1.7447	0.5262	0.3042
$[LDH\ 1 + Epo\ 2]^{3+}$	0.0294	0.0460	0.0172	0.0309	0.0145	0.0084
HT1080				MEAN		
	AIR	AIR	AIR	AIR	Sdev	SE
LDH $(1+2)^{3-}$	0.0583	0.1583	0.1169	0.1112	0.0503	0.0291
$[LDH\ 1 + Epo\ 2]^{3+}$	0.0102	0.0073	0.0103	0.0093	0.0017	0.0010
				MEAN		
	$1\%O_2$	$1\%O_2$	$1\%O_2$	$1\%O_2$	Sdev	SE
LDH $(1+2)^{3-}$	0.5972	0.9044	0.8937	0.7985	0.1744	0.1008
$[LDH\ 1 + Epo\ 2]^{3+}$	0.0102	0.0114	0.0175	0.0130	0.0039	0.0023
				MEAN		
	AnO_2	AnO_2	AnO_2	AnO_2	Sdev	SE
LDH $(1+2)^{3-}$	0.3955	0.9897	1.1920	0.8591	0.4140	0.2393
$[LDH\ 1 + Epo\ 2]^{3+}$	0.0367	0.0830	0.0520	0.0572	0.0236	0.0136
SQD9				MEAN		
	AIR	AIR	AIR	AIR	Sdev	SE
LDH $(1+2)^{3-}$	1.0817	0.6052	0.5538	0.7469	0.2911	0.1682
$[LDH\ 1 + Epo\ 2]^{3+}$	0.0626	0.0346	0.0176	0.0382	0.0227	0.0131
				MEAN		
	$1\%O_2$	$1\%O_2$	$1\%O_2$	$1\%O_2$	Sdev	SE
LDH $(1+2)^{3-}$	4.0672	4.6064	5.0160	4.5632	0.4759	0.2751
$[LDH\ 1 + Epo\ 2]^{3+}$	0.3142	0.1545	0.0572	0.1753	0.1298	0.0750
				MEAN		
	AnO_2	AnO_2	AnO_2	AnO_2	Sdev	SE
LDH $(1+2)^{3-}$	3.1646	4.6193	4.1510	3.9783	0.7426	0.4292
$[LDH\ 1 + Epo\ 2]^{3+}$	0.1600	0.0982	0.0463	0.1015	0.0569	0.0329

Appendix 22

Expression of LDH (1+2), with site 2 modifications in the MDA468 cell line, n=2.

			MEAN	
	AIR	AIR	*AIR*	Sdev
LDH $(1+2)^{3-}$	0.0190	0.0245	*0.0218*	3.877E-03
LDH $(1+2'A')^{3-}$	0.0214	0.0146	*0.0180*	4.846E-03
LDH $(1+2\ Opt)^{3-}$	0.0325	0.0546	*0.0435*	1.566E-02
LDH $(1+2\ Dest)^{3-}$	0.0250	0.0254	*0.0252*	2.817E-04
LDH $(1+E\text{-}Box)^{3-}$	0.0565	0.0511	*0.0538*	3.790E-03
			MEAN	
	$1\%O_2$	$1\%O_2$	*$1\%O_2$*	Sdev
LDH $(1+2)^{3-}$	1.6459	1.9978	*1.8218*	2.488E-01
LDH $(1+2'A')^{3-}$	0.2555	0.1583	*0.2069*	6.871E-02
LDH $(1+2\ Opt)^{3-}$	1.1499	0.9595	*1.0547*	1.347E-01
LDH $(1+2\ Dest)^{3-}$	0.2377	0.1778	*0.2078*	4.237E-02
LDH $(1+E\text{-}Box)^{3-}$	0.5634	0.3682	*0.4658*	1.380E-01
			MEAN	
	AnO_2	AnO_2	*AnO_2*	Sdev
LDH $(1+2)^{3-}$	1.1956	2.2447	*1.7201*	7.418E-01
LDH $(1+2'A')^{3-}$	0.6745	0.2289	*0.4517*	3.151E-01
LDH $(1+2\ Opt)^{3-}$	2.0346	1.3033	*1.6689*	5.170E-01
LDH $(1+2\ Dest)^{3-}$	0.5858	0.1954	*0.3906*	2.761E-01
LDH $(1+E\text{-}Box)^{3-}$	0.9112	0.2678	*0.5895*	4.549E-01

Appendix 23

Expression of LDH (1+2), with site 2 modifications in the SQD9 cell line, n=2.

	AIR	AIR	*MEAN AIR*	Sdev
LDH $(1+2)^{3-}$	1.0817	0.6052	*0.8435*	3.369E-01
LDH $(1+2'A')^{3-}$	0.2470	0.2953	*0.2711*	3.413E-02
LDH $(1+2\ Opt)^{3-}$	0.5100	0.3092	*0.4096*	1.420E-01
LDH $(1+2\ Dest)^{3-}$	0.2117	0.2094	*0.2105*	1.666E-03
LDH $(1+E\text{-}Box)^{3-}$	0.3863	0.3079	*0.3471*	5.541E-02

	$1\%O_2$	$1\%O_2$	*MEAN* $1\%O_2$	Sdev
LDH $(1+2)^{3-}$	4.0672	4.6064	*4.3368*	3.813E-01
LDH $(1+2'A')^{3-}$	1.5473	2.1182	*1.8327*	4.037E-01
LDH $(1+2\ Opt)^{3-}$	1.4691	1.8717	*1.6704*	2.847E-01
LDH $(1+2\ Dest)^{3-}$	0.6129	1.4797	*1.0463*	6.129E-01
LDH $(1+E\text{-}Box)^{3-}$	1.3080	2.2615	*1.7847*	6.742E-01

	AnO_2	AnO_2	*MEAN* AnO_2	Sdev
LDH $(1+2)^{3-}$	3.1646	4.6193	*3.8919*	1.029E+00
LDH $(1+2'A')^{3-}$	1.0063	1.1100	*1.0582*	7.330E-02
LDH $(1+2\ Opt)^{3-}$	1.7519	1.0970	*1.4244*	4.630E-01
LDH $(1+2\ Dest)^{3-}$	0.7927	0.6794	*0.7360*	8.012E-02
LDH $(1+E\text{-}Box)^{3-}$	1.0623	2.0823	*1.5723*	7.213E-01

Appendix 24

Expression of HREs exposed to 16 hours air, hypoxia or anoxia and 3 hours reoxygenation in the A549 lung carcinoma cell line, n=3.

				MEAN		
	AIR	AIR	AIR	AIR	Sdev	SE
PGK $(1)^{3+}$	0.0473	0.0485	0.0655	0.0538	1.02E-02	5.87E-03
PGK $(1)^{3-}$	0.0225	0.0130	0.0173	0.0176	4.76E-03	2.75E-03
PGK $(1+2)^{3+}$	0.0738	0.0302	0.0167	0.0402	2.98E-02	1.72E-02
LDH $(1+2)^{3-}$	0.0603	0.0582	0.0547	0.0577	2.83E-03	1.63E-03
LDH $(1+2)^{3+}$	0.0557	0.0474	0.0354	0.0462	1.02E-02	5.89E-03
LDH $(1+2)^{6-}$	0.0357	0.0661	0.0540	0.0520	1.53E-02	8.85E-03
				MEAN		
	$1\%O_2$	$1\%O_2$	$1\%O_2$	$1\%O_2$	Sdev	SE
PGK $(1)^{3+}$	1.1857	0.9062	1.8573	1.3164	4.89E-01	2.83E-01
PGK $(1)^{3-}$	0.5047	0.2297	0.5452	0.4265	1.72E-01	9.92E-02
PGK $(1+2)^{3+}$	1.0226	0.8009	0.8517	0.8917	1.16E-01	6.71E-02
LDH $(1+2)^{3-}$	1.2390	2.7851	1.6792	1.9011	7.97E-01	4.60E-01
LDH $(1+2)^{3+}$	1.1885	0.8404	1.1130	1.0473	1.83E-01	1.06E-01
LDH $(1+2)^{6}$	1.6115	0.9812	1.7286	1.4405	4.02E-01	2.32E-01
				MEAN		
	AnO_2	AnO_2	AnO_2	AnO_2	Sdev	SE
PGK $(1)^{3+}$	0.9023	0.8182	1.0725	0.9310	1.30E-01	7.49E-02
PGK $(1)^{3-}$	0.8581	0.3150	0.3440	0.5057	3.05E-01	1.77E-01
PGK $(1+2)^{3+}$	1.2464	1.0176	0.9181	1.0607	1.68E-01	9.73E-02
LDH $(1+2)^{3-}$	1.2753	1.0749	3.6977	2.0160	1.46E+00	8.44E-01
LDH $(1+2)^{3+}$	0.9135	0.5846	0.3965	0.6315	2.62E-01	1.51E-01
LDH $(1+2)^{6-}$	0.7566	0.8857	0.5352	0.7258	1.77E-01	1.02E-01

Appendix 25

Expression of HREs exposed to 16 hours air, hypoxia or anoxia and 3 hours reoxygenation in the HCT116 lung carcinoma cell line, n=2.

	Epo $(1+2)^{5+}$	PGK $(1+2)^{3+}$	LDH $(1+2+3)^{3+}$	LDH $(1+2)^{3-}$
AIR	0.0678	0.0384	0.0620	0.1572
$1\%O_2$	0.4314	0.4266	0.0947	0.7715
AnO_2	1.1521	0.5047	0.4116	2.6976

Appendix 26

Expression of HREs exposed to 16 hours air, hypoxia or anoxia and 3 hours reoxygenation in the T47D breast carcinoma cell line, n=3.

				MEAN		
	AIR	AIR	AIR	AIR	SDEV	SE
PGK $(1)^{3+}$	0.0490	0.2032	0.1046	0.1189	0.0781	0.0451
PGK $(1)^{3-}$	0.0367	0.0501	0.0600	0.0489	0.0117	0.0068
PGK $(1+2)^{3+}$	0.2197	0.1681	0.0481	0.1453	0.0881	0.0509
LDH $(1+2)^{3-}$	0.0949	0.0446	0.0197	0.0531	0.0383	0.0221
LDH-A $(1+2)^{3+}$	0.1009	0.0326	0.0149	0.0495	0.0454	0.0263
LDH $(1+2)^{6-}$	0.0333	0.0392	0.0223	0.0316	0.0086	0.0049
				MEAN		
	1% O_2	1% O_2	1% O_2	1% O_2	SDEV	SE
PGK $(1)^{3+}$	6.1095	10.9309	5.6738	7.5714	2.9176	1.6865
PGK $(1)^{3-}$	1.1633	0.9630	2.0672	1.3978	0.5883	0.3401
PGK $(1+2)^{3+}$	4.3233	4.6637	3.0591	4.0154	0.8455	0.4887
LDH $(1+2)^{3-}$	7.9604	6.5871	6.0558	6.8677	0.9828	0.5681
LDH-A $(1+2)^{3+}$	2.7323	3.1546	1.5881	2.4917	0.8105	0.4685
LDH $(1+2)^{6-}$	2.7006	2.6049	3.6285	2.9780	0.5654	0.3268
				MEAN		
	AnO_2	AnO_2	AnO_2	AnO_2	SDEV	SE
PGK $(1)^{3+}$	11.2185	5.3939	8.5280	8.3801	2.9151	1.6850
PGK $(1)^{3-}$	2.8164	4.5616	4.5575	3.9785	1.0064	0.5817
PGK $(1+2)^{3+}$	8.3183	10.6633	8.5356	9.1724	1.2957	0.7490
LDH $(1+2)^{3-}$	9.7893	8.2928	9.3087	9.1303	0.7640	0.4416
LDH-A $(1+2)^{3+}$	5.2870	3.5641	2.6612	3.8374	1.3341	0.7712
LDH $(1+2)^{6-}$	3.4208	5.6884	5.9270	5.0121	1.3832	0.7996

Appendix 27

Expression of HREs exposed to 16 hours air, hypoxia or anoxia and 3 hours reoxygenation in the WiDr colon carcinoma cell line, n=3.

				MEAN		
	AIR	AIR	AIR	AIR	Sdev	SE
PGK $(1)^{3+}$	0.1428	0.1982	0.0988	0.1466	4.98E-02	2.88E-02
PGK $(1)^{3-}$	0.1326	0.1027	0.0869	0.1074	2.32E-02	1.34E-02
PGK $(1+2)^{3+}$	0.0708	0.0869	0.0860	0.0812	9.06E-03	5.24E-03
LDH $(1+2)^{3-}$	0.1520	0.0921	0.0860	0.1100	3.65E-02	2.11E-02
LDH $(1+2)^{3+}$	0.1046	0.0489	0.0574	0.0703	3.00E-02	1.73E-02
LDH $(1+2)^{6-}$	0.0837	0.1042	0.0807	0.0895	1.28E-02	7.39E-03
				MEAN		
	$1\%O_2$	$1\%O_2$	$1\%O_2$	$1\%O_2$	Sdev	SE
PGK $(1)^{3+}$	1.9825	2.3981	4.7199	3.0335	1.48E+00	8.53E-01
PGK $(1)^{3-}$	5.8576	4.6303	4.6544	5.0474	7.02E-01	4.06E-01
PGK $(1+2)^{3+}$	1.1014	4.6544	4.7065	3.4874	2.07E+00	1.19E+00
LDH $(1+2)^{3-}$	6.5913	4.5976	4.7065	5.2985	1.12E+00	6.48E-01
LDH $(1+2)^{3+}$	2.4594	1.9264	1.9397	2.1085	3.04E-01	1.76E-01
LDH $(1+2)^{6-}$	0.8892	2.7203	3.4545	2.3547	1.32E+00	7.64E-01
				MEAN		
	AnO_2	AnO_2	AnO_2	AnO_2	Sdev	SE
PGK $(1)^{3+}$	4.7265	3.8493	5.6102	4.7287	8.80E-01	5.09E-01
PGK $(1)^{3-}$	4.3877	3.5568	2.1931	3.3792	1.11E+00	6.40E-01
PGK $(1+2)^{3+}$	2.2891	2.1931	1.7888	2.0903	2.66E-01	1.53E-01
LDH $(1+2)^{3-}$	5.1581	4.3640	4.2861	4.6027	4.83E-01	2.79E-01
LDH $(1+2)^{3+}$	2.6489	3.0543	2.7462	2.8165	2.12E-01	1.22E-01
LDH $(1+2)^{6-}$	2.4902	3.8353	1.6067	2.6440	1.12E+00	6.49E-01

Appendix 28

Effect of 8-cl-cAMP on the expression of a variety on PGL3 HRE vectors in the MDA468 cell line, n=3.

0uMol

	AIR	AIR	AIR	*MEAN AIR*	Sdev	SE
PGK (1) $^{3+}$	0.0098	0.0099	0.0085	*0.0094*	0.0007	0.0004
PGK (1) $^{3-}$	0.0041	0.0025	0.0029	*0.0032*	0.0008	0.0005
LDH (1+2+3) $^{3+}$	0.0274	0.0128	0.0105	*0.0169*	0.0092	0.0053
Glut (1+2) $^{2+}$	0.0627	0.0268	0.0166	*0.0354*	0.0242	0.0140
Glut (1+2+3) $^{1+}$	0.0503	0.0194	0.0229	*0.0309*	0.0169	0.0098

	AnO_2	AnO_2	AnO_2	*MEAN AnO 2*	Sdev	SE
PGK (1) $^{3+}$	1.0135	0.5988	0.4791	*0.6971*	0.2804	0.1621
PGK (1) $^{3-}$	0.0747	0.1020	0.0529	*0.0766*	0.0246	0.0142
LDH (1+2+3) $^{3+}$	0.2787	0.0858	0.0452	*0.1366*	0.1248	0.0721
Glut (1+2) $^{2+}$	0.3754	0.1512	0.0556	*0.1941*	0.1642	0.0949
Glut (1+2+3) $^{1+}$	0.1545	0.0714	0.0341	*0.0866*	0.0617	0.0356

0.3uM

	AIR	AIR	AIR	*MEAN AIR*	Sdev	SE
PGK (1) $^{3+}$	0.0128	0.0164	0.0107	*0.0133*	0.0029	0.0017
PGK (1) $^{3-}$	0.0023	0.0023	0.0030	*0.0025*	0.0004	0.0002
LDH (1+2+3) $^{3+}$	0.0115	0.0217	0.0233	*0.0188*	0.0064	0.0037
Glut (1+2) $^{2+}$	0.0238	0.0345	0.0226	*0.0270*	0.0065	0.0038
Glut (1+2+3) $^{1+}$	0.0213	0.0354	0.0234	*0.0267*	0.0076	0.0044

	AnO_2	AnO_2	AnO_2	*MEAN AnO 2*	Sdev	SE
PGK (1) $^{3+}$	1.5523	0.6731	0.5256	*0.9170*	0.5551	0.3209
PGK (1) $^{3-}$	0.1877	0.1207	0.0757	*0.1280*	0.0564	0.0326
LDH (1+2+3) $^{3+}$	0.1888	0.1450	0.1209	*0.1516*	0.0344	0.0199
Glut (1+2) $^{2+}$	0.1679	0.2205	0.1075	*0.1653*	0.0565	0.0327
Glut (1+2+3) $^{1+}$	0.0769	0.0993	0.0569	*0.0777*	0.0212	0.0123

1uM

	AIR	AIR	AIR	*MEAN AIR*	Sdev	SE
PGK (1) $^{3+}$	0.0138	0.0140	0.0088	*0.0122*	0.0030	0.0017
PGK (1) $^{3-}$	0.0021	0.0033	0.0025	*0.0026*	0.0006	0.0003
LDH (1+2+3) $^{3+}$	0.0240	0.0223	0.0229	*0.0231*	0.0009	0.0005
Glut (1+2) $^{2+}$	0.0251	0.0534	0.0294	*0.0360*	0.0153	0.0088
Glut (1+2+3) $^{1+}$	0.0196	0.0285	0.0192	*0.0224*	0.0053	0.0030

	AnO_2	AnO_2	AnO_2	*MEAN AnO 2*	Sdev	SE
PGK (1) $^{3+}$	1.1896	0.7265	0.3499	*0.5382*	0.2663	0.1539
PGK (1) $^{3-}$	0.0947	0.1983	0.0679	*0.1331*	0.0922	0.0533
LDH (1+2+3) $^{3+}$	0.1305	0.1504	0.1132	*0.1318*	0.0263	0.0152
Glut (1+2) $^{2+}$	0.1614	0.3901	0.1235	*0.2568*	0.1885	0.1090
Glut (1+2+3) $^{1+}$	0.0726	0.1515	0.0626	*0.1071*	0.0629	0.0363

3uM

	AIR	AIR	AIR	*MEAN AIR*	Sdev	SE
PGK (1) $^{3+}$	0.0138	0.0126	0.0099	*0.0121*	0.0020	0.0012
PGK (1) $^{3-}$	0.0032	0.0036	0.0030	*0.0033*	0.0003	0.0002
LDH (1+2+3) $^{3+}$	0.0152	0.0204	0.0167	*0.0174*	0.0027	0.0016
Glut (1+2) $^{2+}$	0.0240	0.0431	0.0216	*0.0296*	0.0118	0.0068
Glut (1+2+3) $^{1+}$	0.0216	0.0453	0.0256	*0.0309*	0.0127	0.0073

	AnO_2	AnO_2	AnO_2	*MEAN AnO_2*	Sdev	SE
PGK (1) $^{3+}$	1.2201	0.7052	0.3233	*0.7495*	0.4501	0.2601
PGK (1) $^{3-}$	0.1622	0.1510	0.0512	*0.1214*	0.0611	0.0353
LDH (1+2+3) $^{3+}$	0.1209	0.0940	0.1049	*0.1066*	0.0135	0.0078
Glut (1+2) $^{2+}$	0.1828	0.1842	0.1054	*0.1575*	0.0451	0.0261
Glut (1+2+3) $^{1+}$	0.0686	0.0981	0.0442	*0.0703*	0.0270	0.0156

10uM

	AIR	AIR	AIR	*MEAN AIR*	Sdev	SE
PGK (1) $^{3+}$	0.0163	0.0167	0.0131	*0.0154*	0.0019	0.0011
PGK (1) $^{3-}$	0.0034	0.0036	0.0036	*0.0035*	0.0001	0.0000
LDH (1+2+3) $^{3+}$	0.0169	0.0247	0.0206	*0.0207*	0.0039	0.0023
Glut (1+2) $^{2+}$	0.0359	0.0538	0.0283	*0.0394*	0.0131	0.0076
Glut (1+2+3) $^{1+}$	0.0282	0.0304	0.0223	*0.0270*	0.0042	0.0024

	AnO_2	AnO_2	AnO_2	*MEAN AnO_2*	Sdev	SE
PGK (1) $^{3+}$	1.6818	0.7419	0.4594	*0.9610*	0.6400	0.3699
PGK (1) $^{3-}$	0.1736	0.1429	0.0625	*0.1263*	0.0574	0.0332
LDH (1+2+3) $^{3+}$	0.1406	0.1873	0.1617	*0.1632*	0.0234	0.0135
Glut (1+2) $^{2+}$	0.2111	0.3395	0.1046	*0.2184*	0.1176	0.0680
Glut (1+2+3) $^{1+}$	0.0907	0.1465	0.0717	*0.1030*	0.0389	0.0225

30uM

	AIR	AIR	AIR	*MEAN AIR*	Sdev	SE
PGK (1) $^{3+}$	0.0252	0.0135	0.0145	*0.0178*	0.0065	0.0038
PGK (1) $^{3-}$	0.0042	0.0061	0.0036	*0.0047*	0.0013	0.0007
LDH (1+2+3) $^{3+}$	0.0251	0.0248	0.0205	*0.0235*	0.0026	0.0015
Glut (1+2) $^{2+}$	0.0493	0.0456	0.0363	*0.0437*	0.0067	0.0039
Glut (1+2+3) $^{1+}$	0.0358	0.0382	0.0302	*0.0347*	0.0041	0.0024

	AnO_2	AnO_2	AnO_2	*MEAN AnO_2*	Sdev	SE
PGK (1) $^{3+}$	2.4832	0.5662	0.6736	*1.2410*	1.0771	0.6226
PGK (1) $^{3-}$	0.1347	0.1702	0.1261	*0.1437*	0.0234	0.0135
LDH (1+2+3) $^{3+}$	0.2076	0.1795	0.1450	*0.1774*	0.0314	0.0181
Glut (1+2) $^{2+}$	0.2953	0.2436	0.1089	*0.2159*	0.0963	0.0556
Glut (1+2+3) $^{1+}$	0.1154	0.1613	0.0641	*0.1136*	0.0486	0.0281

100uM

	AIR	AIR	AIR	*MEAN AIR*	Sdev	SE
PGK (1) $^{3+}$	0.0467	0.0264	0.0174	*0.0302*	0.0150	0.0086
PGK (1) $^{3-}$	0.0070	0.0068	0.0049	*0.0062*	0.0011	0.0007
LDH (1+2+3) $^{3+}$	0.0440		0.0366	*0.0403*	0.0052	0.0037
Glut (1+2) $^{2+}$	0.0826	0.0730	0.0510	*0.0689*	0.0162	0.0094
Glut (1+2+3) $^{1+}$	0.0605	0.0511	0.0553	*0.0556*	0.0047	0.0027

	AnO_2	AnO_2	AnO_2	*MEAN AnO_2*	Sdev	SE
PGK (1) $^{3+}$	2.8892	1.0485	0.6455	*1.5277*	1.1961	0.6914
PGK (1) $^{3-}$	0.1598	0.1576	0.1275	*0.1483*	0.0181	0.0104
LDH (1+2+3) $^{3+}$	0.4111	0.2190	0.1540	*0.2614*	0.1337	0.0773
Glut (1+2) $^{2+}$	0.3101	0.3175	0.1357	*0.2545*	0.1029	0.0595
Glut (1+2+3) $^{1+}$	0.1314	0.1354	0.0946	*0.1205*	0.0225	0.0130

Appendix 29

Effect of 8-cl-cAMP on the expression of a variety on PGL3 HRE vectors in the HT1080 cell line, n=3.

0uMol

				MEAN		
	AIR	AIR	AIR	*AIR*	Sdev	SE
PGK (1) $^{3+}$	0.0510	0.1130	0.1191	*0.0944*	0.0377	0.0218
PGK (1) $^{3-}$	0.1310	0.1457		*0.1383*	0.0104	0.0074
LDH (1+2+3) $^{3+}$	0.0250	0.0343	0.0310	*0.0301*	0.0047	0.0027
Glut (1+2) $^{2+}$	0.2590	0.2014	0.0983	*0.1862*	0.0814	0.0471
Glut (1+2+3) $^{1+}$	0.1133	0.3153	0.0570	*0.1619*	0.1358	0.0785
				MEAN		
	AnO_2	AnO_2	AnO_2	*AnO_2*	Sdev	SE
PGK (1) $^{3+}$	1.1080	1.0089	1.6168	*1.2446*	0.3261	0.1885
PGK (1) $^{3-}$	1.4710	1.1346		*1.3028*	0.2379	0.1687
LDH (1+2+3) $^{3+}$	0.3150	0.2250	0.2808	*0.2736*	0.0454	0.0263
Glut (1+2) $^{2+}$	0.8030	0.6286	0.6108	*0.6808*	0.1062	0.0614
Glut (1+2+3) $^{1+}$	0.5324	0.2819	0.3438	*0.3860*	0.1305	0.0754

0.3uMol

				MEAN		
	AIR	AIR	AIR	*AIR*	Sdev	SE
PGK (1) $^{3+}$	0.0760	0.0510	0.1196	*0.0822*	0.0347	0.0201
PGK (1) $^{3-}$	0.1100	0.1000		*0.1050*	0.0071	0.0050
LDH (1+2+3) $^{3+}$	0.0215	0.0247	0.0288	*0.0250*	0.0037	0.0021
Glut (1+2) $^{2+}$	0.1939	0.2381	0.0897	*0.1739*	0.0762	0.0440
Glut (1+2+3) $^{1+}$	0.1517	0.1379	0.0541	*0.1146*	0.0528	
				MEAN		
	AnO_2	AnO_2	AnO_2	*AnO_2*	Sdev	SE
PGK (1) $^{3+}$	0.6874	0.8690	1.3261	*0.9608*	0.3291	0.1902
PGK (1) $^{3-}$	0.7920	0.9270		*0.8595*	0.0955	0.0677
LDH (1+2+3) $^{3+}$	0.2069	0.3612	0.2655	*0.2779*	0.0779	0.0450
Glut (1+2) $^{2+}$	0.7370	1.0630	0.6327	*0.8109*	0.2244	0.1297
Glut (1+2+3) $^{1+}$	0.4386	0.5110	0.3642	*0.4379*	0.0734	0.0424

1uMol

				MEAN		
	AIR	AIR	AIR	*AIR*	Sdev	SE
PGK (1) $^{3+}$	0.0547	0.0740	0.1126	*0.0804*	0.0295	0.0171
PGK (1) $^{3-}$	0.1120	0.0909		*0.1015*	0.0149	0.0106
LDH (1+2+3) $^{3+}$	0.0249	0.0321	0.0283	*0.0285*	0.0036	0.0021
Glut (1+2) $^{2+}$	0.2308	0.1936	0.0999	*0.1748*	0.0675	0.0390
Glut (1+2+3) $^{1+}$	0.2007	0.1203	0.0755	*0.1322*	0.0635	0.0367
				MEAN		
	AnO_2	AnO_2	AnO_2	*AnO_2*	Sdev	SE
PGK (1) $^{3+}$	0.9037	0.6916	1.1703	*0.9218*	0.2399	0.1386
PGK (1) $^{3-}$	0.7697	0.9070		*0.8384*	0.0971	0.0689
LDH (1+2+3) $^{3+}$	0.3209	0.2034	0.2602	*0.2615*	0.0587	0.0340
Glut (1+2) $^{2+}$	0.8665	0.6457	0.4545	*0.6556*	0.2062	0.1192
Glut (1+2+3) $^{1+}$	0.3356	0.3724	0.3843	*0.3641*	0.0254	0.0147

3uMol

	AIR	AIR	AIR	*MEAN AIR*	Sdev	SE
PGK (1) $^{3+}$	0.1117	0.0812		*0.0965*	0.0215	0.0153
PGK (1) $^{3-}$		0.1026		*0.1026*		0.0000
LDH (1+2+3) $^{3+}$	0.0275	0.0221		*0.0248*	0.0038	0.0027
Glut (1+2) $^{2+}$	0.0890	0.1964		*0.1427*	0.0760	0.0539
Glut (1+2+3) $^{1+}$	0.1831	0.0992	0.0745	*0.1189*	0.0569	0.0329

	AnO_2	AnO_2	AnO_2	*MEAN AnO_2*	Sdev	SE
PGK (1) $^{3+}$	1.2391	0.7877		*1.0134*	0.3192	0.2264
PGK (1) $^{3-}$		0.9064		*0.9064*		0.0000
LDH (1+2+3) $^{3+}$	0.2466	0.1964		*0.2215*	0.0355	0.0252
Glut (1+2) $^{2+}$	0.4145	0.6612		*0.5378*	0.1744	0.1237
Glut (1+2+3) $^{1+}$	0.4584	0.4009	0.5076	*0.4556*	0.0534	0.0309

10uMol

	AIR	AIR	AIR	*MEAN AIR*	Sdev	SE
PGK (1) $^{3+}$	0.0646	0.0876	0.0859	*0.0794*	0.0128	0.0074
PGK (1) $^{3-}$	0.1289	0.1266		*0.1277*	0.0017	0.0012
LDH (1+2+3) $^{3+}$	0.0261	0.0248	0.0221	*0.0243*	0.0021	0.0012
Glut (1+2) $^{2+}$	0.2402	0.1883	0.0689	*0.1658*	0.0878	0.0508
Glut (1+2+3) $^{1+}$	0.1112	0.1185	0.0886	*0.1061*	0.0156	0.0090

	AnO_2	AnO_2	AnO_2	*MEAN AnO_2*	Sdev	SE
PGK (1) $^{3+}$	0.8948	0.8254	0.8471	*0.8558*	0.0355	0.0205
PGK (1) $^{3-}$	0.7786	1.0371		*0.9078*	0.1828	0.1296
LDH (1+2+3) $^{3+}$	0.3148	0.2727	0.2351	*0.2742*	0.0399	0.0230
Glut (1+2) $^{2+}$	0.8999	0.6582	0.5006	*0.6862*	0.2011	0.1163
Glut (1+2+3) $^{1+}$	0.3470	0.3501	0.4715	*0.3895*	0.0710	0.0410

30uMol

	AIR	AIR	AIR	*MEAN AIR*	Sdev	SE
PGK (1) $^{3+}$	0.1513	0.0840	0.0607	*0.0987*	0.0471	0.0272
PGK (1) $^{3-}$		0.1248	0.1194	*0.1221*	0.0038	0.0027
LDH (1+2+3) $^{3+}$	0.0436	0.0242	0.0277	*0.0318*	0.0103	0.0060
Glut (1+2) $^{2+}$	0.1334	0.1828	0.2490	*0.1884*	0.0580	0.0335
Glut (1+2+3) $^{1+}$	0.2182	0.0813	0.0838	*0.1277*	0.0783	0.0453

	AnO_2	AnO_2	AnO_2	*MEAN AnO_2*	Sdev	SE
PGK (1) $^{3+}$	1.6173	0.7193	1.1062	*1.1476*	0.4504	0.2604
PGK (1) $^{3-}$		0.9913	1.7520	*1.3716*	0.5379	0.3815
LDH (1+2+3) $^{3+}$	0.4520	0.2540	0.3201	*0.3421*	0.1008	0.0583
Glut (1+2) $^{2+}$	0.8440	0.7521	0.9226	*0.8396*	0.0854	0.0493
Glut (1+2+3) $^{1+}$	0.6076	0.2727	0.5329	*0.4711*	0.1758	0.1016

100uMol

	AIR	AIR	AIR	*MEAN AIR*	Sdev	SE
PGK (1) $^{3+}$	0.0602	0.0643	0.1497	*0.0914*	0.0505	0.0292
PGK (1) $^{3-}$	0.1787	0.0938		*0.1362*	0.0601	0.0426
LDH (1+2+3) $^{3+}$	0.0369	0.0216	0.0549	*0.0378*	0.0167	0.0096
Glut (1+2) $^{2+}$	0.2788	0.1391	0.1250	*0.1809*	0.0850	0.0491
Glut (1+2+3) $^{1+}$	0.1688	0.1082	0.0725	*0.1165*	0.0487	0.0281

	AnO_2	AnO_2	AnO_2	*MEAN AnO_2*	Sdev	SE
PGK (1) $^{3+}$	1.4425	0.7966	1.4583	*1.2325*	0.3776	0.2182
PGK (1) $^{3-}$	2.1914	0.8589		*1.5252*	0.9422	0.6682
LDH (1+2+3) $^{3+}$	0.4570	0.2781	0.3792	*0.3714*	0.0897	0.0518
Glut (1+2) $^{2+}$	1.0160	0.7702	0.6443	*0.8102*	0.1890	0.1093
Glut (1+2+3) $^{1+}$	0.5664	0.5273	0.4309	*0.5082*	0.0697	0.0403

Appendix 30

HRE activity after 8 hours +/- a PKA analog followed by 16 hours air or anoxia and 3 hours reoxygenation in the MDA 468 cell line, n=3.

Control

				MEAN		
	AIR	AIR	AIR	*AIR*	Sdev	SE
Epo (1+2) $^{3+}$	0.0249	0.0796	0.0456	*0.0500*	0.0276	0.0160
PGK (1+2) $^{3+}$	0.0339	0.0158	0.0181	*0.0226*	0.0099	0.0057
LDH-A (1+2+3) $^{3+}$	0.0178	0.0393	0.0495	*0.0355*	0.0162	0.0093
LDH (1+2) $^{3-}$	0.0146	0.0198	0.0239	*0.0194*	0.0047	0.0027
VEGF (1+2) $^{3+}$	0.0210	0.0655	0.0128	*0.0331*	0.0283	0.0164
Glut-1 (1+2) $^{2+}$	0.0627	0.0268	0.0166	*0.0354*	0.0242	0.0140
Glut-1 (1+2+3) $^{1+}$	0.0503	0.0194	0.0229	*0.0309*	0.0169	0.0098
				MEAN		
	AnO_2	AnO_2	AnO_2	*AnO_2*	Sdev	SE
Epo (1+2) $^{3+}$	0.1104	0.5248	0.2826	*0.3059*	0.2082	0.1203
PGK (1+2) $^{3+}$	1.2301	0.9287	0.9722	*1.0437*	0.1629	0.0942
LDH-A (1+2+3) $^{3+}$	0.0598	0.1476	0.2478	*0.1517*	0.0941	0.0544
LDH (1+2) $^{3-}$	0.5268	1.7318	1.7939	*1.3508*	0.7143	0.4129
VEGF (1+2) $^{3+}$	0.0536	0.0229	0.0274	*0.0346*	0.0166	0.0096
Glut-1 (1+2) $^{2+}$	0.3754	0.1512	0.3289	*0.2852*	0.1183	0.0684
Glut-1 (1+2+3) $^{1+}$	0.1545	0.0714	0.0341	*0.0866*	0.0617	0.0356

10uM 8-cl-cAMP

				MEAN		
	AIR	AIR	AIR	*AIR*	Sdev	SE
Epo (1+2) $^{3+}$	0.0191	0.1857	0.1935	*0.1328*	0.0985	0.0570
PGK (1+2) $^{3+}$	0.1479	0.0372	0.0369	*0.0740*	0.0640	0.0370
LDH-A (1+2+3) $^{3+}$	0.0196	0.0734	0.1533	*0.0821*	0.0673	0.0389
LDH (1+2) $^{3-}$	0.0185	0.0378	0.0667	*0.0410*	0.0242	0.0140
VEGF (1+2) $^{3+}$	0.0112	0.0320	0.0700	*0.0377*	0.0298	0.0172
Glut-1 (1+2) $^{2+}$	0.0359	0.0538	0.0283	*0.0394*	0.0131	0.0076
Glut-1 (1+2+3) $^{1+}$	0.0282	0.0304	0.0223	*0.0270*	0.0042	0.0024
				MEAN		
	AnO_2	AnO_2	AnO_2	*AnO_2*	Sdev	SE
Epo (1+2) $^{3+}$	0.1089	0.6450	0.5033	*0.4191*	0.2778	0.1606
PGK (1+2) $^{3+}$	0.7155	0.8774	0.7952	*0.7961*	0.0809	0.0468
LDH-A (1+2+3) $^{3+}$	0.1095	0.2663	0.5238	*0.2999*	0.2092	0.1209
LDH (1+2) $^{3-}$	0.8827	3.0451	3.2575	*2.3951*	1.3141	0.7596
VEGF (1+2) $^{3+}$	0.0259	0.0369	0.0977	*0.0535*	0.0387	0.0224
Glut-1 (1+2) $^{2+}$	0.2111	0.3395	0.1046	*0.2184*	0.1176	0.0680
Glut-1 (1+2+3) $^{1+}$	0.0907	0.1465	0.0717	*0.1030*	0.0389	0.0225

10uM Forskolin

				MEAN		
	AIR	AIR	AIR	*AIR*	Sdev	SE
Epo (1+2) $^{3+}$	0.0346	0.2110	0.3021	*0.1825*	0.1360	0.0786
PGK (1+2) $^{3+}$	0.8861	0.0315	0.0609	*0.3262*	0.4851	0.2804
LDH-A (1+2+3) $^{3+}$	0.0748	0.1032	0.2200	*0.1327*	0.0769	0.0445
LDH (1+2) $^{3-}$	0.0417	0.0144	0.0500	*0.0354*	0.0186	0.0107
VEGF (1+2) $^{3+}$	0.0163	0.0353	0.0818	*0.0445*	0.0337	0.0195
Glut-1 (1+2) $^{2+}$	0.0166	0.0112	0.0104	*0.0128*	0.0034	0.0019
Glut-1 (1+2+3) $^{1+}$	0.0185	0.0653	0.0112	*0.0317*	0.0293	0.0170
				MEAN		
	AnO_2	AnO_2	AnO_2	*AnO_2*	Sdev	SE
Epo (1+2) $^{3+}$	0.0873	0.4699	0.4139	*0.3237*	0.2066	0.1194
PGK (1+2) $^{3+}$	0.9507	0.4970	0.7978	*0.7485*	0.2308	0.1334
LDH-A (1+2+3) $^{3+}$	0.2618	0.2409	0.4023	*0.3017*	0.0878	0.0507
LDH (1+2) $^{3-}$	1.4180	0.6747	3.5607	*1.8845*	1.4985	0.8662
VEGF (1+2) $^{3+}$	0.0269	0.0417	0.0672	*0.0453*	0.0204	0.0118
Glut-1 (1+2) $^{2+}$	0.0231	0.0228	0.0282	*0.0247*	0.0030	0.0018
Glut-1 (1+2+3) $^{1+}$	0.0865	0.1707	0.2463	*0.1678*	0.0799	0.0462

Appendix 31

HRE activity after 8 hours +/- a PKA analog followed by 16 hours air or anoxia and 3 hours reoxygenation in the HT1080 cell line, n=3.

Control				*MEAN*		
	AIR	AIR	AIR	*AIR*	Sdev	SE
Epo (1+2)$^{3+}$	0.0336	0.1426	0.0459	*0.0740*	0.0597	0.0345
PGK (1+2)$^{3+}$	0.0246	0.0154	0.0393	*0.0264*	0.0120	0.0070
LDH (1+2+3	0.0250	0.0273	0.0343	*0.0289*	0.0048	0.0028
LDH (1+2)^{3}	0.0888	0.1899	0.0878	*0.1222*	0.0587	0.0339
VEGF (1+2)$^{3+}$	0.0075	0.0070	0.0063	*0.0069*	0.0006	0.0003
Glut (1+2)$^{2+}$	0.4634	0.2014	0.3021	*0.3223*	0.1322	0.0764
Glut (1+2+3)	0.2200	0.1664	0.0388	*0.1417*	0.0931	0.0538
				MEAN		
	AnO_2	AnO_2	AnO_2	*AnO $_2$*	Sdev	SE
Epo (1+2)$^{3+}$	0.2170	1.0011	0.5431	*0.5871*	0.3939	0.2277
PGK (1+2)$^{3+}$	1.4039	0.8163	1.2018	*1.1407*	0.2985	0.1726
LDH (1+2+3	0.5121	0.7453	0.2250	*0.4941*	0.2606	0.1507
LDH (1+2)$^{3-}$	1.2992	1.1933	0.8008	*1.0978*	0.2625	0.1518
VEGF (1+2)$^{3+}$	0.0258	0.0154	0.0143	*0.0185*	0.0063	0.0037
Glut (1+2)$^{2+}$	1.1346	0.6286	0.7649	*0.8427*	0.2618	0.1513
Glut (1+2+3)	0.5008	0.3758	0.1239	*0.3335*	0.1920	0.1110
10uM 8-cl-cAMP				*MEAN*		
	AIR	AIR	AIR	*AIR*	Sdev	SE
Epo (1+2)$^{3+}$	0.0184	0.0626	0.0823	*0.0544*	0.0327	0.0189
PGK (1+2)$^{3+}$	0.0646	0.0353	0.0876	*0.0625*	0.0262	0.0151
LDH (1+2+3	0.0261	0.0228	0.0248	*0.0246*	0.0017	0.0010
LDH (1+2)$^{3-}$	0.0327	0.1300	0.0950	*0.0859*	0.0493	0.0285
VEGF (1+2)$^{3+}$	0.0183	0.0120	0.0155	*0.0153*	0.0031	0.0018
Glut (1+2)$^{2+}$	0.1883	0.1207	0.2402	*0.1831*	0.0599	0.0346
Glut (1+2+3)	0.2409	0.0491	0.0716	*0.1206*	0.1049	0.0606
				MEAN		
	AnO_2	AnO_2	AnO_2	*AnO $_2$*	Sdev	SE
Epo (1+2)$^{3+}$	0.1585	0.4079	0.4564	*0.3410*	0.1305	0.0754
PGK (1+2)$^{3+}$	0.8948	0.4584	0.8254	*0.7262*	0.1915	0.1107
LDH (1+2+3	0.3148	0.3252	0.2727	*0.3042*	0.0227	0.0131
LDH (1+2)$^{3-}$	0.6164	0.6939	0.5852	*0.6318*	0.0457	0.0264
VEGF (1+2)$^{3+}$	0.0279	0.1339	0.0248	*0.0622*	0.0507	0.0293
Glut (1+2)$^{2+}$	0.6582	0.4124	0.8999	*0.6568*	0.1990	0.1150
Glut (1+2+3)	0.6957	0.0979	0.3252	*0.3729*	0.2464	0.1424
10uM Forskolin				*MEAN*		
	AIR	AIR	AIR	*AIR*	Sdev	SE
Epo (1+2)$^{3+}$	0.1585	0.0913	0.2411	*0.1637*	0.0750	0.0434
PGK (1+2)$^{3+}$	0.0333	0.0775	0.0305	*0.0471*	0.0263	0.0152
LDH (1+2+3	0.1363	0.0260	0.0354	*0.0659*	0.0611	0.0353
LDH (1+2)$^{3-}$	0.0495	0.2400	0.5266	*0.2721*	0.2402	0.1388
VEGF (1+2)$^{3+}$	0.0233	0.0162	0.0418	*0.0271*	0.0132	0.0077
Glut (1+2)$^{2+}$	0.2258	0.1242	0.1607	*0.1702*	0.0515	0.0298
Glut (1+2+3)	0.0741	0.0934	0.0528	*0.0734*	0.0203	0.0117
				MEAN		
	AnO_2	AnO_2	AnO_2	*AnO $_2$*	Sdev	SE
Epo (1+2)$^{3+}$	0.5032	0.7575	1.7280	*0.9962*	0.5278	0.3051
PGK (1+2)$^{3+}$	2.4150	0.5939	0.9109	*1.3066*	0.7944	0.4592
LDH (1+2+3	0.8852	0.6850	0.5237	*0.6980*	0.1479	0.0855
LDH (1+2)$^{3-}$	2.3375	0.5628	1.2045	*1.3683*	0.7337	0.4241
VEGF (1+2)$^{3+}$	0.0418	0.0477	0.1585	*0.0826*	0.0537	0.0310
Glut (1+2)$^{2+}$	1.2503	0.6919	0.3879	*0.7767*	0.3571	0.2064
Glut (1+2+3)	0.1330	0.3489	0.2806	*0.2542*	0.0901	0.0521

Appendix 32

HRE activity after 8 hours +/- a PKA analog followed by 16 hours air or anoxia and 3 hours reoxygenation in the SQD9 cell line, n=3.

Control

				MEAN		
	AIR	AIR	AIR	*AIR*	Sdev	SE
Epo $(1+2)^{3+}$	0.1485	0.1580	0.0514	*0.1193*	0.0590	0.0341
PGK $(1+2)^{3+}$	0.2402	0.0720	0.0901	*0.1341*	0.0923	0.0534
LDH $(1+2+3)^{3+}$	0.3567	0.3079	0.1738	*0.2795*	0.0947	0.0547
LDH $(1+2)^{3-}$	0.6052	0.5538	1.0817	*0.7469*	0.2911	0.1682
VEGF $(1+2)^{3+}$	0.0164	0.0291	0.0120	*0.0192*	0.0089	0.0052
Glut $(1+2)^{2+}$	0.2209	0.3485	0.0682	*0.2125*	0.1403	0.0811
Glut $(1+2+3)^{2+}$	0.0715	0.2702	0.0481	*0.1299*	0.1220	0.0705
				MEAN		
	AnO_2	AnO_2	AnO_2	*AnO_2*	Sdev	SE
Epo $(1+2)^{3+}$	1.0473	0.7834	0.5516	*0.7941*	0.2480	0.1434
PGK $(1+2)^{3+}$	2.4075	2.5952	1.6155	*2.2061*	0.5200	0.3006
LDH $(1+2+3)^{3+}$	1.0407	0.6015	0.5293	*0.7238*	0.2768	0.1600
LDH $(1+2)^{3-}$	4.6193	4.1510	3.1646	*3.9783*	0.7426	0.4292
VEGF $(1+2)^{3+}$	0.0208	0.0209	0.0128	*0.0182*	0.0046	0.0027
Glut $(1+2)^{2+}$	0.7585	0.9398	0.1601	*0.6195*	0.4080	0.2358
Glut $(1+2+3)^{2+}$	0.2901	0.3983	0.0690	*0.2525*	0.1678	0.0970

10uM 8-cl-cAMP

				MEAN		
	AIR	AIR	AIR	*AIR*	Sdev	SE
Epo $(1+2)^{3+}$	0.0395	0.0782	0.0514	*0.0564*	0.0198	0.0114
PGK $(1+2)^{3+}$	0.0785	0.2058	0.0901	*0.1248*	0.0704	0.0407
LDH $(1+2+3)^{3+}$	0.0288	0.1738	0.3739	*0.1922*	0.1733	0.1001
LDH $(1+2)^{3-}$	0.4689	0.3678	0.5106	*0.4491*	0.0735	0.0425
VEGF $(1+2)^{3+}$	0.0102	0.0289	0.0164	*0.0185*	0.0095	0.0055
Glut $(1+2)^{2+}$	0.0245	0.0297	0.0759	*0.0434*	0.0283	0.0163
Glut $(1+2+3)^{2+}$	0.0218	0.0181	0.0530	*0.0310*	0.0192	0.0111
				MEAN		
	AnO_2	AnO_2	AnO_2	*AnO_2*	Sdev	SE
Epo $(1+2)^{3+}$	0.3754	0.2720	0.5516	*0.3996*	0.1414	0.0817
PGK $(1+2)^{3+}$	1.0955	3.4238	1.6155	*2.0449*	1.2221	0.7064
LDH $(1+2+3)^{3+}$	0.1548	0.5293	1.4272	*0.7037*	0.6539	0.3780
LDH $(1+2)^{3-}$	2.3177	3.3826	3.6187	*3.1063*	0.6931	0.4006
VEGF $(1+2)^{3+}$	0.0116	0.0497	0.0208	*0.0274*	0.0199	0.0115
Glut $(1+2)^{2+}$	0.1370	0.0173	0.6206	*0.2583*	0.3194	0.1846
Glut $(1+2+3)^{2+}$	0.0374	0.0408	0.2240	*0.1007*	0.1068	0.0617

10uM Forskolin

				MEAN		
	AIR	AIR	AIR	*AIR*	Sdev	SE
Epo $(1+2)^{3+}$	0.2364	0.1452	0.0619	*0.1478*	0.0873	0.0504
PGK $(1+2)^{3+}$	0.1553	0.2261	0.1209	*0.1674*	0.0537	0.0310
LDH $(1+2+3)^{3+}$	0.2981	0.1249	0.4011	*0.2747*	0.1395	0.0807
LDH $(1+2)^{3-}$	0.5161	0.9946	0.3609	*0.6238*	0.3303	0.1909
VEGF $(1+2)^{3+}$	0.0175	0.0307	0.0125	*0.0203*	0.0094	0.0054
Glut $(1+2)^{2+}$	0.2357	0.0371	0.0417	*0.1048*	0.1133	0.0655
Glut $(1+2+3)^{2+}$	0.0802	0.0272	0.0264	*0.0446*	0.0308	0.0178
				MEAN		
	AnO_2	AnO_2	AnO_2	*AnO_2*	Sdev	SE
Epo $(1+2)^{3+}$	1.8716	0.6580	0.3984	*0.9760*	0.7864	0.4546
PGK $(1+2)^{3+}$	3.3423	2.4287	1.7055	*2.4922*	0.8203	0.4742
LDH $(1+2+3)^{3+}$	1.1680	0.6302	0.3155	*0.7045*	0.4311	0.2492
LDH $(1+2)^{3-}$	2.6251	3.1452	2.0649	*2.6117*	0.5402	0.3123
VEGF $(1+2)^{3+}$	0.0207	0.0466	0.0171	*0.0281*	0.0161	0.0093
Glut $(1+2)^{2+}$	0.7166	0.1335	0.2010	*0.3504*	0.3190	0.1844
Glut $(1+2+3)^{2+}$	0.2420	0.0507	0.0796	*0.1241*	0.1031	0.0596

Appendix 33

Expression of the dissected LDH-A elements 8 hours +/- a PKA analog followed by 16 hours air or anoxia and 3 hours reoxygenation in the HT1080 cell line, n=3.

Control

				MEAN		
	AIR	AIR	AIR	*AIR*	Sdev	SE
LDH $(1+2)^{3-}$	0.0888	0.1899	0.0878	*0.1222*	0.0587	0.0339
LDH $(1)^{3+}$	0.0027	0.0048	0.0074	*0.0049*	0.0023	0.0013
LDH $(2)^{3+}$	0.0032	0.0036	0.0044	*0.0037*	0.0006	0.0003
LDH $(3)^{3+}$	0.0059	0.0055	0.0086	*0.0067*	0.0017	0.0010
				MEAN		
	AnO_2	AnO_2	AnO_2	*AnO 2*	Sdev	SE
LDH $(1+2)^{3-}$	1.2992	1.1933	0.8008	*1.0978*	0.2625	0.1518
LDH $(1)^{3+}$	0.0047	0.0064	0.0090	*0.0067*	0.0022	0.0013
LDH $(2)^{3+}$	0.0029	0.0050	0.0050	*0.0043*	0.0012	0.0007
LDH $(3)^{3+}$	0.0051	0.0040	0.0103	*0.0045*	0.0008	0.0005
10uM 8-cl-cAMP				*MEAN*		
	AIR	AIR	AIR	*AIR*	Sdev	SE
LDH $(1+2)^{3-}$	0.0327	0.1300	0.0950	*0.0859*	0.0493	0.0285
LDH $(1)^{3+}$	0.0037	0.0057	0.0022	*0.0039*	0.0018	0.0010
LDH $(2)^{3+}$	0.0023	0.0026	0.0036	*0.0029*	0.0007	0.0004
LDH $(3)^{3+}$	0.0041	0.0027	0.0053	*0.0041*	0.0013	0.0008
				MEAN		
	AnO_2	AnO_2	AnO_2	*AnO 2*	Sdev	SE
LDH $(1+2)^{3-}$	0.3148	0.3252	0.2727	*0.3042*	0.0227	0.0131
LDH $(1)^{3+}$	0.0083	0.0078	0.0048	*0.0069*	0.0015	0.0009
LDH $(2)^{3+}$	0.0044	0.0035	0.0049	*0.0043*	0.0006	0.0003
LDH $(3)^{3+}$	0.0049	0.0043	0.0052	*0.0048*	0.0004	0.0002
10uM Forskolin				*MEAN*		
	AIR	AIR	AIR	*AIR*	Sdev	SE
LDH $(1+2)^{3-}$	0.0495	0.2400	0.5266	*0.2721*	0.2402	0.1388
LDH $(1)^{3+}$	0.0070	0.0093	0.0023	*0.0062*	0.0036	0.0021
LDH $(2)^{3+}$	0.0035	0.0039	0.0039	*0.0037*	0.0002	0.0001
LDH $(3)^{3+}$	0.0141	0.0081	0.0086	*0.0102*	0.0033	0.0019
				MEAN		
	AnO_2	AnO_2	AnO_2	*AnO 2*	Sdev	SE
LDH $(1+2)^{3-}$	2.3375	0.5628	1.2045	*1.3683*	0.7337	0.4241
LDH $(1)^{3+}$	0.0126	0.0145	0.0060	*0.0110*	0.0036	0.0021
LDH $(2)^{3+}$	0.0030	0.0046	0.0048	*0.0041*	0.0008	0.0005
LDH $(3)^{3+}$	0.0190	0.0067	0.0103	*0.0120*	0.0051	0.0030

Appendix 34

Expression of the dissected LDH-A elements 8 hours +/- a PKA analog followed by 16 hours air or anoxia and 3 hours reoxygenation in the SQD9 cell line, n=3.

Control

				MEAN		
	AIR	AIR	AIR	*AIR*	Sdev	SE
LDH $(1+2)^{3-}$	0.6052	0.5538	1.0817	*0.7469*	0.2911	0.1682
LDH $(1)^{3+}$	0.0472	0.0557	0.0380	*0.0470*	0.0089	0.0051
LDH $(2)^{3+}$	0.0648	0.0499	0.0452	*0.0533*	0.0102	0.0059
LDH $(3)^{3+}$	0.0425	0.0220	0.0600	*0.0415*	0.0190	0.0110
				MEAN		
	AnO_2	AnO_2	AnO_2	*AnO 2*	Sdev	SE
LDH $(1+2)^{3-}$	4.6193	4.1510	3.1646	*3.9783*	0.7426	0.4292
LDH $(1)^{3+}$	0.0761	0.0560	0.0657	*0.0659*	0.0100	0.0058
LDH $(2)^{3+}$	0.0260	0.0606	0.0431	*0.0432*	0.0173	0.0100
LDH $(3)^{3+}$	0.0373	0.0238	0.0619	*0.0410*	0.0193	0.0111

10uM 8-cl-cAMP

				MEAN		
	AIR	AIR	AIR	*AIR*	Sdev	SE
LDH $(1+2)^{3-}$	0.4689	0.3678	0.5106	*0.4491*	0.0735	0.0425
LDH $(1)^{3+}$	0.0091	0.0188	0.0160	*0.0146*	0.0050	0.0029
LDH $(2)^{3+}$	0.0382	0.0103	0.0332	*0.0273*	0.0149	0.0086
LDH $(3)^{3+}$	0.0155	0.0118	0.0362	*0.0212*	0.0132	0.0076
				MEAN		
	AnO_2	AnO_2	AnO_2	*AnO 2*	Sdev	SE
LDH $(1+2)^{3-}$	2.3177	3.3826	3.6187	*3.1063*	0.6931	0.4006
LDH $(1)^{3+}$	0.0153	0.0361	0.0263	*0.0259*	0.0104	0.0060
LDH $(2)^{3+}$	0.0264	0.0159	0.0467	*0.0296*	0.0157	0.0091
LDH $(3)^{3+}$	0.0178	0.0133	0.0375	*0.0229*	0.0128	0.0074

10uM Forskolin

				MEAN		
	AIR	AIR	AIR	*AIR*	Sdev	SE
LDH $(1+2)^{3-}$	0.5161	0.9946	0.3609	*0.6238*	0.3303	0.1909
LDH $(1)^{3+}$	0.0126	0.0225	0.0129	*0.0160*	0.0056	0.0033
LDH $(2)^{3+}$	0.0616	0.0150	0.0102	*0.0289*	0.0284	0.0164
LDH $(3)^{3+}$	0.0291	0.0171	0.0164	*0.0209*	0.0071	0.0041
				MEAN		
	AnO_2	AnO_2	AnO_2	*AnO 2*	Sdev	SE
LDH $(1+2)^{3-}$	2.6251	3.1452	2.0649	*2.6117*	0.5402	0.3123
LDH $(1)^{3+}$	0.0182	0.0327	0.0262	*0.0257*	0.0072	0.0042
LDH $(2)^{3+}$	0.0320	0.0155	0.0155	*0.0210*	0.0095	0.0055
LDH $(3)^{3+}$	0.0296	0.0181	0.0272	*0.0250*	0.0060	0.0035

Appendix 35

Expression of Egr-1, Epo.Egr-1 and Epo exposed to 16 hours air or hypoxia, +/- 5Gy and 1 to 6 hours reoxygenation in the HT1080 cell line, n=3.

1 hour reoxygenation

					Mean Egr-1	Sdev	SE
AIR	0.1463	0.1057	0.1371	0.1928	*0.1455*	0.0360	0.0180
5Gy	0.0804	0.0875	0.0379	0.4546	*0.1651*	0.1942	0.0971
$1\%O_2$	0.0379	0.0368	0.0947	0.1480	*0.0794*	0.0532	0.0266
$1\%O_2$ + 5Gy	0.0290	0.0388	0.0250	0.2353	*0.0820*	0.1023	0.0512
					Mean Epo.Egr-1	Sdev	SE
AIR	0.2712	0.1893	0.2139	0.2518	*0.2316*	0.0369	0.0184
5Gy	0.1600	0.1568	0.0297	0.5517	*0.2246*	0.2264	0.1132
$1\%O_2$	0.8093	0.7000	0.7117	0.4738	*0.6737*	0.1420	0.0710
$1\%O_2$ + 5Gy	0.6285	0.5600	0.1582	1.4180	*0.6912*	0.5271	0.2635
					Mean Epo	Sdev	SE
AIR	0.0411	0.0588	0.0712	0.1424	*0.0784*	0.0444	0.0222
5Gy	0.0400	0.0344	0.0112	0.2751	*0.0902*	0.1239	0.0620
$1\%O_2$	1.0944	2.2497	0.6942	0.9675	*1.2515*	0.6861	0.3431
$1\%O_2$ + 5Gy	1.5323	1.0854	0.1703	3.9057	*1.6734*	1.5925	0.7963

3 hours reoxygenation

					Mean Egr-1	Sdev	SE
AIR	0.0510	0.0459	0.0876	0.1533	*0.0845*	0.0495	0.0248
5Gy	0.0784	0.1128	0.4582	0.2684	*0.2295*	0.1735	0.0867
$1\%O_2$	0.0265	0.0334	0.1242	0.1450	*0.0823*	0.0611	0.0305
$1\%O_2$ + 5Gy	0.0482	0.1490	0.3855	0.1788	*0.1904*	0.1416	0.0708
					Mean Epo.Egr-1	Sdev	SE
AIR	0.1121	0.6813	0.0361	0.0963	*0.2314*	0.3017	0.1508
5Gy	0.1693	0.3548	0.4689	0.3552	*0.3370*	0.1241	0.0620
$1\%O_2$	0.2570	0.6480	0.2246	0.9480	*0.5194*	0.3445	0.1722
$1\%O_2$ + 5Gy	0.3926	0.6760	2.2822	1.0130	*1.0909*	0.8336	0.4168
					Mean Epo	Sdev	SE
AIR	0.0155	0.0483	0.0574	0.1615	*0.0707*	0.0632	0.0316
5Gy	0.0403	0.0939	0.1560	0.2316	*0.1304*	0.0824	0.0412
$1\%O_2$	0.5743	1.4335	0.4691	3.2054	*1.4206*	1.2659	0.6329
$1\%O_2$ + 5Gy	0.9771	3.2093	5.6815	2.4063	*3.0685*	1.9715	0.9857

6 hours reoxygenation

					Mean Egr-1	Sdev	SE
AIR	0.0572	0.0443	0.0899	0.1654	*0.0892*	0.0543	0.0272
5Gy	0.1232	0.0143	0.0366	0.2163	*0.0976*	0.0920	0.0460
$1\%O_2$	0.0480	0.0335	0.0530	0.0803	*0.0537*	0.0196	0.0098
$1\%O_2$ + 5Gy	0.0902	0.0053	0.0432	0.1597	*0.0746*	0.0665	0.0333
					Mean Epo.Egr-1	Sdev	SE
AIR	0.0823	0.2534	0.1392	0.4381	*0.2283*	0.1570	0.0785
5Gy	0.1955	0.0243	0.0478	0.3046	*0.1431*	0.1317	0.0658
$1\%O_2$	0.2268	0.5692	0.2631	1.1685	*0.5569*	0.4357	0.2178
$1\%O_2$ + 5Gy	0.6768	0.0666	0.1655	0.6482	*0.3893*	0.3183	0.1591
					Mean Epo	Sdev	SE
AIR	0.0419	0.0474	0.0338	0.2081	*0.0828*	0.0837	0.0419
5Gy	0.0181	0.0114	0.0204	0.1665	*0.0541*	0.0750	0.0375
$1\%O_2$	0.6315	1.4913	0.8696	3.4182	*1.6027*	1.2635	0.6317
$1\%O_2$ + 5Gy	0.5577	1.5571	0.3251	1.5699	*1.0025*	0.6548	0.3274

Appendix 36

Expression of Egr-1, Epo.Egr-1 and Epo exposed to 16 hours air or hypoxia, +/- 5Gy and 1 to 6 hours reoxygenation in the MDA 468 cell line, n=3.

1 hour reoxygenation

				Mean		
				Egr-1	Sdev	SE
AIR	0.07080	0.75687	0.34751	*0.3917*	0.3452	0.1993
5Gy	0.91511	0.33743	0.33308	*0.5285*	0.3348	0.1933
1%O_2	0.05534	0.53589	0.30766	*0.2996*	0.2404	0.1388
1%O_2 + 5Gy	1.10242	0.31854	0.25841	*0.5598*	0.4709	0.2719
				Mean		
				Epo.Egr-1	Sdev	SE
AIR	0.0251	0.3127	0.2093	*0.1823*	0.1457	0.0841
5Gy	0.1925	0.1035	0.1505	*0.1488*	0.0445	0.0257
1%O_2	0.0638	0.8291	1.3302	*0.7410*	0.6378	0.3682
1%O_2 + 5Gy	0.6355	0.7278	0.8494	*0.7376*	0.1073	0.0620
				Mean		
				Epo	Sdev	SE
AIR	0.0018	0.0460	0.0176	*0.0218*	0.0224	0.0129
5Gy	0.0992	0.0276	0.0159	*0.0476*	0.0451	0.0260
1%O_2	0.1642	2.2119	1.0272	*1.1344*	1.0280	0.5936
1%O_2 + 5Gy	0.6547	1.9105	0.5273	*1.0309*	0.7645	0.4414

3 hours reoxygenation

				Mean		
				Egr-1	Sdev	SE
AIR	0.20690	0.74131	0.22780	*0.3920*	0.3027	0.1748
5Gy	0.18643	0.13297	0.22241	*0.1806*	0.0450	0.0260
1%O_2	0.40707	0.07834	0.14911	*0.2115*	0.1730	0.0999
1%O_2 + 5Gy	0.15469	0.09652	0.19065	*0.1473*	0.0475	0.0274
				Mean		
				Epo.Egr-1	Sdev	SE
AIR	0.0731	0.1886	0.4129	*0.2249*	0.1728	0.0998
5Gy	0.0769	0.0358	0.1481	*0.0870*	0.0568	0.0328
1%O_2	0.2501	0.0889	0.8230	*0.3873*	0.3858	0.2227
1%O_2 + 5Gy	0.2234	0.0758	0.7864	*0.3619*	0.3749	0.2165
				Mean		
				Epo	Sdev	SE
AIR	0.0092	0.0436	0.0119	*0.0216*	0.0192	0.0111
5Gy	0.0061	0.0147	0.0126	*0.0111*	0.0045	0.0026
1%O_2	0.1836	0.0869	0.6394	*0.3033*	0.2951	0.1704
1%O_2 + 5Gy	0.1505	0.2588	0.6982	*0.3692*	0.2900	0.1675

6 hours reoxygenation

				Mean		
				Egr-1	Sdev	SE
AIR	1.23632	0.35278	0.18544	*0.5915*	0.5647	0.3260
5Gy	0.06359	0.26599	0.41937	*0.2497*	0.1785	0.1030
1%O_2	0.45375	0.26313	0.04221	*0.2530*	0.2060	0.1189
1%O_2 + 5Gy	0.02889	0.26763	0.18637	*0.1610*	0.1214	0.0701
				Mean		
				Epo.Egr-1	Sdev	SE
AIR	0.3198	0.1072	0.1174	*0.1815*	0.1199	0.0692
5Gy	0.0273	0.0765	0.2193	*0.1077*	0.0997	0.0576
1%O_2	0.6162	0.3734	0.0546	*0.3480*	0.2817	0.1626
1%O_2 + 5Gy	0.0250	0.2221	0.1617	*0.1363*	0.1010	0.0583
				Mean		
				Epo	Sdev	SE
AIR	0.0056	0.0425	0.0113	*0.0198*	0.0198	0.0115
5Gy	0.0068	0.0249	0.0105	*0.0141*	0.0096	0.0055
1%O_2	0.1380	1.3238	0.1507	*0.5375*	0.6810	0.3932
1%O_2 + 5Gy	0.1554	1.0362	0.3224	*0.5047*	0.4679	0.2701

Appendix 37

Expression of Egr-1, Epo.Egr-1 and Epo exposed to 16 hours air or hypoxia, +/- 5Gy and 1 to 6 hours reoxygenation in the DU145 cell line, n=3.

1 hour reoxygenation			*Mean*
			Egr-1
AIR	0.5083	1.2205	*0.8644*
5Gy	3.0042	2.0243	*2.5142*
1%O_2	0.1513	1.0702	*0.6107*
1%O_2 + 5Gy	0.6481	1.5205	*1.0843*
			Mean
			Epo.Egr-1
AIR	0.2932	0.4581	*0.3756*
5Gy	1.5432	0.6306	*1.0869*
1%O_2	0.4488	1.0426	*0.7457*
1%O_2 + 5Gy	0.8398	1.4122	*1.1260*
			Mean
			Epo
AIR	0.0829	0.0617	*0.0723*
5Gy	0.1161	0.0542	*0.0852*
1%O_2	1.2426	1.3846	*1.3136*
1%O_2 + 5Gy	1.0723	1.7624	*1.4173*

3 hours reoxygenation			*Mean*
			Egr-1
AIR	0.7312	1.6016	*1.1664*
5Gy	0.8417	1.1791	*1.0104*
1%O_2	0.4520	0.4770	*0.4645*
1%O_2 + 5Gy	0.4402	0.5286	*0.4844*
			Mean
			Epo.Egr-1
AIR	0.1072	0.6466	*0.3769*
5Gy	0.0381	0.2308	*0.1345*
1%O_2	0.6537	0.6000	*0.6268*
1%O_2 + 5Gy	0.0982	0.5733	*0.3357*
			Mean
			Epo
AIR	0.1030	0.0456	*0.0743*
5Gy	0.0262	0.0315	*0.0288*
1%O_2	4.0903	0.4132	*2.2518*
1%O_2 + 5Gy	0.5912	0.8374	*0.7143*

6 hours reoxygenation			*Mean*
			Egr-1
AIR	0.4864	1.0006	*0.7435*
5Gy	0.4651	0.9442	*0.7046*
1%O_2	0.3798	0.8800	*0.6299*
1%O_2 + 5Gy	0.3532	0.8684	*0.6108*
			Mean
			Epo.Egr-1
AIR	0.2295	0.3136	*0.2715*
5Gy	0.2424	0.3092	*0.2758*
1%O_2	0.4526	0.6428	*0.5477*
1%O_2 + 5Gy	0.5072	0.5777	*0.5424*
			Mean
			Epo
AIR	0.0953	0.0365	*0.0659*
5Gy	0.0863	0.0414	*0.0639*
1%O_2	3.2840	1.3180	*2.3010*
1%O_2 + 5Gy	1.7409	1.1367	*1.4388*

Appendix 38

Expression of Egr-1, Epo.Egr-1 and Epo exposed to 16 hours air or hypoxia, +/- 5Gy and 6 hours reoxygenation in the HepG2 cell line, n=1.

6 hours reoxygenation

	Egr-1	Epo.Egr-1	Epo
AIR	0.7789	0.1531	0.2098
5Gy	0.6751	0.2472	0.1963
1%O_2	0.8553	0.3415	0.4200
1%O_2 +5Gy	0.6505	0.4002	1.0042

Appendix 39

Expression of Egr-1, Epo.Egr-1 and Epo exposed to 16 hours air or hypoxia, +/- 5Gy and 3 hours reoxygenation in the HCT116 cell line, n=1.

3 hours reoxygenation

	Egr-1	Epo.Egr-1	Epo
AIR	0.7667	0.1301	0.0410
5Gy	0.9488	0.5940	0.0611
1%O_2	0.6642	0.2734	0.1261
1%O_2 +5Gy	1.6096	1.1890	0.8282

Appendix 40

Expression of Egr-1, Epo.Egr-1 and Epo exposed to 16 hours air or hypoxia, +/- 5Gy and 1 to 6 hours reoxygenation in the WiDr cell line, n=1.

3 hours reoxygenation

	Egr-1	Epo.Egr-1	Epo
AIR	5.3162	0.3933	0.3098
5Gy	4.3274	0.7734	0.2872
1%O_2	5.8863	1.6046	8.5924
1%O_2 +5Gy	9.7263	2.3431	10.3657

Appendix 41

Expression of CArG.Epo versus CArG multimers exposed to 16 hours air or hypoxia and 3 hours reoxygenation in the HT1080 cell line, n=2.

3 hours reoxygenation

			MEAN
	CArG.Epo	CArG.Epo	*CArG.Epo*
AIR	0.0638	0.1756	*0.1197*
5GY	0.0624	0.1255	*0.0939*
1%O_2	0.4935	1.4253	*0.9594*
1% O_2+5GY	0.7495	1.0729	*0.9112*
			MEAN
	$CArG^5$	$CArG^5$	*$CArG^5$*
AIR	0.0118	0.0300	*0.0209*
5GY	0.0096	0.0237	*0.0167*
1%O_2	0.0054	0.0257	*0.0155*
1% O_2+5GY	0.0122	0.0114	*0.0118*
			MEAN
	$CArG^{10}$	$CArG^{10}$	*$CArG^{10}$*
AIR	0.0090	0.0311	*0.0201*
5GY	0.0139	0.0141	*0.0140*
1%O_2	0.0103	0.0182	*0.0143*
1% O_2+5GY	0.0116	0.0091	*0.0103*

Appendix 42

Expression of CArG.Epo versus CArG multimers exposed to 16 hours air or hypoxia and 1 hour reoxygenation in the MDA 468 cell line, n=2.

1 hour reoxygenation

			MEAN
	CArG.Epo	CArG.Epo	*CArG.Epo*
AIR	0.0148	0.0239	*0.0193*
5GY	0.0128	0.0231	*0.0180*
1%O_2	0.8111	0.9561	*0.8836*
1% O_2+5GY	0.8042	0.8056	*0.8049*
			MEAN
	$CArG^5$	$CArG^5$	*CArG* ^{5}
AIR	0.0297	0.0276	*0.0286*
5GY	0.0232	0.0269	*0.0250*
1%O_2	0.0278	0.0260	*0.0269*
1% O_2+5GY	0.0248	0.0312	*0.0280*
			MEAN
	$CArG^{10}$	$CArG^{10}$	*CArG* ^{10}
AIR	0.0232	0.0273	*0.0253*
5GY	0.0250	0.0315	*0.0283*
1%O_2	0.0262	0.0356	*0.0309*
1% O_2+5GY	0.0233	0.0298	*0.0266*

Appendix 43

Expression of CArG.Epo versus CArG multimers exposed to 16 hours air or hypoxia and 3 hours reoxygenation in the DU145 cell line, n=2.

1 hour reoxygenation

			MEAN
	CArG.Epo	CArG.Epo	*CArG.Epo*
AIR	0.0819	0.1081	*0.0950*
5GY	0.0783	0.0744	*0.0763*
1%O_2	1.9144	2.5929	*2.2537*
1% O_2+5GY	1.5296	1.3590	*1.4443*
			MEAN
	$CArG^5$	$CArG^5$	*CArG* ^{5}
AIR	0.0616	0.0643	*0.0629*
5GY	0.0396	0.0693	*0.0544*
1%O_2	0.1098	0.0643	*0.0870*
1% O_2+5GY	0.0341	0.0511	*0.0426*
			MEAN
	$CArG^{10}$	$CArG^{10}$	*CArG* ^{10}
AIR	0.0941	0.0862	*0.0902*
5GY	0.0847	0.0561	*0.0704*
1%O_2	0.0795	0.0841	*0.0818*
1% O_2+5GY	0.0595	0.0446	*0.0520*

Appendix 44

HRE activity when exposed to hypoxia and radiation with 3 hours reoxygenation, in the HT1080 cell line, n=3 (except Epo n=4)

3 hours reoxygenation

					Mean Epo (1+2) $^{5+}$	Sdev	SE
AIR	0.0155	0.0483	0.0574	0.1615	0.0707	0.0632	0.0316
5Gy	0.0403	0.0939	0.1560	0.2316	0.1304	0.0824	0.0412
1%O_2	0.5743	1.4335	0.4691	3.2054	1.4206	1.2659	0.6329
1%O_2 + 5Gy	0.9771	3.2093	5.6815	2.4063	3.0685	1.9715	0.9857

			Mean PGK (1+2)$^{3+}$	Sdev
AIR	0.0497	0.1790	0.1143	0.0914
5Gy	0.3634	0.3367	0.3501	0.0189
1%O_2	1.1920	3.5608	2.3764	1.6750
1%O_2 + 5Gy	6.1536	5.7383	5.9460	0.2937

			Mean LDH (1+2+3)$^{3+}$	Sdev
AIR	0.0563	0.1224	0.0894	0.0467
5Gy	0.2360	0.2140	0.2250	0.0156
1%O_2	0.7314	1.1385	0.9349	0.2879
1%O_2 + 5Gy	3.3382	1.3716	2.3549	1.3906

			Mean LDH (1+2)$^{3-}$	Sdev
AIR	0.0889	0.3673	0.2281	0.1969
5Gy	0.4963	0.4503	0.4733	0.0326
1%O_2	1.8598	5.5887	3.7243	2.6367
1%O_2 + 5Gy	12.2372	4.4226	8.3299	5.5257

Appendix 45

HRE activity when exposed to hypoxia and radiation with 1 hour reoxygenation in the MDA 468 cell line, n=3

1 hour reoxygenation

	(EPO 1+2)$^{5+}$	PGK (1+2)$^{3+}$	LDH (1+2+3)$^{3+}$	LDH (1+2)$^{3-}$
AIR	0.0176	0.0168	0.0467	0.0330
5Gy	0.0159	0.0108	0.0312	0.0236
1%O_2	1.0272	0.6925	0.1524	2.3865
1%O_2 +5Gy	0.5273	0.3470	0.0723	1.2143

Appendix 46

HRE activity when exposed to hypoxia and radiation with 1 hour reoxygenation in the DU145 cell line, n=2 (LDH (1+2); Epo[5]), n=1 (PGK (1+2); LDH (1+2+3)).

1 hour reoxygenation

	Epo $(1+2)^{5+}$	PGK $(1+2)^{3+}$	LDH $(1+2+3)3+$	LDH $(1+2)^{3-}$
AIR	0.0723	0.0529	0.0506	0.0321
5Gy	0.0852	0.2265	0.0727	0.0801
$1\%O_2$	1.3136	1.3523	0.4642	1.0610
$1\%O_2$ + 5Gy	1.4173	4.7317	0.9843	2.9356

Appendix 47

HRE activity when exposed to hypoxia and radiation with 6 hours reoxygenation in the HepG2 cell line, n=1

6 hours reoxygenation

	Epo $(1+2)^{5+}$	PGK $(1+2)^{3+}$	LDH $(1+2+3)^{3+}$	LDH $(1+2)^{3-}$
AIR	0.2098	0.3603	0.3590	0.3373
5Gy	0.1963	0.3562	0.4665	0.4671
$1\%O_2$	0.4200	2.2628	0.9728	2.4385
$1\%O_2$ +5Gy	1.0042	2.1784	2.6100	3.6868